The study of a mesoscale model applied to the prediction of offshore wind resource.

James Geraint Hughes

A Doctoral Thesis

Submitted in part fulfilment of the requirements
for the award of
Doctor of Philosophy of Loughborough University.
January 2014

Certificate of originality

This is to certify that I am responsible for the work submitted in this thesis, that the original work is my own except as specified in acknowledgments or in footnotes, and that neither the thesis nor the original work contained therein has been submitted to this or any other institution for a degree.

Signed:

Date:

Abstract

The Supergen wind research consortium is a group of research centres which undertake research primarily aimed at reducing the cost of offshore wind farming. Research is undertaken to apply the WRF mesoscale NWP model to the field of offshore wind resource assessment to assess its potential as an operational tool. WRF is run in a variety of configurations for a number of locations to determine and optimise a level of performance and assess how accessible that performance might be to an end user. Three studies set out to establish a level of performance at two different sites and improve performance through optimisation of model setup and post processing techniques. WRF was found to simulate wind speed to an appreciable level by reference to similar studies, though performance was found to vary throughout the course of the model runs and depending on the location. An average correlation coefficient of 0.9 was found for the Shell Flats resource assessment at 6-hourly resolution with an RMSE of 1.7ms^{-1}. Performance at Scroby Sands was not at as high a level as that seen for Shell Flats with an average correlation coefficient for wind speed of 0.64 with an RMSE of 2ms^{-1}. A range of variables were simulated by the model in the Shell Flats investigation to test the flexibility of the model output. Wind direction was produced to a moderate level of accuracy at 10-minute resolution while aggregated stability statistics showed the model had a good appreciation of the frequency of cases observed. Areas of uncertainty in model performance were addressed through model optimisation techniques including the generation of two ensembles and observational nudging. Both techniques were found to add value to the model output as well as improving performance. The difference between performance observed at Shell Flats and Scroby Sands shows that while the model clearly has inherent skill it is sensitive to the environment to which it is applied. In order to maximise performance, as large a computing resource as possible is recommended with a concerted effort to optimise model setup with the aim of allowing it to perform to its best ability. There is room for improvement in the application of mesoscale NWP to the field of offshore wind resource assessment but these results confirm an inherent skill in model performance. With the addition of further validation, improvements to model setup on a case by case basis and the application of optimisation techniques, it is anticipated

mesoscale NWP can perform to a level which would justify its adoption operationally by the industry. The flexibility which can be offered relating to spatial and temporal coverage as well as the range of variables which can be produced make it an attractive option to developers if performance of a consistently high level can be established.

Acknowledgements

I would like to begin by thanking my supervisor Prof. Simon Watson, firstly for giving me the opportunity to undertake this journey and secondly for all the support along the way. Simon, I felt very much at home undertaking this research with you. Your thoughts over the last three years have been instructive and helpful, which helped me take the work through a range of fascinating and diverse areas. I really felt you trusted me throughout the project which gave me the confidence to produce this research of which I am truly proud, as I hope you are too. I unreservedly thank the other members of Simon's research group, Scott, Cian, Peter, Rolando and John, who have all been helpful, friendly and supportive throughout my time, which has meant a lot to me. Heartfelt thanks goes to the people of CREST who provide an enjoyable, simulating environment in which to work. A special mention goes to those who started their journey as a PhD student at CREST at the same time as me, to Adam, Ben and Bianca, it has been a consummate privilege.

My thanks go to Prof. Gareth Harrison (University of Edinburgh) and Dr. Tom Betts (Loughborough University) for agreeing to be the examiners of this work. I owe a great debt of gratitude to the EPSRC, specifically the Supergen wind consortium, who funded this research. I also thank Loughborough University and CREST for providing the environment and facilities for me to undertake my research over the past three years. A special mention goes to the IT support staff, to David, Ray and Gavin in the departmental facility and Dr Laurence Hurst at the HPC facility who provided a superb level of service throughout my time.

A big thanks goes to my previous academic institutions, the University of Northampton and the University of Birmingham. My time at these institutions has been instrumental in my personal and academic development for which I am truly grateful.

My deepest thanks go to my family, in particular my Mum, Dad and Sister, Zena, John and Hannah, to whom I would like to dedicate this doctorate. Your love, support and belief have been unwavering and helped me every step of my journey, I am so lucky to have you behind me, I thank you from the bottom of my heart.

Table of Figures

Table of Tables

1 Introduction

1.1 Research context

1.1.1 The changing climate

Natural climate change has been happening on Earth throughout its history. A function of the energy received from the sun, long-term climate on the earth is dictated by the three axes upon which the earth rotates. In their seminal paper Hays, Imbrie and Shackleton (1976) presented to the world the three orbital (or Milankovitch) cycles of the Earth, which exist on timescales of 23,000, 42,000 and 100,000 years. The orbital cycles manifest as long-term climate drivers as they correspond to variations in the amount of incident solar radiation received by the Earth. Earth's global energy begins as incident radiation from the Sun which is then subject to a range of processes upon entering the Earth's atmosphere. One such process, which acts to maintain the temperature of Earth's climate, is the greenhouse effect, the product of a number of naturally occurring gases in the atmosphere. Greenhouse gases do not interact with the short wavelength energy received from the sun as it enters the atmosphere, but do act to insulate the planet by retaining longwave infrared energy as it radiates away from the surface (Figure 1.1).

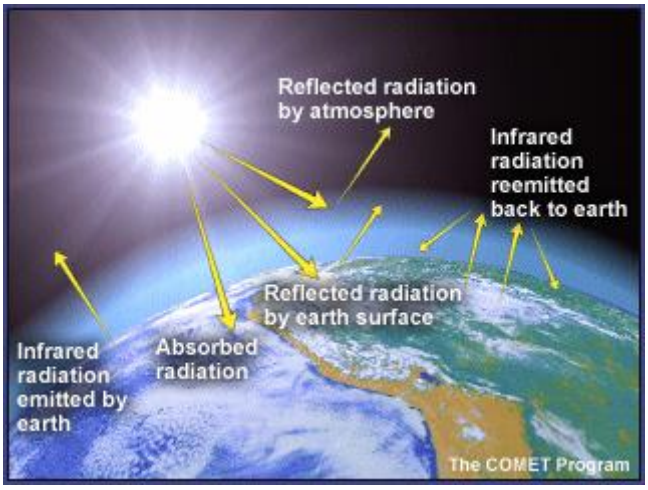

Figure 1.1 Schematic of solar energy receipt highlighting the Greenhouse Effect (UCAR, Date Unknown)

While Earth's climate has experienced periodic natural change through its history, there is a growing sense of unease at the negative impact humans have had

and will continue to have, upon the natural balance of the Earth's climate. In the UK for example, public perception is that the frequency of extreme weather events is increasing (for example Mckie 2013) while on a global scale, for example, annual sea ice reduction in the Arctic has rendered the North-West passage navigable to ocean vessels. A desire of national leaders to pool resources and undertake research into climate change, led to the formation of the IPCC (Intergovernmental Panel on Climate Change) in 1988. Since then the IPCC has been conducting research to gauge the extent of the human effect upon the climate of the planet and how it might change in the future. Since the Industrial Revolution, human society has evolved around advances in technology driven by energy extracted from fossil fuels. Combustion of fossil fuels releases carbon dioxide, which mixes into the air and augments the natural greenhouse effect. The concept of anthropogenically induced climate change is not new. While an awareness of the impact of greenhouse gas emission has led to a significant improvement in the efficiency of many of the methods which contribute to the changing climate, the increase in global population and contribution of large developing countries means that the human footprint continues to grow (WMO 2012 & Figure 1.2.).

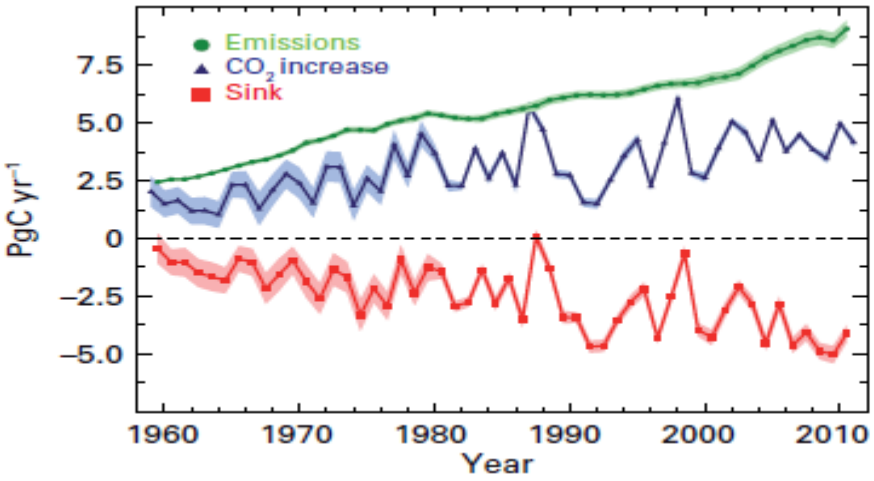

Figure 1.2 Annual emissions in PgC (Petagrams of carbon) from fossil fuel combustion and other industrial processes, the annual atmospheric increase, and the amount of carbon sequestered by sinks each year Ballantyne et al., 2012 and Levin, 2012.

Projections of future climate change from the IPCC were delivered in 2007 covering a range of scenarios based on projected variations in socio-economic factors such as growth in population and wealth (Figure 1.3) described in Meehl et al (2007). Projections of global temperature rise range from 1 to 6°C depending on the

scenario, even if concentrations of CO_2 were held at the level seen in the year 2000, temperature would continue to rise as CO_2 makes its way into the atmosphere from surface stores. Ultimately, according to the IPCC, the planet is resigned to temperature rise, the degree of which can still be moderated by the actions of society now.

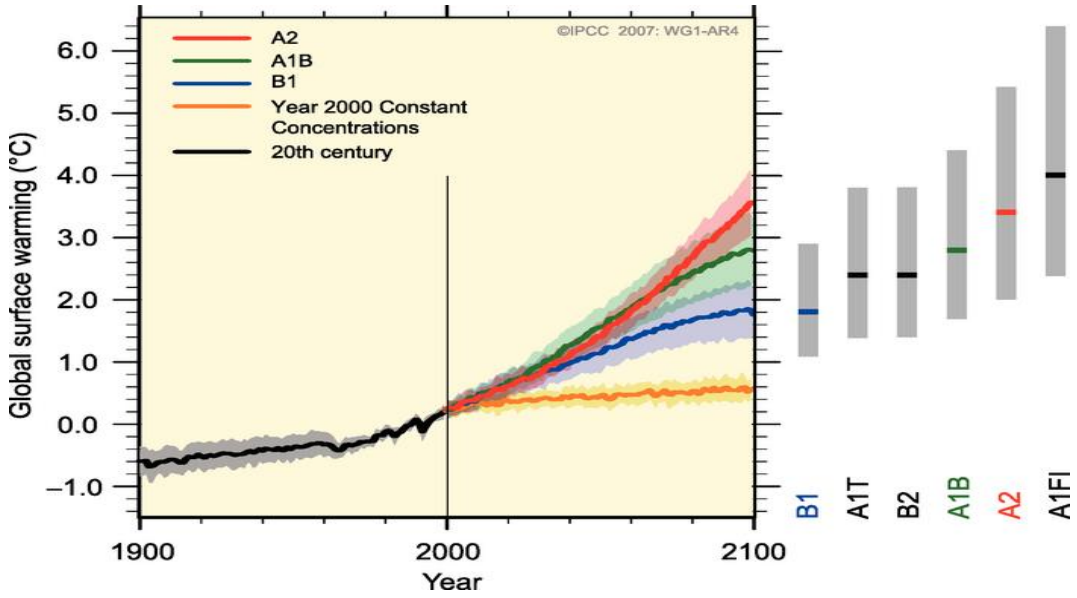

Figure 1.3 IPCC Multi-Model Averages and Assessed Ranges for Surface Warming, model projections with error bars of future climate for a range of scenarios based on projections of global socio-economic change (Meehl et al, 2007).

1.1.2 The response to increasing GHG emissions.

Combined with the damage being done to the Earth's climate, is an awareness in developed nations that dependence on fossil fuels needs to be reduced. For example prices are subject to those who own the resource, which will increase as supply becomes limited before eventually running out. As a result, times are changing for the means by which global energy is produced. Through the Climate Change Act of 2008, UK governmental policy has implemented a legally binding measure to mitigate greenhouse gas emissions, translating to a reduction in greenhouse gas emissions by 80% on 1991 levels by 2050 (Great Britain. Climate Change Act, 2008). One of the areas targeted to make the most significant steps toward achieving this target is the energy sector. The energy sector is a significant source of carbon dioxide (Figure 1.4) thus decarbonising the energy sector or at

least reducing the amount produced will have a significant impact upon national emissions.

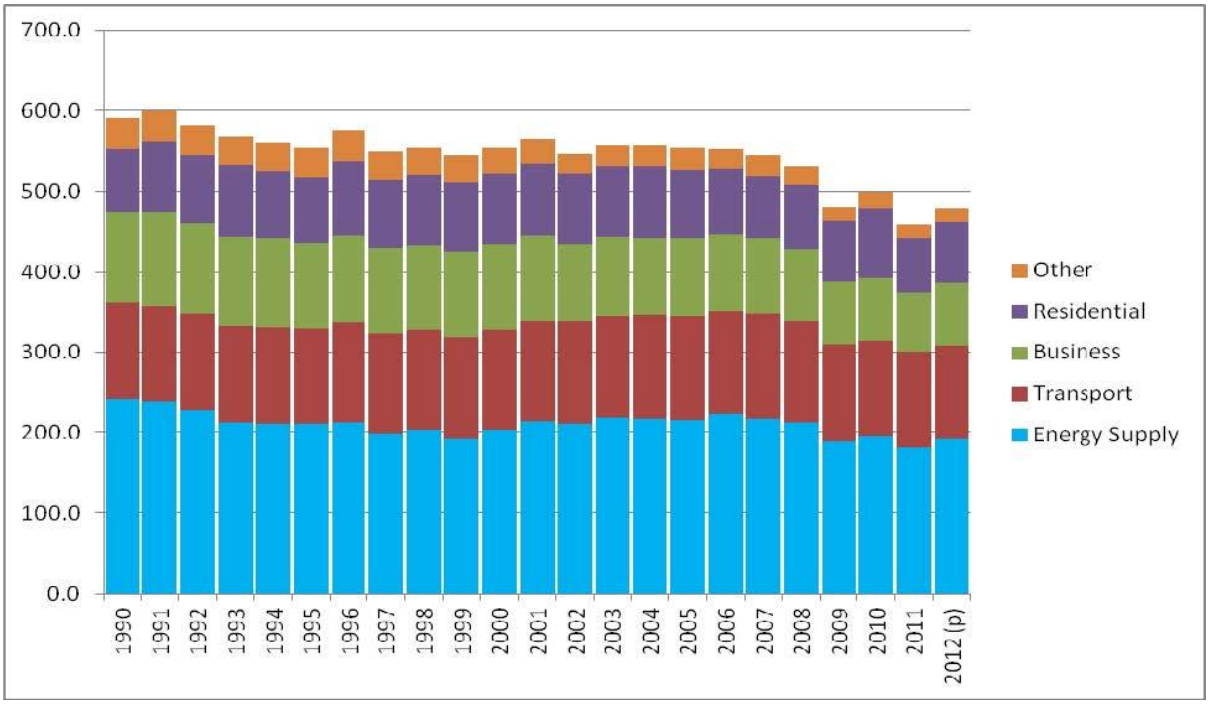

Figure 1.4 Carbon dioxide emissions by source, 1990-2012 (provisional), (Megatons) (DECC, 2013)

1.1.3 Wind energy in the UK

As part of the Electricity Act 1989, in a move to adopt sustainable energy generation methods, the British government offered the NFFO (Non fossil fuel obligation). The NFFO was an incentive scheme through which energy distributors bought energy from non-fossil fuel generators at a fixed price over long term contracts. The NFFO stimulated movement in the UK renewable energy market which resulted in the development of the UK's first two offshore wind farms, Gunfleet sands and Blythe. The NFFO has since been replaced by the Renewables Obligation (RO) which defines a proportion of energy which suppliers must obtain from renewable sources. The amount of renewably-sourced energy increases each year from 3% in the first year (2002/2003) to 15.4% in 2015/2016. The move towards adopting offshore wind power on a large scale has been stimulated by the awarding of offshore wind farm sites by the UK Crown Estate. Three rounds have been undertaken thus far whereby interested parties submit tenders for the lease of particular areas of UK waters in which they can develop a wind farm. Rounds one and two have been completed with many of the round two farms close to- or fully

operational, with a peak awarded capacity of 8.5GW. In 2008 the UK Climate change act was introduced which committed the UK to reducing emissions of the six primary greenhouse gases identified in the Kyoto treaty by 80% of 1990 levels for the year 2050. The significance of the act was felt throughout the UK, including the energy industry. In 2010, after another tendering process, awards of round three offshore wind farm sites were announced with a total capacity of approximately 25GW. Rounds one and two provided many lessons for the industry, particularly in the UK, from which to learn about developing an offshore wind farm. Many plans have now been consented, though due to the scale of the projects, round three sites are not expected to begin generation until around 2015 and construction is set to begin in 2014 (RenewableUK, 2013). Offshore wind energy in the UK is a viable source of energy which could become a fundamental part of the energy supply in the future. A well-developed infrastructure and tendering process demonstrates the ability of the country to adopt and incorporate such technology, but several stumbling blocks lie in the way of the developer's path to bringing an offshore wind power station online.

A wind turbine is a rotating machine driven by the kinetic energy transferred to its rotors by an incident wind. The power a turbine may extract from the wind can be calculated using the following formula (Equation 1) after Manwell et al (2002), where P=power, C_p = specific heat at constant pressure, A = swept area, ρ=density and U=wind speed;

$$P = \frac{1}{2} C_p A \rho U^3$$

Equation 1.1

A wind turbine is limited from extracting 100% of the kinetic energy from the incoming wind, because essentially net flow would drop to zero after the turbine blocking the incoming flow. Instead a rule called Betz's law calculates the maximum performance of a wind turbine, by reference to actuator disk theory, to be 59.3% (Betz, 1966). Practically, wind turbines rarely extract such a proportion of the energy more commonly achieving 75-80% of the Betz limit for the given wind speed (Burton et al, 2001). The technology exists to build multi gigawatt sized wind farms in the UK's territorial waters, which combined with the experience of the British offshore wind industry and tendering process means the potential for wind farm penetration in

the UK energy market is high. Technology, opportunity and availability are thus not the inhibiting factors in wind farm installations, the limiting factor is cost. As a rule of thumb offshore turbines cost about £3million per megawatt, which puts the cost of a gigawatt farm into the billions, however the associated costs begin far sooner than the production and installation of the turbines with tens of millions of pounds spent by developers in the planning phase.

1.2 Supergen Wind

Supergen Wind is a research consortium of seven UK research groups established by the EPSRC. The purpose of the Supergen Wind project is “To undertake research to achieve an integrated, cost-effective, reliable & available Offshore Wind Power Station.” (Supergen Wind, 2012). Supergen Wind is involved in extensive research throughout the planning, designing, installing and operating a wind farm. For the second phase of the Supergen Wind project, part of the renewal commitment was to dedicate time to a new field of research for Supergen Wind: wind resource assessment. A key challenge facing wind farm developers is securing the huge capital investment required to build a wind farm. Briefly, a wind resource assessment is required for any wind farm project to estimate energy generation and potential profits. Output from the wind resource assessment is of great importance to the developers when securing capital for the project as it directly relates to potential revenue for investors. A preliminary estimate of the wind resource is made to gain traction for a wind farm project, but as part of the planning phase a detailed site assessment must be made to satisfy investors, yield projections and designers. Costs of such a site assessment are typically on the order of millions of pounds, per mast, providing an area of research which the Supergen Wind consortium decided would be of significant interest to the industry if cost savings could be achieved or methods improved. Under the initial structure of the Supergen Wind research hierarchy, wind resource assessment was attached to ‘The Farm’ branch of research, under the direction of Professor Simon Watson at Loughborough University.

1.3 Wind Resource Assessment

1.3.1 Introduction

A wind resource assessment is simply an appraisal of the wind conditions for a site of interest, with the intention of providing useful information relating to the amount and efficiency of power which can be extracted. The variables of most interest are wind speed and direction; wind speed is ultimately the most important because it solely determines the amount of energy which can be produced. Wind direction is important to understand because of implications of fetch and potential array losses due to wake effects. After wind speed and direction, a number of other variables are important to supplement the quality of a resource assessment as they relate to the efficiency with which the turbines can utilise the wind speed, for example variables such as turbulence, humidity, temperature and stability. Stability is a measure of the atmospheric buoyancy, which is of particular interest in large wind farm arrays due to the effect it has on wake propagation. Knowledge of the wind resource at a prospective wind farm site is critical to completing the design specifications for the machinery which needs to operate at the site. Given that offshore turbines are essentially marinised onshore turbines, it is of great importance to understand the tolerances which will have to be built into the machines to ensure they complete their intended operations. Wind resource assessments are usually utilised at three times during the lifetime of a wind farm; a preliminary assessment which acts as a feasibility study; a detailed wind resource assessment which provides figures for output projections; and design requirements and a short term look ahead forecast for predicting farm output.

1.3.2 Preliminary site assessment

A preliminary assessment of the average wind conditions is usually undertaken by reference to a statistical or modelled dataset as a ‘quality check’ of the intended site to give a basic impression of the potential yield. Assuming the preliminary resource assessment provides enough confidence to the developer, a more detailed site assessment is required to provide more specific information about the wind conditions, both for more specific yield projections and turbine design specifications. Finally once the farm is operational short term forecasts are continually required to provide the operator with the clearest information by which to

choose their farm and turbine optimisation strategy to extract the maximum amount of power from the facility. A preliminary assessment is usually part of a feasibility survey, at such an early stage in a wind farm project the outlay for such a project will be minimal so the data comprising the study will usually already be available. There are several options for producing an early stage assessment, depending on the resource and expertise of the developer. Many consultants produce a shaded map representative of the average wind speed over a given period (for example Figure 1.5). Wind atlases are a popular option at the early stage as key information is easily accessible and immediately available. Wind atlases from different sources often contain some of the same data but gain value from privately owned datasets by the consultants.Mmore data can also be integrated if available such as point observations or satellite data, but would increase the monetary and workforce cost. A wind atlas can readily be compiled from existing free data such as reanalysis data sets. Many wind resource products are produced and validated at or just above ground level (Nunalee and Basu, 2012) where data is in more plentiful supply thanks to coverage by surface stations and buoys etc. but not necessarily directly applicable to turbines with a hub height of 90m. In addition to a wind atlas, average values of wind speed and direction at a point within an area of interest are the first step of a resource assessment. Average values give a good insight into the generic conditions received at a site, but understanding the variability is essential for accurate production estimates and design specifications for the machinery. Supplementary to the mean value, standard deviation can be readily calculated to give an impression of general variation in a series.

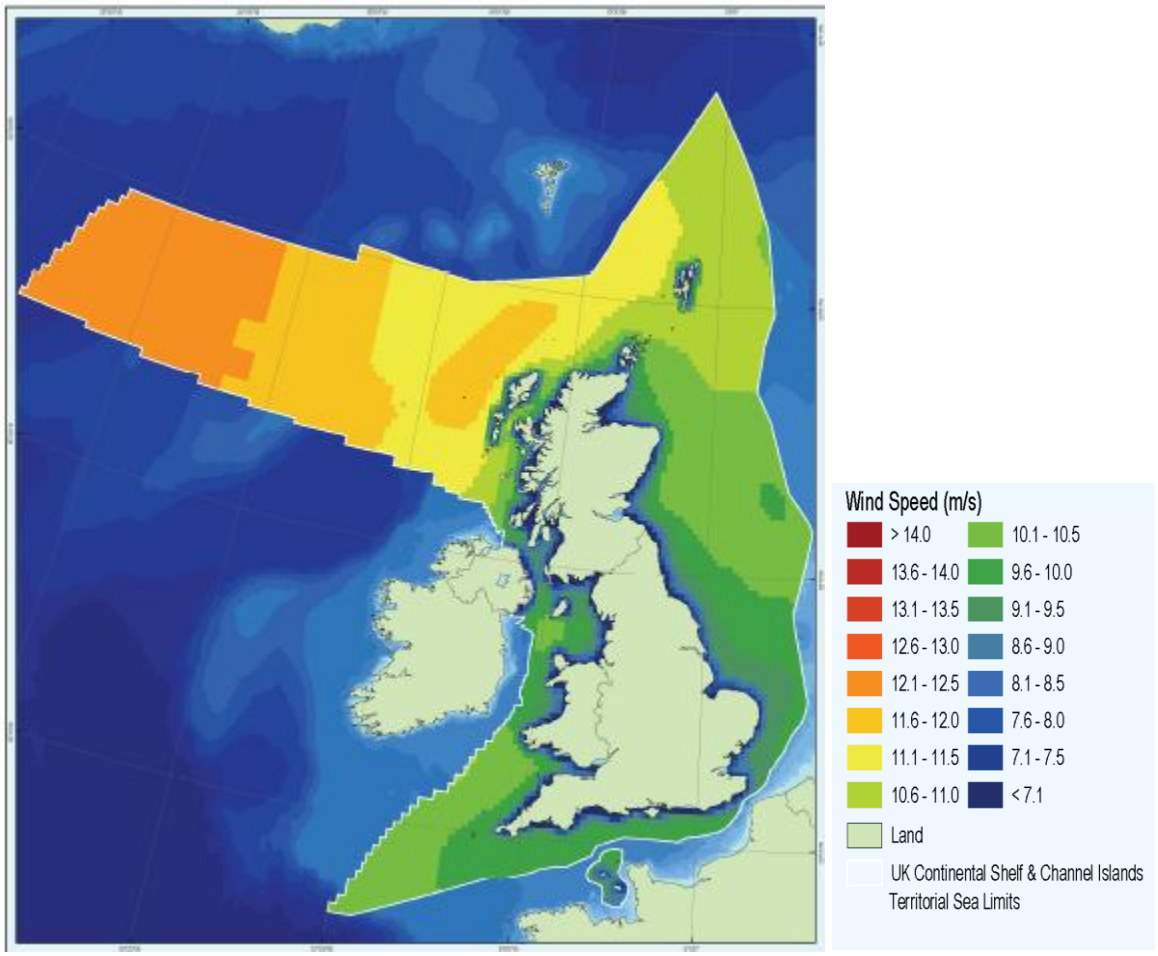

Figure 1.5 Atlas of UK Marine Renewable Energy Resources. 2008. ABPmer. Date of access (27 February 2013) © Crown Copyrighthttp://www.renewables-atlas.info/.

1.3.3 Detailed wind resource assessment

Once a preliminary feasibility study has been undertaken, detailed site investigations are undertaken by the developer to establish the processes required to build and operate the desired wind farm. The second stage of the resource assessment has to be specific to the site of interest to provide more detailed information of wind farm productivity. Atmospheric features, such as a sea breeze circulation, an internal boundary layer, or a low level jet may exist in a region subject to a wind resource assessment. In such a case, the application of a low level based study such as a surface level wind atlas may not be applicable even if the wind statistics were scaled to be for turbine hub height because the relevant features are not accounted for (Nunalee and Basu, 2012). To be confident in the performance of a resource assessment tool, validation is required at turbine hub height. The major, long-term wind resource assessment provides a far more detailed description of the

wind resource at a site of interest. Long term descriptive statistics focus on the variability of a number of variables at a site over a range of heights. Wind speed and wind direction are primarily measured from which turbulence and shear can be calculated. The duration of the campaign will afford an insight into the variability of the wind field over seasonal timescales. A long-term wind resource assessment should be undertaken over the course of at least a year (Bailey et al, 1997) to capture seasonal change, but preferably longer to establish a wider context for the period observed. Currently, a wind resource assessment for a prospective wind farm site must be carried out using cup anemometry according to IEC standard 61400-12-1 (IEC, 2005), the anemometers themselves must be validated and calibrated according to standard 61400-12-1. The need for certification is to ensure safety and consistency regarding the design of turbines used for a particular site, based on the resource assessment. A cup anemometer is a rotational device which spins at a speed proportional to that of the incident wind. Cup anemometers are a popular instrument because they are cheap yet accurate (Pedersen, 2003) to around 1% of the observed wind speed (Kristensen, 1999). It is necessary to validate anemometers to the correct standard to ensure they perform as intended; properties such as inertia affect the response to a change in wind speed which must be accounted for. To confirm each anemometer complies with the initial validation they must also be calibrated before being operationally deployed. Accuracy of 1% is very high and provides the standard which new methods of offshore wind resource assessment must aspire to. In addition to wind speed and direction, modern met masts are typically equipped to measure other atmospheric properties for example sunlight, rainfall and humidity. Doing so expands the knowledge provided by the resource assessment which can allow the calculation of other variables important to the developer such as stability (which will be discussed shortly).

Typically the detailed wind resource at a site is measured through an observational campaign, which for an offshore site costs on the order of millions of pounds per mast. The size of round three sites in the UK may require a developer to install multiple masts ramping the cost up further. More than one mast may be required because extrapolating for large distances from one point observation source is inappropriate, which is one of the limitations of in situ observations. One option available to a developer is to obtain additional information from other sources rather

than erecting multiple masts. Historical spatially extensive data can be obtained from reanalysis products (discussed in chapter 2) which contain a range of observational datasets. Similarly, satellite data can be acquired which provides surface wind speed over the ocean, but is not as temporally flexible as a reanalysis product nor does it offer a range of heights. In cases where a site is close to a shoreline and an observational series nearby is available, a measure correlate predict study (MCP) might be undertaken where data from the site of interest is correlated with the onshore site for an overlapping period and then historical output for the wind farm site is produced by extrapolating from the onshore site through the regression equation achieved in the correlation analysis. Atmospheric features which dominate long term studies are synoptic scale features such as pressure systems and weather fronts. Such large scale features are low frequency, passing on the order of days.

1.3.4 Short term operational forecasts

Once a wind farm is operational the need for wind resource assessments remains present, but over a different timescale. Predictions of impending conditions are required to forecast farm output and optimise the control strategy. Short term forecasts must capture small scale atmospheric features which will correspond to high frequency changes in wind speeds which occur at timescales on the order of hours and below. Such atmospheric features might be convective systems or be due to regional topography.

1.3.5 Stability

Stability is an atmospheric property which describes the future tendency of an air parcel once vertically perturbed. Stability is discussed more technically in chapter 2. Stability is of interest to the wind farm operator because of the effect it has on energy production of a wind farm due to the effect it has on wind shear, turbulence and turbine wake dissipation. Because it is not an absolute quantity, stability is approximated potentially via a number of methods. As well as directly calculating stability, it can be of use to relate stability to other variables produced in the resource assessment to try and provide more information to the end user. For example stability could be linked to a particular wind direction, time of day or weather type, knowledge of which can then be used to interpret the wind resource assessment more intricately.

1.3.6 Summary

Wind resource assessments are required throughout the process of developing and operating a wind farm and there is a need for alternative options by which to generate them to reduce the cost of offshore wind farming. The method must be able to perform in a long term low resolution historical context to capture large scale synoptic processes which dominate the seasonal variations. The method must also perform in the short term at a high resolution to forecast wind fields dominated by small scale, short term features. Ultimately a range of products exist which can augment an observational wind resource assessment campaign but none are acceptable methods by which to do so in isolation. Supergen Wind 2 is undertaking research into the cost reduction and optimisation of wind resource assessment to see if an alternative method can be applied more successfully to support an observational resource assessment campaign initially and looking farther ahead potentially replacing the need for an observational campaign and dramatically reducing development costs.

1.4 High resolution numerical modelling

Numerical weather prediction (NWP) is the process of simulating atmospheric evolution by solving a number of governing equations representing atmospheric processes. The dawn of NWP transformed meteorology from an observational science into a predictive science. As computers have improved and models have been refined, the performance of NWP models has improved comprehensively. Figure 1.6 shows that a weeklong forecast now is as accurate as a 5-day forecast 15 years ago with a similar gain seen in the 5 day forecasts compared to the 3-day forecasts 15 years ago. Numerical modelling is very flexible in the range of outputs which can be produced from spatial fields to time series outputs and Hovmöller diagrams (time/latitude plots). NWP models can be run retrospectively to simulate for periods in the past and global NWP models can be run to forecast future conditions. NWP models exist in a range of guises which typically relates to the resolution at which they operate. Mesoscale models are NWP models which simulate at a resolution on the order of kilometres (Janjc et al, date unknown), in some cases down to a few hundred metres. Such flexibility allows the resolution of some small scale phenomena and local topographic features which are missed by coarser global models yet mesoscale models retain the ability to simulate the large scale

atmospheric features which drive the local circulations. Being able to perform at a high resolution is critical to the success of NWP in the field of wind resource assessment and is discussed in Chapter 2 with some practical examples. NWP models have to simulate extensive atmospheric variables to accurately represent reality which means they are available to output from the model at any point in the modelled domain. For example a spatial field of wind shear could be produced or a time series of stability for a range of locations.

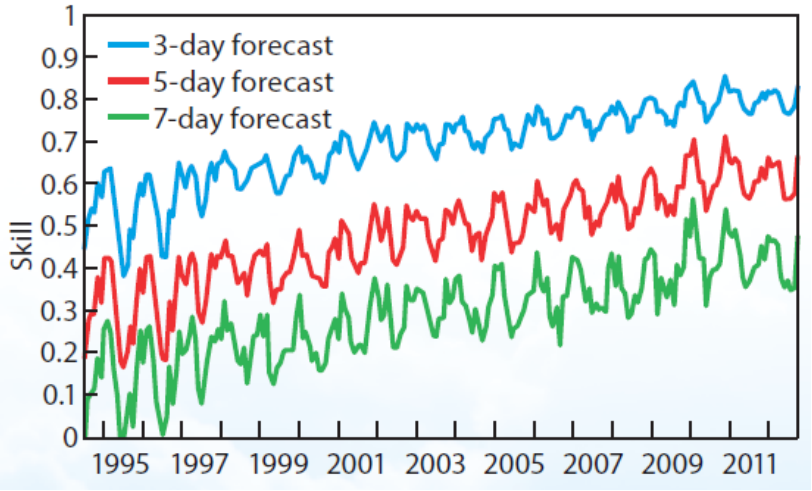

Figure 1.6 ECMWF ensemble forecasts for the 500 hPa geopotential height indicate that for the northern hemisphere extratropics there have been gains in predictability of between one and a half and two days per decade (e.g. the five-day forecast is now as skillful as the three-day forecast in the mid-1990s) (ECMWF 2012).

1.5 Application of a mesoscale NWP model to wind resource assessment

NWP models are relied upon daily by many industries across the world that base big decisions on model outputs, for example, energy trading. NWP models are capable of operating at a high resolution for any location on the globe. They are able to produce output at any vertical level for a wide range of variables that match and exceed what can be observed in situ. NWP models can be run on a range of computing systems depending on what is available to the end user. Accessing such technology is becoming easier with increasingly powerful computers and readily available models, while input data can also be obtained with ease from a range of sources. What remains is validation of mesoscale NWP models as operational wind resource assessment tools, which requires comparison against observational data.

Acquiring offshore met mast data is very difficult, firstly because it is very expensive to collect and thus not much data actually exists and secondly because typically the only possessors of such data are wind farm developers who are often reluctant to share it. There is a face value for such offshore data which combined with the desire of wind farm developers to restrict competitors from obtaining such data means very little is available to the research community.

There are two areas within mesoscale NWP of particular relevance to wind resource assessment which need to be addressed as part of the validation process. Performance at high resolution, required for producing accurate simulations for a single point, is reliant on the accurate representation of small scale features which are approximated by parameterisation schemes within the model as functions of resolved variables. Such approximations are fundamental to the model process, providing input regarding sub-grid scale processes which feed back to the larger circulation. Many studies using the WRF mesoscale model review the performance of the PBL (planetary boundary layer) parameterisation schemes find that no single scheme performs best outright. Instead different schemes tend to favour particular conditions (eg Draxl et al, 2012), which has led to uncertainty in model performance when representing sub-grid processes. The second area for investigation concerns the provision of accurate atmospheric conditions to the model, both initially over the entire domain from which to begin the simulation and as boundary conditions to provide tendency terms over the duration of the run. Uncertainty in initial and boundary conditions is present through all forms of NWP. The more accurate the input data is the better chance the model has of correctly simulating the atmospheric evolution, where any inaccuracies lead to a divergence in solutions between what is simulated and observed. Challenges exist within mesoscale NWP modelling which require investigation but there is significant potential to employ such technology as a wind resource assessment tool. One of the strengths of NWP models is their adaptability to different applications as a function of model setup. Extensive setup options, from physics to dynamics and domain setup, can improve model performance and a number of techniques also exist for the same purpose, a number of which are summarised next.

1.6 Optimising model performance

Traditional weather models have been applied to many different situations but remain dedicated weather forecasting models. There are many components to a weather model which can be tuned to optimise performance for particular application, in this instance offshore wind resource assessment.

1.6.1 Model setup

A diverse range of setup options exist for the user to tailor the model run, aspects such as domain setup, physics modules or dynamical options can be modified or selected where appropriate. Domain selection plays an important role in determining the level of accuracy to which the NWP is able to simulate atmospheric features, the domain must be large enough to allow the model to resolve the synoptic scale drivers (e.g. pressure systems), yet also exist at a resolution which accounts for local features such as topography or land/water interfaces etc. Dynamical options such as vertical damping or time integration options are available to adjust some of the model runtime properties which may help optimise the numerical stability or efficiency of the run. For example in mountainous terrain engaging vertical damping can help maintain numerical stability which could be breached by the associated large vertical gradients. Physics options which serve to account for particular processes can be changed, often by using different modules such as parameterisation schemes, to modify performance for given conditions If a particular set of conditions is known to prevail at a location then the most appropriate scheme could be selected to optimise performance for that location.

1.6.2 Ensembles/uncertainty

In meteorology an ensemble is a collection of model runs, or ensemble members, which simulate the same concurrent period. Each ensemble member is different by virtue of some form of perturbation, for example a different set of initial conditions, modified physics equations or an offset initialisation time. Viewed as a whole, the ensemble is a collection of individual time series which vary through time, an example of which is shown in Figure 1.7. Ensembles are generated to account for uncertainty in the modelling process. Already mentioned was the uncertainty regarding performance at sub-grid scales, which for the purposes of offshore wind resource assessment specifically relates to the PBL scheme. Also mentioned was

the fact that there are numerous methods in existence which account for processes in the PBL, selection of which appears dependent on the prevailing conditions and location. Such a scenario provides the ideal opportunity to employ an ensemble system which can account for a variety of conditions by employing different PBL schemes simultaneously. A similar approach can be used to employ an ensemble to reduce uncertainty in the provision of initial conditions to the model. Specific variables could be modified to generate the members, or different input sources used, or runs could be initialised at different times.

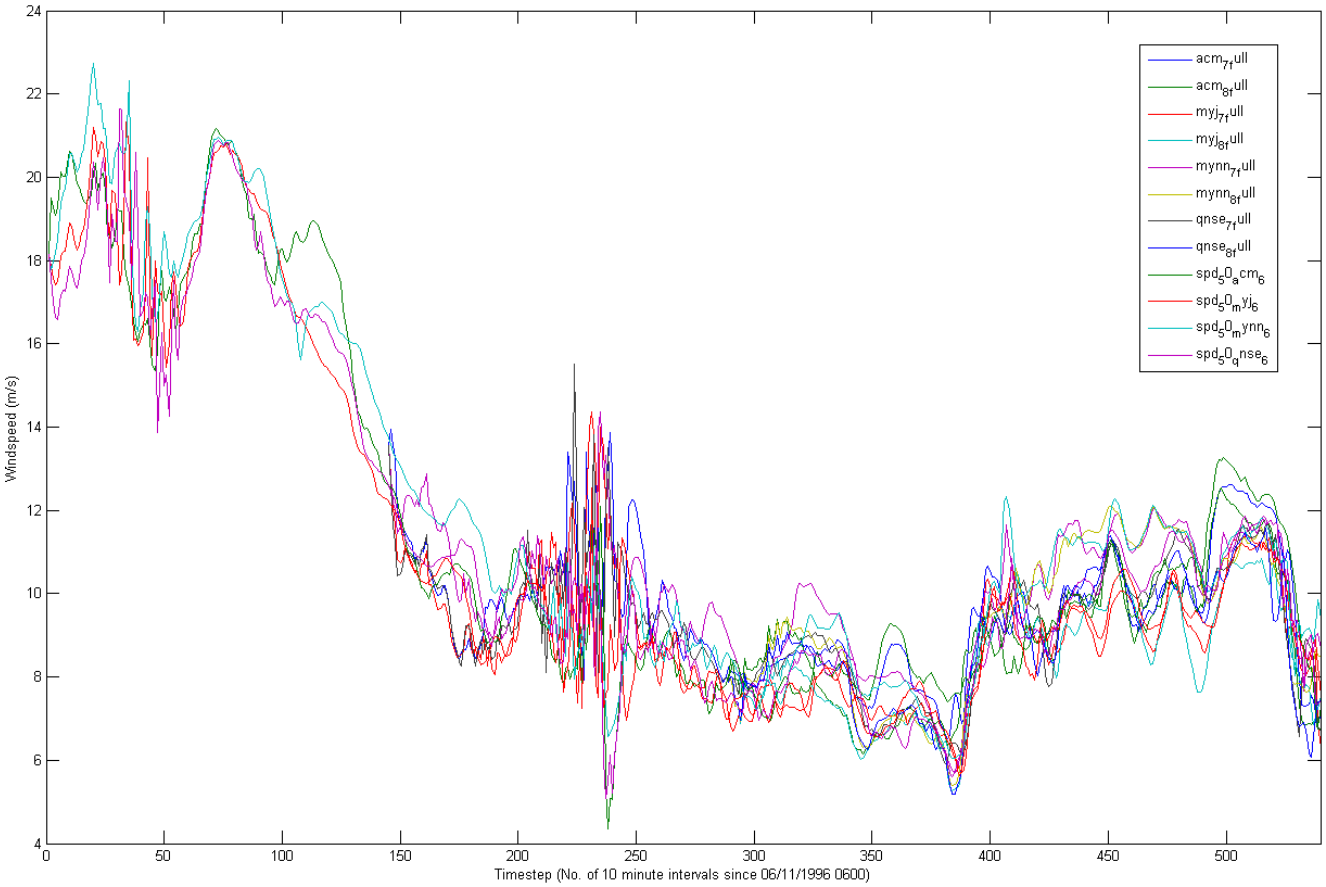

Figure 1.7 Ensemble members for a run beginning on the 6th of November 1996.

1.6.3 Nudging

Nudging is a modelling technique whereby observational data is incorporated into the model run through an assimilation process which provides a reference for the model solution to tend towards over the course of the simulation. Observational data for nudging can be point data from one or many locations or gridded data for the whole domain. Where nudging data is present in the modelled domain a relaxation zone exists around the nudged point with the influence of the nudging

value decreasing with distance. Nudging is a valuable technique to NW as the incorporation of even a single series might help the model maintain an accurate impression of the correct atmospheric features. In reality, there might be observational series available to those undertaking a wind resource assessment, both retrospectively for a site assessment and predicatively for those providing operational forecasts so it is important to validate the use of nudging as an optimisation technique.

1.6.4 Summary

The offshore wind farming industry has the potential to provide a considerable amount of the UK's electricity requirement, which would help the country achieve its renewable energy generation targets, reduce carbon emissions and reduce energy dependency on external sources. Currently the process of offshore wind farming is very expensive, prohibitively so in some cases, and thus only available to a handful of organisations. Even well-funded organisations require external investment which, combined with the significant engineering feat associated with developing and operating a wind farm, translates to a slow growth in the industry. In order to accelerate the development process of offshore wind farms, costs must be reduced. Several avenues are being investigated in Supergen Wind 2, including the field of offshore wind resource assessment. To comply with the IEC wind turbine certification standard 61400-12-1, wind resource assessments, upon which turbines are designed to, must be undertaken using calibrated anemometry. Offshore, the cost of a meteorological mast is in the region of millions of pounds. This research intends to identify the potential of NWP as a wind resource assessment tool, which in the future might be accepted independently within certification standards or as an augmentation to physical instrumentation, to reduce the cost in the planning phase of a wind farm. Performance of NWP as a wind resource assessment tool also extends to the operational phase of a wind farm where detailed knowledge of the impending short-term wind conditions for a site will help optimise operation, increasing productivity and profit. Ultimately there are questions regarding specific aspects of mesoscale NWP which need investigating as part of the validation process, but there is significant potential for the application of mesoscale NWP models to the field of offshore wind resource assessment.

1.7 Aims and objectives

1.7.1 Primary aim

Scientific research ultimately exists to answer questions. Central to this research is the question “How well can a mesoscale NWP model perform as a wind resource assessment tool?”. Primarily, this research aims to test the hypothesis that a mesoscale NWP model can be applied successfully as a wind resource assessment tool. More specifically, the NWP model will be subjected to validation against 2 UK offshore observational series, considering the implications for both long and short term assessments. Model setup will then be optimised for performance as a wind resource assessment tool based upon results of the initial validation work. Performance will be reviewed in absolute terms against the observational series but also in the context of other resource assessment techniques. Success of the project will be determined by the contribution of knowledge to the field of NWP in offshore wind resource assessment. Ultimately the goal is inform whether NWP models can perform suitably as resource assessment tools, after which the model would be introduced and applied industrially by developers, reducing costs and achieving the aim of the Supergen Wind consortium. Details of the contributory objectives which will need to be fulfilled in order to achieve the project aim are discussed below.

1.7.2 Contributory Objectives

The objectives of this research are listed and then discussed in further detail below;

1. To select and implement an appropriate NWP model
2. To develop a methodology by which to quantitatively assess model performance.
3. To run the model and simulate the wind resource along with associated variables at sites where observed data is available for comparison
4. To consider model performance as a function of computing resource and identify related operational limits of model performance
5. To innovatively optimise model setup for offshore wind resource assessment
6. To consider the practicality of the modelling approach used

1.7.2.1 To select and implement an appropriate NWP model

Selection of an NWP model will depend on its ability to fulfil the main requirements of this study. In order to be of use to parties interested in undertaking a wind resource assessment, the model should be readily available and accessible on a range of computing systems. Undertaking a wind resource assessment requires the model to capture synoptic features which drive the local circulation, as well as simulate at a high resolution to account for local features and produce an output from which a time series for a site of interest can be extracted. Thus the chosen model should be academically proven as a valid high resolution atmospheric model and ideally be used operationally to confirm confidence in its performance by national weather centres. A description and review of the chosen model will form a key part of the literature review for this project. Acquisition and implementation of the model will be discussed in the methods section alongside details of the modelling process including data preparation and post processing.

1.7.2.2 To develop a methodology by which to quantitatively assess model performance.

Once a model is selected and observational data is available for validation, a domain setup must be designed to produce an output of desired variable for comparison against observations. Domain setup relates to the area which will be simulated by the model and the resolution of the grid upon which the simulation will be performed. Selecting a domain setup is a compromise between running the model at the highest resolution possible but within practical time and resource constraints. The aim being to maximise the available computing power but doing so without making model runs last too long and take up too much disk space. Domain setups vary due to the constraints provided by the different computing systems and the application. Setup is described for each computing system in the relevant methods section for each investigation. Once the model has been run and output produced, quantitative statistics are required to validate model performance. There will usually be an element of qualitative assessment in any analysis, which often adds vital information, but to be comparable to other studies and provide a universal metric by which useful results can be disseminated to interested parties,

quantification is necessary. The techniques used to assess model performance are discussed in the methods section.

1.7.2.3 To run the model and simulate the wind resource along with associated variables at sites where observed data is available for comparison

Mentioned earlier were the two critical temporal periods over which wind resource assessments are undertaken. Short term forecast windows are of interest in the operational phase of a wind farm and long term studies of climatic variability is most important in the planning phase. Because the use of a mesoscale NWP model is feasible for both applications, it is important to assess model performance at the two timescales. As such the investigation will be conducted at a temporal resolution which is representative of the assessment requiring the shortest timestep, data from which can then be analysed directly at the higher temporal resolution and modified to investigate performance for the lower temporal resolution. One continuous yearlong resource assessment will be undertaken, comprised of shorter runs of 4 days at 10 minute resolution to look at performance through the seasonal cycle. Additionally 2 sets of several 90 hour runs equating to over 100 days each will be undertaken to focus on the performance of the model in isolated windows at a temporal scale equivalent to that at which the mesoscale model should have most success. The grouped runs are intended for benchmarking and optimisation exercises which can be considered as individual case studies. Focus of the research will be oriented towards comparison of observed and modelled wind speed as the variable which ultimately determines wind farm output. Wind direction is of great importance in farm design, determining factors such as the orientation of turbine rows. Furthermore wind direction offers another variable by which to evaluate model performance. While producing a wind resource assessment foremostly requires the production of wind speed and direction for a site, it might also include variables which contribute to the efficiency of wind turbines. Since the Supergen Wind 2 project is concerned with offshore wind, turbine installations are likely to be of a significant size to maximise space and resource. In large turbine arrays, wake losses can account for a significant amount of power deficit (Hansen et al, 2012). Turbine wake persistence is known to be dependent upon atmospheric stability, thus an impression of stability conditions are of great value to a potential operator. Stability can be estimated from

calculations of temperature and windspeed at two heights; the inclusion of humidity would add value as virtual potential temperature could be calculated giving more information on atmospheric energy. Since stability can thus be approximated from observations, it will also be approximated from model output of the same variables.

1.7.2.4 To consider model performance as a function of computing resource and identify related operational limits of model performance

Being able to run the selected numerical model on a range of computers is important so that the technology is available as widely as possible. High availability affords the best chance of getting the technology noticed and accepted by those in the industry, the feedback from which might in turn help develop the model. While it is of benefit to be able to run the model on different machines it is important to understand how the specifications and thus capability of the computer might affect the model run, for example through enforced setup choices. The model will be run on a number of computing facilities to test the dependence of performance of available computing resource and identify any associated operational boundaries. Considering the computing resource is an important practical consideration for potential end users of the technology who will not all have the same computing resources available and need to know what performance they can expect and should account for. Operational limits of the model will be considered given a particular computing resource, for example the maximum spatial resolution may be dependent upon the computing resource which will limit the size of the spatial features the model is able to resolve. Such a consideration is of utmost importance when considering a resource assessment setup for a particular application. For example if resolution is low, the model may only be able to resolve large features, which might give an indication of wind speed trend but won't be able to capture smaller features.

1.7.2.5 To innovatively optimise model setup for offshore wind resource assessment

Benchmarking model performance is important to gain an understanding of baseline performance, however, mesoscale models are primarily weather forecasting tools, not specifically set up as wind resource assessment tools. From the benchmarking exercise, methods will be developed with the intention of improving

model performance by optimising setup for wind resource assessment. Consideration will be placed not only on improving the skill of the model output to more accurately represent the observed variables, but also understanding model performance and accounting for it. For example, the dynamic nature of the atmosphere means that there will be times when the model performs well and times when it performs poorly, if some method can be adopted which is able to identify periods when model performance is likely to be better or worse, the end user has more information about how to use the output. Practicality is a key consideration in this research, given that deterministic models are some way off a perfect forecast, the goal is about providing as much information as possible to the end user to help inform their decision. Optimisation will consider the dynamical, physical and domain setups of the model process. Techniques will include observational nudging, the generation of ensembles and the comparison of boundary layer schemes. All the techniques will be investigated in the literature review and applied to the modelling process with the results presented in a separate section detailing the difference in performance due to the optimisation techniques.

1.7.2.6 To consider the practicality of the modelling approach used

The priority of the research is to design and execute an investigation which will determine the application of an NWP model to wind resource assessment. However, for the findings to be of practical use to the industry, the following question must also be considered a priority: “How accessible is this technology?”. One stream of research is concerned with the model performance on various computing facilities and this is one example of the dedication to fully answer the research question. Throughout the research, consideration will be made of the process and a key part of the discussion will focus on the practical implications associated with actually applying this technology operationally.

1.8 Investigation structure

In order to address all of the objectives, three studies will be undertaken. Once the outcomes of each research thread have been established and discussed, the work will be brought together in the final discussion chapter where the overall performance of the NWP model as a resource assessment tool will be discussed. The final discussion chapter will focus on the feasibility of the application of NWP to

wind resource assessment. Model performance will be a key factor but so will the process of undertaking the analysis, it is of key interest to the industry to know not only how good the technology is but how accessible it is. The three studies are presented below.

1.8.1 Performance benchmarking at Scroby Sands

Firstly a benchmarking exercise will be performed at the Scroby Sands site to gain an initial impression of model performance over the course of a year. Wind speed will be the focus of the benchmarking investigation because it is solely the most important variable in a wind resource assessment and thus the variable to which model setup will be optimised. Wind speed will be simulated by the model without any observational nudging on two computing systems. Model setup will be selected appropriately for the corresponding computing resource. Aggregated statistics will give a description of the general state of model performance while analysis of the individual runs will highlight more specific traits of model performance which might relate to dependencies and areas for optimisation. Undertaking the runs on two computing systems, with setup optimised for the different systems used, will address the question of model performance and limitations arising from and related to, the available computing resource. Runs comprising this section of the investigation will be undertaken over short periods from 1-4 days at 10 minute temporal resolution which will provide information of model performance at short and longer temporal resolutions. Investigating both temporal resolutions is important to address the suitability of mesoscale model performance as a resource assessment tool both operationally and in the planning phase when the requirements are slightly different. Furthermore, series will be temporally filtered to investigate the performance of the model through different temporal scales, from high resolution at which small scale features are parameterised to longer lower resolution where atmospheric features are directly resolved by the model.

1.8.2 Long-term resource assessment

Long-term performance of the chosen NWP model will be tested by conducting a resource assessment for the second mast at Shell Flats for a period of a year and a half. For the long term resource assessment investigation, wind direction and temperature will be included as further means by which to compare model performance to observations. While wind speed remains the priority, wind direction is

a variable of importance in a wind resource assessment for planning farm layout, and turbine optimisation. Temperature allows the calculation of a stability parameter which is of operational use in calculating farm output as it pertains to the persistence of turbine wakes. Model input will be augmented by the integration of observational data at hourly intervals obtained from Mast 1 at Shell Flats as an investigation into improving performance in the short term. Two months will be simulated without nudging in addition to the resource assessment to provide an insight into the impact of the technique. As a deliverable to the Supergen wind projects an exemplar wind farm was developed at Loughborough University as a forum upon which various streams of research could be applied. The fictional Supergen Exemplar farm was located near to the Dogger Bank round three tender site shown in Figure 1.8. In total 256 turbines comprise the farm in a diamond array shown in Figure 1.9, the turbines are the Supergen Exemplar 5MW turbines giving the farm a nameplate capacity of 1.28GW.

Figure 1.8 Location of the Supergen Exemplar wind farm Google, 2013.

A year long resource assessment will be produced for the centrepoint of the Supergen Exemplar site. The full assessment will be performed for the central point of the farm with a further 3 months run for the four extreme points at the edge of the

farm to gain an impression of the variability across the farm. Wind speed, wind direction and temperature at multiple heights will be produced to detail the resource as well as the stability. One key aspect to communicate is an evaluation of the methodology by which the model could be used. The continuous resource assessment will be produced through the concatenation of shorter runs both for the Shell Flats and exemplar resource assessments.

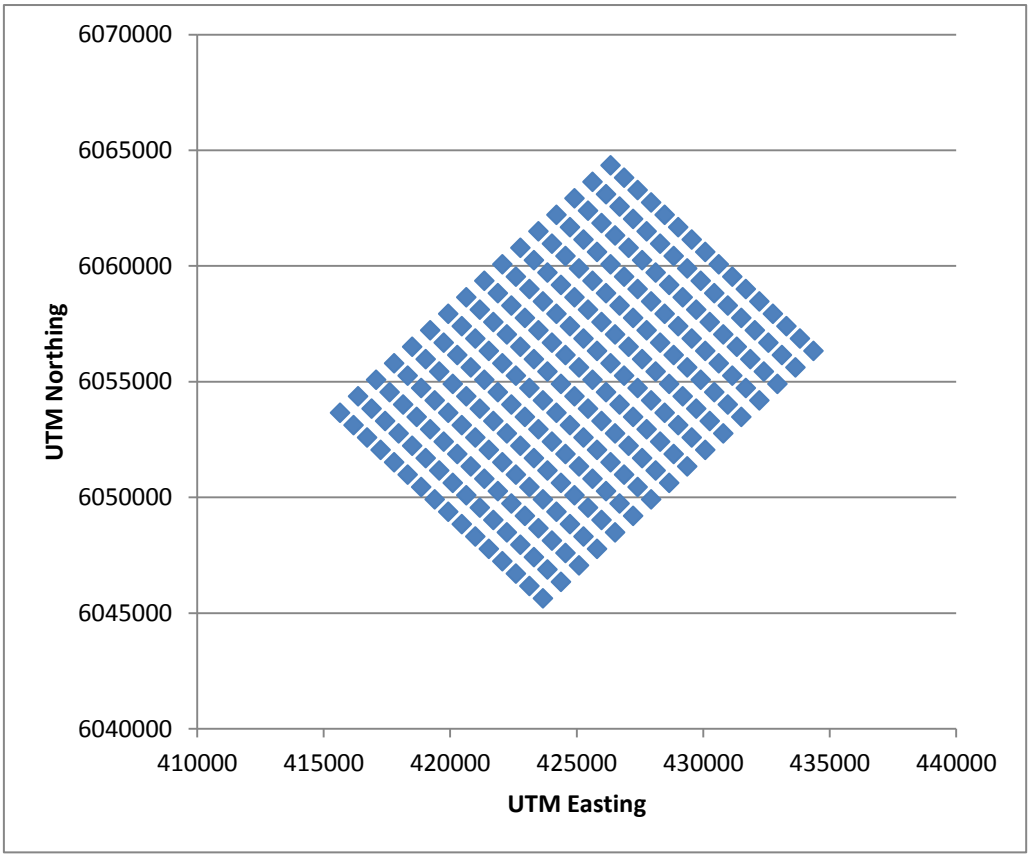

Figure 1.9 Initial layout of the turbines in the Supergen Exemplar wind farm (Watson, 2012)

1.8.3 Optimisation of model performance

To address the remaining objectives, the last investigation is composed of a number of optimisation techniques aimed at improving model performance as well as accounting for model dependencies throughout the runs. At the time of conception, the optimisation techniques used in this work were novel for the field of wind resource assessment. Since the work has been undertaken, a couple of studies (eg Deppe et al, 2013; Draxl et al, 2012) have employed similar techniques using an ensemble, to investigate the performance of the WRF model as a resource assessment tool. It is encouraging that others had similar ideas for the development of the model into an operational resource assessment tool. Due to the timing, while

simply applying the technique is no longer an exclusive property of this work, the location and setup used in this work is. Observational nudging will be employed to use the local skill of a nearby mast assuming wind conditions to be broadly similar over the given distance. An ensemble will be developed to account for two prominent sources of error in NWP simulation of relatively high resolution wind fields, namely the performance of the model in the boundary layer and uncertainty in the accuracy of the initial conditions. Two ensembles will initially be created before being combined to produce one ensemble mean and spread. One will use different boundary layer schemes available to investigate performance in the boundary layer of each scheme but also attempt to account for deficiencies within each yet combining several. Uncertainty in initial conditions will be addressed by employing a time offset ensemble system (TOES). The same as a lagged ensemble, TOES is comprised of members physically similar only initialised at different times and combined over the period for which they are concurrent. The benefit of a lagged ensemble is that initial conditions are represented more than once, but also that by combining runs, the model has information from after the initialisation to help steer it more towards observations, while retaining the large scale skill.

1.9 Thesis structure

Chapter 2 provides a review of literature concerned with the application of an NWP model to the field of offshore wind resource assessment. The theory of NWP is discussed in chapter 3. Chapter 4 presents the methods by which the application of an NWP model as a wind resource assessment tool is investigated. Chapter 5 is a presentation of the results from the benchmarking investigation undertaken to address objectives 2 & 3. Chapter 6 provides results from the production of a wind resource assessment which addresses objective 3. Chapter 7 contains results of the investigation into optimisation of the model setup for wind resource assessment (objective 5). Results from the three research themes are then discussed in Chapter 8 which addresses objectives 4 & 6 discusses the results in the context of wind resource assessment to address the overriding aim. Conclusions are drawn in chapter 9 and suggestions for future work are detailed in chapter 10.

2 Literature review

2.1 Introduction

This review of literature will begin with an overview of the process of wind resource assessment, describing a number of methods which can be and are used. Inadequacies of observational campaigns were identified in the introductory chapter and provide the impetus for this research, a review of potential NWP (Numerical Weather Prediction) based solutions are presented, with the focus on mesoscale models. A selection of research articles, relating to the performance of WRF in a wind resource assessment context is presented.

2.2 Wind resource assessment

Traditionally, meteorology was an observational science where phenomena were recorded through some physical manifestation, for example wind direction was measured by reference to the orientation of a wind vane. The move to simulation and prediction of the weather revolutionised meteorology and is now a fundamental part of everyday life. However, traditional methods are still an integral part of modern meteorology, particularly regarding offshore wind resource assessment. Mentioned in the introduction was the fact that wind resource assessments, used to specify design requirements for wind turbines, must be undertaken using cup anemometers (IEC, 2005). The reasons are simple and relate to the well-tested and trusted record of the cup anemometer which can be easily validated and calibrated on a site specific basis. In the UK, weather stations in some form have been around for approximately a hundred years, with their growth most rapidly increasing in the last 50 years or so. Observational coverage is relatively dense compared with most countries, however for wind farm developers, not extensive enough. The overwhelming majority of meteorological stations are land-based, though some exist near the coast. Ultimately, a wind farm developer has to install a meteorological mast themselves to meet the criteria of IEC standard 61400-12-1, but as much information about the site of interest is beneficial. One technique which has been employed to extend the scope of a wind resource assessment, particularly for sites which are closer to the coast, is MCP (measure correlate predict). MCP involves the correlation of two series over an overlapping period to then infer the behaviour of one based on the variation of the other for an unobserved period. For example a wind farm

developer would install a meteorological mast at a site of interest and collect a year's worth of data, however, they ideally would like a longer time series to establish the context of that year more generally. Then, if a nearby meteorological station existed with a longer recording history, the two series could be correlated. Conditions at the offshore site for the duration of the onshore series could be predicted from the onshore site using the information from the correlation analysis. Another option which exists for wind farm developers to gain a better understanding of conditions at a site of interest, is the use of satellite-derived data such as SAR (Synthetic Aperture Radar). SAR employs an active microwave sensor which images the amount of backscattered signal for a unit area (Badger et al 2010). Typically, the SAR sensors track the relative motion of surface roughness elements over the sea, generated by surface wind stress (Badger et al 2010). Postprocessing the results provides a 10m wind speed at resolutions up to 1km x 1km (e.g. Horstmann et al, 2004). Results from SAR can be very impressive, for example Hasager et al (2011) obtained a correlation coefficient, between a range of observation stations and their SAR output, of 0.78 alongside an RMSE of 1.17ms^{-1}. However, a number of limitations exist with SAR data alone, for example the post-processing relies on the assumption of a logarithmic wind speed profile. SAR is also affected by the presence of objects in the scan region, for example features like algal blooms can affect the signal backscatter, producing a false wind speed reading when processed. Finally, satellite-derived observations are constrained temporally by the periodicity of the satellite's pass over a site of interest and can only infer values for wind speed, so ultimate output could be considered constrained by comparison to other techniques. However, products exist which contain satellite data as well as observational data from multiple other sources which is all homogenised onto a standard grid. These are known as reanalysis products. Reanalysis products are not typically used independently in wind resource assessments because the resolution at which variables are available, both temporally and spatially, is too coarse for the requirements of developers. However, they are a useful source of data from which dynamical downscaling and NWP tools can be run. Two reanalysis products are discussed in the theory chapter, providing more information regarding the general background of reanalysis data and individual properties of the two products used in this research.

2.3 The potential of mesoscale NWP in wind resource assessment

Identification of NWP as a viable option by which offshore wind resource assessments could be undertaken, arises from the potential of the technology alongside strengths which address inadequacies in alternative methods. Mesoscale NWP models offer the ability to dynamically simulate variables at relatively high resolution compared to reanalysis products while also capturing the large scale synoptic processes which drive the local circulation. The mesoscale relates to a specific spatial domain, ranging from metres to thousands of kilometres (Janjic et al., date unknown). Alternative methods do exist but many come with drawbacks. For example, direct observations offshore are very expensive as well as being temporally and spatially restricted (e.g. Hasager et al, 2008). Statistical methods of approximating meteorological variables can offer some potential to wind resource assessment, particularly in the very short term, where persistence forecasting outperforms most dynamical models out to around three hours. However, statistical methods mostly employ linear assumptions which are inappropriate for atmospheric science because the atmosphere is a nonlinear system. Reanalysis products demonstrate flexibility as potential offshore wind resource assessment tools, by providing global coverage for extensive time periods. However, a number of questions remain about the validity of their use. A reanalysis product is essentially a low resolution global model run, albeit comprehensively nudged using observations. For a wind resource assessment, developers want output at a relatively high resolution compared to that available in reanalysis products, as local effects (Garcia-Diez et al, 2012) on the wind flow are important to consider in terms of turbine/farm performance. Mesoscale models are intended to operate at grid resolutions on the order of kilometres, allowing the resolution of local and regional circulations (Santos-Alamillos et al 2013). The temporal and spatial availability of reanalysis data is well suited to historic resource assessment campaigns and when used to initialise a mesoscale NWP model, would produce a high resolution output of a suite of variables which could be used to produce a wind resource assessment for any global location. The ability of mesoscale models to dynamically downscale input also means that global forecast data could be used to initialise such a model in order to predict impending wind fields at higher resolution for shorter timescales, for example in operational forecasting. Such abilities give mesoscale NWP certain advantages over other resource assessment techniques.

2.4 WRF

2.4.1 Selection

The NWP model to be used in this research is the WRF (Weather Research and Forecasting) model (Skamarock et al, 2008; Janjic, 2003). WRF was selected for a number of reasons. Firstly, it is a highly flexible model with extensive tunable parameters available to an end user. Secondly it is readily available from the developers (NCEP/NCAR/UCAR/NOAA) and very well-maintained, along with a range of essential and utility programs. Thirdly, WRF is very widely utilised in the research field, applied to a full spectrum of atmospheric investigations which includes high resolution simulations (for example Litta and Mohanty 2008), which are relevant in the application to wind resource assessment. Finally, a number of US governmental organisations are satisfied with the level performance of WRF such that it is used in a number of operational forecasting systems including the hurricane forecasting system, HWRF.

2.4.2 Applicability of WRF to offshore wind resource assessment

A selection of studies which utilise WRF is presented to justify the models application to the field of wind resource assessment. An end-user must be confident that WRF is able to perform well at high resolution simulations and add value to the input data. Tastula et al (2012) undertook an investigation into the performance of WRF as compared against the ERA-Interim reanalysis product which was also used as initialisation and boundary data for the model run. They studied the performance of the model in the boundary layer which is of particular relevance to this study. Findings showed the model to offer a higher level of performance than the ERA-interim reanalysis product for the vast majority of variables studied apart from surface pressure. However this was attributed to the provision of buoy data which was incorporated into the ERA-Interim product but not the WRF model run. The US army are investigating the operational use of WRF, at very high resolution for a mesoscale model, at 0.3-3km for the purposes of very short term forecasting and nowcasting applications (Dumais et al, 2009). For some locations, the use of WRF to create a wind resource assessment product has already been undertaken, with Peña et al (2011) producing a wind atlas for the South Baltic region. Such an application was essential because of the complete lack of observational data to the south of the region, while output was validated at locations in the domain where observational

series were available from Danish and German masts. WRF has the potential to perform well as a wind resource assessment tool and has already been applied in the production of a wind atlas, which makes the next step validating performance for use as a site assessment tool, both in a historical long-term context and short-term operational context. Zhao et al (2012) review a system which is operational in China whereby GFS forecast data is downscaled by WRF and passed through a Kalman filter for the purpose of day ahead forecasting. They found the system to perform with an acceptable level of error (16.47% normalised RMSE) and that it was a profitable undertaking which increased wind energy penetration in China.

Some traits of the model itself and setup options have been identified which should be considered when undertaking such a study. The limit to the potential performance of the model is somewhat constrained by computing resource. In order to optimise a model run, outright resolution is often compromised to achieve a quicker model runtime and reduced computational requirements. In theory, the higher the simulated resolution, the better model performance would be as more processes are able to be directly resolved. However, Gibbs et al (2011) found that increasing resolution around the 4km range yielded diminishing returns with respect to the subsequent extra requirement in computing resource and instead suggested utilising larger spatial domains and vertical resolution to try and improve resolution of the larger scale features. Operationally, WRF has been shown to possess a high surface wind speed bias (for example Mass and Ovens 2011; Jiminez and Dudhia 2012), Knowledge of such a bias is beneficial, because it can be accounted for. Such a bias, however, might cause problems in model simulations which involve a coastal interface.

2.4.3 Stability

The potential for using WRF as a tool to simulate stability has not been examined significantly to date. The successful application would be of great interest to developers. The majority of studies have only really considered the performance of WRF as a wind speed prediction tool. Some studies have examined the performance of WRF under different stability conditions. For example Munoz-Esparza et al (2011) look at the performance, as predictors of wind speed, of a range of PBL schemes at FINO 1 under different stability classes, but there is much scope to expand the research into the representation of stability by WRF. For example

Munoz-Esparza et al, (2012) look at the performance of a number of PBL schemes within WRF as predictors of Obukhov length compared to observations at FINO 1. They found that, generally, the schemes provide a good representation of the stability class but impart a slight bias, where the magnitude of stable conditions tended to be under-predicted while the magnitude of unstable and neutral conditions tended to be enhanced compared to observations. Calculation of stability is subject to input from the model parameterisation schemes, which means at short timescales and high resolution, just like the wind variables, there is less confidence in the accuracy of the model output. If the model can be shown to provide a decent representation of atmospheric stability, it would be of great benefit to wind farm developers in refining potential farm output forecasts.

2.5 PBL parameterisation

2.5.1 Introduction

Numerous parameterisation schemes are required to run a numerical model, for example convection/ cumulus schemes, land surface models (LSM) and planetary boundary layer (PBL) schemes. In the context of wind resource assessment research, the parameterisation scheme of most interest is the PBL scheme because it solves for the region in which turbines operate and is thus an integral contributor to model performance. PBL schemes are described by the order of the equations they solve and the locality of the data points which they use. The theory behind PBL parameterisation is discussed in the subsequent theory chapter which covers properties of schemes such as order, level and locality.

2.5.2 Review of individual schemes

Two PBL schemes are most commonly used with WRF: the local Mellor-Yamada-Janjic (herein MYJ) level 2.5 scheme (Mellor and Yamada, 1982; Janjic, 2001), and the Yonsei University (herein YSU) non-local first order closure scheme. Three further PBL schemes available with WRF are discussed in further detail: the MYNN (Mellor Yamada Nakanishi Niino) 2.5, the QNSE (Quasi Normal Scale Elimination) and the ACM2 (Asymetric Convective Model) , alongside the aforementioned MYJ and YSU schemes.

2.5.2.1 First order closure schemes

2.5.2.1.1 YSU

In the nonlocal YSU (Hong et al., 2006) scheme, TKE (Turbulent kinetic energy) is explicitly resolved rather than approximated (Misenis and Zhang, 2010). Turbulent fluxes due to non-local gradients are represented by counter gradient terms, which under stable conditions are generally small and thus neglected (Holtslag and Boville, 1993). The entrainment layer at the top of the boundary layer is explicitly treated (Challa et al. 2009).

2.5.2.1.2 ACM2

The nonlocal ACM2 (Pleim, 2007) PBL scheme closes the same turbulence equations as the YSU scheme but approaches mixing through the boundary layer in a different way. Local diffusion is combined with non-local mixing under convective conditions, where the non-local mixing is explicitly simulated. Such a combination allows mass and momentum transport through the depth of the PBL between remote layers as well as local transport between adjacent layers. Under neutral and stable conditions the ACM2 scheme is able to switch off the non-local transport component to only account for local diffusion (Pleim, 2007).

2.5.2.2 1.5 order closure schemes

2.5.2.2.1 MYJ level 2.5

A development of the Mellor Yamaha (1982) model by Janjic (2001), the MYJ level 2.5 is a 1.5 order closure scheme. A prognostic equation is included for calculating TKE (Turbulent Kinetic Energy), however, the remaining 2nd order terms, such as the velocity-temperature covariance, remain simplified by equations (Suselj and Sood, 2010). Vertical turbulent mixing is represented by eddy diffusivity which is a function of TKE, a master length scale and a term dependent on TKE, buoyancy, and shear (Hanna et al., 2010). The master length mixing scale in the MYJ 2.5 is a function of height and is used in the vertical redistribution term and the dissipation term (Olson and Brown, 2009). MYJ 2.5 was intended for application to stability conditions from stable to slightly unstable (Mellor and Yamada, 1982), with performance deteriorating in increasingly unstable conditions.

2.5.2.2.2 MYNN level 2.5

The MYNN level 2.5 (Nakanishi and Niino, 2004) PBL scheme is a local 1.5 order closure scheme based on the Mellor Yamaha model (Mellor and Yamaha 1982), like the MYJ scheme. As in the MYJ scheme, the additional prognostic equation is of TKE, however the crucial difference between MYJ and MYNN is the master length scale derivation which goes into calculating the local eddy diffusivity. The master mixing length for the MYNN PBL schemes is a function of three independent length scales concerning the surface layer length, the buoyancy length and the turbulent layer length (Olson and Brown 2009; Nakanishi and Niino 2009).

2.5.2.2.3 QNSE level 2.5

The QNSE (Sukoriansky et al. 2005) PBL scheme is a 1.5 order closure model which, like the MYJ and MYNN schemes, includes a prognostic term for calculating TKE. Unlike any of the other schemes, spectral theory is applied to simulate diffusivity, in particular, under stable conditions. Due to its tailoring to stable conditions, the QNSE scheme is not particularly widely used in general WRF studies.

2.5.3 Performance

Generally, the consensus from the literature is that no single PBL scheme is a readily identifiable single best performer. A selection of examples will follow which identify particular schemes to be favourable, but in the vast majority of cases, performance is dependent upon the occurrence of particular conditions (for example Draxl et al 2013; Munoz-Esparza et al, 2012).

2.5.3.1 Performance of individual schemes

Mentioned in the description of each scheme was the different calculation of mixing length in the MYJ and MYNN schemes, used in determining the PBL depth. Olsen and Brown (2009) compared the MYJ and MYNN level 2.5 schemes in a low-level jet study. They found that the MYNN scheme developed larger TKE and a deeper, more realistic, mixing depth than the MYJ scheme which generally under predicted depth. The MYNN scheme was found to produce accurate levels of TKE in general but, on occasion, to an unrealistic level. They also noted that while the MYNN scheme performed best by comparison to a number of variables, the MYJ scheme simulated wind speed most accurately. It is important to accurately represent the boundary layer depth so that contributory processes to turbulence within the layer can be accounted for and passed to the main model solver, for the

impact upon the general circulation to be established. The studies presented so far give an interesting insight into the variability of performance exhibited by the PBL schemes depending on conditions, however, most of the studies are conducted onshore. In a study which produced a wind atlas for the south Baltic, Peña et al (2011) found a clear difference between performances of the PBL schemes when used over sea compared to land, but as with the majority of other studies, found no particular scheme to be a preferable option. Draxl et al (2012) found that performance of the PBL schemes at the coastal site of Høvsøre was highly dependent upon stability. For unstable conditions, the YSU scheme was found to perform best. Under near stable and neutral conditions, the ACM2 scheme was found to be the best performer, while under stable conditions the MYJ scheme was preferable. A study by Santos-Alimillos et al (2013) reviewed the performance of WRF as a function of physical setup, which included looking at the performance of the YSU and MYNN PBL schemes at four sites over southern Spain with the focus on wind power prediction. They found the YSU scheme to outperform the MYNN scheme. In an offshore study using the FINO 1 mast data, Munoz-Esparza et al (2012) found the MYNN scheme to be the most versatile high performer through different stability classes. The studies presented cover a range of topics and locations describing some of the observed qualities and tendencies of the PBL schemes of interest. However, the main findings of most are the variability in performance of the schemes and a dependence upon prevailing conditions, both atmospheric and physical. Since conditions invariably differ between sites, extrapolation of results from any of the above mentioned studies to the locations of this research is unwise. The results from these studies is used as a guide and has helped select a methodology by which it is hoped results can generate greater knowledge to be contributed to the field.

2.6 Mesoscale modelling offshore wind

The application of WRF to topics related to wind resource assessment has been previously discussed in section (2.4) which reviewed the suitability of WRF for this research. A number of studies have investigated the application of WRF in a wind energy context (e.g. Shimada and Ohsawa, 2011; Storm et al, 2009; Chin et al, 2010). The lack of available offshore data for validation translates to a relative paucity of directly relevant studies which makes defining a level of performance

difficult. Peña et al (2011) produced a comprehensive wind resource assessment for the south Baltic as a commissioned wind atlas. A four-year period from January 2007 to December 2011 was simulated using a two domain WRF setup. The south Baltic Sea was the area for which the wind atlas was produced and model performance was validated by extracting point data from the model runs for the offshore FINO research platforms, Horns Rev II and the onshore coastal site at Høvsøre from which observational data were obtained. Model output was also compared to quikSCAT and SAR satellite data to validate model performance spatially. Performance as validated against the observational data showed an RMSE of around 2ms^{-1} and no state dependence relating to location, height level or number of samples. Good agreement was found between the 5km model output and the 25km quikSCAT wind field, while a greater discrepancy was found by comparison to the high resolution (1km) SAR data. Kwun et al (2009) looked at the surface wind representation of WRF offshore over three days. They found correlations between observed and modelled hourly wind speed to be 0.6304 and 0.6483 for the YSU and MYJ PBL schemes respectively. RMSE for the daily values was 1.1360 and 1.1680 ms^{-1} for the YSU and MYJ PBL schemes respectively. Shimada and Ohsawa (2011) looked at the performance of WRF as a wind resource assessment tool at an offshore site in Japan. A complex model setup, including FDDA (four dimensional data assimilation), was employed at ten minute resolution. They found the model to perform well at replicating observed wind speed variability displaying a correlation coefficient of 0.8, however an RMSE of 46% of the mean annual wind speed was calculated. RMSE as a percentage of the annual mean wind speed is a strange metric to use and is provided in the paper by reference to a plot which suggests a value of around 5-6ms^{-1} which would translate to an RMSE of around 2.75ms^{-1}. The three studies discussed above, provide the most relevant statistics for comparison to the work undertaken in this study which will use correlation and RMSE as measures by which to assess model performance. Table 2.1 summarises the performance achieved by each of the studies and also includes statistics from three other studies, conducted over land, to serve as a measure by which to judge the results achieved in this research. It is clear from the values that model performance is highly location dependent, with average correlations ranging from 0.48 to 0.94 and average RMSE from 1.1ms^{-1} to 2.8ms^{-1}. For the offshore environment, the average correlation coefficient is 0.72 and average RMSE is approximately 1.95ms^{-1}. It is important to consider the parameters of each

investigation upon review as these may also affect the performance figures obtained. For example, the high correlation achieved by Raubenheimer et al (2012) was obtained for a study undertaken at diurnal temporal resolution. Sampling every 12 hours would remove changes in wind speed below 12 hours, which is suited to the effective resolution of a mesoscale model. In contrast, the 10-minute temporal resolution of the Shimada and Ohsawa (2011) study would test the high resolution performance of WRF by including shorter changes in wind speed caused by smaller scale atmospheric features which are more difficult for the model to resolve related to the effective resolution of the model grid.

Table 2.1 Collection of statistics describing accuracy of WRF as a predictor of wind speed

Study	Notable setup options	Resolution	Correlation coefficient	RMSE
Shimada and Ohsawa	ARW, FDDA, MYJ, SST	10 minute	0.8	46% mean ~2.75ms^{-1}
Kwun et al 2009	ARW, MYJ	Correlation – hourly RMSE - daily	0.64	1.1 ms^{-1}
Pena et al, 2011	ARW	Hourly	-	2 ms^{-1}
Raubenheimer et al, 2012	ARW	Diurnal	0.94	>1 ms^{-1}
Nawri et al, 2012	ARW	Monthly	0.57	-
Liu et al, 2012	ARW	Hourly	0.483	2.8 ms^{-1}

2.7 Summary

This review of literature has sought to present the foundations for the research undertaken in the project and the current understanding. The application of mesoscale NWP models to offshore wind resource assessment is entirely justified based upon the successful operational use of such technology in other fields. For the adoption of such techniques by the industry, more studies must be undertaken to evaluate the broader potential of such models. Many examples of WRF as a wind resource tool have been sourced, but still the available literature does not exist on a

large enough scale and with enough consistency between the studies to justify confidence in the model for operational use. Far fewer studies using WRF as an offshore wind simulation tool exist because of data restrictions for comparison. Furthermore, very few studies at all exist which consider the model's performance in a more complete context as an offshore wind resource assessment tool by using it to predict a suite of variables, for example stability, of interest to wind farm developers. Thus the conclusions of this review of literature are that;

1. More studies need to be undertaken using consistent performance metrics (such as correlation and RMSE) by which to assess model performance in as diverse locations and temporal periods as possible.

2. More thorough investigations of the potential uses of NWP models as offshore wind resource assessment tools should be undertaken to more wholly establish the potential benefits to the industry. For example, NWP models are able to simulate a wide range of variables which could be used by developers.

3. The identification, or lack thereof, of an optimal setup (specifically PBL scheme) suggests an area of uncertainty which requires comprehensive investigation for industrial application. If one ideal setup does not exist, the definition of a range of setups given particular conditions should be provided or at least established. Such a set of conditions will most likely change depending on location.

3 Theory

3.1 Introduction

An introduction to numerical modelling is provided and the WRF modelling system is described. The components of the modelling system most relevant to offshore wind resource assessment are introduced and described. A number of techniques, which can be applied to NWP are presented with a view to incorporation into the main study as a means of improving/augmenting model performance, are then discussed.

3.2 Introduction to numerical modelling

Weather forecast models are a form of numerical weather prediction (NWP), which is a means of predicting future atmospheric development by solving a series of physically derived equations. Numerical models are an approximation of reality, limited by computational resources because the complexity of the atmosphere is simply too great to represent in its entirety. In the modelled system, the most important processes are fully resolved while other process which cannot be explicitly calculated due to computational restrictions, are approximated by parameterisations based on values of other variables, represented in Figure 3.10. NWP models exist in a variety of guises generally classified by physical and temporal constraints on the operational boundaries of the model. Mesoscale models are examples of limited area models where only part of the globe is simulated. Limited area models were designed to provide a more high resolution output than GCM's both temporally and spatially. This flexibility has particular appeal in resource assessment research because the model can incorporate large scale atmospheric features such as pressure systems and produce relatively high resolution output. Mesoscale models possess the full suite of physical equations as in GCM's but by running for a reduced spatial domain they are less computationally demanding.

3.2.1 Underlying Principles

There are a number of fundamental principles which underpin numerical weather prediction. The most important are the primitive equations which perform the calculations which simulate the atmosphere as required by the investigator. Other important concepts which are implicit in NWP, particularly for the WRF-NMM model, are atmospheric chaos and the hydrostatic assumption.

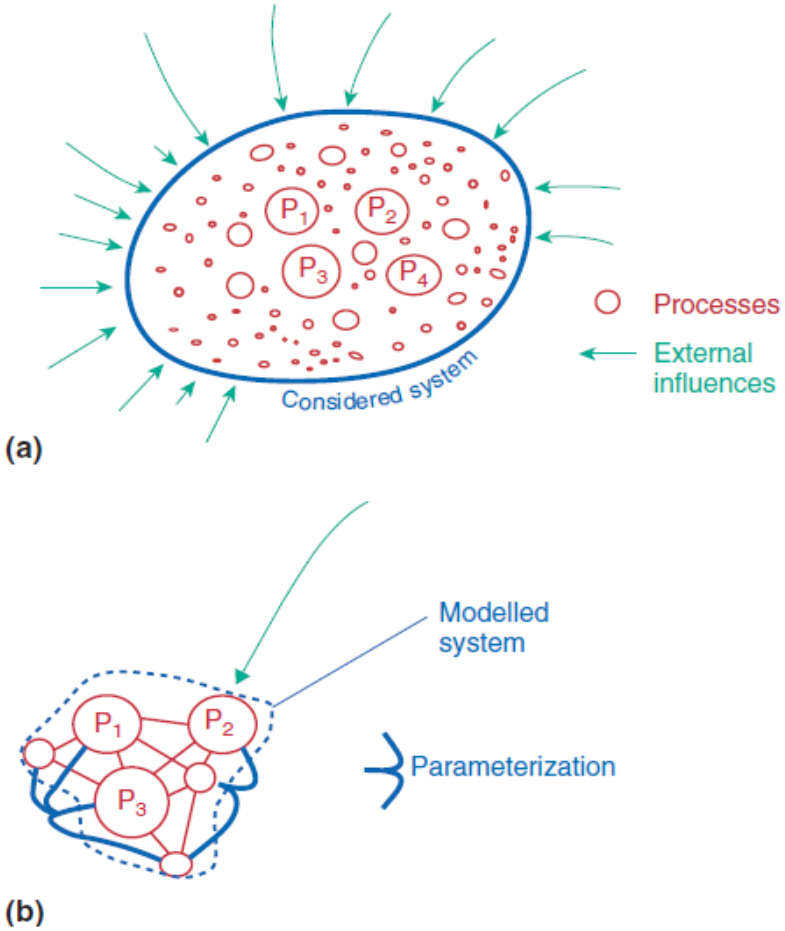

Figure 3.10 Sketches of (a) a real system, in which an infinite number of processes Pi (open circles) is present, and upon which an infinite number of external forces (arrows) act; (b) a modelled system, in which only a limited number of processes (open circles) and their interactions are represented, and in which the number of external forces is also limited (arrow). Parameterisations are indicated by solid lines crossing the dashed-line border of the model (von Storch, 2001).

3.2.1.1 Primitive Equations

NWP models operate by adhering to fundamental dynamic and thermodynamic principles. These principles account for the evolution of the atmosphere by ensuring the conservation of momentum (eq. 3.1), mass (eq. 3.2), state (eq. 3.3), energy (eq. 3.4) and moisture (eq. 3.5) in all phases through solving the primitive equations where v = horizontal wind vector, F = Friction, Ω = Coriolis parameter, T = temperature, t = time, ρ = density, p = pressure, $\emptyset$ = geopotential, α = specific volume, C_p = specific heat at constant pressure, E = evaporation, C =

condensation, *Q* = energy applied, *q* = specific humidity, *R* = the gas constant (Kalnay, 2003).

Momentum

$$\frac{dv}{dt} = -\alpha\nabla\rho - \nabla\emptyset + F - 2\Omega \times \mathrm{v}$$

Equation 3.2

Mass

$$\frac{\delta\rho}{\delta t} = -\nabla \cdot (\rho v)$$

Equation 3.3

State

$$\rho\alpha = RT$$

Equation 3.4

Energy

$$Q = C_p \frac{dT}{dt} - \alpha\frac{dp}{dt}$$

Equation 3.5

Moisture

$$\frac{\partial\alpha q}{\partial t} = -\nabla \cdot (\rho v q) + \rho(E - C)$$

Equation 3.6

The primitive equations are applied to individual parcels of air and account for the evolution of the meteorological parameters in accordance with the values of the previous time-step. Newton's second law relates to the conservation of momentum which asserts that in an inertial frame, a body will react to an applied force and maintain momentum in the same direction at constant velocity until another force is applied. To apply the principle to the Earth, apparent forces have to be included which arise because the Earth is a rotating body and the atmosphere is a fluid. On Earth the apparent forces in order of magnitude are the Coriolis and Centrifugal forces (Kalnay, 2003). Accounting for all the forces acting upon particles in the atmosphere forms the basis of NWP, from which weather forecasts can eventually be produced. The three forces of most importance to atmospheric motion are the Pressure Gradient force, the Coriolis force and the Friction force and comprise the conservation of momentum equation (eq 3.1). The Pressure Gradient force arises from gradients in temperature and density of air and causes large scale motion as air moves from areas of high concentration (pressure) to low. Friction acts in the opposite direction to the pressure gradient force and arises from energy dissipation resulting from contact with other molecules which can be either stationary solid

objects or due to viscous forces present in the fluid. The Coriolis force is an apparent force which accounts for the motion of air parcels relative to that of the Earth as it rotates ‘underneath’. The faster the rotation of the earth, the stronger the Coriolis force and thus it is strongest at the poles (Barry and Chorley, 2003). The strength of Coriolis force is also proportional to the velocity of the particle upon which it acts. There is a wide range of NWP products available including several mesoscale models. The variation between the models arises from the methods by which the primitive equations are solved. Processes such as time integration procedures and parameterisation schemes vary depending on the model developers. Variation in the output of different models is a product of the differing solving processes from one another and leads to differing performance under particular conditions, for example one model may produce more accurate outputs under stable conditions because certain parts of the model approximate the stable conditions more accurately.

3.2.1.2 Atmospheric Chaos

Mentioned earlier was that atmospheric modelling is an approximation of reality not a direct representation, i.e. the fact that not all processes are fully represented induces a certain error in the model output, but one which is known and can be accounted for. One of the most important factors which affect the accuracy of weather prediction is the inherent chaos of the atmospheric system. Atmospheric chaos is the theory, originally proposed by Edward Lorenz in 1963, which relates to the sensitivity of the atmospheric system to perturbations. The atmosphere is a dynamic deterministic system which means there are no random inputs, the system simply evolves from the initial conditions but, the sensitivity to the initial conditions is very high and divergence from similar starting states can happen very quickly which is why long term weather prediction is near impossible (Kellert, 1993).Chaos can be induced simply by not setting the NWP model up correctly as well as misrepresentation of initial conditions to the model. All NWP models solve their primitive equations at incremental time steps. If the increments are too large, for example longer than the shortest wave resolved by the system, the numerical system may become unstable and induce chaotic behaviour (Lorenz, 1989). Numerical stability can be improved by reducing the time step increment but this is at the expense of computational efficiency as more processes are calculated for the same temporal domain. Accounting for atmospheric chaos is not a direct priority for

the model developers because there is little that can be done at the modelling stage. One solution is the ensemble approach which takes multiple output forecasts run for the same temporal and spatial domain but which vary in either initial conditions or model setup. Ensemble outputs provide a spread of results which can be manipulated as desired by the researcher, for example by producing a weighted average.

3.2.1.3 Effective grid resolution

One of the conceptual properties of numerical modelling relates to the grid resolution of the model run being undertaken. Since calculations for the resolved variables are undertaken on a discrete grid, any features/motions/entities existing at a scale below the distance between two points cannot be directly resolved. However, even if the feature is larger than one grid point spacing, the number of grid points it covers will determine how successfully the model is able to simulate it and this principle is the effective resolution of the model. What size is the smallest feature the model can resolve? The answer is related to the grid resolution and clearly will be above 1Δ (where Δ is the grid spacing). Effective grid resolution is found to be roughly 4-7 Δ (Bryan et al. 2003; Skamarock 2004). For example, to resolve features on the order of a few hundred kilometres, a grid spacing on the order of tens of kilometres would be required (Kang, 2009). Mesoscale NWP models are most appropriate for application to wind resource assessment because they can cover large spatial areas yet operate at a relatively high resolution to capture some regional features. When selecting the resolution of the innermost domain, a user must decide where the compromise between resolution and efficiency lies for their study. Some papers report that increasing grid resolution beyond a certain level does not justify the increased requirement in computing resource (Gibbs et al, 2011). The manifestation of effective grid resolution, in the context of wind resource assessment, translates to the frequency of wind speed change which the model can resolve. Short-term high frequency changes in wind speed are caused by small scale atmospheric features such as turbulent structures, while long-term low frequency change is caused by large scale features such as fronts or pressure systems, represented in the Van der Hoven (1957) spectrum in Figure 3.11. The Van der Hoven spectrum shows two significant peaks in the spectral density of wind speed, one at around four days and one at around one minute. The significance of these

peaks respective to mesoscale modelling is that the 4 day peak represents long-term changes in wind speed caused by synoptic scale features which would be resolved by a mesoscale model running at 2km grid resolution. The one minute peak however, represents short term changes in wind speed caused by turbulent structures that would not be resolved by the model but approximated by parameterisation schemes.

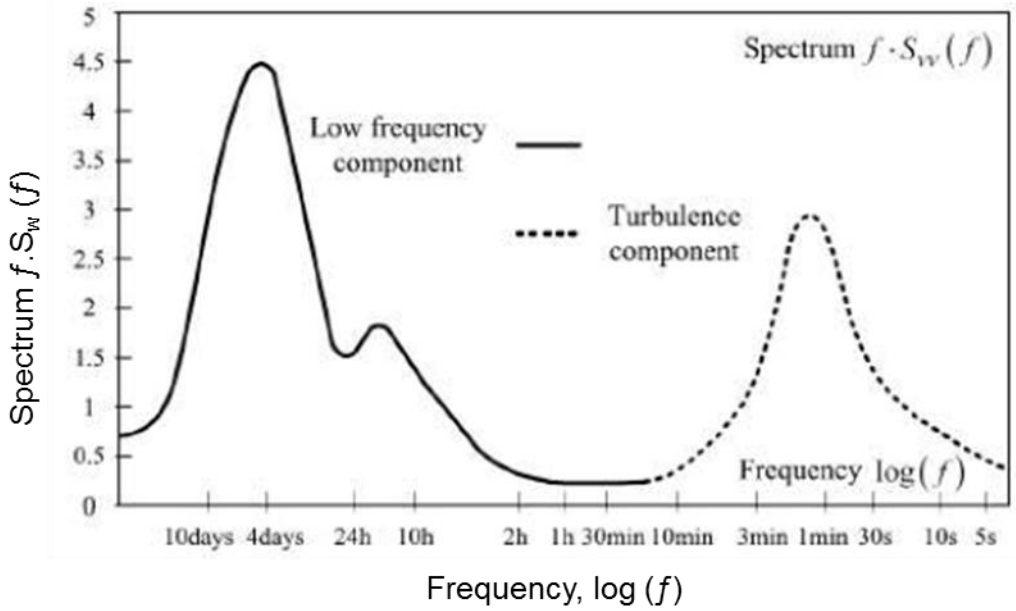

Figure 3.11 Van der Hoven (1957) spectrum for wind speed adapted by Munteanu et al, (2008).

3.3 WRF

3.3.1 Description

Developed as a replacement for the MM5 mesoscale model, WRF is a fully compressible non-hydrostatic mesoscale model and is available with two dynamical cores. The NMM (Nonhydrostatic mesoscale model) core (Janjic 2003) is used operationally in a number of systems by its developer NCEP (the National Centre for Environmental Prediction). The other core, ARW (advanced research WRF, Skamarock et al, 2008), was developed by NCAR (the National Centre for Atmospheric Research) for the research community. ARW is regarded as the more advanced core but requires more specific care regarding setup. The NMM core is more robust and in one study which compared the two dynamical cores by simulating the same period, using the same setup and resources as far as possible, the models performed similarly though the NMM core displayed a lower systematic bias (Jorba et al, 2008). Selection of which core to use is typically determined by the

application, operational applications of WRF, such as the hurricane forecasting system HWRF, tend to employ the NMM core. Research applications benefit from the greater physical flexibility available with ARW core. While developed independently the cores share many similarities, for example the vertical coordinate system, mass conservation and terrain following coordinate system (Skamarock, 2005). Where the cores primarily differ is in their model grid staggering, the selection of equations, variables and conservation properties and finally their time integration methods (Skamarock, 2005). Ultimately, performance differences between the cores exist, but they are attributed more to the differences in the physics employed, rather than the dynamical solver (Skamarock, 2005). One of the main practical manifestations of the differences between the cores relates to the computational efficiency. NMM is the more numerically efficient core, running faster and less intensively than ARW. Unless run in a global setup (which is computationally expensive and restricts resolution), WRF is unable to account for processes external to the modelled domain and therefore requires boundary conditions for the duration of every run to satisfy conservation equations.

3.4 PBL parameterisation

3.4.1 Introduction

PBL schemes approximate atmospheric fluxes of heat, momentum and moisture in the boundary layer (Deppe et al, 2013) as functions of variables resolved by the model (Suselj and Sood, 2010). The parameterized fluxes cannot be resolved explicitly by the model, either because it is too computationally demanding to do so, or because the processes operate at a higher resolution than the model (Teixeira et al, 2008). The estimation of heat and moisture fluxes is a part of the PBL scheme which involves assumptions about how the variables combine to represent the relevant friction velocities and exchange coefficients through the layer (Borge et al. 2008).

3.4.2 Fundamental principles

Approximating turbulence within the boundary layer is the key task of the PBL parameterisation. Closure of the nonlinear terms which contribute to turbulence is one of the major challenges faced by the PBL schemes. The order of closure of the parameterisation scheme describes the turbulent anisotropy (direction dependant) terms approximated, which are sets of variables calculated by the scheme either

explicitly or implicitly. The set of variables described by a first order closure scheme are the state variables (u, v, w, T and q), which are the three dimensional wind vectors (E/W, N/S and vertical), temperature and specific humidity respectively (Stensrud, 2007), which vary independently in first order schemes. The first set of variables provide a basic description of the boundary layer, though in reality the turbulent fluxes are far more complex and not independent. Higher order schemes account for this increasing complexity by incorporating more variables and introducing interactions between variables. In order to fully close the first order turbulence equations, the involvement of at least one second order term is required. Likewise, closure of the second order terms involves at least one third order term, which is a triple correlation term. Essentially the closure problem is infinite and currently broken by including an assumption, that terms of a certain order are functions of the preceding lower order terms. For example, a first order closure scheme assumes that all second order terms are a function of the first order terms, where a second order closure assumes third order turbulence is a function of first and second order terms. The second anisotropic variable set (second order closure) includes covariance terms and in third order closure schemes a triple correlation term is present. Intervening order schemes, include a (some) calculation(s) implicit in the next order of turbulent anisotropy (e.g. Mellor and Yamada 1982) but not the full suite, thus the scheme is of an intermediate order. The other major defining property of PBL schemes is locality, which describes the number of known data points used when calculating an unknown variable. Local PBL schemes relate the unknown fluxes to known values at the same grid point (Stensrud, 2007). Non-local PBL schemes have the freedom to utilise any number of data points in the vertical, to approximate the unknown turbulent fluxes, potentially the full depth of the boundary layer (Stensrud, 2007). The two approaches both have advantages, for example a non-local scheme is beneficial in an unstable convective layer where the deep mixing motion is translated to the variable fluxes through the layer (Bright and Mullen, 2002). The advantage of a local scheme is computational efficiency and when coupled to a high order closure scheme, more complex calculations are intended to provide a detailed appraisal of fluxes through the layer, such that using information from the full depth is unnecessary (Stensrud, 2007).

3.4.3 Local versus non-local closure

First order closure schemes are considered simpler than higher order schemes (e.g. Challa et al, 2009) because of reduced complexity of the equations solved and quantities calculated. However first order schemes tend to be non-local which utilise information from, potentially, the full depth of the boundary layer. The manifestation of the individual qualities of local and non-local techniques was identified by Shin and Hong (2011) who found non-local schemes to perform favourably compared to local schemes under unstable conditions for a range of variables during an observational field campaign. Under stable conditions, the higher order local schemes offered better performance, despite the fact that neither non-local nor local schemes performed particularly well. Similarly, Challa et al (2009) looked at coastal mesoscale circulations using the MYJ and YSU schemes and found the non-local YSU scheme to perform better than the local MYJ for a range of predicted mean variables. In a study of PBL depth, Xie et al (2012) compared the performance of local versus non-local schemes and found that the local PBL schemes (MYJ and Boulac) produced a much shallower PBL than was simulated by the non-local schemes (YSU and ACM2). By reference to observations, they found the deeper solutions of the non-local solutions to be more representative of reality.

3.5 Importance of Input Data

The modelling process has to be considered with respect to the input data by which the model run is initialised, not simply the model itself in isolation. A famous acronym in the modelling community pertaining to this consideration is GIGO (garbage in garbage out). A description of two well-used reanalysis products is provided shortly, with both being used in research to initialise NWP models. While different reanalysis datasets utilise much of the same data as one other, there are inherent differences between the individual products which can have an impact upon the success of the modelling campaign depending on them as input data. For the purposes of an offshore wind resource assessment by a mesoscale NWP model, large scale features are required to be well defined in the reanalysis output in order to allow the model the best chance of accurately simulating the resultant processes through the domain. Ultimately, the reanalysis datasets might provide different perspectives of the atmosphere for a given time because of the observations of which they are comprised, the data assimilation method and the NWP model run to

produce the output. For example, one reanalysis dataset may have a more dense observation network in a particular region, which is not shared internationally, to the detriment of alternative reanalysis products. Such an occurrence should improve the accuracy of that product in that particular area which should in theory provide more accurate initial conditions to an NWP model providing the best opportunity for good performance.

3.6 Reanalysis products

A meteorological reanalysis product is a global dataset of reanalysed variables, the output of an assimilation system which synthesises NWP (numerical weather prediction) model output and observational data (Kalnay et al., 1996). The concept was developed in the 1980's when data assimilation was a technique used to produce operational datasets combining observations from multiple sources (e.g. Bengtsson et al. 1982), such as satellites surface stations and ocean buoys. Many users found the assimilated data to be of insufficient quality which prompted the movement (Bengtsson and Shukla, 1988 and Trenberth and Olson, 1988) to reanalyse the observations into a standardised format. The assimilation process creates a global state of the atmosphere (Uppala et al., 2005) for a given time-step. The NWP model simulates the atmospheric evolution and is augmented during the course of the model run by observations, where they exist from the multiple data sources, within the model domain. Essentially, the simulation is nudged by tendency terms towards observations of reality. The objective of a reanalysis product is to present all possible variables in a single gridded dataset for the globe. Reanalysis products are an important source of homogenised global atmospheric data that are readily accessible to those who cannot produce such datasets independently and, as a result, many research projects have been conducted solely using reanalysis data, for example Heikkila et al., (2010), Zhao and Fu (2009) and Brodeau et al., (2010). The accuracy of reanalysis products depends on the amount of observational data which can be assimilated to help nudge the simulation towards observations. Most recently the biggest advancement has been in remote sensing by satellite (see table 3.2) which has significantly increased the spatial coverage and resolution of observations.

Table 3.2 Average daily counts of various types of observation supplied to the ERA-40 data assimilation process over five selected periods, (Uppala et al, 2005)

Observation Type	1958-66	1967-72	1973-78	1979-90	1991-2001
SYNOP/SHIP	15313	26615	28187	33902	37049
Radiosondes	1821	2605	3341	2274	1456
Pilot Balloons	679	164	1721	606	676
Aircraft	58	79	1544	4085	26341
Buoys	0	1	69	1462	3991
Satellite radiances	0	6	35069	131209	181214
Satellite winds	0	0	61	6598	45671
Scatterometer	0	0	0	0	7575

One of the major achievements of global reanalyses is the international collaboration which has arisen from the need for data. Meteorological agencies across the world have united and donated data, all converted to the same WMO BUFR format (Uppala et al. 2005), which is available to all the partner institutions for use in their reanalysis products. The data sharing endeavour is a platform from which continual development of reanalysis products will develop. With the majority of data being available to all agencies, the main differences between reanalysis products of very recent times and in the future will be down to the analysis model and the data assimilation technique. Two of the more extensively used reanalysis products are discussed in the theory chapter with a view to incorporation into this investigation of the offshore wind resource.

3.6.1 ERA-40

The ERA-40 (ECMWF 40-year Reanalysis) dataset is a reanalysis product from the European Centre for Medium range Weather Forecasts (ECMWF). Based in Reading, UK, the ECMWF is an independent organisation comprised of 18 member and 15 co-operating European states that all contribute to the project and utilise the variety of outputs from the facility. Numerical simulation for the process was undertaken using the ECMWF IFS (Integrated Forecast system) model. Observations were assimilated into each model run using a 3D-Var (3-dimenional variational analysis) method, whereby observations in all three physical domains are included at a given time-step. ERA-40 is available from 1957-2002 at 1.0° resolution, variables are available on 60 vertical levels. The IFS model was able to run at a higher resolution and employ a 4D-Var assimilation process, where data from

alternative time-steps are also available. However, neither of the techniques were employed in favour of computational efficiency (Uppala et al, 2005). ERA-40 has been used in numerous studies, in addition to providing input to dynamical NWP models. One area of particular strength for reanalysis products is their spatial coverage. The relative motion of the atmosphere around the globe is difficult to represent with point measurements because of uncertainty in the intervening space. This is the benefit of a homogenised dataset, such as a reanalysis product, where all quantities are conserved on a global scale. Crooks and Grey (2005) performed a statistical analysis of the influence of the 11-year solar cycle upon atmospheric temperature and zonal winds as well as a number of large scale atmospheric proxies such as the Quasi-Biennial Oscillation (QBO), El-Niño Southern Oscillation (ENSO), North Atlantic Oscillation (NAO) and volcanic signatures. All of the atmospheric variables investigated were extracted from the ERA-40 product. The influence of the 11-year solar cycle was confirmed as having a direct influence on terrestrial variables as relationships to equatorial temperature and zonal wind (seen as a seasonal response) were identified. Another key use of reanalysis products is in the historical collection of global variables they possess. Such capacity is useful in two ways. Firstly it allows an investigation a good historical length over which the study can be conducted. Secondly, it is ideal input to regional scale NWP models which cannot conserve variables globally and need input at the model domain boundaries for the duration of their runs. Dynamical downscaling processes coarse resolution input data through an NWP model to simulate conditions at a higher resolution than the original input data. Essentially, the model simulates the evolution of the atmosphere dynamically, considering regional features which do not exist at the resolution of the original product. Heikkila et al (2010) downscaled ERA-40 data at two resolutions: 30 km and 10 km, approximately 0.3 and 0.1 times the resolution of the ERA-40 output. The results of the downscaling were compared to high resolution observational data obtained from a network of stations situated in complex terrain within Norway. The results indicate the downscaled model output is able to significantly improve the quality of the output afforded by ERA-40. It is important to consider the benefits of ERA-40 along with its constraints. It is readily available from the BADC (British Atmospheric Data Centre) with an academic licence and provides a good appraisal of the global atmosphere for the period it covers according to many studies which have used it. While 1.0 degree resolution is not particularly high

compared to current reanalysis products, it does make the file sizes smaller for a given area which, for example, speeds up the download process and is less intensive on computing resources. However it is 7 years old now and the main shortcomings which relate to the products now available are the assimilation methods and data availability at the time of production. The dataset described next is a more recent product and is available at a higher resolution.

3.6.2 CFSR

A number of American governmental centres have produced reanalysis products beginning, in the mid 1990's, with the NCEP/NCAR (National Centre for Environmental Prediction) (National Centre for Atmospheric Research) reanalysis. One of the most recent products is the CFSR (Climate Forecast Systems Reanalysis) (Saha et al, 2010) product which was released in 2010. The CFSR product covers the period from 1979 to 2012 and is available at 0.5° resolution, where variables are available on 64 model levels. The CFS (Climate Forecast System) model system which assimilates observations is comprised of three parts. The atmospheric model used in producing the CFSR is the widely used GFS (Global Forecast System) model and forms one part of the CFS. Next is the MOM (Molecular Ocean Model) which is used to drive the atmospheric model as opposed to using the observed SST (Sea Surface Temperature) field as in most other reanalysis products. The final part of the CFS is the coupling between the oceanic and atmospheric model components. Data assimilation in the CFSR is 3D-Var, like ERA-40, but modified from its older sibling the NCEP/NCAR reanalysis. SSU (Stratospheric Sounding Unit) satellite data was incorporated into the CFSR for its duration which provided observations of CO_2. Liléo and Petrik (2011) found the CFSR to correlate well with observed wind speeds when looking at the wind resource over a number of sites in Sweden. The study looked at the performance of other reanalysis products, which were the original NCEP/NCAR reanalysis and the MERRA (Modern-Era Retrospective analysis for Research and Application) reanalysis. The MERRA product was released at a similar time to the CFSR and thus is available with more recent data and technology. Ultimately, Liléo and Petrik (2011) found the MERRA and CFSR reanalysis products outperformed the NCEP/NCAR product with the MERRA coming out slightly ahead, but suggested caution when applying their results to other locations. When applied as model input data, Carvalho et al (2012)

found the CFSR product to perform well, providing accurate initial conditions to the WRF model to a similar standard as the 4D-Var ERA-Interim product.

3.7 Techniques used to improve model performance

Performance of WRF has been discussed for a range of applications including wind resource assessment. The effect upon performance that model setup can have, both physically and dynamically, has been presented. After model setup, a number of further options exist to improve model performance, which is discussed in the following section.

3.7.1 Nudging

Nudging a model run involves the incorporation of observational data into a model run over its duration at every boundary update. There are two types of nudging available with WRF: objective analysis and observational nudging. In observational nudging observational time series‘ close to points of interest can be integrated into the model run to provide more accurate local information. Objective analysis operates across the entire model grid as opposed to single points within the domain as is the case when using observational nudging. Nudging relaxes the model solution towards the nudged sources to preserve the ‘known’ atmospheric structures provided by the nudging series (Deng and Stauffer 2005; Otte 2007). In WRF, observational nudging is achieved through a four dimensional data assimilation (FDDA) process, where the difference between the nudging series and the model simulation at each time step is calculated and imposed upon the model run as an artificial forcing term (Otte, 2007). The number of variables which can be nudged is extensive, and thus depends on the priorities of the researcher as to what extra variables might be of benefit to the model performance. Objective analysis involves incorporating the observations into the model input data to give the best first guess of the atmosphere at the initialisation of the run, to provide the best opportunity of correctly representing the initial conditions. Gryning et al (2013) found that observational nudging of wind, temperature and humidity improved the simulation of wind speed in absolute terms as quantified by RMSE. Shimada and Ohsawa (2011) included analysis FDDA in their study to nudge the model run towards the analysis for the duration of the model run, which yielded a high correlation coefficient to observed wind speed of 0.8.

3.7.2 Ensembles

3.7.2.1 Introduction

Ensembles were introduced in chapter 1 as a technique by which to augment the scope of an NWP simulation by running the same case multiple times with some features of the model system perturbed to generate different solutions. Classically, the individual perturbations which generate the ensemble members reflect sources of uncertainty within the model system. A perfect ensemble would account for every source of uncertainty through the modelling process to produce members which exactly follow observations (Anderson, 1996, Hamill, 2001). One of the benefits of running an ensemble is the information which can be obtained from analysis of the members' behaviour relative to one another, particularly if the differences between the members are known and might explain the observed discrepancy. Ultimately, an ensemble is a single product comprised of its members. One of the great strengths of ensemble generation is the potential to produce a probabilistic output, providing a distribution suggesting the likely location of the correct value. Alternatively, ensemble members are often combined to produce a mean value, which is more often used when a limited number of members are available. It is generally accepted that an ensemble mean will have a lower error than any individual member (Whitaker and Loughe, 1998; Leith 1974; Murphy 1988). An extension of the ensemble mean method involves weighting the members to accentuate confidence or uncertainty accordingly (for example Lu et al, 2007). However, such a technique requires justification based on previous experience. National forecasting centres which employ operational ensemble forecast systems undertake statistical post-processing of the ensemble to produce calibrated probability forecasts (Grimit and Mass, 2007). Calibration of the ensemble is desirable but also computationally expensive and time consuming. Uncalibrated ensemble systems have been investigated against their calibrated counterparts and were shown to be skilful tools (eg Arribas et al., 2005, Buizza et al., 2005), albeit lacking the confidence associated with a calibrated product.

3.7.2.2 Application to the field of offshore wind resource assessment

Clearly the main focus of an ensemble is the difference between its members, i.e. the method of perturbation, which is related to a particular area of uncertainty. Depending upon the application of the simulation, different areas of uncertainty might

be more highly prioritised. Two areas of uncertainty were identified as being particularly relevant to the field of offshore wind resource assessment. The first relates to the initial conditions provided to the model, which is a source of uncertainty in every NWP simulation, and the second is more specific to this research which is the representation of physical processes in the planetary boundary layer.

Initial conditions are the values of required variables provided to the model at the start of a run by the input data. The accuracy of the input data is clearly limited by its grid resolution with each mass point representing a portion of the surrounding area. Accuracy of the initial conditions is imperative to the success of the model run. The further departed the input data is from reality, the less chance the model has of correctly simulating the evolution of the atmosphere as it will effectively be doing it from a different state. The closer a set of initial conditions is to reality, the less quickly a model solution is likely to diverge from reality. An ensemble approach is thus a very useful technique to apply to the uncertainty associated with initial conditions as multiple runs can be undertaken. Perturbation of the initial conditions relates to the study in question, for example different data sources might be available or specific variables might have a bias associated with them which could be accounted for using an ensemble. Another option by which to perturb the initial conditions is to initialise members at different times and generate an ensemble for the overlapping period. This time offset ensemble system (TOES), also known as a lagged ensemble (Hoffman and Kalnay 1983), preserves the same model setup for the duration of a run and is consisted of members initialised at different times. Originally, lagged ensembles were applied to medium range simulations on the order of 6-10 days (Dalcher et al. 1988, van den Dool and Rukhovets 1994), before shorter timescales were considered and the performance benefit of generating a lagged ensemble was evident (e.g. Hou et al. 2001, Lu et al 2007 and Walser et al. 2004). A lagged ensemble is a flexible method by which to account for some uncertainty in initial conditions, but another benefit is the reinitialisation effect achieved by staggering initialisation times to generate an ensemble mean. Lo et al (2008) compared the solutions of a continuous year-long run with a run for the same period but which was reinitialised every 29 days. The model setups were otherwise identical and they found that the reinitialised run performed better than the continuous run due to the regular update of large scale atmospheric structures provided by the input

data. While the runs for this work will be much shorter, the principle still stands and by generating an ensemble mean of the staggered runs, the effect of reinitialisation will be incorporated into the run.

Uncertainty in the planetary boundary layer is associated with the techniques applied in mesoscale NWP models to represent the processes which occur throughout the layer and are implicit in modifying the larger scale circulation resolved by the model. Parameterisation schemes, discussed earlier in section 2.7, are functions of resolved variables which provide an approximation of the fluxes which occur through the PBL. Since the processes are sub-grid and thus not directly resolved, a degree of uncertainty is attributed to the accuracy with which the layer is represented and thus the feedback effect translated to the larger scale circulation resolved by the mode. As previously mentioned, a number of PBL schemes exist for WRF and no one scheme proves an obvious first choice with different schemes excelling depending upon conditions. Creating an ensemble by running the same simulation using different PBL schemes is one way to ensure the best performing scheme always has an influence. Generating a PBL ensemble is a novel approach to addressing the uncertainty of model performance in the boundary layer. Only recently have other studies employed a similar approach, for example Deppe and Gallus (2013) who were motivated by results in studies by Harrison et al. (1999) and Stensrud et al. (2000) which showed the potential of perturbing WRF model physics to be an efficient way of generating a forecast ensemble. In the context of wind resource assessment, Nunalee and Basu (2013) conclude the use of multi-physics ensembles to be of benefit in producing more accurate predictions.

3.7.2.3 Ensemble spread

Ensemble spread is simply the distribution of ensemble members for a given point in time. Spread of the ensemble members is considered a measure of uncertainty, with larger (smaller) spread of ensemble members corresponding to larger (smaller) model uncertainty (Grimit and Mass, 2007). Practical investigations of the linear correlation between ensemble spread and model error have highlighted a lack of any strong relationship between the two series (e.g., Buizza 1997, Stensrud et al, 1999, Hamill and Colucci, 1998), though correlation has been shown to improve using forecast bias correction (Stensrud and Yussouf, 2003). The strongest linear link between ensemble spread and model error appears to occur when

ensemble spread is anomalously high or low (Whitaker and Loughe, 1998, Grimit and Mass, 2002). Such behaviour is associated with the state dependence of the metrics (Grimit and Mass 2007), which some studies (Toth 1992; Ziehmann 2001) suggest should be viewed in a climatological rather than instantaneous context. For example, the inference is that the magnitude of a forecast error is more likely to be greater (reduced) when a variable is close to its climatological extreme (mean) value (Grimit and Mass, 2007; Whitaker and Loughe, 1998).

3.8 The modelling environment

Two concepts which pertain to the application of NWP as a wind resource assessment tool are presented below. Discussed first is the concept of stability, its impact on wind resource assessment and farm output and how it can be accounted for as part of an NWP derived wind resource assessment. Secondly, the concept of weather typing is presented. Weather typing has no direct influence on the wind resource assessment, but as will be argued, is a useful tool to consider alongside an NWP output.

3.8.1 Stability

Stability is an atmospheric property which describes the tendency of an air parcel after a perturbation in the vertical direction. In a stable atmosphere, upon perturbation, an air parcel will return to its original level. In a neutral atmosphere, an air parcel will remain at the level it was perturbed to, while in an unstable atmosphere an air parcel will continue travelling in the direction of the perturbation. The implication of atmospheric stability in extracting energy from the wind mostly translates to the effect it has upon mixing between horizontally orientated atmospheric layers, which affects both the vertical wind profile and the wake dissipation after a turbine. Manifestation of varying stability on the vertical wind profile tends to be considered, for wind energy applications, in terms of variations in shear (e.g. Rareshide et al 2009, Wagner et al 2009) and turbulence intensity (e.g. Tindal et al 2008). Ultimately, the inter-layer mixing which is affected by stability will determine the degree of energy redistribution between layers. For the incident turbines, the ones which receive the wind first, this will affect the amount of lift each blade will generate across its diameter and for downwind turbines there is also the

wake effect to consider. In an unstable atmosphere, enhanced mixing promotes energy transfer between adjacent atmospheric layers which has the effect of dissipating turbine wakes faster than under neutral conditions. In a stable atmosphere, turbine wakes persist further than under neutral conditions because there is no additional source of momentum from neighbouring layers. As a result, stable conditions typically lead to a greater power deficit for downwind turbines (Barthelmie and Jensen, 2010; Türk and Emeis, 2010; Hansen et al, 2012). While ultimately determined by the relative thermodynamic state of the atmosphere, stability can vary as a function of other atmospheric variables. For example at high velocities laminar flow tends to dominate inhibiting turbulent structures. Figure 3.12 shows an example of this where the highest wind speeds tend to be dominated by neutral conditions and lower wind speeds corresponding to more unstable conditions.

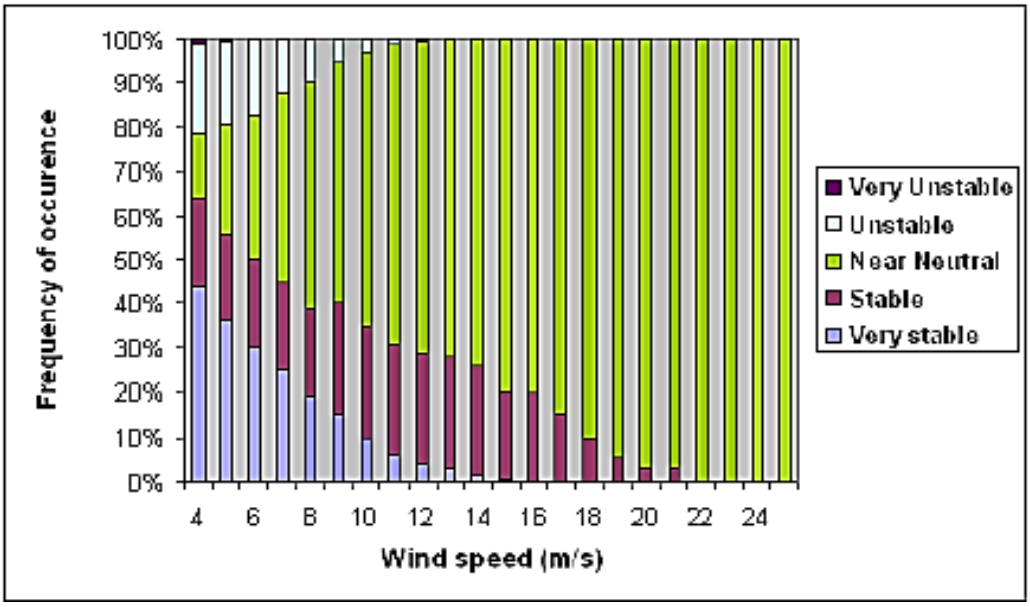

Figure 3.12 Stability as a function of wind speed at Vindeby (Motta and Barthelmie, 2005)

Different metrics exist for representing atmospheric stability and are generally related to the type of research application. The Obukhov length (L) is a scaling parameter used specifically within the surface layer (Stull 1998; Joffre 1984) and is a function of heat and momentum fluxes (Wharton and Lunquist, 2012b; Mahrt et al, 1998). The Obukhov length is one of the key dimensional scales used in Monin-Obukhov similarity theory (MOST) which describes turbulence and non-dimensionalised mean flow in the atmospheric surface layer (roughly the lowest 10% of the PBL). In this

work, the Obukhov length is derived from the Richardson number. There are two methods for calculating the Richardson number depending upon the variables available. The gradient Richardson number requires temperatures and wind speeds at two heights, calculated in Equation 3.7 with the conversion criteria to Obukhov length described in Equation 3.8 after Stull (1988) and used in Zoumakis and Kelessis, (1991). The bulk Richardson number (Equation 3.9) requires temperature at two heights but wind speed at one. Conversion to Obukhov length is shown in Equation 3.10 after Grachev and Fairall (1997) used in Hansen et al (2012). In these calculations, temperature at the lower height is subtracted from temperature at the higher level, which is why the gravity constant does not have a negative sign because the force is acting in the same direction as the temperature gradient as calculated.

$$Ri_{z'} = \frac{g}{\overline{T}} \frac{(\frac{\Delta\theta_v}{\Delta z})}{(\frac{\Delta u}{\Delta z_u})^2} \qquad \text{Equation 3.7}$$

$$L = \frac{z'}{Ri} \qquad Ri < 0 \qquad \text{Equation 3.8}$$

$$L = \frac{z'(1 - 5Ri)}{Ri} \qquad 0 < Ri < 0.2$$

$$Ri_b = \frac{g}{\overline{T}} \frac{z\Delta T + (\frac{g}{Cp} * dz)}{U^2} \qquad \text{Equation 3.9}$$

$$L = \frac{z}{10Ri_b} \qquad Ri < 0 \qquad \text{Equation 3.10}$$

$$L = z/(\frac{10Ri_b}{1 - 5Ri_b}) \qquad Ri > 0$$

Where *z'* relates to the approximate height (m), *dz* relates to the change in height, *g* is gravitational acceleration (9.81ms^{-2}), θ_v is virtual potential temperature (°K), C_p is the specific heat of dry air at constant pressure (1004 J K^{-1} kg^{-1}), $\bar{T}$ is the temperature (°C) and *u* is wind speed (ms^{-1}). Richardson number has been shown to be dependent upon the length scale over which it is calculated (Reiter and Lester 1968), which means if any comparisons are made is important to be consistent regarding the levels over which the Richardson values are calculated to try and reduce any sources of discrepancy. Once the Richardson number has been calculated and mapped to provide the Obukhov length, the stability can be classified. A range of classification schemes exist developed for varying applications, provided in Table 3.3 is the scheme used in this research.

Table 3.3 Stability classes in relation to Obukhov Length (L) van Wijk et al (1990)

Obukhov length (m)	Atmospheric stability class
-200 < L < 0	Very Unstable (VU)
-1000 < L ≤ -200	Unstable (U)
|L| > 1000	Neutral (N)
200 ≤ L < 1000	Stable (S)
0 ≤ L < 200	Very Stable (VS)

3.8.2 Weather typing

Weather typing is a classification system which describes the synoptic state of the atmosphere for a given area, in this case the British Isles. Originally a subjective classification devised by Lamb (1972), a synoptic chart is classified firstly by the dominant pressure system (where present) and then by the wind direction. Jenkinson and Collison (1977) then developed the objective Lamb weather typing system (Table 3.4) by quantifying the atmospheric setting from daily gridded sea level pressure. Knowledge of the dominant air source and air mass properties affords the ability to infer general information about atmospheric conditions. For example, if the weather type was a cyclonic westerly (26 CW), the wind would be coming from a westerly direction with cyclonic tendency. The source of the airmass is to the North-West of the UK so it is likely to be relatively cold and the flow brings the air over the Atlantic which means the air is likely to contain a lot of water vapour. Because the scale of weather typing is synoptic, only large scale features are of

interest which tend to move slowly. As a result, weather typing is typically carried out on a daily basis assuming persistence of the synoptic features for that day.

Table 3.4 Numerical designation of the lamb weather type categories

Lamb Weather Type (LWT) codes					
-1	U	-9	non-existent		
0	AC			20	C
1	ANE	11	NE	21	CNE
2	AE	12	E	22	CE
3	ASE	13	SE	23	CSE
4	AS	14	S	24	CS
5	ASW	15	SW	25	CSW
6	AW	16	W	26	CW
7	ANW	17	NW	27	CNW
8	AN	18	N	28	CN

A number of basic principles are required for making use of weather type analysis, most importantly is remembering that any inferences made are relative, much like discussing pressure systems. For example, a Northerly flow is likely to bring cooler air than is currently affecting the UK while a Southerly flow might bring warmer air, so that weather types do not offer absolute values for variables. This touches on one of the important principles of weather typing, namely the relative temperature of an airmass based on its origin. Very basically, due to the differential heating of the Earth, if an air mass originated South of the UK, it is likely to bring warmer air while from the North the air is likely to be cooler. Some instances do exist where this might not be the case. For example, if a Northerly air mass passes over the Atlantic to the West of the UK before reaching the country, the air will be modified through heating from the Atlantic Ocean due to the northerly transport of warmer water by the Gulf Stream. The ambient conditions affecting the UK at the time of interest are also an important consideration when performing a weather typing analysis. In the winter, the landmass is likely to be cold, at times colder than the surrounding water bodies, so a North-Westerly flow may well bring relatively warm air. Consideration of the modifications which may have been imparted to an

airmass is also important. For example, an air mass may have originated North of the UK, travelled South past the UK then circulated back around to influence the country. The journey South is likely to have warmed the airmass, equally if it has travelled over water it is likely to be holding more water than if it had come from a pure northerly flow as warm air holds more water. The dominant pressure systems will allow a tracing of the track of an airmass, and also provide some information about the atmospheric conditions. Anticyclonic conditions are associated with calm weather, low wind speeds and temperature extremes. For example, in the summer a high pressure circulation can lead to very high temperatures due to cloudless skies, whereas the same conditions in winter could lead to very cold temperatures. Cyclonic pressure is associated with more unsettled weather such as: higher wind speeds, clouds and precipitation. These principles can be established very quickly either by visual analysis or for an experienced user using simple knowledge of the weather types. Once the weather type is established, suggestions can be made of likely conditions and this is where the potential value lies to the field of wind resource assessment. As large scale pressure fields tend to be well simulated by NWP models, subsequent weather typing analysis would provide another perspective on likely conditions. For example, Figure 3.13 shows a South-Westerly weather type. The airmass originates in the Arctic but circulates round a low pressure system north of the UK and moves eastwards across the Atlantic. On its journey south, the airmass will be warming and becoming more saturated as it travels over the Atlantic. By contrast to NWP forecasts, weather typing offers no direct quantification of variables but an insight into the likely properties of the atmosphere and some impression of its likely evolution.

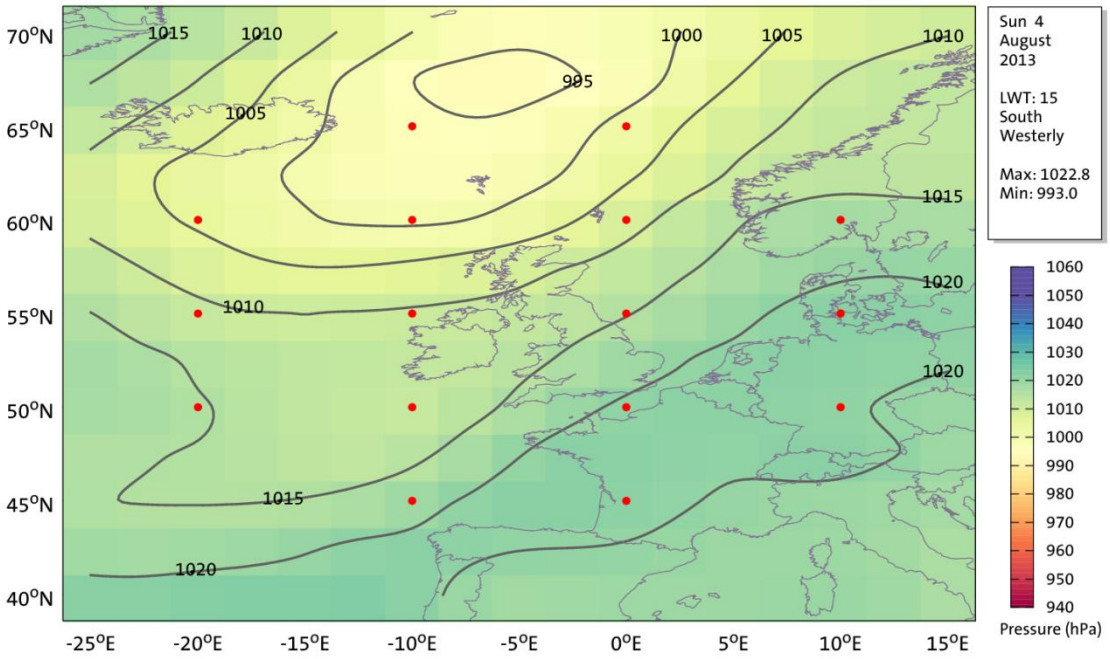

Figure 3.13 Example of South-Westerly weather type. Red points mark the locations at which pressure is sampled for the objective classification (Horseman, 2013).

The time of year will help determine the impact of the airmass coming into contact with the UK land mass. In winter, the land is likely to be colder than the air flowing over it from a South-Westerly flow which would chill the overlying air, forcing water to condense leading to cloud formation. In the summer when the airmass might still possess some coldness from its origins, the underlying land would warm the air above generating convective clouds most likely producing rain as the air is forced to rise. Weather typing is a simple technique which can provide a metric to be used alongside the output of an NWP model. By identifying the behaviour of variables under particular weather types, the reverse process could be used operationally by referring to the forecasted weather type and extrapolating the behaviour of the variables. The synoptic scale of weather typing fits well with mesoscale NWP simulations which resolve synoptic scale features wind confidence, upon which a weather typing analysis could be performed.

4 Method

4.1 Introduction

This chapter describes the process by which the potential of WRF as a wind resource assessment model is assessed. Facets of the project upon which progression is entirely dependent are discussed first, before setting up the model and analysing the output for the three investigation threads is described. As a relatively inductive study, there is little existing research to inform the process by which to undertake the research to achieve the aims, so the methodology of this work itself is one of the major achievements. From the development of the investigation and designing of the studies, to the careful selection of model output and analysis techniques, the methods applied to two novel locations are presented in the following chapter.

4.2 Dependencies of the research

This work is dependent upon observational data against which to validate model performance and the availability of computing systems on which to run the model. It is critical to validate model output against observations, not only to quantify performance as a resource assessment tool, but also as a means to investigate model shortcomings. Offshore observational data is often proprietary and since making observations offshore is prohibitively expensive, companies who own these data are reluctant to share them without significant compensation. Even if data are available, there are requirements to which it must adhere in order to be of use to the study, for example regarding data quality, resolution and format, which form a considerable part of the selection process. It is also critical to acquire the use of computing resources on which to run the model. The computationally intensive nature of mesoscale modelling requires significant processing resource, combined with significant storage capacity for both model input and output. Given the wide audience of potential users to which this research might be relevant, undertaking runs on computing facilities with varying levels of performance was important to provide some context into the capability of machines with different specifications. The observational data obtained for this research and the computing resources acquired are discussed below in turn.

4.2.1 Observational data

Two observational data series' were sourced for this work through connections within the Supergen Wind consortium, one from Scroby Sands, the other from Shell Flats (Figure 3.14). Temporal resolution of the data from both sites is 10 minutes, which for wind speed is an average of the anemometer data sampled at 1Hz. Scroby Sands meteorological mast is located at 52.67° lat, 1.79° lon, recording: temperature, wind speed and wind direction at 33 and 51 metres, from 1995 to 2000. Missing data was a significant challenge and selection of runs was heavily influenced by data availability. Two masts were erected at Shell Flats, Mast 1 is located at 53.86° lat, -3.29° lon, recording wind speed, wind direction, temperature, relative humidity, pressure, rainfall and solar radiation with instruments sited at 12, 20, 30, 50, 70, 80 and 82m above HAT (highest astronomical tide). The second mast at Shell Flats is located at 53.88° lat, -3.20° lon, some 9km from Mast 1. Observations at Mast 2 were made at 12, 20, 30, 40 and 52m above HAT, recording the same variables as Mast 1. Not all instruments were installed at every height and the investigation is set up to use the required data available from both masts at comparable heights.

4.2.2 Computing resources

4.2.2.1 CREST03

To begin with, the only computing resource available for the project was the departmental server CREST03, a Dell PowerEdge™ 2930 server with dual quad core Intel® Xeon® X5355 processors, 32GB FBD RAM and 2TB hard-drive storage, running Linux x84_64 GNU/Linux. The GCC (GNU Compiler Collection) compiler suite is available on CREST03. As a shared resource, without a batch queuing system, runs on CREST03 were undertaken in serial mode on one processor so as to not monopolise the facility. Given the relatively restricted amount of computing power available, it was decided WRF-NMM be run on CREST03 due to its superior computational efficiency. Despite the performance gain afforded by running WRF-NMM, considerations had to be made regarding the physical setup of the model for the desired runs, detailed in chapter 5.1.2.

Figure 4.14 Selection of Offshore met. masts and nearby onshore stations (McQueen and Watson, 2006)

4.2.2.2 HECToR

Obtaining computing time on a high performance computing cluster was always an aim of the project in order to maximise model performance as far as possible. With this in mind an application was made for a class 2a computing account on HECToR (High-End Computing Terascale Resource), the UK's national supercomputing facility. HECToR has 2816 compute nodes, each with two 16-core AMD Opteron 2.3GHz Interlagos processors and 32Gb of memory. Aside from significant processor power, HECToR possesses advanced data communication hardware such that each 16-core socket is coupled with a Cray Gemini routing and communications chip which translates to data latency between two nodes of around 1-1.5μs. HECToR runs Linux and is available with many selectable modules and

compilers for example gfortran, PGI, Intel and Cray. A class 2a account (grant Q198891) initially provided 300kAu's (thousand allocation units) of computing time on HECToR and 150GB of hard disk storage. With little knowledge of how intensive the early runs would be they were simply undertaken and monitored. It was obvious early on that more hard disk space was required and while 150GB was initially allocated, a request for more space saw an expansion to 500GB which allowed multiple runs to be undertaken simultaneously. The budget was completely used and again after a request the project was generously awarded more resource, this time in the form of an extra 100kAu's. Furthermore an additional 6 months were provided to extend the project. A second computing account on HECToR was applied for to undertake the set of runs comprising the performance optimisation investigation. Lessons learned from the first account identified the need for more computing time and hard disk storage. A class 1b account was applied for in the November 2012 RAP (resource allocation panel) which was assessed by review and awarded to the same research grant as the earlier class 2 account (grant Q198891). The awarded account provided 1,500kAu's and 1.5TB of hard disk storage as requested. Such a resource allowed the simultaneous undertaking of 6 runs which facilitated a much faster run turnaround period than was possible with the previous account.

4.2.2.3 Hydra

One of the aims of the research was to undertake yearlong resource assessments for the Supergen exemplar site and Shell Flats, which required a lot of model runs. Since applying for a HECToR computing account can only be done during particular periods through the year, an application was made for time on the Loughborough University HPC (high performance computing) cluster Hydra, to allow a more flexible work program. Hydra is comprised of 161 compute nodes, each having two six-core Intel Westmere Xeon X5650 CPUs and 24GB of memory. Hydra runs Linux and offers PGI, Intel, gfortran and Bull compilers. A computing account on Hydra was awarded which provided 354816 core hours of computing time and 1Tb of hard disk storage.

4.2.2.4 Compilation of model and ancillaries

WRF is well supported and highly versatile in that it is provided with multiple configuration options for a range computing systems and compilers. Access to WRF requires an account from the model website, after which the model and ancillaries

can be downloaded. For this research WRF version 3.3 was used throughout the investigations to provide a level of consistency. Four processes comprise the modelling flow (pre-processing, observation integration (where applicable), model running and postprocessing) are compiled individually. WRF and the pre-processor WPS, require the following libraries; a Fortran 90/95 compiler, a C compiler, Perl and netCDF. In order to pre-process GRIB 2 data, for example when using CFSR data, the following libraries are also required for compilation; JasPer, PNG and zlib. Observations were integrated into the model run for nudging using Obsgrid.exe, a WRF utility program which requires the presence of the netCDF library. Post processing on CREST03 was undertaken using WPP (WRF Post Processor, now UPP) and NCL (Ncar command language) scripts, these programs require the NCL libraries and the NCAR graphics package. Post processing on Hydra and HECToR was undertaken using RIP4, which requires netCDF and the NCAR graphics package. The NCAR graphics package is also required to build some of the WPS utility programs which can help the setting up of model runs.

4.2.2.5 Modelling process

Once the model components are successfully compiled, runs can be undertaken. To begin, input for the model run must be prepared which is done using the WRF Pre-processing System (WPS) executables. All three WPS executables are controlled by information in the namelis.wps file which specifies temporal and spatial domains. The namelist file is a text file and can either be populated manually or generated by a utility program such as WRF domain wizard. WRF domain wizard is a GUI tool which is very helpful in selecting model domains and can be used to generate the namelist.wps file. Initially in the pre-processing stage, input data is sourced and transferred onto a model grid by the ungrib program. Land surface data is provided with the WPS and the geogrid program extracts data for the domains of interest at a requested resolution. Metgrid.exe is the final WPS program to be run which combines the atmospheric and surface input data together which can then be used to run the model. If nudging forms part of the model input, this is the point where Obsgrid is run to integrate an observational series into the model input. Input files are then copied to the model run directory where another namelist file controls the parameters of the model run. Physical and temporal parameters are the same as set in the pre-processing namelist, while the model namelist includes dynamics

options for the run. Two executables form the model solver process, first a preliminary program generates the WRF input and boundary files interrogated by the model over the course of the run, then the solver itself executes the simulation. WRF output files are spatial grids containing a wide array of variables produced at time intervals set in the namelist. Most postprocessors comprise a 'translation' step to manipulate the raw output from the models Arakawa grid onto a more standard format such as a lat-lon grid, from which variables can be extracted. This work is concerned with extracting variables from a single point to compare against observations. WRF outputs variables on a discrete grid, which means the space between the gridpoints is vacant. Post processing tools offer the option to interpolate variables for sites of interest which lie between grid points. In this work model domains were all designed to have a mass grid point at the centre of the domain, co-located with the site of interest so post processed output from the model would be 'true' rather than interpolated by software accounting for the point being located between two model grid points. Two post processing techniques were used in this work and are described below.

4.2.2.6 Post processing

4.2.2.6.1 RIP4

RIP4 (Read Interpolate Plot version 4) was used for the majority of the model post-processing in this research, specifically for the runs undertaken with WRF-ARW. ARW solves on a different model grid to NMM, which requires a different post processing technique by which to extract the variables. RIP4 has two stages, where firstly a data preparation executable extracted a range of state variables from the model grid and maps them onto an intermediate RIP format for selected time periods. Secondly the RIP4 postprocessor processes the intermediate data to extract and display variables as requested in the RIP4 namelist. RIP4 is able to produce time series' or plots for variables by a range of temporal and spatial media. It is also able to spatially interpolate to provide values for variables between model points. RIP4 is controlled by the specification of values through a namelist file for both post-processing stages with critical features such as location, time step and vertical level all explicitly stated for each run.

4.2.2.6.2 WPP and NCL

The WRF Post Processor (WPP) is a utility provided by the model developers which extracts selected variables, controlled by a namelist, from output of the WRF-NMM. Much like the data preparation stage of RIP4, model output is translated from the model grid to a standard grid. NCL (NCAR Command Language) scripts were then used to select wind speed and direction from the WPP output for a specific grid point which coincided with the location of Scroby Sands. Outputted variables were stored in a comma delimited format using a command in the NCL script.

4.2.2.7 Analysis

After post-processing, model output is stored as a text file for each day's worth of running. A FORTRAN script was written to concatenate the multiple daily text files which comprised a whole run. Once the model runs were completed and post processed, output was copied back to a desktop PC where analysis of the output was undertaken. Model output was processed, manipulated and compared to observations using Matlab © software maintained by the university's IT services.

5 Benchmarking model performance at Scroby Sands

5.1 Introduction

As identified in the literature review, little previous research has been undertaken investigating the performance of WRF as a wind resource assessment tool and none at all has been published regarding the locations used in this study. As a result, this research is novel and effectively inductive because there is no level of performance to directly compare against. It is therefore necessary to undertake an investigation to define a level of baseline performance. As well as establishing a baseline performance, early model runs will help identify tendencies in performance and inform the direction of further investigations.

5.2 Method

An investigation which compared simulated to observed wind speed was required to establish a benchmark for model performance. The investigation was conducted for a site at Scroby Sands from which mast data were available. Two configurations of WRF were developed to investigate the impact of computing resource upon model performance. The two configurations would be run for the same cases so a direct performance comparison could be made. Temporal filters were developed and applied to focus on model performance at different temporal resolutions. Wind speed was simulated for Scroby Sands at 10 minute temporal resolution and 50m height.

5.2.1 Computing setup

The class 2a HECToR account was obtained to run a comprehensive setup of WRF-ARW for the same run period as those simulated using the WRF-NMM on CREST03. NMM runs were undertaken on the departmental server, CREST03 which was limited in physical storage space. ARW runs were undertaken on HECToR which, despite being able to undertake more demanding runs, was also constrained by hard disk space restriction. Around three runs could be undertaken simultaneously on HECToR due to the restriction of the 500GB hard disk space, as each model run including post-processing was around 100-150GB. 256 cores (8 nodes, 256GB of memory) were used for each benchmarking run undertaken on HECToR.

5.2.2 Selection of run duration

As was mentioned in the literature review, it is well known in numerical weather prediction (NWP) that the time frame of a simulation will help determine the method to be used. For example, a high quality short-term forecast, on the order of minutes to an hour, can be obtained by assuming persistence. An alternative to persistence with a greater degree of complexity and sensitivity, also favoured in the short term, is an ARIMA (Auto Regressive Integrated Moving Average) model. When the timescales lengthen, dynamical solutions become more necessary as accuracy improves and overtakes statistical and persistence models. A simple persistence investigation was undertaken using data from the Scroby Sands mast to identify the error associated with the technique and inform the selection of model run lengths. Figure 5.15 shows the absolute error of the persistence forecast with increasing lead time. Accuracy of the persistence forecast drops significantly to begin with, before appearing to smooth out with increasing forecast horizon after around 180 minutes, which suggests that model simulations should be at least three hours in length.

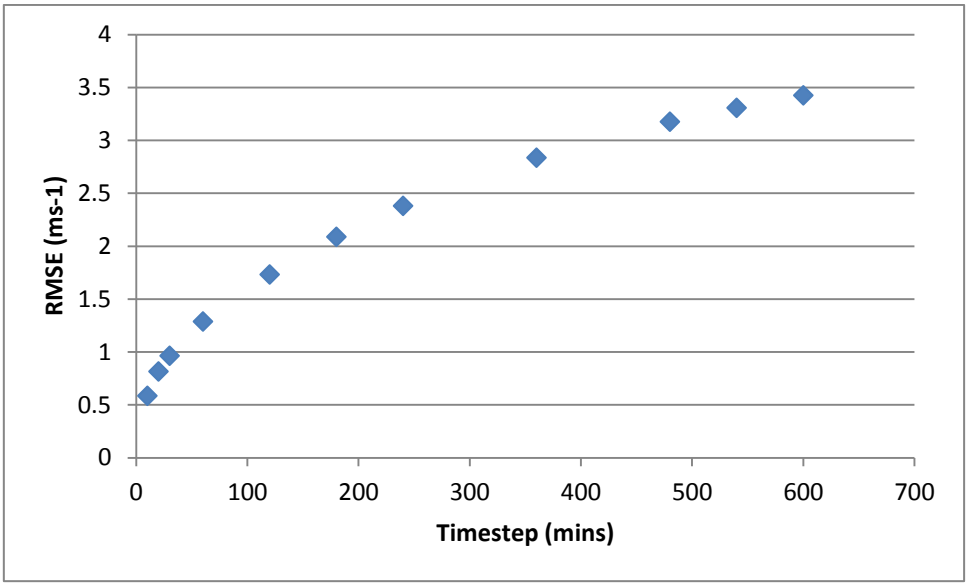

Figure 5.15 RMSE for the prediction of wind speed at Scroby Sands data assuming persistence as a function of timestep into the future

5.2.3 Selection of run periods

Case studies for the benchmarking runs were undertaken during the year of 1996, since relatively complete data from Scroby Sands were available for that year. Data from Scroby Sands were available at 33m and 51m and ten minute averaged temporal resolution. To include a variety of synoptic and seasonal conditions, three

cases from the beginning (3rd), middle (10th) and end (26th) of each month, were arbitrarily chosen to comprise the study. In two cases (early August and late November), runs could not be undertaken due to missing data. Three cases were undertaken from a different start date, again due to data availability. These were- early June (started on the 4th), early September (4th) and mid August (20th). Several initial feasibility runs had been undertaken to gain knowledge of the model, but as a novel study and with little experience, a variety of run lengths were operated to provide insight into the optimal run length. Runs undertaken at the beginning of the month were 24 hours long, late month runs were 36 hours long and the mid-month runs were 90 hours long, apart from the January and March cases which were 24 hours long. In total 80 days were simulated in the 34 benchmarking runs, accounting for around 22% of the year. A meteorological mast is located at Hemsby (figure 4.14) which is around 6km north west of Scroby Sands. Hourly wind speed data at 10m height were obtained from Hemsby to provide a context by which to judge model performance by using both series as predictors of wind speed observed at Scroby Sands. In the postprocessing stage the first six hours of each run were discarded to allow for model spin-up when calculating statistics but were retained in most plots to provide a little more overlap between model and observations.

5.2.3.1 Model setup

It is important to state from the outset that this investigation is not a comparison of the two WRF dynamical cores. While both NMM and ARW are used in the two configurations which are compared against one another, the dynamical cores are simply a setup selection, based upon a compromise of computational efficiency and outright performance. Results cannot be used as a direct means of comparison of the two model cores because the conditions are not the same.

5.2.3.2 Physical setup

5.2.3.2.1 Configuration 1, NMM-Setup

Model runs were undertaken on CREST03 to illustrate the potential of WRF given a relatively available yet not particularly powerful computing resource. In order to provide a compromise between performance and computing resource, the more numerically efficient WRF-NMM solver was used. To maintain the requirement of large spatial coverage in combination with high resolution centred over the site of

interest at Scroby Sands, a five domain setup was used for the NMM-setup runs described in Table 5.5. Four sequentially nested domains at increasingly high resolution were located over Scroby Sands within the parent domain shown in Figure 5.16. The NMM-setup runs were initialised from the 1.0° ERA-40 reanalysis product which provides variables on a spatial resolution of around 110km at the latitude of the UK. 65 vertical levels on which the gridpoints were located were used in each of the domains, with a concentration in the lower part of the atmosphere to give greater resolution in the PBL. Sixteen levels exist below 500m at heights very similar to those described for the ARW setup in the next section.

Table 5.5 Domain description of NMM-setup runs

Domain	Resolution (km)	Grid configuration
1 (Parent)	~84km	18 x 18
2	~28km	22 x 22
3	~9km	28 x 28
4	~3km	22 x 22
5 (Innermost)	~1km	19 x 22

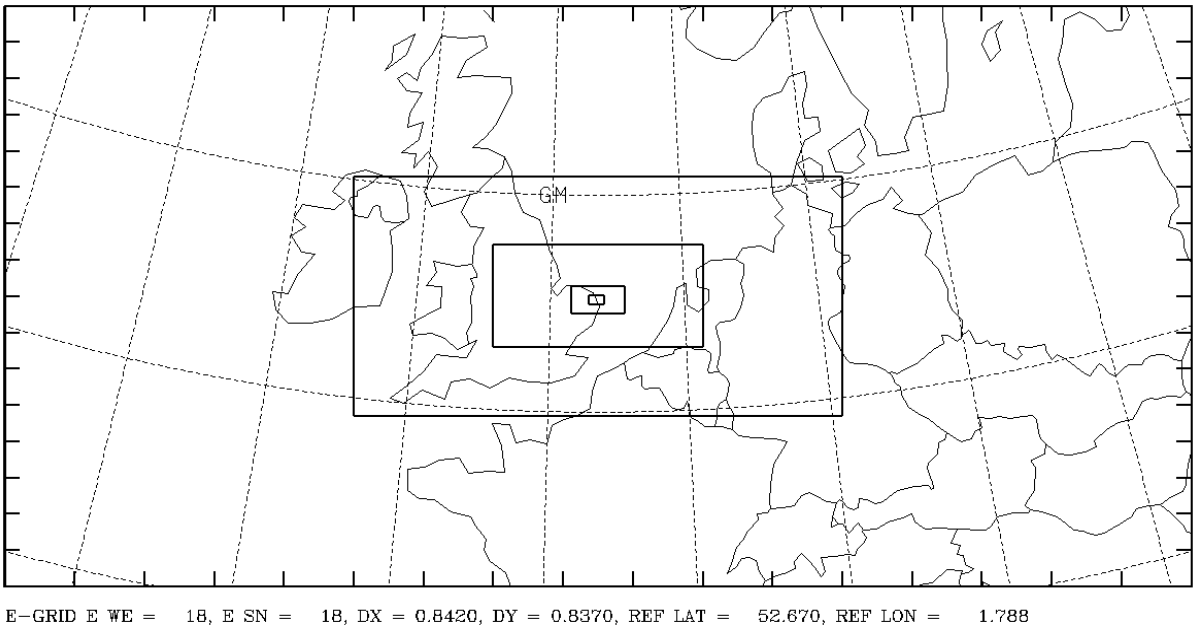

Figure 5.16 Model domains used for the NMM-setup runs

5.2.3.2.2 Configuration 2, ARW-setup

For the ARW-setup runs a larger computing resource was available which was utilised by running the model for much larger domains. A larger domain gives more space to simulate synoptic scale features and track their movement over the course of the run which is pivotal to contributing to the wind observed at the site of interest. The parent domain covered a much larger area at a far higher effective resolution than the parent domain of the NMM-setup. By using a higher resolution outer domain, fewer nests were required to reach the high resolution desired for the innermost domain. Having an outer resolution of 18km allows a higher resolution input to be used, which provides more information from which the model can simulate. Two further domains were nested within the parent domain providing an inner resolution of 2km shown in Figure 17 and described in Table 5.6. Nests were offset for the ARW-setup runs to give more space for the model to simulate features originating over the Atlantic, where many weather systems which influence the UK originate. For the ARW-setup runs the 0.5° CFSR reanalysis product was used to initialise the model, which equated to a grid spacing of around 55km. During the testing phase, breaches of the CFL (Courant Friedrichs Levy) criterion in the vertical plane were causing the model run to stop. The number of vertical levels was reduced to 50 vertical model levels which resolved the issue of numerical stability. Vertical levels were fairly evenly distributed apart from close to the surface where again more levels were concentrated to improve resolution in the PBL. 15 levels were located below 500m at 0, 20, 40, 65, 90, 110, 130, 150, 170, 190, 230, 270, 330, 405, and 490m.

Table 5.6 Model domains used for the ARW-setup runs

Domain	Resolution (km)	Grid configuration
1 (Parent)	18	178 x 130
2	6	208 x 169
3 (Innermost)	2	241 x 169

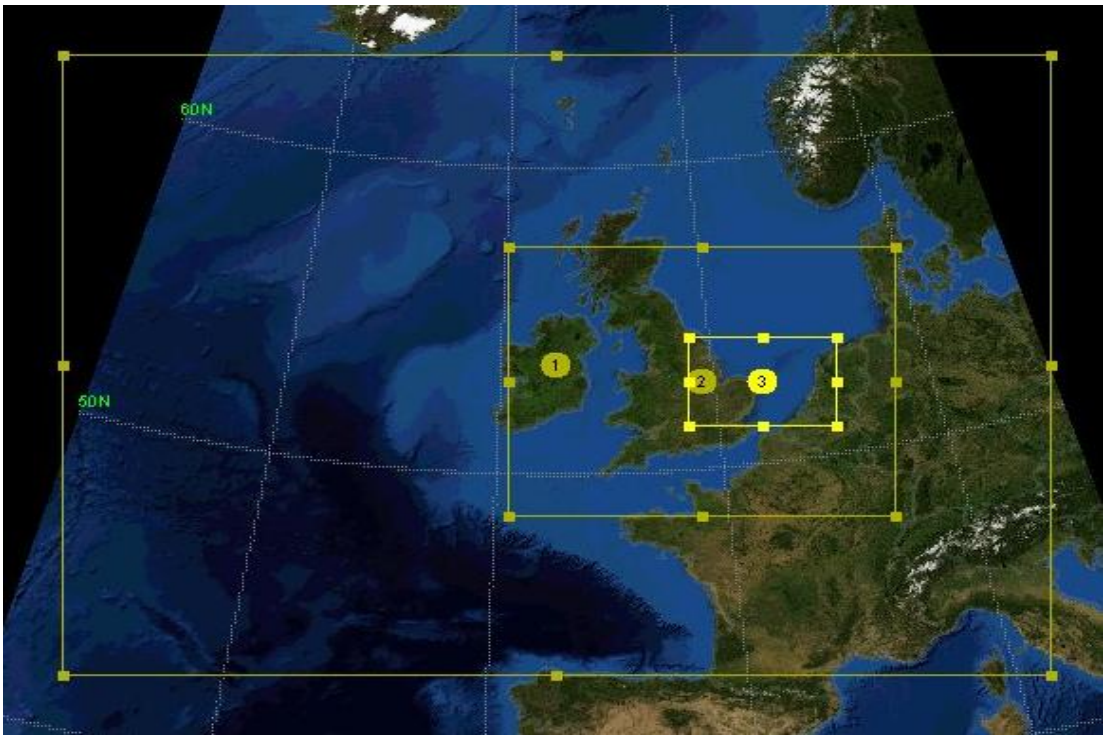

Figure 5.17 Location and coverage of domains for the ARW-setup runs.

5.2.3.3 Dynamical setup

As the first set of runs in the investigation, little was known about performance relative to dynamical setup, particularly for the sites used here, which is why it was important to undertake the benchmarking runs. Dynamically the model options were very similar between the ARW- and NMM-setup runs. The MYJ PBL scheme was selected because of its adoption by many other studies and because it was shown to perform better in the offshore environment (Kwun et al, 2009) than the other PBL scheme widely used with WRF, the YSU. In both setups, to account for boundary layer processes, feedback was switched on allowing two-way information flow between the domains. Cumulus parameterisation was switched off in the innermost domain of the ARW setup and the innermost two domains of the NMM setup to allow resolution of convective structures which becomes appropriate at around 5km. A full list of the dynamical options used is presented in Table 5.7.

Table 5.7 Dynamical options used in both ARW- and NMM-setups for the benchmarking runs.

Model Parameter	Setup
Vertical model levels	65/50 (NMM/ARW)
Nesting Feedback	On
PBL Scheme	Mellor-Yamada-Janjic (MYJ)
Cumulus scheme	Betts-Miller-Janjic
Radiation scheme - Long wave	GFDL
Radiation scheme - Short wave	GFDL
Microphysics option	Ferrier (new Eta) microphysics
Surface layer physics	Monin-Obukhov (Janjic)
Land surface option	Unified Noah land-surface model

5.2.4 Model output

Once the runs were undertaken model output had to be compared to observations. 50 metre wind speed at ten minute resolution for Scroby Sands was extracted from model output using the WPP method for the NMM-setup runs and the RIP4 method for the ARW-setup runs. Descriptive statistics were produced by calculating the mean and standard deviation values for each modelled and observed run. It was important to quantify absolute error of model performance as well as the accuracy with which variability was reproduced to provide results of use for the investigation. Absolute error was represented in this work by the RMSE (Root Mean Squared Error) statistic, which effectively reports the average absolute model error over the course of a run using Equation 5.11.

$$RMSE = \sqrt{\frac{\sum_{t=1}^{n}(O^t - F^t)^2}{n}} \qquad \text{Equation 5.11}$$

Where O^t is the observed windspeed at timestep t, F^t is the forecast or modelled windspeed at the corresponding timestep and n is the number of

timesteps. Pearson's product moment correlation coefficient (Equation 12) was selected as the method by which to quantify model accuracy in reproducing observed variability. In equation 5.12 n is the number of samples, i is the instantaneous observation, X^t is the observed value, Y is the modelled value and the bar signifies the mean value of the corresponding series. Pearson's correlation coefficient describes the covariance between two variables divided by their standard deviation which quantifies the strength of a relationship on a scale from -1 to 1. Perfect relationships where a unit change in one variable corresponds to the same degree of change in the other variable will have a correlation of 1 or -1 depending on the direction of the relationship. In a positive correlation both variables change in the same direction, whereas in a negative relationship, one goes up as the other goes down. A correlation coefficient of zero indicates no relationship exists between the two variables. A strong correlation implies the model is able to simulate the magnitude, timing and direction of wind speed change closely reflecting that observed. Timing of change is constrained by the temporal resolution at which the correlation analysis is performed. Of course some consideration must be paid to the fact that at 10 minute resolution, the highest resolution used in this work , wind speed may have changed dramatically.

$$r = \frac{\sum_{i=1}^{n}(X_i - \bar{X})(Y_i - \bar{Y})}{\sqrt{\sum_{i=1}^{n}(X_i - \bar{X})^2}\sqrt{\sum_{i=1}^{n}(Y_i - \bar{Y})^2}} \qquad \text{Equation 5.12}$$

5.2.5 Temporal filtering

Initial analyses were performed at 10 minute temporal resolution to match that of the observations. Such a temporal resolution is able to capture features below the resolved physical scale of the model. As a result the small, sub-grid scale features giving rise to short term changes in wind speed, which would be represented at 10 minute resolution, are approximated by the parameterisation schemes within WRF. Temporal filters were applied as a means of reducing the higher frequency variation to give priority to larger scale features operating over longer timescales which are resolved by the model. A simple moving average filter was initially applied as a feasibility study on the benchmarking performance investigation. The filter was

applied to both model and observational series at intervals of 3, 9 and 17 timesteps covering periods of 30, 90 and 170 minutes after Equation 5.13. In the equation x is the input wind speed, U is the filtered wind speed, n is the length of the timeseries, j is the timestep of the filtered windspeed and M is the order of the moving average filter. In order to preserve validity and compare like with like, the Scroby Sands observations were also filtered in the same way.

$$U_{(n)} = \frac{1}{M} \sum_{j=-(M-1)/2}^{(M-1)/2} x[n+j] \qquad \text{Equation 5.13}$$

Initially, the moving average filter was applied as a feasibility study to see if the filtering process worked as intended. Once proven, it was decided to proceed with the moving average filter but also test a different filter to address some problems with the application of the moving average filter. A more subtle filter was ultimately desired which would have a lesser effect upon the filtered series and preserve some of the key features to a greater extent than the moving average filter. Furthermore, the application of a moving average filter meant sacrificing a number of observations at each end of the runs to have enough observations to calculate the moving average, where ideally a filter would preserve the full length of the series. A review of temporal filters identified the Butterworth filter as a potential candidate with which to proceed. A Butterworth filter is designed to be reliable and consistent for permitted frequencies in the passband. A Butterworth filter also allows a degree of flexibility after the cut-off frequency, depending on the order of the filter which determines the strength of the frequency roll-off. Ultimately a lower order Butterworth filter retains more features present in the original series than a higher order scheme would. A first order, lowpass Butterworth filter was developed using the FDESIGN.LOWPASS tool in Matlab ©. Sampling frequency of the observations was set at 0.0017Hz (10 minutes). Three versions of the Butterworth filter were a implemented at timescales of 60, 180 and 360 minutes which corresponded to cut-off frequencies of 2.8×10^{-4} Hz, 9.2×10^{-5} Hz and 4.6×10^{-5} Hz, respectively. The Matlab © developed Butterworth filter was able to operate over the entire time series preserving all the features allowing a longer comparison than the moving average filter.

5.3 Establishing a baseline performance

5.3.1 Baseline statistics

Thirty four test cases from 1996 were undertaken for the site at Scroby Sands using the two different modelling configurations of WRF defined in the methods chapter. For ease of comparison, distinction between the configurations will be made evident by referring to the runs by their dynamical core of WRF. It is again stressed this is not a comparison of the two dynamical cores but an investigation of the restrictions associated with a particular level of computing resource. Results from configuration 1, optimised for a more restricted computing setup using the NMM dynamical core, will be presented under the name NMM-setup. Results from the second configuration, optimised for a high performance computing resource using the ARW dynamical core, are named ARW-setup. Descriptive statistics pertaining to the predicted, for both model setups, and observed wind speed can be found in Table 5.8 for the 34 cases run during 1996. Average wind speed observed at Scroby sands was 7.92ms^{-1}. For the same period the ARW-setup runs simulated an average windspeed of 8.62 ms^{-1} which was an overestimation by 0.7 ms^{-1}, while the NMM-setup runs produced an average of 7.07 ms^{-1}, an underestimation of around 0.9ms^{-1}. Average standard deviation is a measure of spread which, in this work, is used as an indicator of the variation present in a series. Average standard deviation was observed to be 2.5 ms^{-1}, while it was simulated by the ARW- and NMM-setup to be 2.6 and 2 ms^{-1} respectively. It can be seen that there is little difference in standard deviation across the three series, indicating that the variation in wind speed is captured reasonably well by the models, especially for the ARW-setup. Correlation analysis provides more information about the variability within the modelled series' relative to the variable of interest, i.e. the observations. An average correlation of 0.35 for the NMM-setup runs shows a weak relationship between model and observations but is at least positive indicating the direction of change is correct. Correlation is far better for the ARW-setup runs at a reasonable value of 0.65, which implies a moderate relationship between the two series', but is lower than the hourly correlation between observations at Scroby Sands and the onshore station at Hemsby of 0.75. Absolute error between modelled and observed wind speed is quantified in terms of root mean squared error (RMSE). RMSE for the NMM-setup

runs is 3.5ms^{-1}, but for the ARW-setup runs, is lower at 2.2 ms^{-1}. Referring back to the persistence statistics calculated for the Scroby Sands data provides an opportunity to compare model performance against a simple forecasting technique. WRF initially performs poorly compared to persistence on 10 minute intervals but becomes a preferable option to persistence after 180 minutes or 3 hours. The correlation between observed wind speed at Scroby Sands and Hemsby showed the highest correlation coefficient in 25 of the 34 test cases run, whereas the ARW-setup runs performed best in 7 cases and NMM-setup runs in the remaining 2 runs. In the two cases where the NMM-setup achieved the highest correlation, the ARW-setup once outperformed Hemsby. In the remaining cases where the wind speed at Hemsby showed the strongest correlation, the NMM-setup series outperformed the ARW-setup series on three occasions. In 8 of the 24 runs when the ARW-setup runs were outperformed by the Hemsby wind speed time series, the ARW-setup correlation was within 0.05 of the value achieved by the Hemsby wind speed time series. Apart from two situations, all the runs in which the model (in either setup) outperformed the Hemsby wind speed time series, displayed a correlation coefficient less than 0.7. Runs with the highest correlations were all achieved using the Hemsby wind speed time series, though the ARW-setup did produce 4 runs with a correlation over 0.9.

Table 5.8 Statistics based on 10 minute 50m wind speed for 34 runs at Scroby Sands throughout 1996 for the ARW-setup and NMM-setup runs and hourly 10m wind speed for the Hemsby met station.

	NMM-setup	ARW-setup	Observations	Hemsby
RMSE (ms^{-1})	3.47	2.19	N/A	N/A
Correlation Coefficient (CC)	0.35	0.64	N/A	0.75
Average (ms^{-1})	7.07	8.62	7.92	5.26
Standard deviation (ms^{-1})	1.97	2.58	2.50	1.87

5.3.2 Analysis of baseline performance

To help analyse the modelled and observed wind speed, an arbitrary measure of wind speed variability in time, referred to by frequency was established as follows;

- High frequency variation – rapid changes on the order of 1-3 timesteps (10 – 30 mins).
- Medium frequency variation – changes sustained on the order of 6-18 timesteps (1 – 3 hours).
- Low frequency variation – Trends in the timeseries on the order of 36+ timesteps (6 + hours).

Preliminary results indicate that both configurations of the model exhibit skill, though to varying degrees. Standard deviation values suggest that ARW-setup runs give levels of variation similar to that observed, while NMM-setup runs have a lower standard deviation indicating a more suppressed range in comparison. Correlation results suggest that ARW-setup runs do not fully replicate the timing and magnitude of observed wind speed variability, though there is a clear relationship while the NMM-setup runs exhibit little likeness to observations. By comparison, observations from the nearby onshore station at Hemsby do reflect the change in the Scroby series very well despite the difference in temporal resolution. In most instances of sustained wind speed change, as opposed to a high frequency returning event, features in the Scroby series tend to be present in the Hemsby series, supporting the presence of a strong correlation between the two series. Instances where significant high frequency variation is exhibited at Scroby Sands but little in the way of medium or low frequency features is observed, sees performance of the Hemsby series as a predictor of the Scroby series fall quite far below the average correlation. An example in which the dominant mode of variability is high frequency is evident in the 04/09/1996 case (Figure 5.20). This is most likely due to the different sampling frequencies of the Hemsby (hourly) and Scroby (ten-minute) data. The case of 26/10/1996 is an interesting case because the Hemsby data and ARW output appear very similar, in that both predictors expected the same pattern to be seen at Scroby Sands. As it transpires, agreement between the predictors did not translate to be the observed sequence of events observed at Scroby Sands for the case beginning on 26/10/1996 shown in Figure 5.21. Results from the 26/10/1996 case are of

importance because they clearly show that change in wind speed seen at Hemsby does not always reflect the change seen at Scroby Sands despite the close proximity

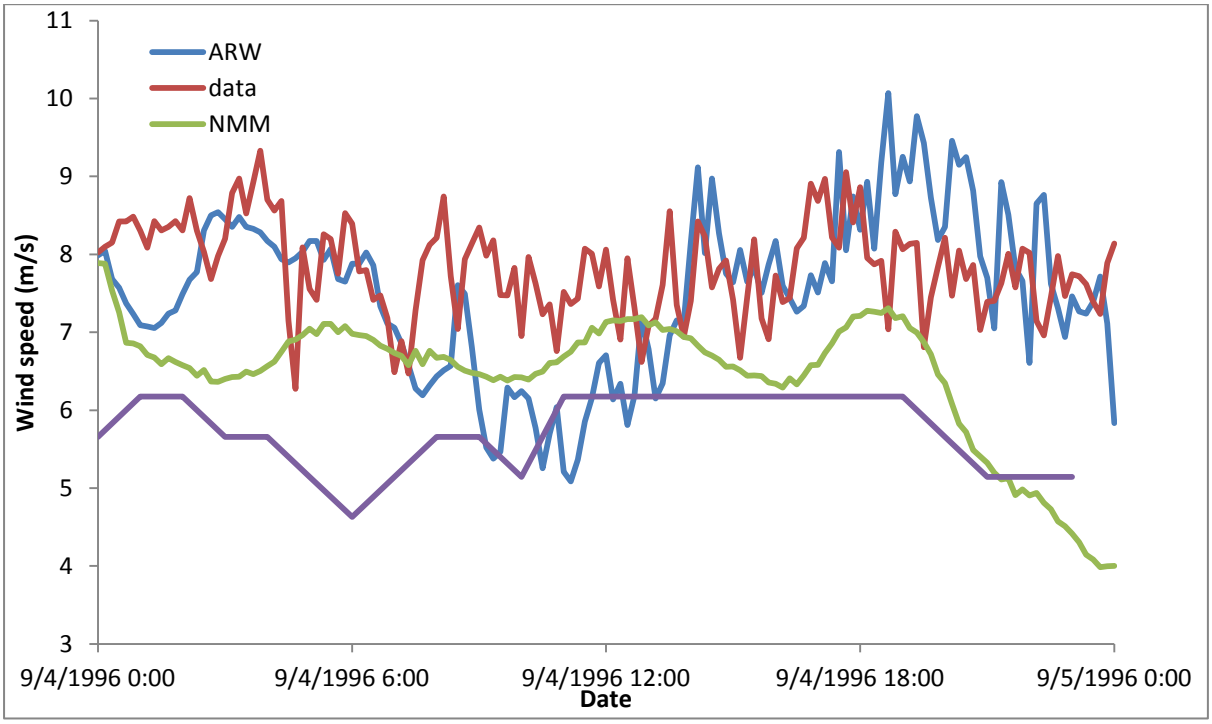

Figure 5.18 Wind speed for the 04/09/1996 case as simulated using both model configurations and observed at Hemsby and Scroby Sands.

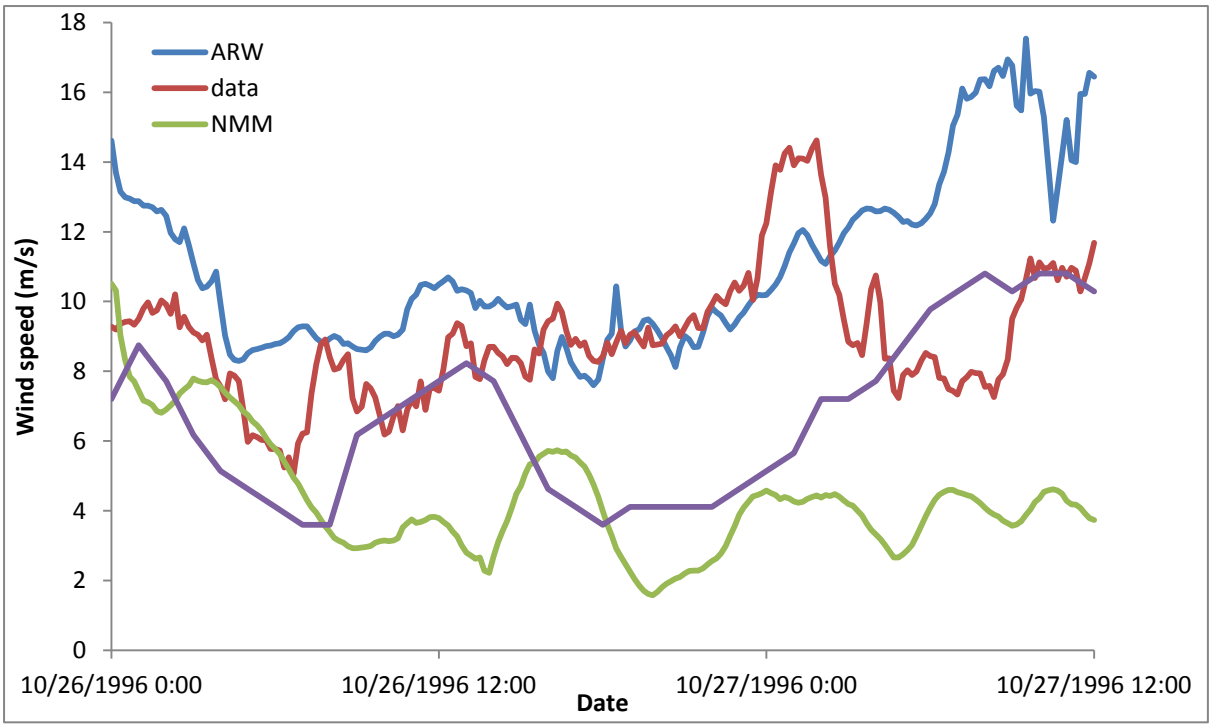

Figure 5.19 Wind speed for the 26/10/1996 case as simulated using both model configurations and observed at Hemsby and Scroby Sands.

To put these benchmark results into context a comparison can be made to similar research. Shimada and Ohsawa (2011) (herein SAO) conducted a yearlong resource assessment for the Shirahama observatory in Japan. WRF-ARW was initialised from 1.0° FNL (NCEP Final Analysis) data, incorporated FDDA (four dimensional data assimilation) and was updated from high resolution SST input. The correlation coefficient between model and observations was found to be 0.81 and the RMSE was 46% of the annual mean. In terms of correlation coefficient, the SAO study shows significantly higher values than either of the configurations used in this research. When RMSE is converted to percentage of annual mean, the NMM-setup runs achieve a value of 49%, while the ARW-setup runs achieve 25%, far lower than the value found by SAO. Techniques such as high resolution SST update and FDDA were used by SAO to improve model performance. High resolution SST data is an attempt to provide more information to the model regarding the thermal properties of the air over the sea, which can lead to a more successful simulation of small scale features such as convection which in turn can have an impact on local high frequency wind speed change. Data assimilation is a process which incorporates data into the WRF boundary files over the course of the run. The value of such techniques is evident in the high correlation coefficient achieved, however absolute error remains large compared to the results found in this benchmarking exercise, suggesting a potential area for improvement and an element of location dependence. In another study by Kwun et al (2009) which looked at representation of wind speed for three days from a range of sites around the Korean peninsula, eastern Asia. They found a correlation coefficient between observed and modelled hourly wind speed to be 0.6304 and 0.6483 for the YSU and MYJ PBL schemes respectively. While daily RMSE values were found to be 1.1360 and 1.1680 $^{ms-1}$ for the YSU and MYJ schemes respectively. Comparison against the results from Shimada and Ohsawa (2011) suggests the mode is capable of performing to a higher standard in terms of capturing wind speed variability, but results from Kwun et al (2009), show that model performance can vary with location. RMSE shows absolute error achieved in this work was lower than was seen by Shimada and Ohsawa (2011), however it remains large compared to results obtained by Kwun et al (2009) albeit for mean daily values and large in the context of wind resource assessment.

5.4 Analysis of individual runs

Average results give an initial impression of performance, but to fully understand model performance and identify areas for improvement, analysis of the individual runs is required. A selection of individual runs is presented to illustrate more closely particular features, model traits and capabilities of each setup. Figure 5.22 shows the 10/10/1996 case, in which the observed wind speed displays a significant degree of variability in the high frequency range as well as some medium and low frequency variability. Such a complex case, in which wind speed varies to a moderate extent in all three frequency ranges, presents a good test of a model's ability to accurately simulate the controlling dynamic features resulting in such wind speed variability. Change in medium frequency variability is well reproduced by the ARW-setup, with timing, magnitude and direction of change generally reflecting observations. High frequency change is less well reproduced in the ARW-setup as the modelled and observed series' diverge from one another on occasion. 10/10/1996 is an example of a statistically high quality run using the ARW setup, the correlation coefficient is high at 0.89 and the RMSE of 2.0 ms^{-1} is below the ARW-setup average of 2.1 ms^{-1}. Output for the 10/10/1996 test case produced using the NMM setup did not perform as well as the ARW-setup, but did manage to account for some of the medium frequency features, such as the slow rise in the middle of the run and the drop then rise at the end. Data from Hemsby show that similar trends in wind speed are seen at Scroby sands, but the Hemsby data do not offer a precise reflection of medium-high frequency events at Scroby Sands. 10/10/1996 is one of the runs where the model statistically outperforms the Hemsby data. An interesting feature exists at the very beginning of this run, where wind speed in neither model is correct, implying an inaccuracy, for Scroby Sands at least, is present in the input data. This serves as a reminder of the challenge facing NWP that any model is reliant on the quality and accuracy of the input data it is initialised from. Any initial inaccuracy indicates a misrepresentation of initial conditions, from which the model is less likely to be able to correctly simulate atmospheric evolution.

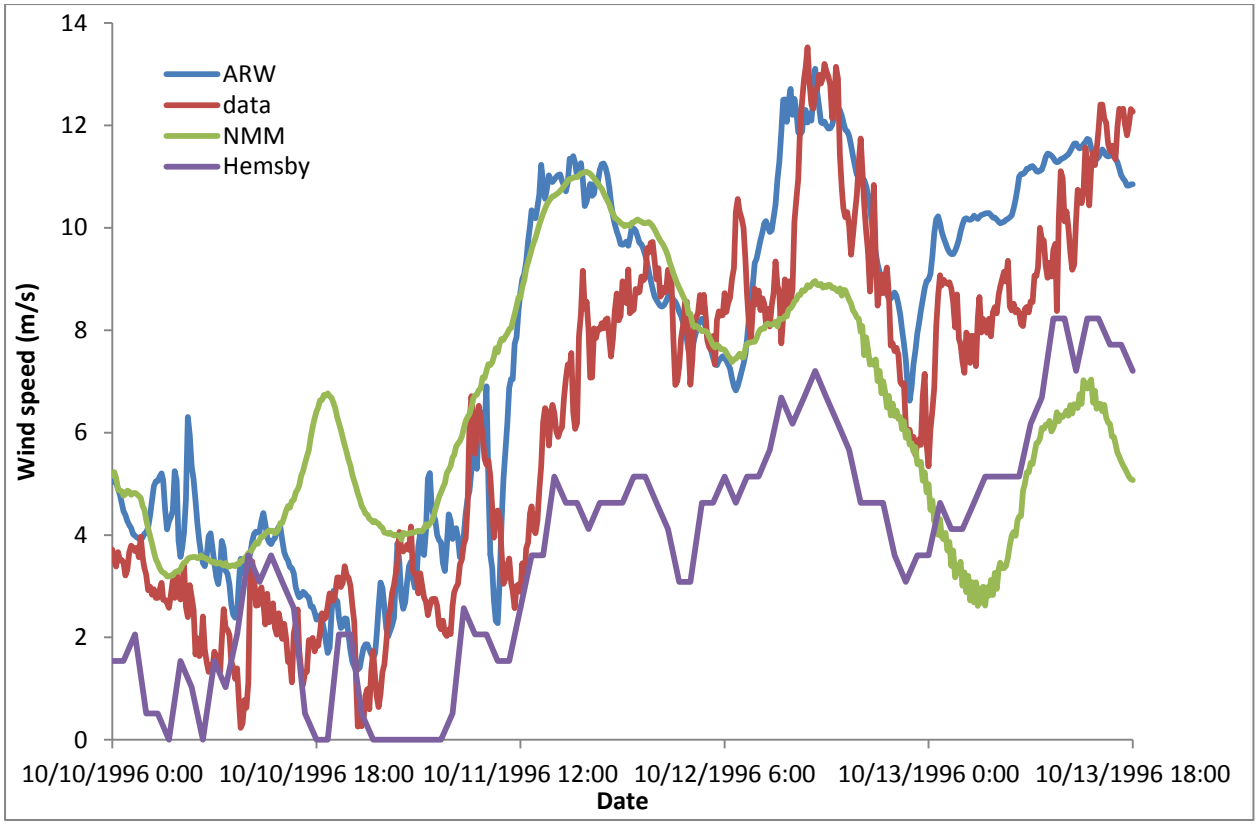

Figure 5.20 Wind speed at 50m and 10 minute resolution, simulated by the ARW-setup, NMM-setup and observations for a 90 hour run beginning 10/10/1996. Stats for ARW, NMM and Hemsby, Correlation coefficient (0.885, 0.479, 0.883) RMSE (2.03, 3.11, N/A ms^{-1}).

Another good example of the variability in model performance is provided by the 26/12/1996 test case. It is one of the very few instances where an NMM-setup series statistically outperforms the ARW-setup series (Figure 5.23). Observations of the wind speed display predominantly high frequency variation superimposed on a low frequency decline then rise. In the middle of the run there is a medium frequency ramp up and recovery (1) which is pivotal to the performance of the ARW-setup series. The ramp up in speed is well timed in the ARW-setup series but its magnitude is overestimated and the recovery down completely missed (2). From here (2) the ARW-setup series reproduces many observed features but with a large positive bias, seen as a positive vertical offset from the observations. Performance of the ARW-setup series is very good initially, with the divergence in the middle of the run akin to a practical demonstration of chaotic divergence represented by the Lorenz attractor, where two paths begin close together but some features are not quite captured accurately by the model and at point (2) the series diverge. It is

unknown as to the reason for this particular divergence seen at (2), which could be a chaotic feature or an inaccuracy in the model physics. The NMM-setup run is a good example of the lack of high and medium frequency variation when running using this setup. Observations are characterised by a soft sloped V-shaped trend through (3). A similar trend is displayed by the NMM-setup (4), however no sign of high frequency variation is seen neither is the small ramp event in the middle of the run at (1). Despite the lack of variability, replication of the general trend by the NMM-setup is relatively good with a correlation coefficient of 0.69 and a RMSE of 1.45 ms^{-1} which is far below the average value for all the runs (3.47 ms^{-1}). Hemsby data display an expected negative bias due to the lower height at which wind speed are recorded. As with the majority of the test cases, wind speed at Hemsby provides a good representation of wind speed at Scroby Sands. In this particular case of 26/12/1996, most of the important features present in the Scroby Sands series are visible in Hemsby, evidenced by the high correlation value.

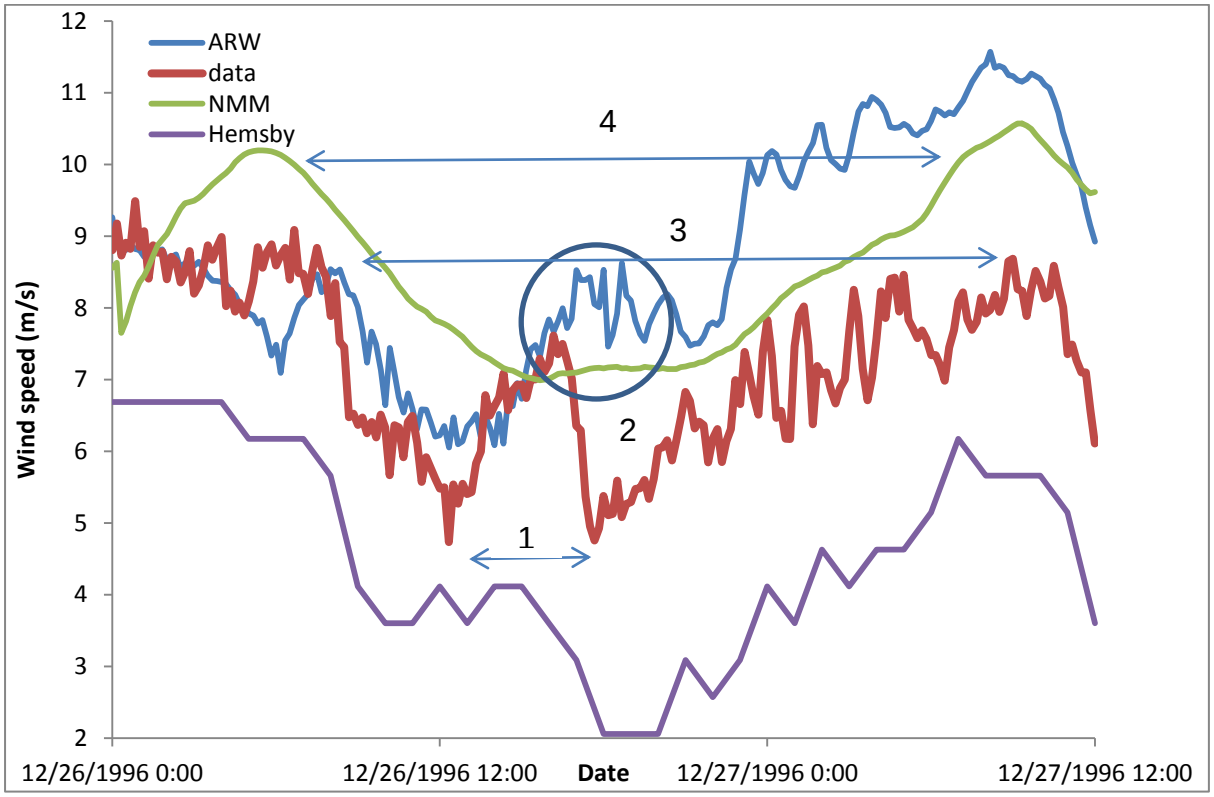

Figure 5.21 10 minute 50m wind speed as simulated by WRF-ARW, WRF-NMM along with observations for a 36 hour run beginning 26/12/1996. Stats for ARW, NMM & Hemsby, CC (0.450, 0.694, 0.868), RMSE (2.07, 1.64 ms^{-1}).

For all 34 individual runs, correlations for both model configurations were considered by reference to average wind speed (modelled and observed), standard deviation, and the coefficient of variation. No significant relationship was identified between correlation and the type of wind experienced in terms of speed, with the model seeming to show equal aptitude for low and high wind speeds (Figure 5.24). However the model does perform slightly better when standard deviation is higher, shown in Figure 5.25. These limited results show that the model performs with consistency and has no bias towards particular wind speed conditions, but is able to better simulate wind speed in a series where variation is relatively high compared to the mean wind speed. A lack of model bias is a positive sign for the application of NWP to the field of offshore wind resource assessment. The preference shown for higher levels of variability indicates the potential for some form of classification scheme which might help add value to model output and offer an insight into the potential level of model performance.

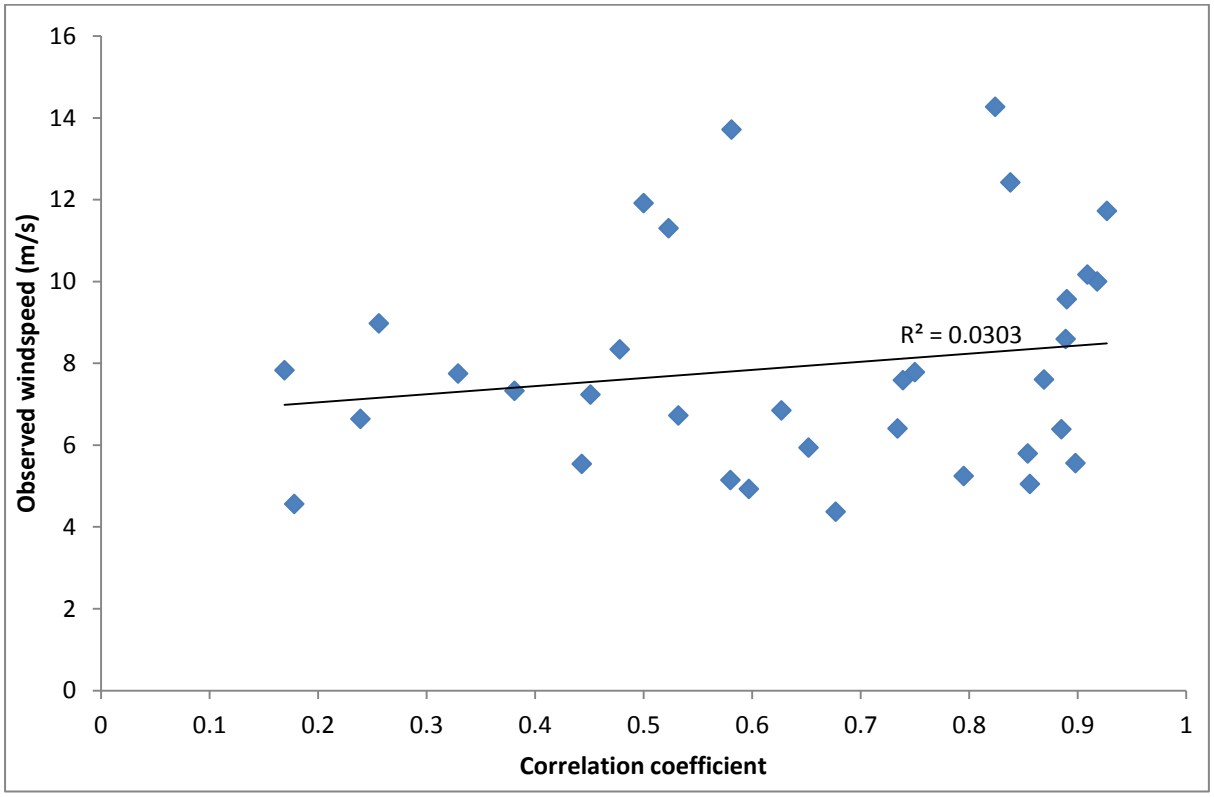

Figure 5.22 Scatterplot and correlation coefficient pertaining to the relationship between observed and simulated (ARW-setup) wind speed, by reference to observed wind speed.

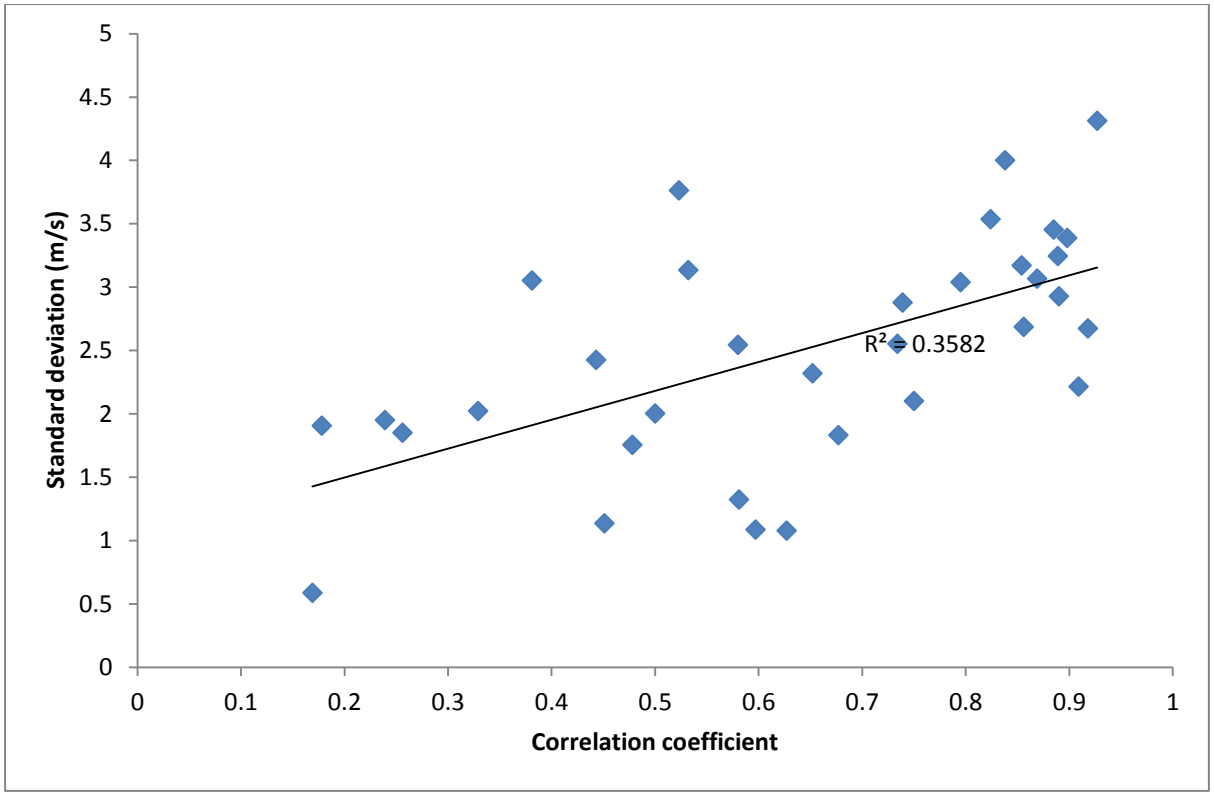

Figure 5.23 Scatterplot and correlation coefficient pertaining to the relationship between observed and simulated (ARW-setup) wind speed, by reference to observed standard deviation.

5.5 Model performance as a function of computing resource

Use of the two WRF cores in this research is not a comparison of one against the other, but a setup choice designed to deliver maximum efficiency given a particular computing resource. It is evident from the results in Table 13 that by restricting the computing resource, the NMM-setup runs performed much less accurately than the ARW-setup runs. RMSE was higher for the NMM-setup than the ARW-setup and particularly high as a potential wind resource assessment tool. Variability was poorly captured as indicated by the low correlation coefficient and was not of a level comparable to either the ARW-setup or the Hemsby series. An example of the typically observed behaviour of both models is shown in Figure 5.26, where the NMM-setup run shows no appreciable high frequency variation but captures the general trend of change in wind speed to some extent. High frequency change is present in the ARW-setup run and is at times reflective of the observations, apart from, most notably, the ramp down and recovery which is observed (1) to be less abrupt than was simulated (2). Most of the observed major low frequency features are present in the ARW-setup run. At the beginning of the run

in Figure 5.26 it is clear to see the two model configurations do not start from the same point, identifying a discrepancy between the two input data sources, ERA-40 and CFSR. As a result the wind speed in the NMM-setup run starts with a negative bias, while in contrast the ARW-setup run starts with a positive bias, compared to observations. The model runs are updated with boundary conditions from the input data every six hours, so performance of the different configurations will be influenced by the input data as well as the physical setup. The ARW setup run is able to converge to the observed pattern of wind speed change for the majority of the run, while the NMM-setup is not. This is a good example of the sensitivity of a model run to initial conditions, in some cases the model is able to recover but in others it cannot.

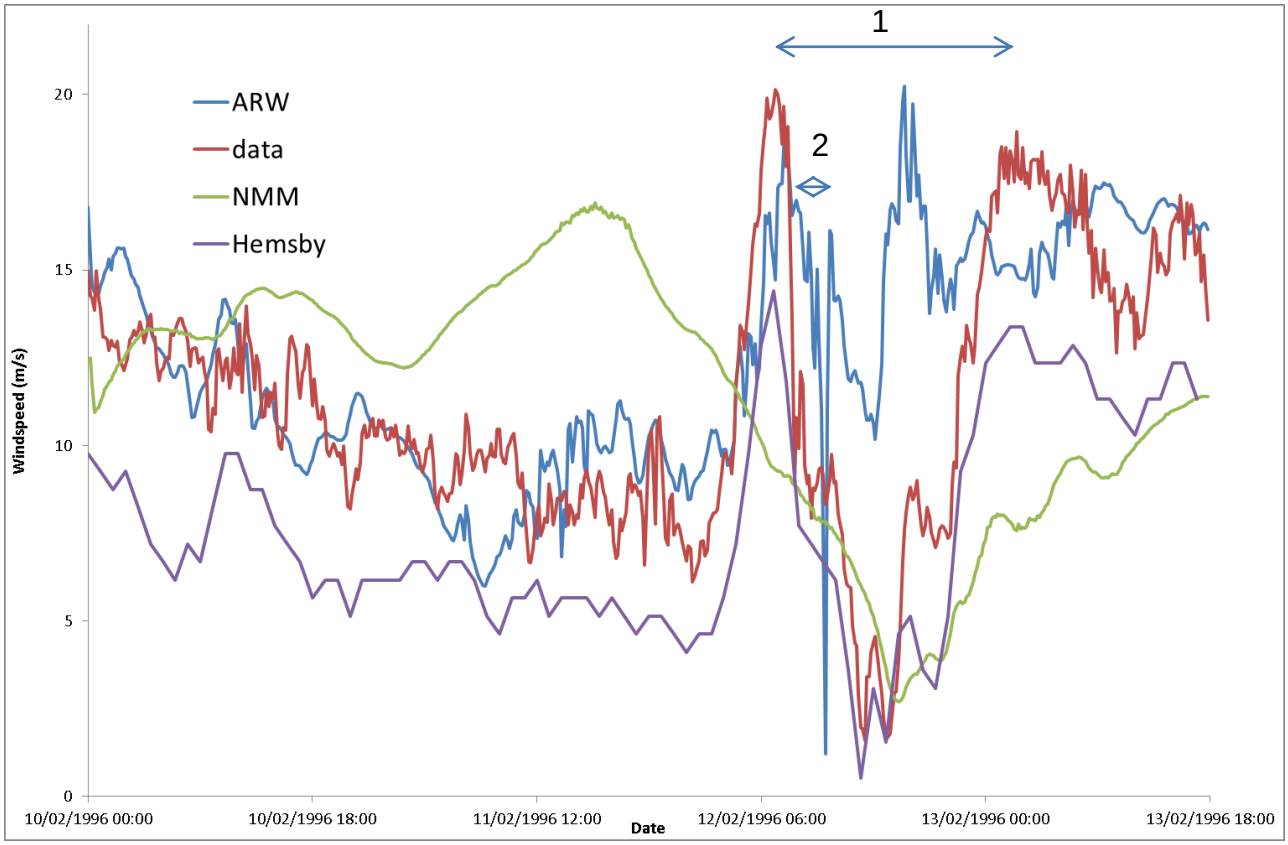

Figure 5.24 Single case study from February 1996 showing observed wind speed at Hemsby (10m) and Scroby Sands (50m) alongside 50m model output from ARW- and NMM –setup runs.

The restriction placed on model setup by the available computing resource, dictates at what level of accuracy the model can perform. Restricted computing resource affects model performance in two major ways. Firstly model setup has to be

optimised for the available computing power which requires a compromise between performance and time. In order to simulate wind speed for a single point, a relatively high resolution domain is required but it must be accompanied by a large spatial domain to capture large scale synoptic processes. To achieve both, a relatively large number of nested domains is required and to maximise computational efficiency the domains tend to be as small as possible. To function optimally, domains need to be as large as possible to allow complete resolution of the atmospheric features, with spatially restricted domains there is a risk features will not be completely captured. The second restriction upon model performance imposed by a limited computing resource is the resolution of input data. Because more nests are required the resolution of the large scale outer domain is very low, for WRF, input data is manipulated onto a model grid from which the model is initialised, so there is little point obtaining input data which exists at a higher resolution than the outer domain because the data will simply be lost when mapped to the input grid. As a result lower resolution data is used which gives less information to the model from which it can simulate. All told the effect of limited computing resource upon model accuracy is potentially significant because of the restrictions placed on the model equations. Ultimately the success of a modelling system is determined by absolute error, in this case represented by RMSE. While it is a good measure of modelling success, there is a lot more information pertaining to the performance of the model which is of great relevance to an end user. It was for this reason that both correlation and RMSE were always considered through this research as the measures by which to judge performance to appreciate the magnitude of difference between model performance and observations but also how well variability is captured. Hughes and Watson (2012) highlighted the importance of seeking to improve model performance by focussing on how well variability is resolved rather than simply aiming to reduce RMSE. By thoroughly identifying the reasons behind observed performance there is a better chance it can be improved. Comparing the results from both model configurations showed how restricting the computing resource effectively reduced the level of detail which the model could resolve to really only produce successful variation in the low frequency range. Given RMSE could be minimised using a reasonably accurate low frequency output and post processing, it might be possible to implement an operational resource assessment tool using a computationally restricted configuration, but to maximise the potential of the mesoscale model,

Hughes and Watson (2012) suggest focussing on improving correlation, which will either result in a direct improvement in RMSE or a greater ability to account for it through bias correction. Options which exist to aid performance such as nudging, data assimilation or ensemble generation, are all computationally intensive and thus inapplicable to a user with limited computing power. From the results of this work it is clear to see that more computing power translates to better model performance. More input data is fed to the model over a larger area at higher resolution, because more processors are available to deal with the extra work. As a result features within the model are better represented and defined in space and time, which feeds more information throughout the model systems down to the parameterisation schemes. Ultimately by giving the model a better representation of the atmosphere it is more likely to simulate evolution with a greater degree of accuracy.

5.6 Considering model performance in the temporal domain

Part of the benchmarking investigation was to identify aspects of the study which were factors in determining model performance. Inspection of individual runs identified a lack of ability in the NMM-setup to reproduce high frequency variation, yet retain some elements of the observed low frequency change. An increased computing resource allowed for larger, higher resolution model input data, larger grids and increased spatial coverage, which were key factors in enabling the ARW-setup runs to offer a significant improvement in performance. Despite producing levels of variation comparable to observations, it is in the high frequency range where ARW-setup runs struggle to capture observed variability. Performance problems at short temporal scales were also present in the work by Nunalee and Basu (2012), where variation in model output appeared damped in comparison to observations. With the innermost model domain resolution being 2 km, the smallest features which can be expected to be well resolved are around 14km in size. Below 14 km the model is able to account for atmospheric features to an extent, but does so through parameterisation schemes, specifically the planetary boundary layer scheme. Given that the temporal resolution of the runs is 10 minutely, it is unlikely that model performance will be best at simulating high frequency change. Atmospheric features responsible for change in wind speed on a 10 minute timescale are likely to be small scale for example turbulent fluctuations, such a scale is below that directly resolved by the model. In order to investigate model

performance on longer timescales at which atmospheric features are directly resolved, temporal filtering was performed on ARW-setup model runs and concurrent observations. Initially the unweighted moving average filter, was applied to the10 minute model output and Scroby Sands observations at intervals of 3, 9 and 17 time steps which corresponded to 30, 90 and 170 minute periods. Subsequently a low-pass Butterworth filter was also developed to filter out frequencies below 60, 180 and 360 minutes. Table 5.9 summarises the average results from all 34 runs. A clear improvement is evident from both of the filtering processes. While filtering will intuitively reduce the variation in a series, the model output must still exhibit similar characteristics to the observations in order for the correlation to improve. Results are improved for the 3 hour time increment by a greater margin using the moving average filter than by the Butterworth filter. Furthermore the performance gap between the model output and observations from the Hemsby series is reduced.

Table 5.9 Average statistics for the 34 ARW-setup cases run after temporal filtering of model output and observations using an unweighted moving average (MA) filter and a lowpass butterworth filter.

	Hemsby Raw	Hemsby MA	NMM Raw	ARW Raw	ARW MA	ARW Butterworth Filtered		
Effective temporal resolution (Minutes)	60	180	10	10	170	60	180	360
Correlation	0.746	0.785	0.350	0.639	0.720	0.662	0.698	0.733
RMSE			3.471	2.196	1.876	2.107	1.957	1.798

Correlation coefficients improve by between 0.06 and 0.08, depending on the filter used, when the considered temporal resolution is extended from 10 minutely to 3 hourly. For the same filtering process RMSE dropped by around 0.2ms^{-1}, or roughly 10%, to 1.9 ms^{-1}. Some runs are better improved by filtering than others, for example on the 03/05/1996 run the initial 10 minute correlation coefficient is 0.58. After filtering the correlation coefficient at 30 minutes is 0.81, at 90 minutes is 0.93

and at 170 minutes is 0.97. Improvement in accuracy is possible by filtering the series if the underlying performance if the model is accurate at the filtered timescales, on a run by run basis this is unknown until the filtering is undertaken, but the general improvement seen across the runs suggests an inherent skill is present. The fact that not every run displays a marked improvement is evidence that the process of filtering will not necessarily improve performance. The 180-minute Butterworth filter was applied to hourly data from Hemsby to see the effect of filtering the observed data. Average correlation between observations from Hemsby and Scroby Sands improved to 0.79, with ARW-setup correlation improving to around 0.7. At hourly resolution, ARW-setup runs outperformed the Hemsby data in 7 of the 34 cases, with a further 8 cases possessing a correlation coefficient only 0.05 less than the Hemsby correlation coefficient. Filtered to a 3-hourly resolution, ARW-setup output outperformed Hemsby in 13 cases and came within a correlation coefficient of 0.05 in a further 4 runs. These results confirm the value of using the model when applied to simulate features of appropriate scale. When done so, model output is as good as a nearby met station yet significantly cheaper and more versatile both in terms of temporal capacity and the variables which can be produced. Temporal averaging affords the ability to compare the model output with observations at an optimal temporal resolution for the 2km model setup. Low and medium frequency features are retained while small, high frequency change are removed.

5.7 Filter performance

As the average statistics suggest, the unweighted moving average and low-pass Butterworth filters are generally close in performance, evident throughout the individual runs. It is important to consider the impact of the filtering process upon the series to which it is being applied. Manipulation of the filtered series is the ultimate purpose of a filter, however the intention of a filtering process is solely to preserve traits of the unfiltered series at a different temporal resolution, with minimal modification of the original features. While the moving average filter provides marginally better results, it is a less discriminating process which has a notable smoothing influence. The Butterworth, filter on the other hand, operates less intrusively and preserves more of the original features in a series which is evident in the run beginning on the 10th of May shown in Figure 5.27.

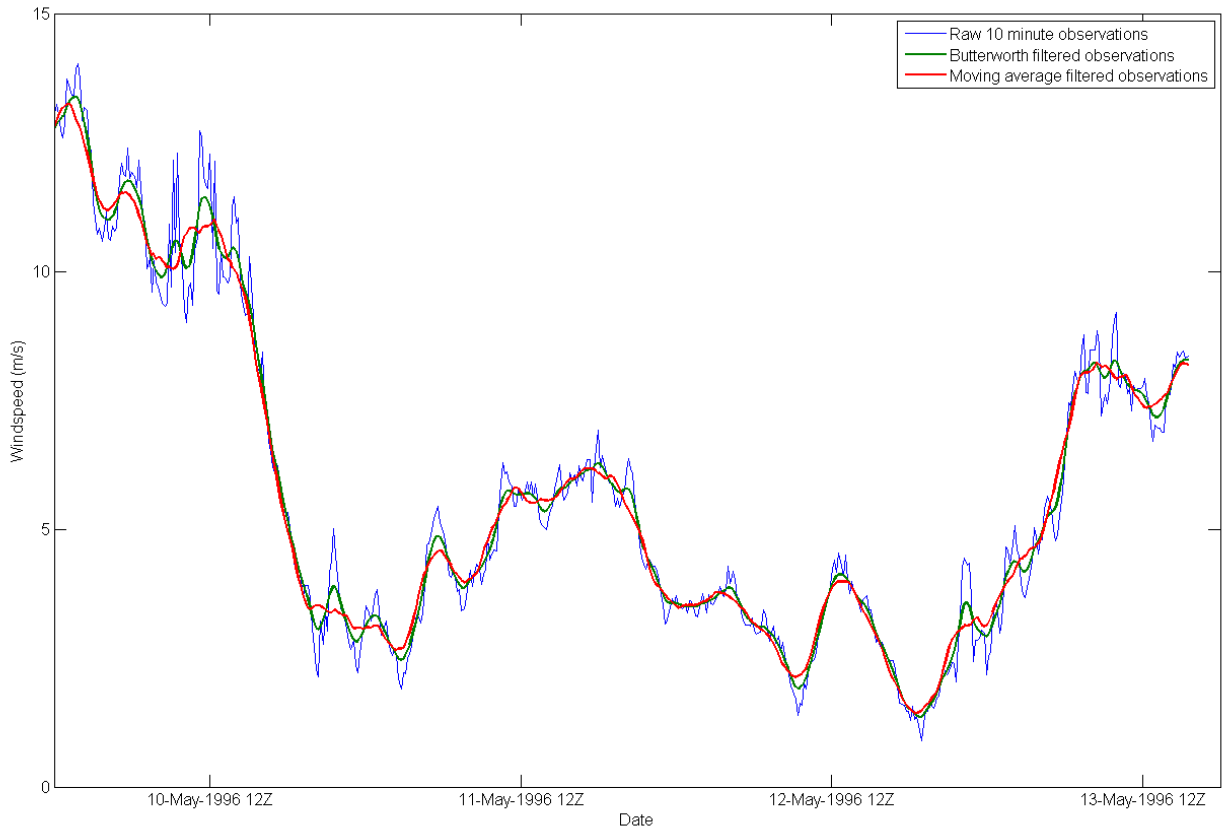

Figure 5.25 Raw 10 minute observations alongside a 17 timestep filtered moving average and 180 minute Butterworth filtered wind speed for the 10th May 1996 case at Scroby Sands.

5.8 Summary

The benchmarking exercise provided baseline statistics relating to model performance as a wind resource assessment tool. Initial results suggested some skill but limited performance which compared unfavourably against local observed data. Model configuration was considered and found to be a factor in determining performance, where performance improved with greater computing resource and a more setup options. Closer inspection of model performance identified high frequency variability range as the area for improvement, which was addressed through the application of temporal filters. Filtering model output and observations to longer timescales showed model performance to be better when temporal resolution was lower. Temporal resolution of wind speed change is directly related to the size of the atmospheric features which cause that change. Numerical models are constrained by their inner grid resolution to be able to directly resolve features below a certain size. The filtering process effectively moved the focus of the simulation

from high frequency features to lower frequency features which the model was able to more accurately simulate because such features were directly resolved and not approximated. When filtered to 3-hourly resolution, the model performed as well as the nearby observational series. Ultimately, the results show that the model is a good resource assessment tool when applied to the correct spatial scale, whereby it simulates large and medium temporal scale features well, which are responsible for the significant changes of interest in a long-term study. Performance is less successful at small scales, which dominate short term resource assessments such as operational forecasting.

6 A long-term study of the wind resource at Shell flats and the Supergen exemplar site

6.1 Method

A long term modelling study was required to validate the performance of WRF as an operational wind resource assessment tool, which would have to provide a resource assessment covering a period of at least a year. This study also afforded the opportunity to test the location dependence of model performance by simulating for a different location, namely Shell Flats. The resource assessment investigation was chosen to provide a look at the model's capacity to simulate other variables critical to wind farm operators, including wind direction and atmospheric stability. Undertaking a study of such length provided the opportunity to characterise model performance and trends in variables through time and by reference to synoptic settings represented by weather type. A year-long resource assessment was produced for the Supergen exemplar site to showcase the potential of WRF as a resource assessment tool and provide a dataset for use by other members of the consortium.

6.1.1 Computing setup

With the initial class 2a computing account on HECToR used for the benchmarking investigation and a waiting period until the RAP allocation of resources for the second HECToR account, computing time on the Loughborough University HPC cluster Hydra was obtained for the resource assessment runs. Hydra was a less powerful computing cluster than HECToR but still offered a comprehensive resource. Model setup was adjusted accordingly to utilise the computing resource efficiently, allowing multiple simultaneous runs to ensure completion on time. Each run was undertaken on 144 cores of Hydra and up to 8 jobs were submitted simultaneously. Given the large number of runs to be undertaken, computational efficiency was key. While some features of the more successful ARW-setup from the benchmarking runs were preserved such as the dynamical core, nesting setup and large spatial coverage, some features changed. For example the YSU PBL scheme was used as a simpler and quicker option for approximating boundary layer processes, rather than the higher order MYJ scheme.

The same computing setup was used for the Supergen exemplar resource assessment using 144 cores for each run on Hydra. Post processing was undertaken in situ in the hydra HPC in serial mode which produced the time series output of desired variables for Shell Flats and the exemplar site. The output was then transferred to the desktop computer for analysis using Matlab ©.

6.1.2 Selection of run periods

6.1.2.1 Shell flats

Data for Shell Flats were available from the two masts, which are around 6km apart, from June 2002 until December 2003. A number of discontinuities were present throughout both the observational series which, as a result, meant the study was split into five parts detailed in Table 6.10. Runs comprising four day periods were undertaken and concatenated to comprise the entire duration of the five periods. Output from the model was produced for Mast 2 to be compared to that observed data series because it provided more consistent continuous data than Mast 1.

Table 6.10 Run period description for the Shell Flats resource assessment

Run Period	Start (00:00)	End (Time stated)	No. of days
1	17/06/2002	03/02/03 (2250)	231
2	09/02/2003	23/03/03 (0420)	43
3	12/04/2003	22/05/03 (0330)	41
4	10/06/2003	19/09/03 (2350)	102
5	22/09/2003	04/12/03 (2350)	72
Total	17/06/2002	04/12/03	489

As a result of the close proximity of the Shell Flats masts, data from Mast 1 would serve a dual purpose. Firstly, it would be used as a yardstick by which to judge model performance as a predictor of Mast 2 by comparing both series against observations from Mast 2. Secondly, data from Mast 1 was incorporated into the model input, using the Obsgrid program, to nudge the simulations towards observations. The nudging process is described in more detail in section 4.4.3. During Period 1, data from Mast 2 were available throughout, while data from Mast 1

were intermittent and available in three parts. As a result, comparisons involving Mast 1 data could only be made during these periods while statistics for the full duration were available between the model and Mast 2. In the fifth period of the assessment, data from Mast 1 were again intermittently available. Nudging could only take place with suitable data, but this also means that comparisons between model performance and inter-mast performance cannot be performed for the final period. To provide another frame of reference by which to assess model performance, output was also validated against an observational series from a land-based station at Squires Gate. Squires Gate is located around 13.5km South-East of Mast 2 at Shell Flats and 19.5km in the same direction from Mast 1. Data from Squires Gate series were missing between 25/5/03 and 01/06/03, which meant that Period 3 could not be compared to data from Squires Gate but the other time frames could. At the end of the resource assessment, the final five days could not be compared to Squires Gate because of a lack of data from the site. Therefore the final period compared to Squires Gate, terminates on the 30th November 2003. Data from Squires Gate comprised hourly wind speed and direction at 10m height. WRF was initialised from the 0.5° 6-hourly CFSR reanalysis product.

6.1.2.2 Supergen exemplar farm

Raw input data for the latter half of 2003, used for the Shell Flats resource assessment, were available on the pre-processing server, CREST03. As a result a wind resource assessment for the Supergen exemplar farm was undertaken from June 2003 – June 2004. The 0.5° CFSR reanalysis product was used as input at six hourly intervals.

6.1.3 Model setup

6.1.3.1 Physical setup

6.1.3.1.1 Shell flats

The nested model domains used are shown in Figure 6.26. Three domains were used in total: a parent domain set at 18km grid resolution; an intermediate domain at 6 km; and an innermost domain from which the outputted variables would be extracted at 2km resolution. The outer domain is comprised of 107 x 90 grid points, the middle domain of 112 x 94 grid points and the innermost domain of 97 x 82 grid points. 40 model levels were used, with a concentration at the surface to

allow a higher level of processing in the PBL. Nine levels were located below 500m at heights of roughly 0, 50, 90, 140, 180, 230, 280, 330, 390 and 460m.

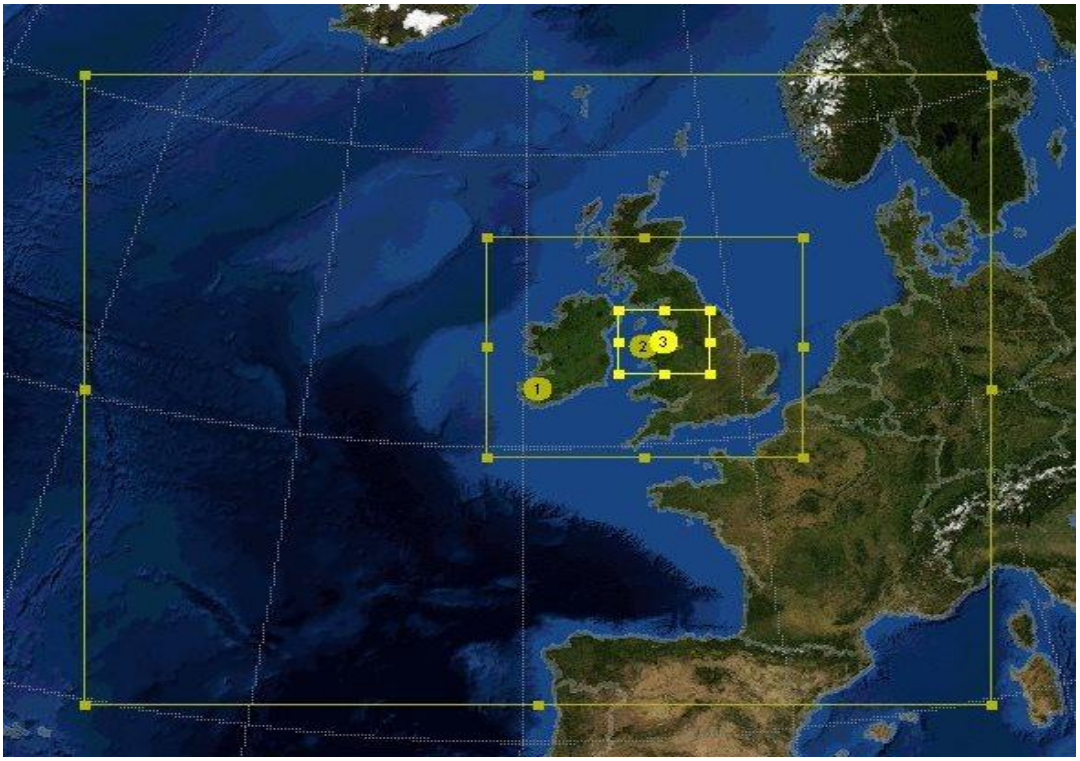

Figure 6.26 Domain locations and positions for the Shell Flats resource assessment.

6.1.3.1.2 Supergen exemplar farm

Domain setup for the Supergen exemplar site followed the same priorities as the Shell Flats site whereby a large spatial coverage at relatively high resolution was adopted to utilise the computing resource and reduce the number of nests used. The nesting setup is shown in Figure 6.27 with the focus of the domains all shifted slightly eastward to reflect the location of the Supergen exemplar site. Resolution is slightly coarser for the Supergen exemplar resource assessment than the Shell Flats runs because a large inner domain was desired to capture the full wind farm extent and surrounding area. An efficiency compromise was achieved by lowering the resolution slightly with the increase in inner domain size to ensure the extra spatial coverage did not increase computing resource excessively. The parent domain for the run was at 27km resolution and comprised 107 x 90 grid points, the middle domain at 9km resolution comprised 112 x 94 grid points and the innermost domain at 3km

resolution comprised 121 x 103 grid points. The vertical grid spacing was the same as that used in the Shell Flats runs.

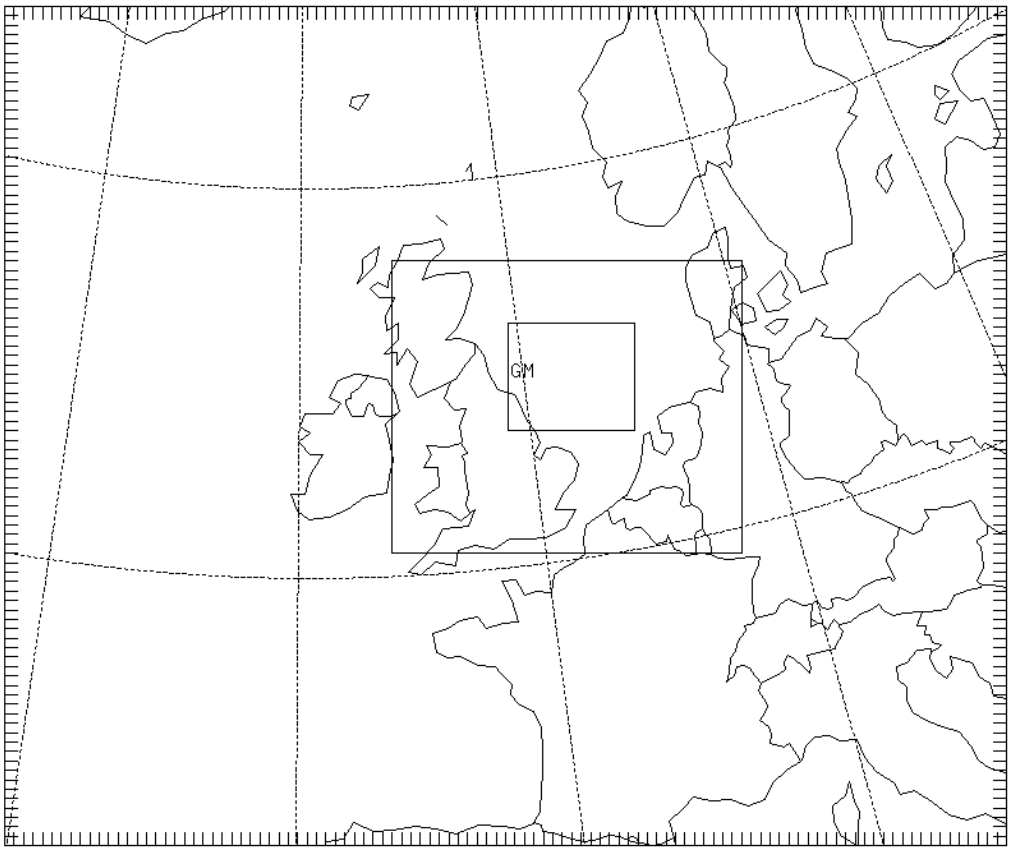

Figure 6.27 Domain setup for the Supergen exemplar site.

6.1.3.2 Dynamical setup

Dynamically, setup for both sets of runs at Shell Flats and the Supergen exemplar site was very similar to the runs undertaken at Scroby Sands with an example of the model namelist is provided in appendix I and a summary of the options in Table 6.11. Convective parameterisation was switched off for the inner domain. The YSU PBL scheme was used and with it being non-local it provided explicit treatment of the boundary layer depth. Additionally it is a numerically efficient scheme. Nesting feedback was switched on to allow two-way information flow between the domains.

Table 6.11 List of dynamical options used in the Shell Flats resource assessment runs.

Model Parameter	Setup
Vertical model levels	40
Nesting Feedback	On
PBL Scheme	Yonsei University (YSU)
Cumulus scheme	Betts-Miller-Janjic
Radiation scheme - Long wave	GFDL
Radiation scheme - Short wave	GFDL
Microphysics option	Ferrier (new Eta) microphysics
Surface layer physics	MM5 Monin-Obukhov scheme
Land surface option	Unified Noah land-surface model

6.1.4

6.1.5 Model output

6.1.5.1 Shell Flats

Wind speed and direction were produced at 10 minute intervals and 40m height for Mast 2 at Shell Flats. For the stability investigation, temperature was produced at 10 minute temporal resolution and 10m and 50m height which was used in conjunction with the 40m wind speed to calculate the bulk Richardson number. Wind direction is a potentially troublesome variable to investigate because of the circular scale on which it is measured. In other research different techniques have been employed to investigate wind direction, for example Jiminez et al (2010) look at the meridional and zonal wind component in daily averages computed from hourly averages, whereas Honrubia et al., (2011) perform RMSE analysis on the raw direction data in degree form. This research followed the method used by Honirubia et al., (2011), which was sufficient to produce comparable results upon which analysis and conclusions could be performed. Wind speed distribution plots are produced in 25 bins so as to provide a standard format for easy comparison between the multiple series and thus the Weibull parameters.

6.1.5.2 *Supergen exemplar site*

All variables produced from the model were available at ten minute temporal resolution. Wind speed was produced at 10, 30, 40, 50, 90 and 160m height for the Supergen exemplar site. Wind direction was produced at 40m. Temperature was produced at 10 and 50m height which combined with the 50m wind speed data was used to calculate the bulk Richardson number for the site.

6.1.6 Nudging

Observational nudging involves assimilating observational data into the model simulation over the duration of the run, described in Section 3.7.1. While large scale model input data are convenient due to global coverage, homogeneous levels and a wide range of variables, coarse resolution might not be exactly representative of conditions at, or near, a site of interest. Nudging the model input is intended to improve the first guess of particular variables at, or close to, a particular site. Given that WRF is updated for the duration of a model run by input and boundary files, observational nudging is performed throughout the whole run. Nudging was employed only for the Shell Flats resource assessment and not the exemplar farm resource assessment. Observations from Mast 1 at Shell Flats were integrated into the runs using the WRF utility program Obsgrid. Obsgrid synthesises observations into the model input to provide the objective analysis and creases a separate file, wrfsfdda_d01, which contains the nudging terms at the surface for the duration of the run. Obsgrid requires observations be processed into a specific format called little-r for ingestion, which was achieved using a custom FORTRAN script. The radius of influence of the observations and the magnitude to which the simulation is nudged, are both options which can be controlled by the user, but were left as default settings in this research. For example a user could afford more weight to an observational series which would increase the shift in the model solution towards the observations. Hourly wind speed at 80m from Mast 1 at Shell Flats was used to nudge the outer domain only, whereby influence of the observations is passed to the inner domains through the nesting process. Wind speed was used in isolation, despite the availability of other variables, to investigate the impact of the procedure and because the simulated variable of most interest is wind speed. This research marks the first step in the nudging investigation to which other variables can be added in further research. To investigate the benefit of observational nudging, the months of July and

October 2003 were run without observational nudging and the results compared to those achieved using nudging.

6.1.7 Stability

Stability at Shell Flats was estimated by classifying the Obukhov length (Table 10) after van Wijk et al (1990). The Obukhov length is an approximation of thermally driven buoyancy within the surface boundary layer which can be estimated from the Richardson number. Two derivations of the Richardson number (gradient and bulk) are used in this investigation, depending upon the variables available. Virtual potential temperature was calculated from observations at Shell Flats using pressure and moisture data at 12m and 82m from Mast 1, which was used to calculate the gradient Richardson number at Mast 1. To have a stability metric comparable between observations and the model, the bulk Richardson number was calculated for both the model and observations at Mast 1 using the same formula. Absolute temperature was used to calculate the bulk Richardson number instead of virtual potential temperature due to a lack of pressure and humidity data from the model. For the model data, temperature at 10m and 50m was used in combination with wind speed at 40m. For the observations, temperature at 12m and 82m was used along with wind speed at 82m. Since absolute rather than potential temperature was used to calculate the Richardson number, a lapse rate term was included to account for the reduction in temperature with height. The modelled near-surface Richardson number (termed rib in the RIP4 user guide) was also provided by the RIP4 postprocessor which calculated the value in units of seconds squared. No formula for the calculation performed by RIP4 could be found but the output is retained for comparison to the other metrics to serve as information for a potential end user. RIP4 is able to produce a dimensionless version of the Richardson number, which was requested in postprocessing, however on several occasions a null value was produced which disrupted the postprocessing so the variable was discarded. Model output of stability is produced for Mast 2 which is important because the observational data used to calculate stability at Shell Flats was from Mast 1 some 6km away from the site simulated by the model. Stability was calculated for the Supergen exemplar site using the bulk Richardson number as calculated from the 10m and 50m temperature values as well as the 50m wind speed in. As with stability at Shell Flats, the bulk Richardson number was then mapped to Obukhov length

before being classified after van Wijk et al (1990) using the values for Obukhov length in Table 6.12.

Table 6.12 Stability classes in relation to Obukhov Length (L) van Wijk et al (1990)

Obukhov length (m)	Atmospheric stability class
-200 < L < 0	Very Unstable (VU)
-1000 < L ≤ -200	Unstable (U)
|L| > 1000	Neutral (N)
200 ≤ L < 1000	Stable (S)
0 ≤ L < 200	Very Stable (VS)

6.1.7.1 Stability by reference to other variables

As a property of the atmosphere, stability is dependent upon a few variables. Part of the stability investigation is to try and reproduce those variables and thus stability as well as possible, but it is also of interest to see how stability relates to other variables which either operate at a larger scale or are already well accounted for. Ultimately just less than 30,000 data points comprised the investigation which ran from June 17th 2002 to February 3rd 2003, with the same discontinuities as the rest of the stability analysis due to data intermittency. Stability variation was looked at as a function of time and state, although time could be considered a state function as it corresponds to variations in temperature. Classification of stability by the different variables was performed through Matlab© scripts which queried one large dataset to aggregate stability statistics as required. In the temporal domain stability was classified by hour and by month, in order to evaluate stability throughout the diurnal and seasonal cycles. In terms of state dependence stability was classified by wind speed, wind direction and weather type. Wind speed was classified into six bins with smaller increments employed lower in the wind speed range where more data were concentrated. Wind direction was binned into eight 22.5 ° sectors with the standard compass points at the centre of each sector, for example the East direction bin included wind directions from 67.5° to 112.5°.

6.1.7.2 *Wind shear and stability*

Wind shear is known to be dependent upon stability (for example Wharton and Lundquist, 2012a) where in unstable conditions shear is minimal due to high levels of turbulent mixing with the opposite true in stable conditions. Thus a means of quality checking a measure of stability is to assess the observed wind shear as a function of stability. Three methods are used in this study to produce the Richardson number either in bulk or gradient form, which is then converted to Obukhov length and finally sorted into a stability class. Using multiple methods to determine stability provides potential for uncertainty if they are not in agreement, which was the case in the analysis at Shell Flats. Ultimately an analysis was necessary to identify the accuracy of both approximations of stability and identify the more appropriate metric. Observational data from Period 1 (17 June 2002 – 16 November 2002) was used to compare the bulk and gradient methods, with the findings generalised to the model output because the same method was used to calculate the bulk Richardson number. Wind shear was represented by the shear exponent (α) calculated in (6.14), where u represents wind speed and z represents height.

$$a = \frac{ln\,(u_2 - u_1)}{ln(z_2 - z_1)} \qquad \text{Equation 6.14}$$

Richardson number was binned in hundredths for the gradient method and thousands in the bulk method (to produce a representative number of bins), then a scatter plot was produced with binned Richardson number as the x value and average shear exponent for the given Richardson bin as the y value. In addition, the binned Richardson scatter plots were also binned by wind speed to identify any relationship between speed, shear and stability.

6.1.8 Weather typing

Weather typing is used in the Shell Flats resource assessment to provide a means of classification by which to assess the prevailing atmospheric conditions alongside the model output. The classification is presented in Table 6.13, where weather type is defined by the dominant pressure circulation (when present) and wind direction. Variables are analysed and compared against themselves as they exist under different weather types. For example, wind speed was qualitatively assessed to see how the frequency of variation and amount of variability differ for

different weather types. Model performance will be investigated to see if a particular weather type corresponds to a particular level of performance. Stability will be classified by weather type to identify any trends which can be used to infer stability based on a synoptic analysis and also to see the comparison between modelled and observed stability when broken down by weather type. Weather type data was obtained from the University of East Anglia's Climate research unit (http://www.cru.uea.ac.uk/cru/data/lwt/) after Jones et al, (2012).

Table 6.13 Numerical designation of the lamb weather type categories

Lamb Weather Type (LWT) codes					
-1	U	-9	non-existent		
0	AC			20	C
1	ANE	11	NE	21	CNE
2	AE	12	E	22	CE
3	ASE	13	SE	23	CSE
4	AS	14	S	24	CS
5	ASW	15	SW	25	CSW
6	AW	16	W	26	CW
7	ANW	17	NW	27	CNW
8	AN	18	N	28	CN

6.1.9 Temporal filtering

Temporal filtering was employed to investigate model performance at different temporal resolutions. The simplicity of a moving average filter makes it an attractive prospect if refined to an acceptable level whereby the smoothing effect is reduced. An exponential moving average filter was applied at the same intervals as the unweighted moving average filter in the Benchmarking investigation at Scroby Sands, to see if a compromise between the moving average and Butterworth filtering techniques could be reached. Exponential weighting affords most weight to the

values in direct proximity to the calculated value (t+0), with weighting decreasing with time from t+0, shown in Equation 6.15.

$$U_{(n)} = \sum_{n=1}^{n} a * (1-a)^{n-1} * x_n \qquad \text{Equation 6.15}$$

Exponential weighting improved the performance of the moving average filter over its unweighted counterpart. To see if the exponential moving average filter performed better than the Butterworth filter the two filters were applied to the 33408 data points comprising Period 1 of the Shell Flats investigation. Correlation analysis was then performed between the raw data and both filtered series. The Butterworth filtered series showed a higher correlation coefficient(r=0.9924) to the original unfiltered series than the exponential moving average filter (r=0.9680). As a result, temporal filtering of the Shell Flats resource assessment data was undertaken using the same Butterworth filter described in 4.3.6. Three versions of the filter were again applied to look at model performance at temporal resolutions greater than 60, 180 and 360 minutes by setting the cut-off frequency appropriately.

6.1.10 Analysis

As in the benchmarking runs, correlation and RMSE were used to quantify the success of the model at capturing observed variability and absolute error. Standard descriptive statistics of mean and standard deviation were also produced to describe variation in the series for observations at Masts 1, 2 and Squires Gate as well as the model output. In addition, a wind rose and two-parameter Weibull distribution (e.g. Lackner et al 2007) were produced from both modelled variables and those observed at Shell Flats Masts 1 and 2. Wind rose and Weibull distribution are commonly used in communicating results from a wind resource assessment. The wind rose was generated using a Matlab© script to bin wind direction and map it to a circular coordinate, colouring the bars depending on the proportion of represented wind speed. The two-parameter Weibull distribution was generated using a number of Matlab© functions. Firstly, a Weibull curve was fitted to the wind speed distribution using the wblfit function, from which the scale and shape parameters were generated. Then the wblpdf function was used to generate the Weibull probability

density function which was plotted against wind speed for both model and observations.

6.2 General appraisal of the wind resource at Shell Flats

6.2.1 Average wind speed

From June 2002 to December 2003 data were obtained from the two offshore meteorological masts at Shell Flats. The same period was also simulated using the WRF setup described in 4.4.3. It is important to reiterate that problems with data intermittency meant that the series was not continuous from June 2002 to December 2003 and the values in Table 8 are representative of the periods where data were available, translating to around 489 days. Data from Mast 2 at Shell Flats are the predictands in this investigation for which the WRF model output, data from Mast 1 at Shell Flats and data from Squires Gate are predictors. In order to characterise the general traits of the two main series of interest, i.e. WRF-ARW model output and observations from Mast 2, descriptive statistics are presented in Table 6.14. Average wind speed is very similar between the series at around 8.3 ms^{-1}, whereas standard deviation in the modelled time series is slightly lower than that observed, indicating a reduced amount of variability is simulated compared to that observed.

Table 6.14 Observed and modelled average wind speed and direction at Shell flats.

		Mast 2 (40m)	WRF-ARW (40m)
Direction (°)	Mean	179.07	193.96
	Standard Deviation	92.62	89.34
Speed (ms^{-1})	Mean	8.37	8.25
	Standard Deviation	4.27	4.04

The distribution of wind speed, as represented by the two- parameter Weibull distribution, provides another important form by which to assess the accuracy of the model as a resource assessment tool. The Weibull distributions for observed and

modelled wind speed are very similar to each other which is summarised in Table 6.15 where the values for the two parameters relating to the Weibull distributions are quantified. Wind speed distribution for the modelled series has slightly larger scale parameter value which relates to the average wind speed which implies a greater proportion of wind speeds in a slightly higher range. The shape parameter of the modelled wind speed is also slightly higher which means the data are slightly more normally distributed than the observed data.

Table 6.15 Description of the two parameter Weibull distribution for Shell Flats as simualted and observed in ms^{-1}.

	Observed	Simulated
Scale parameter (C)	9.24	9.42
Shape parameter (k)	2.02	2.17

6.2.2 Wind direction

Wind direction provides a valuable metric of comparison between the series. Model output presents a slightly more westerly orientated average than is observed at Mast 2 while standard deviation values indicate that spread is similar between the series. Figure 28 shows the wind roses generally agreeing in that the prevailing wind is South-Westerly, which shows the value of producing such plots which confirm the aptitude present in the model which might not be evident from the statistics in Table 6.15. Comparison of the wind roses identifies a more significant North-Easterly component is observed at Mast 2 that is not reproduced by the model. Model output displays a stronger presence of West and North-Westerlies than are observed at Mast 2, while the model also sees more frequent wind coming from the South-East. Further analysis of the model's simulation of wind direction is provided by comparing the wind roses to those observed after classification by month of the year to see if any consistent patterns or significant outliers emerge (Figures 6.29 & 6.30). Visual impressions from the original plot (Figure 6.28) suggest a slight clockwise offset of modelled wind direction compared to that observed which would corroborate with the slightly more westerly tendency and average value.

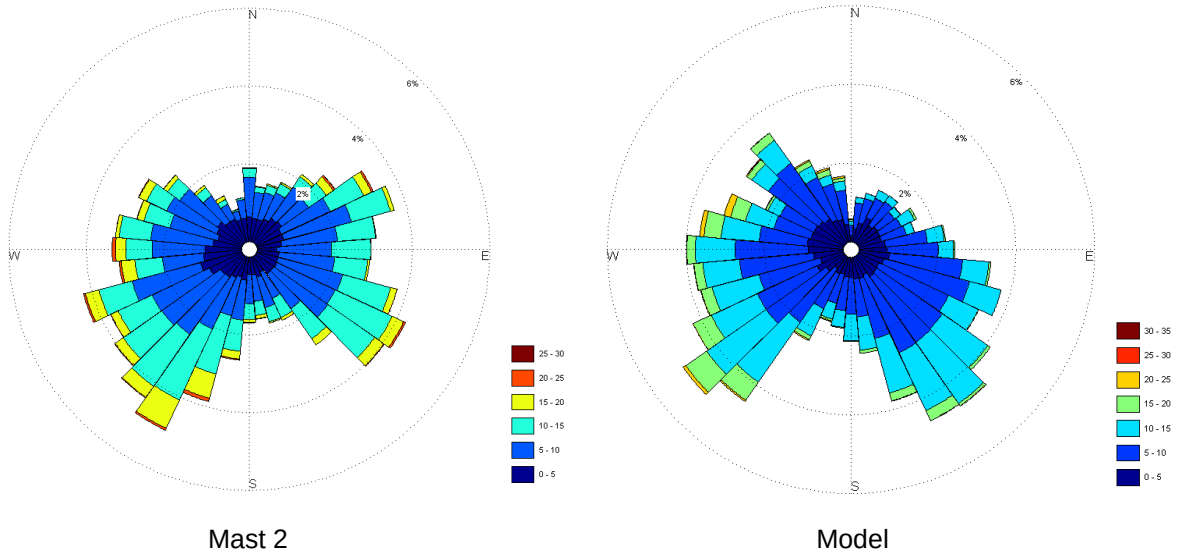

Mast 2 Model

Figure 6.28 Wind roses for Shell Flats as observed at Mast 2 and simulated by WRF from June 2002 to December 2003.

Comparison of individual months generally shows a very good agreement between the model and observations. In some months the distribution of wind direction is unimodal, where a prevailing wind from a single defined sector, for example February, November and December. Unimodal wind regimes imply consistent circulation patterns, which should prove less difficult to simulate. The modelled wind roses for these months tend to reflect observations closely, with the November plot looking to show the best agreement. The February plots show a slight degree of turning between the two series which would agree with a slight westerly bias identified earlier. The December model output has a greater spread of winds in the prevailing direction compared with observations, but in general the series agree well. Bimodal wind regimes possess two distinct prevailing wind directions, such as observed in March, July and October, present more of a challenge to the model because of changing synoptic scale atmospheric influence. Model output again is broadly reflective of the patterns observed. Certainly in the March and July cases the bimodal structure is captured if not quite in the same proportion. The October cases provide an interesting comparison where the two prevailing direction lobes are opposed. Again the structure of the modelled rose is very much like that observed, but simulating a narrower spread in each direction compared to the wider spread observed. Complex wind direction cases are where a wide distribution of prominent prevailing directions is evident. Examples of complex wind distributions are the

January and September cases. The model output broadly reflects that observed, apart from missing a North-easterly component in the September plot, implying a high performance standard is achieved by the model regardless of the type of wind distribution seen.

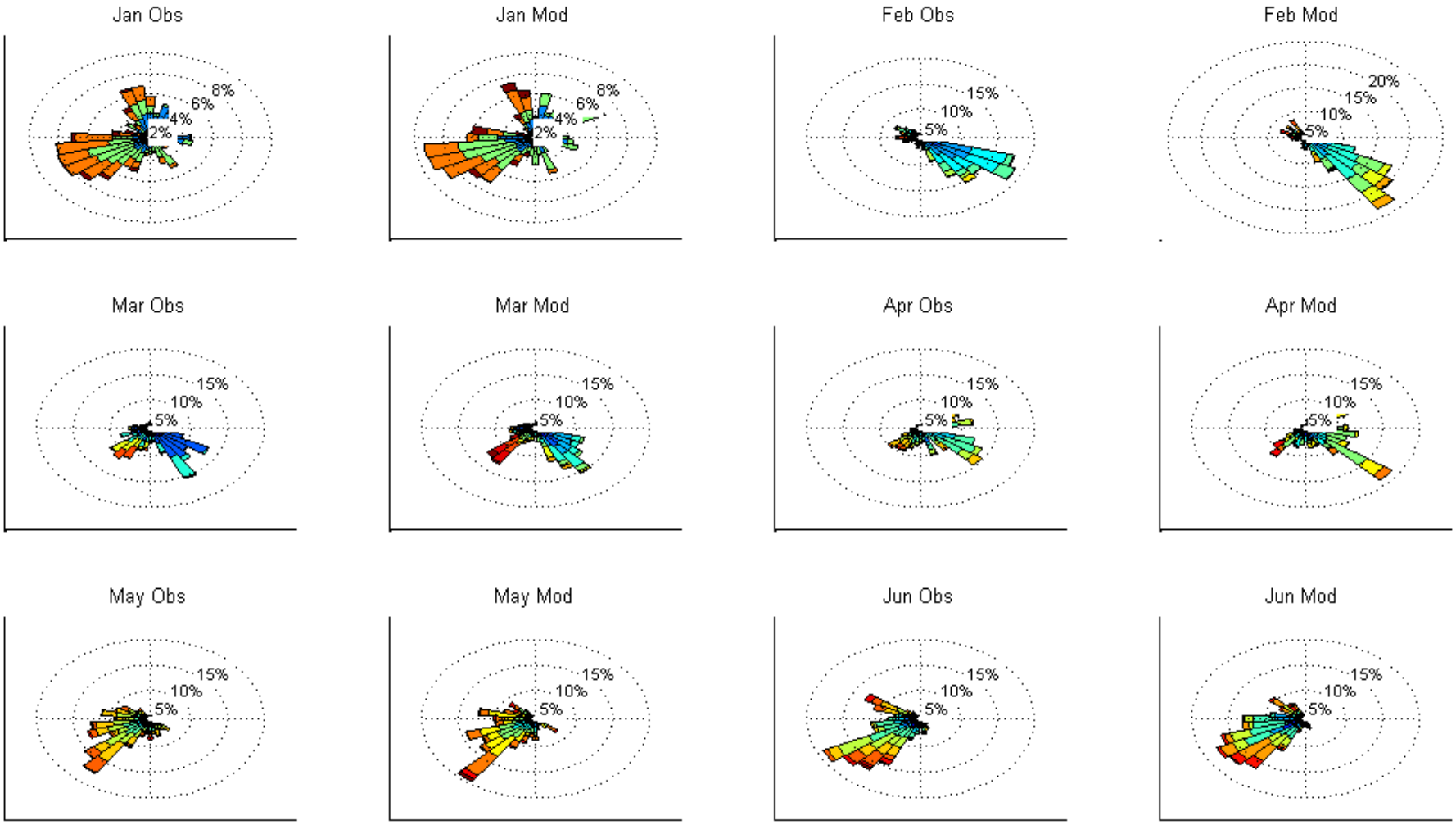

Figure 6.29 Wind direction by month as simulated and observed for Mast 2 at Shell Flats over the 18 month resource assessment for January to June.

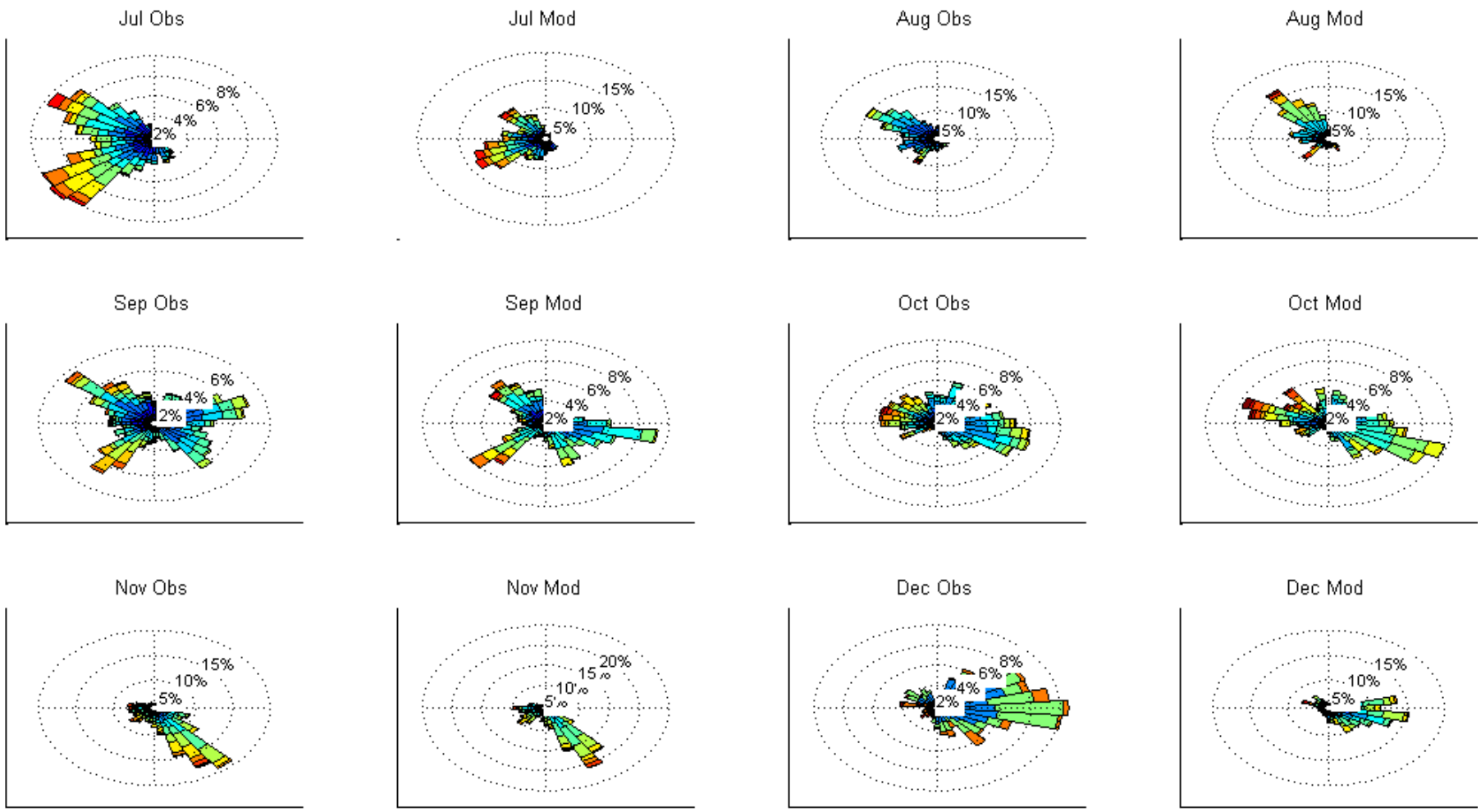

Figure 6.30 Wind direction by month as simulated and observed for Mast 2 at Shell Flats over the 18 month resource assessment for July to December.

6.2.3 Time series analysis

Correlation and RMSE statistics quantify model performance in terms of variability and absolute error. As with the benchmarking comparison at Scroby Sands both series were initially compared at ten minute temporal resolution then filtered, using the lowpass Butterworth filter, at a range of longer temporal resolutions. Correlation values between model output and observations at Mast 2 for the raw and filtered series are presented in Table 6.16. An average correlation coefficient of 0.86 for the ten minute data implies that the model is able to simulate the features which cause change in wind speed at the site very well. Certainly the correlation results at the Shell Flats site are significantly better than those seen in the benchmarking exercise at Scroby Sands. When the series are filtered through increasingly long intervals, the correlation coefficient continually improves to over 0.9 at a temporal resolution of 360 minutes. A similar story is found when analysing the RMSE statistics which are presented in Table 6.17. An RMSE, similar to that established in the benchmarking study, of 2.1 ms^{-1} is achieved at raw temporal resolution of ten minutes, which improves with decreasing temporal resolution by 0.3 ms^{-1} to 1.7 ms^{-1} at 360 minutes. The average correlation coefficient for wind direction at ten minute resolution is 0.6 while RMSE is 78°. Statistically, wind direction is simulated to a similar level as wind speed in the benchmarking investigation at Scroby Sands. Parallels between model performance in both cases is evident, skill and accuracy is present in both but accompanied by notable error. One must bear in mind the comparison being made here, where the observed values are ten minute averages while the simulated values are instantaneous. The importance of this effect is unknown but should be considered when comparing the two series.

Table 16 Correlation coefficient between model simulated wind speed and observations from Mast 2 at Shell Flats in five periods from Jun 2002 to December 2003.

Temporal resolution (min)	Period 1	Period 2	Period 3	Period 4	Period 5	Average
10	0.8827	0.8852	0.8200	0.8176	0.8726	0.8556
60	0.8899	0.8933	0.8315	0.8251	0.8871	0.8654
180	0.9035	0.9094	0.8536	0.8463	0.9037	0.8833
360	0.9170	0.9251	0.8762	0.8685	0.9194	0.9012

Table 6.17 RMSE in ms^{-1} between model simulated wind speed and observations from mast 2 at Shell Flats in 5 periods from Jun 2002 to December 2003.

Temporal resolution (min)	Period 1	Period 2	Period 3	Period 4	Period 5	Average
10	2.1269	2.1100	2.2022	2.0667	2.1005	2.1213
60	2.0496	2.0238	2.1142	2.0035	1.9965	2.0375
180	1.9001	1.8439	1.9386	1.8640	1.8356	1.8764
360	1.7370	1.6531	1.7435	1.7034	1.6670	1.7008

Considering correlation and RMSE as a function of time affords an insight into how variable the model performance was over the course of the resource assessment. Such an analysis can then be used to identify particular episodes of performance and examine the prevailing atmospheric conditions for example by synoptic weather type, to investigate the presence of state dependence in model performance. For example in Figure 6.31, the month of October in 2002 seems to correspond to a moderately high and consistent correlation coefficient between the model and observations, also reflected by lower values in the RMSE plot (Figure 6.32). Aside from during October 2002, performance as a predictor of wind speed is shown to be highly variable over the duration of the wind resource assessment as the model performs to varying standards depending upon the prevailing conditions. Anticyclonic conditions are slow moving and through atmospheric subsidence, tend to promote a stable atmosphere with low turbulence. Such conditions invariably translate to a reduction in the amount of high frequency change in wind speed for periods on the order of days, compared to cyclonic conditions. Results from Scroby Sands imply that the model is more successful at simulating slow moving, low frequency features. In contrast, cyclonic conditions are faster moving and promote more unsettled conditions. Weather typing is one form of classification, of which there are several, known to be an effective measure by which to analyse model performance. Weather typing was employed in this run experimentally to assess its feasibility in a wind resource assessment context, and forms a key part of the model optimisation investigation.

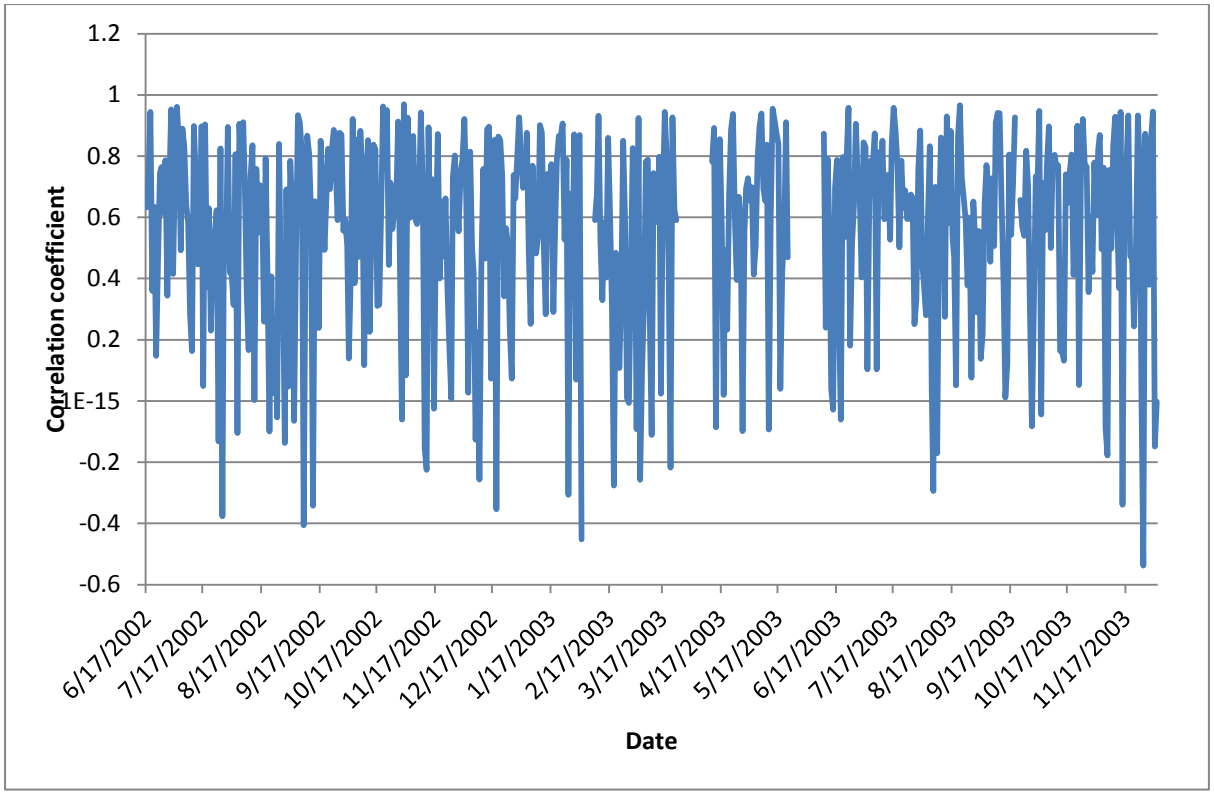

Figure 6.31 Correlation between simulated an observed 50m 10 minute wind speed for the Shell Flats resource assessment.

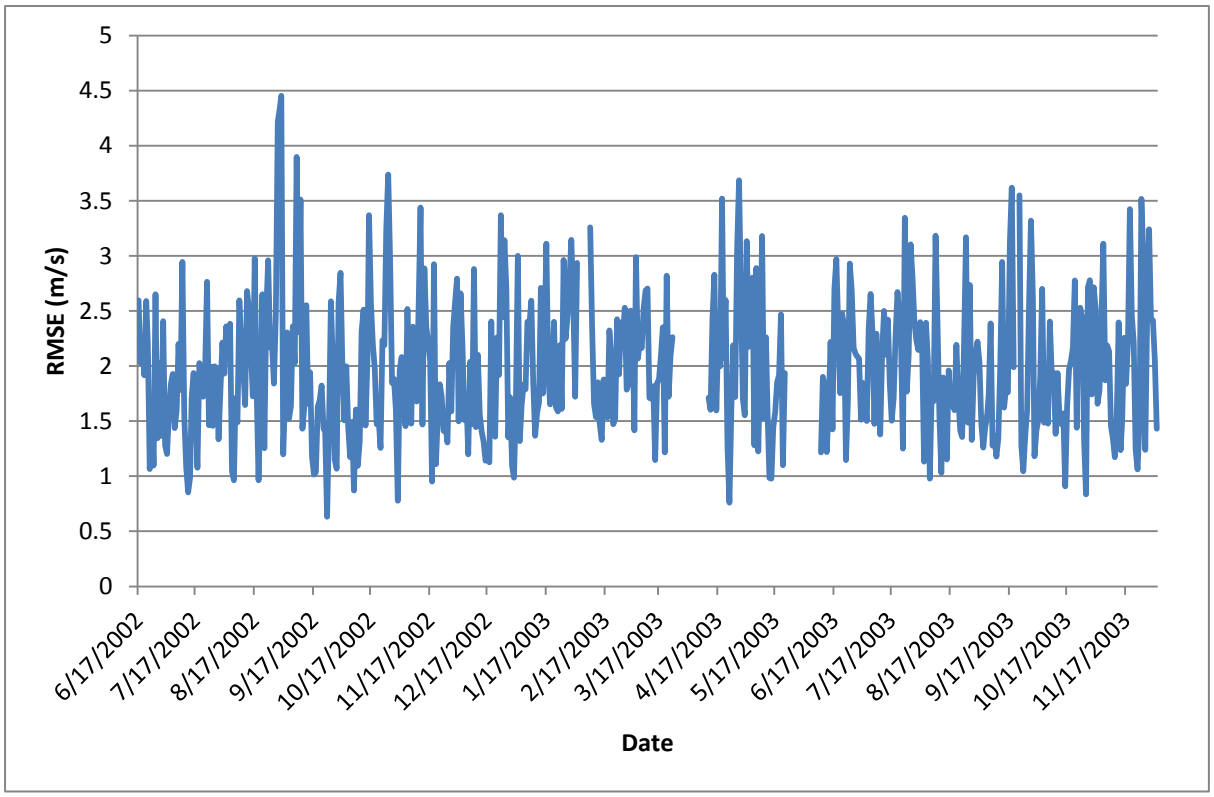

Figure 6.32 RMSE between simulated and observed 50m 10 minute wind speed for the resource assessment at Shell Flats.

6.2.4 Analysis of observational nudging

For two months during the Shell Flats resource assessment investigation, extra model runs were undertaken without observational nudging to establish the effect upon performance of including observations. Only wind speed was nudged to keep the process simple while offering a potential improvement to the most important variable in terms of resource assessment. Collated statistics for both months can be found in Table 6.18, where the performance achieved by observations from Mast 1 is presented for reference. July 2003 provided the first case study, where the correlation coefficient between observed and modelled wind speed was improved by the nudging process. RMSE of the nudged wind speed time series was also found to be lower than the non-nudged series. As a result of nudging wind speed, the correlation coefficient between observed and simulated direction also improved, albeit marginally. Similarly, RMSE for wind direction was slightly improved by nudging wind speed compared against the non-nudged run. October 2003 provided the second case study, in which the correlation coefficient for wind speed was marginally higher for the non-nudged run compared to the nudged run. Similarly, RMSE was marginally higher for the nudged run compared to the non-nudged run, indicating nudging inhibited the models simulation of wind speed in this case study. By contrast, a slight improvement in representation of wind direction was observed, with a higher correlation coefficient and a lower RMSE for the nudged run.

Table 6.18 Statistics for the July and October 2003 case studies comparing performance of observations from Mast 1, a non-nudged model run and a model run nudged by observations from Mast 1 as predictors of 40m wind speed at Mast 2.

		July			October		
		Shell Flats Mast 1	Nudged model (Model + Mast 1)	Non-nudged Model	Shell Flats Mast 1	Nudged model (Model + Mast 1)	Non-nudged Model
Speed	**Correlation coefficient**	0.9340	0.8097	0.7389	0.9194	0.8877	0.8887
	RMSE (ms^{-1})	1.2133	2.1335	2.5847	1.7869	1.9418	1.9289
Direction	**Correlation coefficient**	0.8863	0.7995	0.7904	0.6442	0.6499	0.6221
	RMSE (ms^{-1})	31.5093	44.3640	46.8879	50.6065	53.6024	56.0912

Observational nudging can be beneficial for the modelling process which has been reflected in model performance statistics. However, even incorporation of an observational series near the site of interest does not raise model performance to the same level as the observations used to nudge the model as a predictor for the site of interest. Model performance when simulating a non-nudged variable (wind direction) was shown to be improved, while improvement in performance for wind speed in the first case study outweighed the reduction in model performance seen for wind speed in the second case study. When deciding whether to employ nudging, consideration of the relationship between data from the nudging location and the location to be simulated for, must be made. If a weak relationship exists between the two observational series, nudging will negatively affect the performance of the model. Local roughness can help inform such a decision for example in an offshore context, where both series are derived from offshore masts, whereby less modification of the flow is likely to occur due to the low surface roughness over the sea. Thus one might have more confidence that given the distance is not too far, the observed wind field is likely to be fairly consistent between the two locations. By contrast if the nudging series is an onshore mast, and a modest distance from the site of interest, not only will the onshore mast be subject to local roughness elements, but the larger distance

may also mean the two sites are influenced by different wind fields. Ultimately the application of this work is almost an extension of the use of met masts. It is inevitable that wind farm sites will require a met mast for a long time yet, because of the current state of alternative technologies and the requirements of end users. However, these results show the benefit of incorporating observations from a local site into a model run, potentially expanding the spatial area for which the mast data can be effectively used and saving a developer installing an extra met mast where one will suffice. Such findings are of particular relevance given the large geographical extent of today's offshore farms which may require multiple masts to deliver confident resource assessments across the proposed farm site.

6.3 Evaluation of model performance in the context of local observations

Model performance as a proxy for wind observations at Shell Flats has thus far been considered by comparing model output to observations. To add another dimension to the analysis, model performance will be considered by comparison to two observational series, ten minutely data from Shell Flats Mast 1 (used to nudge the model run) and hourly data from an onshore site at Squires Gate.

6.3.1 Comparison against observations from Mast 1 at Shell Flats

There is little difference between the observed and simulated wind speed statistics at Shell Flats (shown in Table 6.19 and Figure 6.33), suggesting the model is performing to a high standard for this location. Somewhat surprisingly, average wind speed, as both observed and simulated, at 40m level for Mast 2 is greater than the 80m wind speed observed at Mast 1. Without performing a comprehensive site review, the cause of the difference between the sites is unknown, but there could well be an element of local variation, for example resulting from the slightly different prevailing wind direction. Such an investigation should include comparison of values from the same height levels, for example statistics and wind roses for Mast 1 at 40m as well as variation in speed and direction with height. The highest observations were used from each mast in this study to represent the closest level to turbine hub height and provide a practical demonstration of a scenario with observations at different heights. Wind direction at Mast 1 is observed to have a slightly more westerly component than is observed at Mast 2 but displays a similar degree of variation as represented by standard deviation. Difference in wind direction might be

partially resulting from the height difference between the observations as a reduction in height corresponds to reduced friction higher velocity and a stronger Coriolis influence. However the Ekman spiral alone is unlikely to be the sole reason for such a difference. Wind roses for the three series are presented in Figure 33, giving a little more information about the distribution of wind direction. Interestingly the modelled wind rose appears more similar to that observed at Mast 1 than Mast 2. Modelled (for Mast 2) and observed (at Mast 1) wind roses both exhibit a stronger presence of Westerly and South-Easterly flow, while showing little in the way of North-Easterly flow in contrast to observations from Mast 2. The point must be made that wind direction is not nudged in this research, just wind speed in isolation. The similarity between the wind direction simulated for Mast 2 and that recorded at Mast 1 is therefore not a product of a nudging process. Deeper analysis of the three series is required to identify if and where discrepancies exist, as from these results it would seem the observations from Mast 2 contradict the values from the other two series.

Table 19 Observed and modelled 40m average wind speed and direction at Shell flats Mast 2 and observed 80m wind speed and direction at shell flats Mast 1.

		Mast 1 (80m)	Mast 2 (40m)	Model (40m)
Direction (°)	Mean	189.97	179.07	193.96
	Standard Deviation	91.54	92.62	89.34
Speed (ms^{-1})	Mean	8.34	8.37	8.25
	Standard Deviation	4.27	4.27	4.04

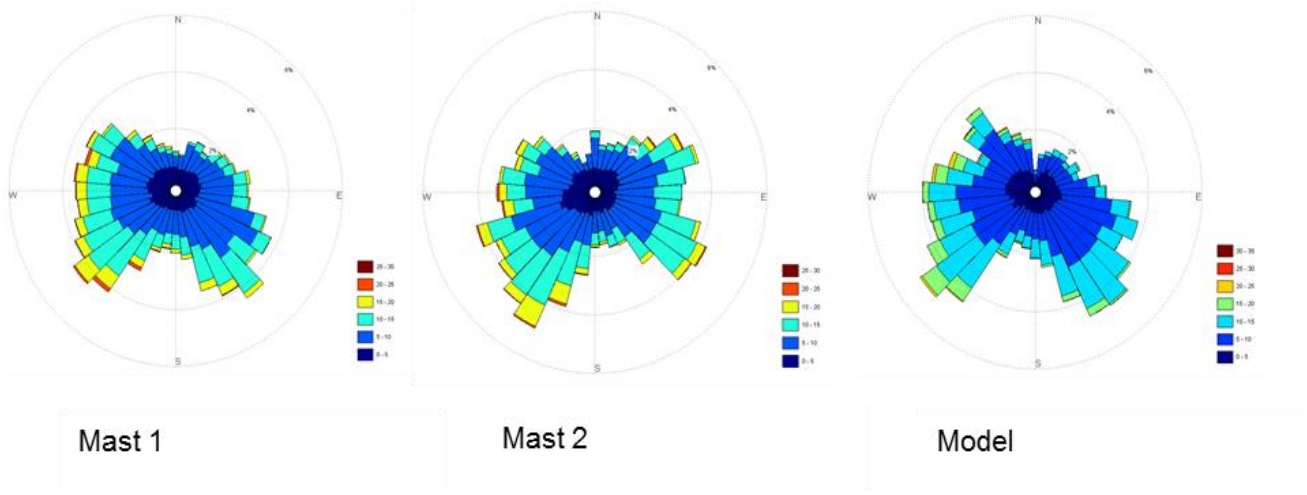

Figure 6.33 Average wind roses (°) for 80m observed at Mast 1 and 40m observed and simulated at Mast 2.

When the relationship between the observed series' is investigated, the benefit of the nearby met mast is apparent. A correlation coefficient of 0.94 is achieved between the two masts at ten minute resolution compared to a value of 0.86 achieved by the model. These statistics imply that variation in the wind observed at Mast 1 is reflective of that seen at Mast 2 which may be due to the low surface roughness, lack of topographical features and close proximity of the masts. However as a predictor of wind speed at Mast 2, observations from Mast 1 display a large RMSE at 1.4 ms^{-1} given the strength of the correlation, which compares to 2.1ms^{-1} achieved by the model.

6.3.2 Comparison against observations from Squires Gate

Hourly values from observations at Shell Flats and the model output were required to undertake the comparison to the observational series at Squires Gate. Due to data availability at Squires Gate, the dates over which the series are compared is different to the five periods for which simulations were undertaken at Shell Flats. By reference to the five simulated periods described in the methods section, period 3 is missing completely, while period 5 is reduced in extent. At hourly resolution, the average correlation coefficient between the 10m Squires Gate series and the 40m observations from Mast two at Shell Flats is 0.59 with an RMSE of 5.09 ms^{-1}, which compares with a correlation of 0.87 and RMSE of 2.12 ms^{-1} when simulated by the model for the same period. Average 10m wind speed at Squires Gate is 4.78 ms^{-1} with a standard deviation of 2.99 ms^{-1}, while average observed and

modelled wind speed is 8.17 and 7.99 ms^{-1}, with a standard deviation of 4.33 and 4.12 ms^{-1} respectively. The RMSE value of Squires Gate as a predictor for Shell Flats is likely to be inflated because of the bias between the two series arising from the height discrepancy, with average wind speed showing the contrast between the two sites. In contrast to the strong relationship seen between Hemsby and Scroby Sands, Squires Gate does not offer potential as a predictor station for the Shell Flats site. Model performance is significantly better in every statistical respect and offers a greater diversity of output in terms of variables, spatial coverage and temporal resolution.

6.4 Investigation of stability

The atmospheric stability at Shell Flats was investigated, both from the onsite measurements and variables extracted from WRF. Stability is an important parameter to understand as it has an impact on turbine wake dissipation and wind shear. Firstly, stability is evaluated from site data using a number of methods. Finally, occurrence of stability is classified using several variables to see if it can be inferred based on predictions of these classification variables.

6.4.1 Evaluation of measures of stability

Scatter plots of average shear exponent by Richardson number (Ri) bin were produced to analyse the relationship between wind shear with stability. Theory dictates (e.g. Wharton and Lundquist, 2012) that shear will be relatively reduced under unstable conditions (when $Ri < 0$), due to increased mixing between layers promoted by the higher levels of convective turbulence. It is then expected that shear increases as conditions become neutral, moving into stable, as layers develop in the flow and mixing is reduced. Figure 6.34 shows the average wind shear for binned bulk and gradient Richardson numbers during period 1.1 of the Shell Flats resource assessment. Binning was undertaken to provide a clearer view of the stability distribution. Both bulk and gradient Richardson, measures agree with theory that shear is lower under unstable conditions and increases at the point where conditions become neutral. Both methods also show a significant divergence after flow becomes stable, suggesting that while shear is likely to be higher in stable conditions there is a large degree of variability. Bulk Richardson number values show a degree of spread in very unstable conditions, where gradient Richardson values do not.

Gradient Richardson number values show a more gentle transition from low shear in unstable conditions to increased shear in neutral and stable conditions compared to the bulk Richardson number values which imply a more pronounced difference between mild cases of both types of stability (stable/unstable). The Richardson number at which the Obukhov length is 80m (the height of the upper observation in the calculations) was calculated by rearranging the Obukhov length mapping equation using the known Obukhov length. The Richardson number at Obukhov length of 80m is 0.0024, which is close to the point on both the scatter plots where dispersion in the shear value starts to occur. It is suggested that the application of the equation is not valid when the Obukhov length is lower than the uppermost measurement because the equation is specifically for use in the surface layer (e.g. Grachev and Fairall 1997). Thus shear values for Richardson numbers above 0.0024 will not necessarily correspond with Monin-Obukhov length similarity theory scaling.

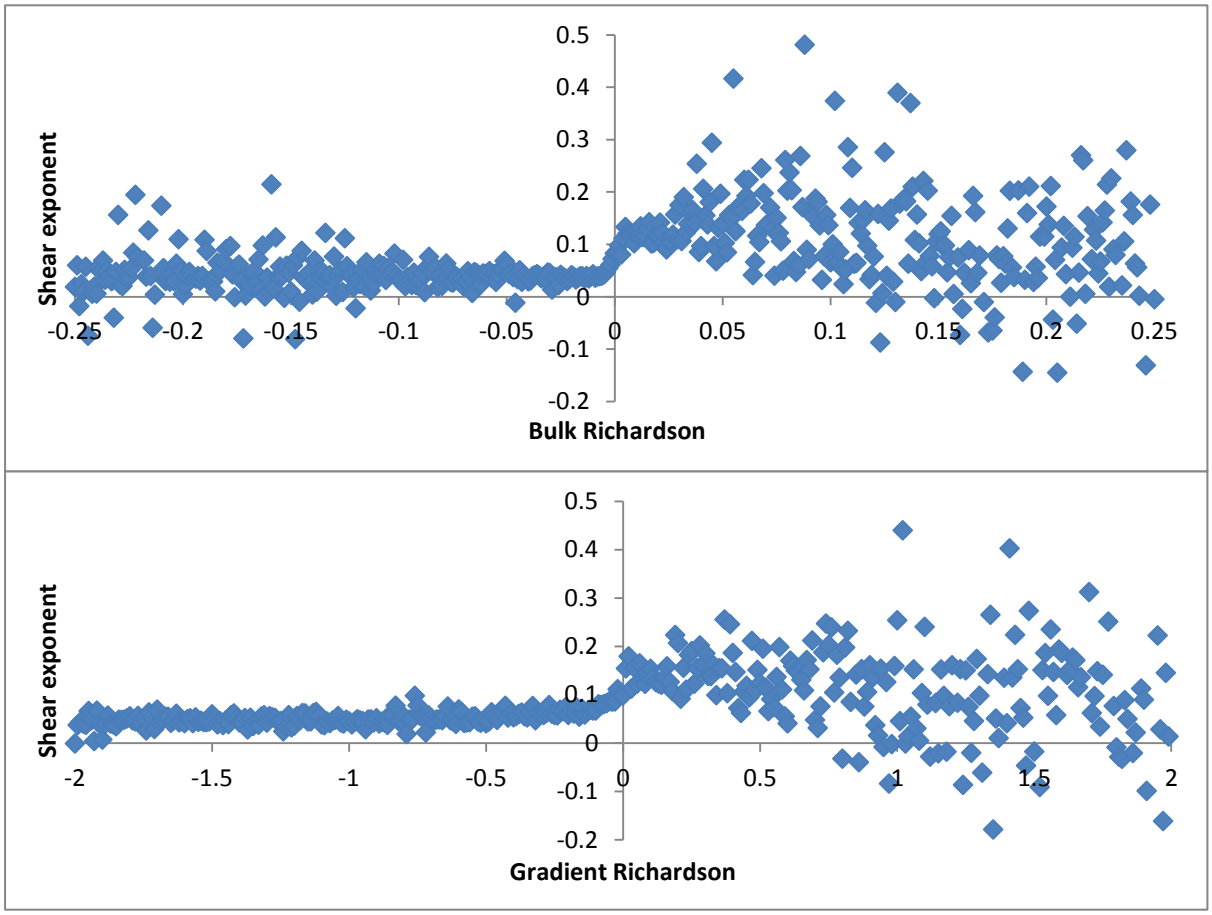

Figure 6.34 Comparison of shear exponent as a function of observed Bulk (top) and Gradient (bottom) Richardson number during period 1.1 at Shell Flats.

Figure 6.35 shows the same scatter plot of bulk Richardson number versus shear exponent, this time using the simulated bulk Richardson number as generated from wind speed and temperature. What this plot shows is the ability of the model to capture the trend in wind shear with stability to a similar extent shown by the bulk Richardson number method performed using observed variables. The modelled shows a greater spread than the observed bulk Richardson plot. There are fewer data points which comprise the modelled plot which could imply a refinement in the methodology used to generate the Richardson number is required. Ultimately the shape of both bulk Richardson plots is very similar. A generally limited spread in the unstable region increases with shear at the point of neutral conditions after which a considerable divergent spread is observed. Use of the bulk Richardson number method as an approximation of stability is thus a justified means of comparison between model and observations.

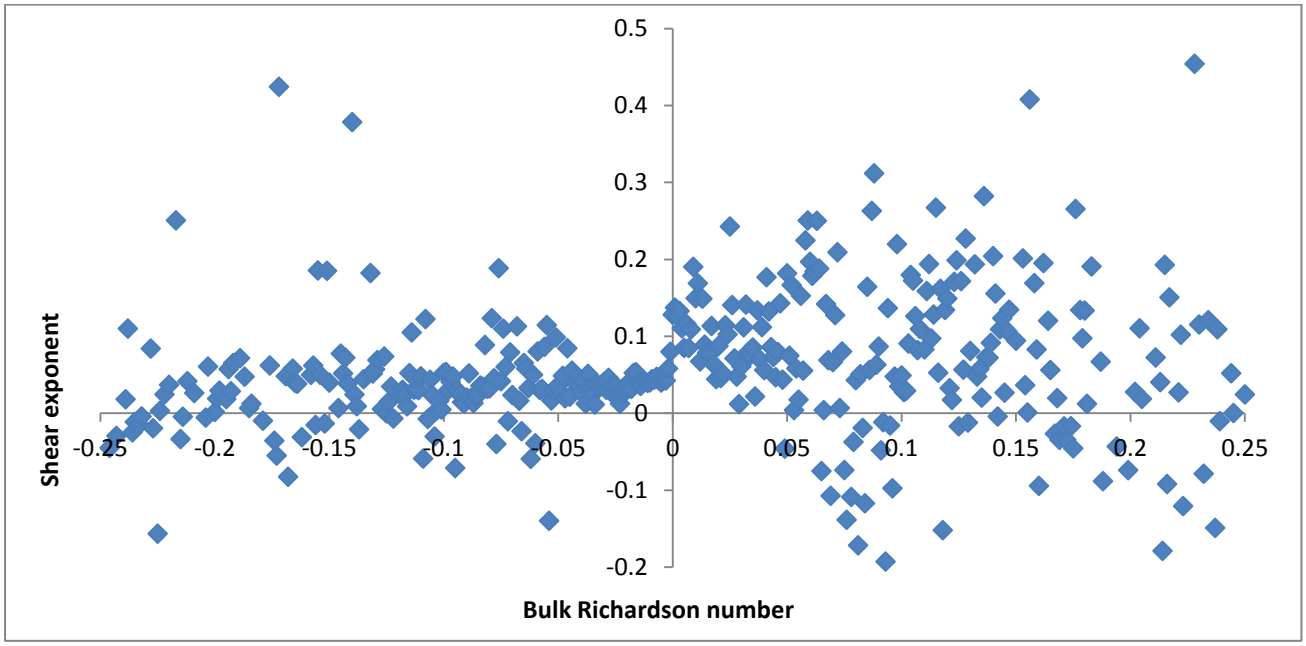

Figure 6.35 Average 70-20m shear as a function of binned bulk Richardson number calculated from modelled variables.

Figure 6.36 shows a scatter plot of Richardson number and wind shear classified by windspeed. Of interest is the grouping of higher wind speeds close to neutral conditions, with the highest speeds appearing to be in neutral conditions. Figure 6.37 shows the model representation of the same variables. The distribution of different wind speed bins is slightly shifted towards the unstable side of neutral conditions in the modelled plot compared to the observed plot. However the two

plots agree that high windspeed events tend to lower levels of shear and near neutral conditions.

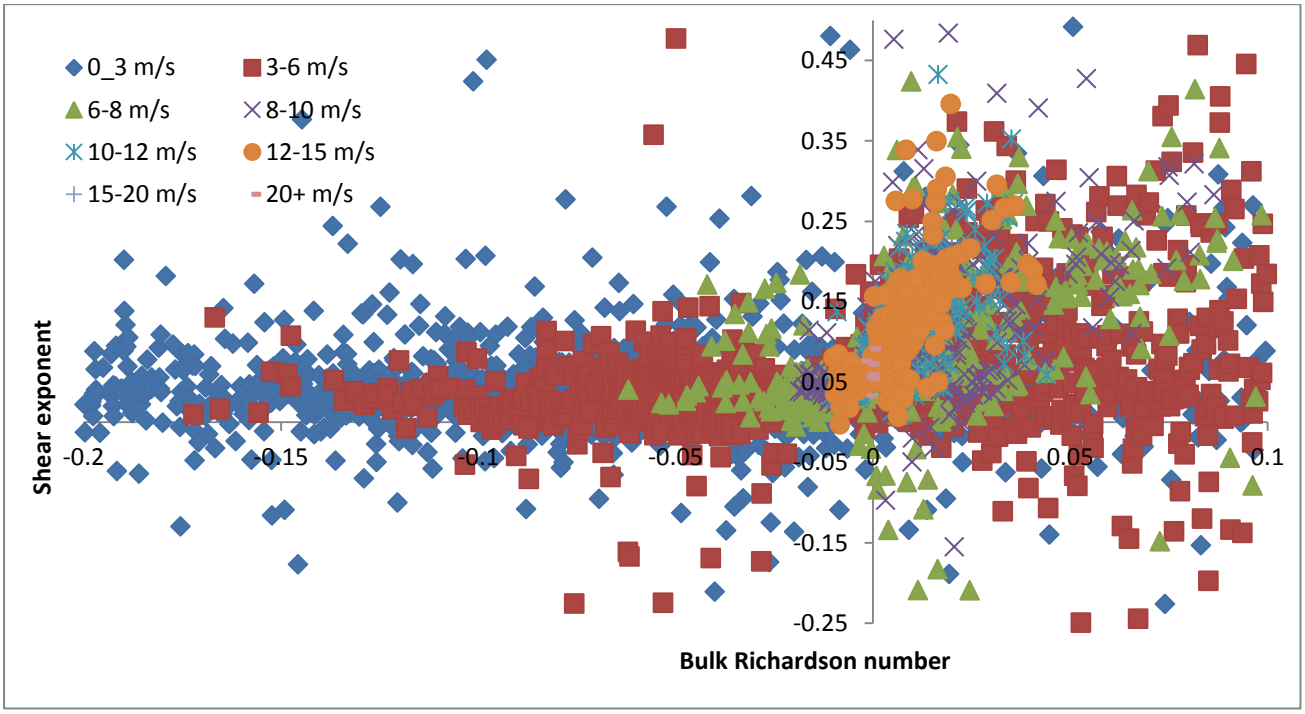

Figure 6.36 Average 70-20m shear as a function of observed bulk Richardson number, classified by wind speed bin.

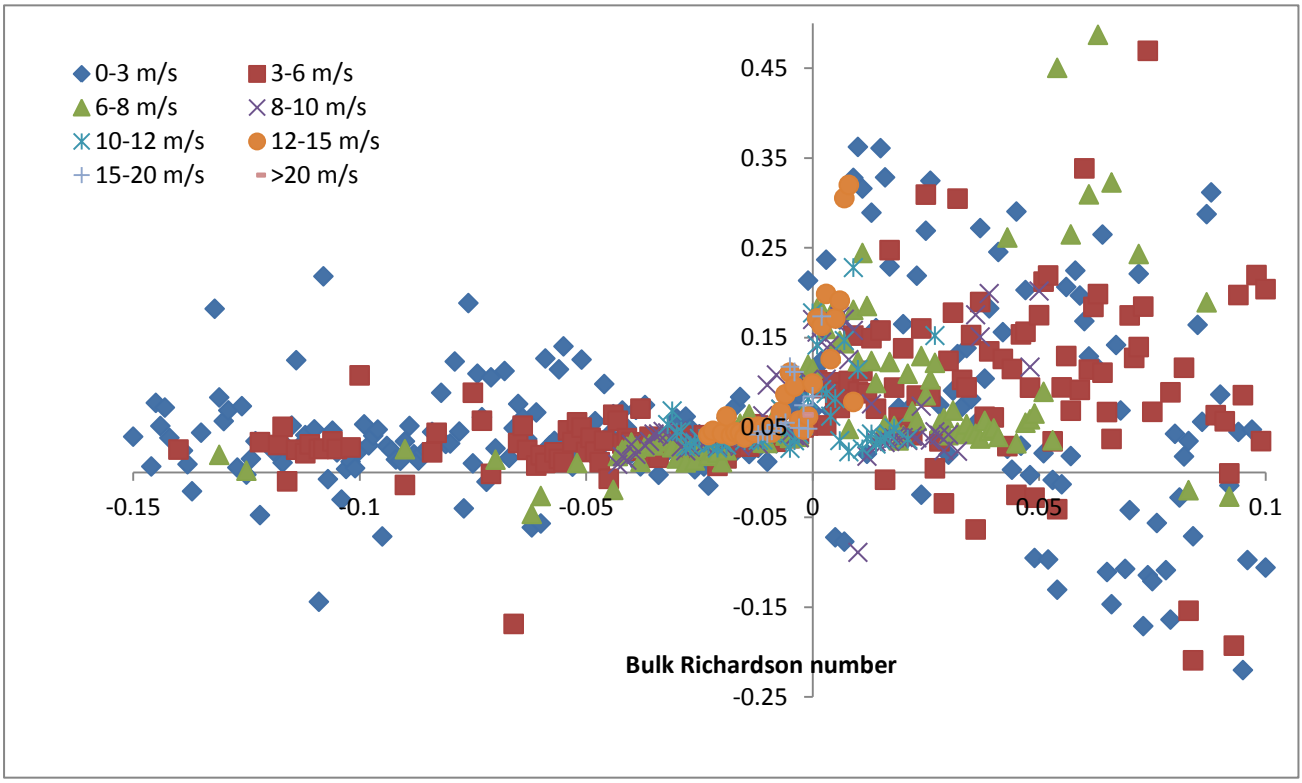

Figure 6.37 Average 70-20m shear as a function of modelled bulk Richardson number, classified by wind speed bin.

6.4.2 Stability at Shell Flats

To begin this section, the frequency of each stability class produced by the four approximation methods is presented and discussed. Stability as grouped by wind speed, wind direction, weather type, seasonal and diurnal cycles are then presented. Most attention will be paid to the bulk Richardson number approximations calculated from model and observations as this provides the comparison between the two sources by which model performance will be judged. Results from the wind speed and direction investigation highlighted some shortcomings in model performance, in particular high frequency variability. While the model may not be able to precisely simulate high frequency changes in wind speed, if it simulates features which can be related to stability while providing a good estimate of wind speed, the value of the model as a resource assessment tool becomes greater. Simulation of stability, both directly and approximately by reference to other variables, will give the wind farm operator more information about the likely conditions which will affect the wind farm. For example, weather type might correspond to the incidence of particular stability class. Given the simulation of a particular weather type the likely stability conditions, and transition from the current state can be inferred. Knowledge of the changing stability would allow a modification to the degree of wake losses currently accounted for. The adoption of such a process operationally would provide a deeper understanding of likely turbine performance and farm output which could be used to alter the wind farm management strategy.

6.4.2.1 General appraisal

The main focus for comparison between model and observations will be using the bulk Richardson number values calculated from observations and variables outputted from the model. Because both gradient and bulk Richardson number methods provide similar approximations of stability with respect to wind shear, some confidence can be afforded to their use as measures of stability. Furthermore it is deemed appropriate to use the bulk Richardson number as the main metric of comparison between model and observations. The gradient Richardson number derived stability class produced from observations (OGR), is included to provide another means of comparison. RIP4 (model postprocessor) generated bulk

Richardson number (BRR), is also present in the analysis for validation against bulk Richardson number as calculated from the other modelled variables to serve as a reference for any potential end users of the feature in RIP4. Once the various methods have been used to calculate a bulk Richardson number, the value is then converted to Obukhov length and classified into stability classes as described in chapter 3. Classification of stability by frequency as simulated and observed is presented in Figure 6.38. Observed stability approximated by gradient Richardson (OGR) number, shows a dominance of very unstable conditions at Shell Flats, with little presence of any kind of stable conditions and minimal occurrence of neutral conditions. Observed bulk Richardson (OBR) values indicate a considerable presence of stable and neutral conditions in contrast to the gradient Richardson values but also show a strong presence of unstable conditions. Distribution of stability as produced from observed and modelled bulk Richardson (MBR) numbers agree on a number of levels. Both show a reasonably even distribution of cases either side of the neutral class, though with more extreme cases observed than simulated. There is a greater occurrence of neutral conditions observed than are simulated and the model produces more stable conditions compared to the slightly more unstable tendency observed. The BRR series agrees to a small extent, in that the dominant conditions are evenly distributed between stable and unstable cases, though a greater proportion of an extreme tendency (very unstable or very stable compared to unstable or stable) is simulated than is observed. OBR stability sees a considerably larger proportion of neutral conditions than is seen in the modelled bulk Richardson (MBR) series and the OGR series. To put these results in a practical context, both simulated measures of stability produced more stable cases than are observed. In reality a farm operator using this model output would expect more stable conditions than actually occur. While this is good because wake recovery promoted by unstable conditions would be greater than expected reducing power loss, it might also result in the imparting of more fatigue to the machines than expected.

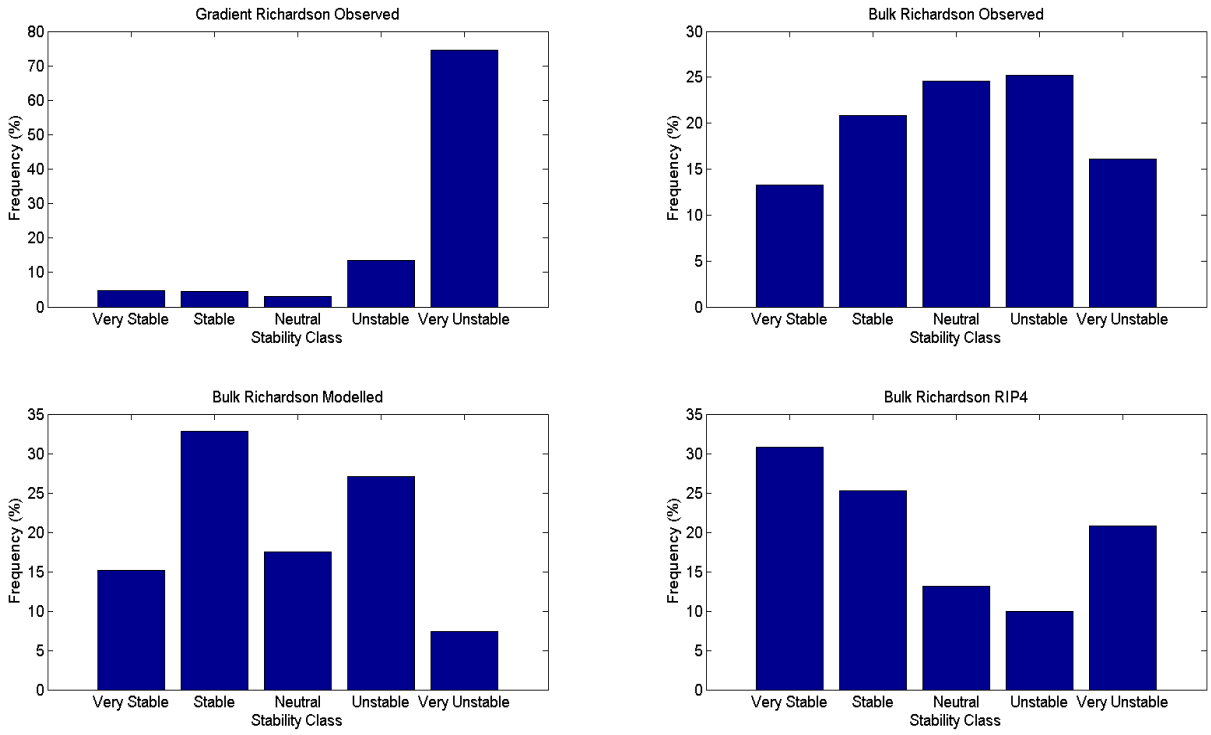

Figure 38 Frequency of stability at Shell Flats Mast 2 from approximations of the bulk and gradient Richardson number as modelled and observed.

6.4.2.2 Stability variation by time

Temporal variability in stability exists on diurnal and seasonal cycles, relative to the incident solar radiation. For with the diurnal variation, Figure 6.39 shows agreement in the general trend of all the metrics for stability throughout the day. A tendency for increasingly stable conditions during the evening and more unstable conditions during the daytime is present in both the modelled and observed time series. Where the different measures disagree is in the proportion of each stability class. To be expected is a dominance of very unstable conditions in the OGR series and to a lesser extent the OBR values. Comparing the calculated OBR and MBR values identifies a less pronounced diurnal change in the modelled values which also display a greater proportion of stable conditions. Stability as represented by BRR shows a trend more akin to the OBR series than the MBR series with a slightly greater proportion of very unstable conditions and a slightly more pronounced variation throughout the series compared to the MBR series.

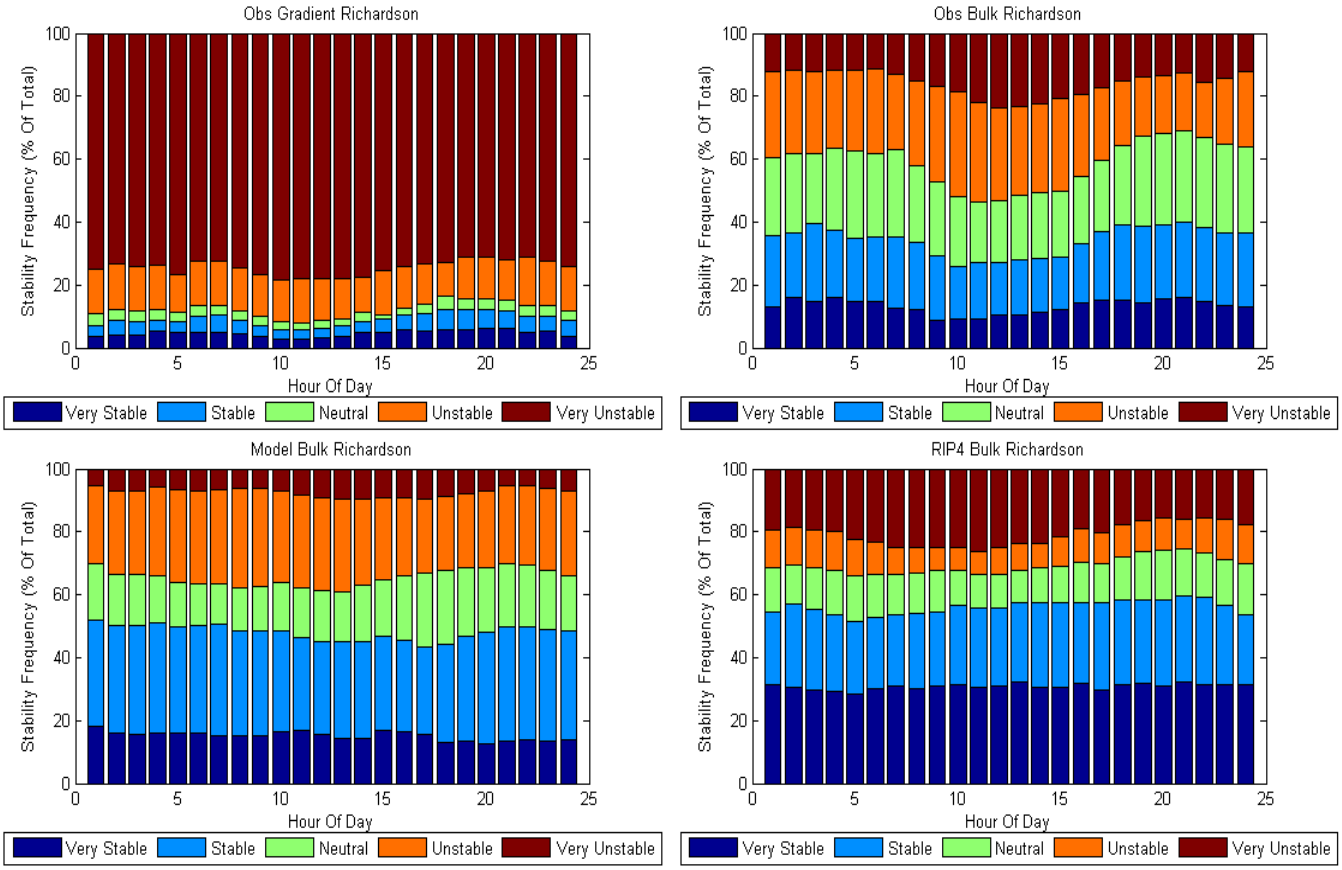

Figure 6.39 Observed and modelled approximations of stability as a function of time at Shell Flats Mast 2.

Stability variation classified by month is presented in Figure 6.40. In general the incidence of stable conditions is highest during the winter and spring months, with the most unstable conditions seen in the summer. As with stability change by hour of day, the plots show that the model seems to capture the observed seasonal trend quite well, aside from the obvious difference in proportions. As with the diurnal variation investigation, MBR shows quite different proportions of each stability class compared to the OBR series. MRR stability shows extensive similarities to the MBR derived stability with a slightly greater incidence of very unstable conditions. December shows a discernible presence of unstable conditions in all the series apart from the BRR, in a similar manner to the June case. Perhaps a better means of comparison between the OBR and MBR series relates to assessing the magnitude of conditions when the atmosphere is less unstable. For example in January and February, again ignoring a degree of discrepancy in proportions, the OBR and MBR series agree that the atmosphere is predominantly not unstable, however where they disagree is in the occurrence of neutral or stable conditions, with the modelled series

favouring a greater proportion of neutral conditions. April and May provide examples of where the model does not capture observed stability well, vastly over predicting the proportion of stable conditions. Further work needs to be done to fully identify the reasons behind these differences but ultimately a discernible level of coherence is evident between the modelled and observed stability as derived from bulk Richardson values.

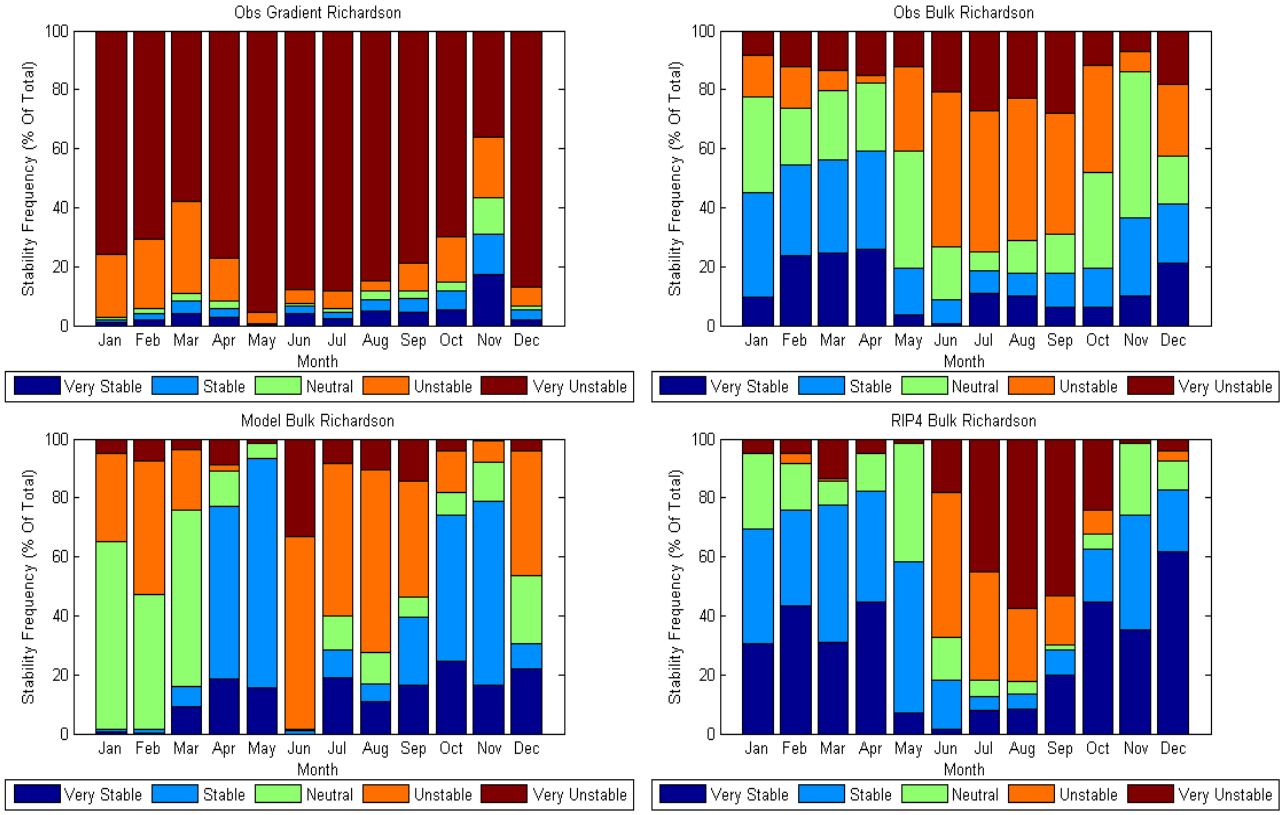

Figure 6.40 Observed and simulated approximations of stability at Shell Flats Mast 2, classified by month.

6.4.2.3 Stability variation by wind speed

Analysis of the trend in stability with wind speed (Figure 41) shows a decrease in unstable conditions in general apart from the highest wind speed bin in the OGR series. The OBR, MBR and BRR series all show an increase in neutral conditions with increasing wind speeds which reaches a majority at high wind speeds which is in agreement with the findings of Motta and Barthelmie (2005). Stability as approximated by OGR shows decreasing levels of the very unstable class as wind speed increases while the three bulk Richardson values show an increase in the number of stable conditions in the mid-speed range before neutral

conditions dominate at high wind speeds. Concentrating on the representations of stability from observations, the contrast between the bulk and gradient methods is especially evident. Increased mixing, promoted by high wind speeds, tends to act to negate thermal stratification required for modes of stability other than neutral. The profile shown by the OBR approximation is more likely representative of reality than that of the OGR series in which a highly unstable atmosphere persists at wind speeds of 20ms^{-1}. Indeed Motta and Barthelmie (2005) found that "high wind speeds are related to near-neutral conditions, while the two extreme stratifications dominate at speeds lower than 10ms^{-1}". The relationship between wind speed and stability as it is calculated here arises from the calculation of the Obukhov length which has a cubic relationship with friction velocity, itself a function of wind speed (Motta and Barthelmie, 2005). It is important to note the number of values comprising each speed bin is not equal, so while for example very unstable conditions do not appear dominant in the MBR plot, there are a greater number of observations in the lower wind speed range.

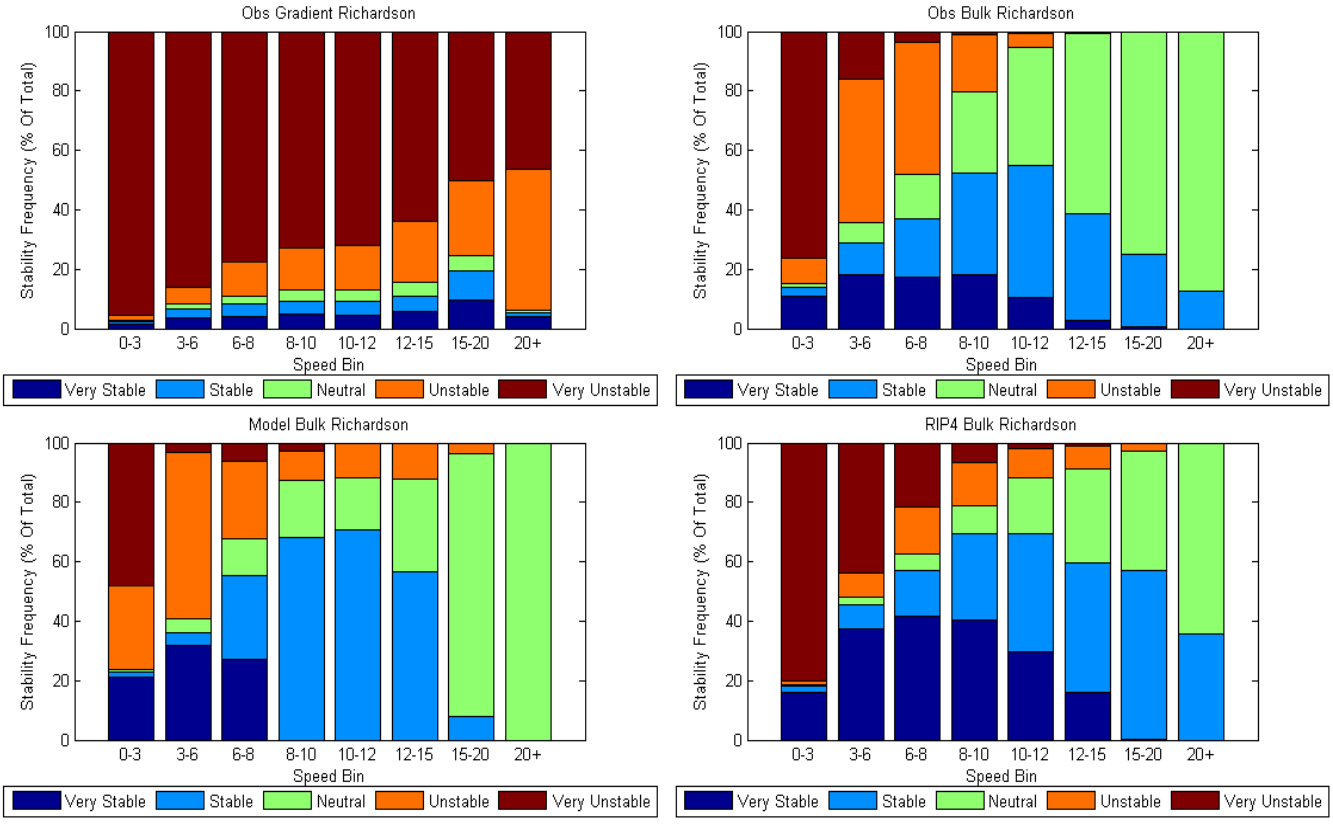

Figure 6.41 Observed and modelled approximations of stability at Shell Flats Mast 2 as a function of wind speed.

6.4.2.4 Stability variation by wind direction

Figure 6.42 shows the general patterns in stability relative to wind direction, where trends are consistent between the model and observation derived values. All measures agree that the greatest proportion of unstable conditions occur when a Northerly or Westerly component is present in the wind direction, the major difference being the proportion of each class. The observed bulk and gradient methods of approximation of Richardson number, show trends akin to one another with an expected difference in proportion of stability class. Increased stable and reduced very unstable conditions are seen in the Southerly direction sectors with more unstable conditions prevailing in Northerly direction sectors. While not always the case, air masses coming from the South are generally warmer than the sea over which they flow, promoting stable conditions, where, by contrast, air masses from the North can be colder than the sea over which they flow giving rise to unstable conditions. Stability during Westerly and Southerly conditions is similarly distributed across the OBR and MBR series, but Easterly and pure Northerly flow is simulated to correspond to a greater proportion of stable conditions than are observed. Such a scenario might point to flow modification by the land sea effect as the air mass passes over the British coastline, which is either missed by the model or erroneously included. The OBR and MBR series agree that more very unstable conditions are likely from winds with an Easterly component compared to those with a southerly component which, to an extent, is supported by the OGR series which shows a slightly greater proportion of very unstable cases in Easterly flow. Contrast is evident between the BRR and both the MBR and OBR series in the Easterly direction bins. The BRR series shows a much greater incidence of very stable cases than is seen in the MBR and OBR series.

Comparisons in this section cannot be definitive for two reasons. Firstly, the wind direction bins for modelled and observed derivations of stability are identified from modelled and observed data respectively, which at times may not reflect one another. Secondly, the number of cases which populate each direction bin are not equal which will affect the proportion of each class when comparing different measures. These plots are thus best used as guides of tendency rather than absolute measures of comparison.

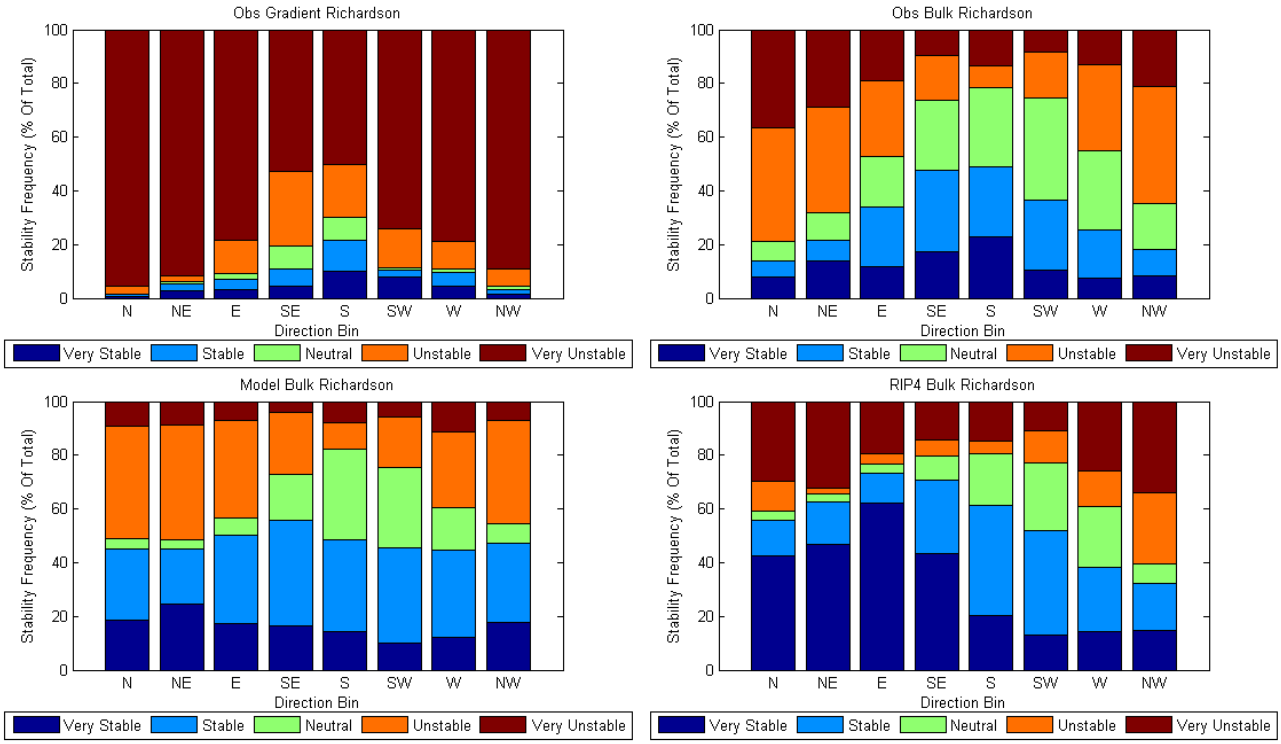

Figure 6.42 Observed and modelled approximations of stability at Shell Flats Mast 2 as a function of wind direction.

6.4.2.5 Stability variation by weather type

Stability, represented by the four measures, as classified by weather type (summarised in Table 6.20) is presented in Figure 6.43. Due to the added information available from a weather typing analysis, more can be learnt from analysis of these plots, but to do so requires greater consideration. Some consistency should be evident between the middle group of weather types (11-18) and the stability by direction plots, because they represent the same entity being wind direction. Some differences will exist between the weather type derived direction and the direction plots in the previous section because of the different sources of information determining the wind direction and the classification method for binning the data. However there are notable consistencies, for example the least unstable conditions include a southerly component, with a similar trend occurring under westerly flow, while easterly flow tends to bring a greater proportion of unstable conditions. The major similarities between the MBR and OBR values are evident under Easterly flow (classes 11, 12, 13, 21, 22, 23). While both MBR and

OBR measures imply conditions are predominantly very unstable, the model simulates a greater incidence of unstable cases than are observed. The highest incidence by far of stable conditions seen in the OGR series occurs during anticyclonic southerly conditions, which is reflected in the OBR and MBR series. The same three measures also see an above average level of stable and neutral conditions in the corresponding cyclonic Southerly type, which implies the source of the air mass does not affect stability when the flow is Southerly. By contrast stability under South-Easterly flow is affected by the airmass source and dominant pressure system, with stable conditions under cyclonic South-Easterly flow, while unstable conditions are seen under anticyclonic South-Easterly flow in the OBR and MBR series. Classification of stability by weather type adds an extra degree of information to the wind direction results by allowing the inference of airmass properties. Results indicate that the meridional component of the wind seems particularly relevant to the stability conditions witnessed at the site as classified by weather type, though only in relative terms compared across the different derivations of Richardson number. What the results also show is a degree of variability in the stability class in every weather type, so while stability can be inferred probabilistically, it appears not to be exclusively related to the weather type.

Table 20 Numerical designation of the Lamb weather type categories.

Lamb Weather Type (LWT) codes		
-1 U	-9 Non-existent	
0 AC		20 C
1 ANE	11 NE	21 CNE
2 AE	12 E	22 CE
3 ASE	13 SE	23 CSE
4 AS	14 S	24 CS
5 ASW	15 SW	25 CSW
6 AW	16 W	26 CW
7 ANW	17 NW	27 CNW
8 AN	18 N	28 CN

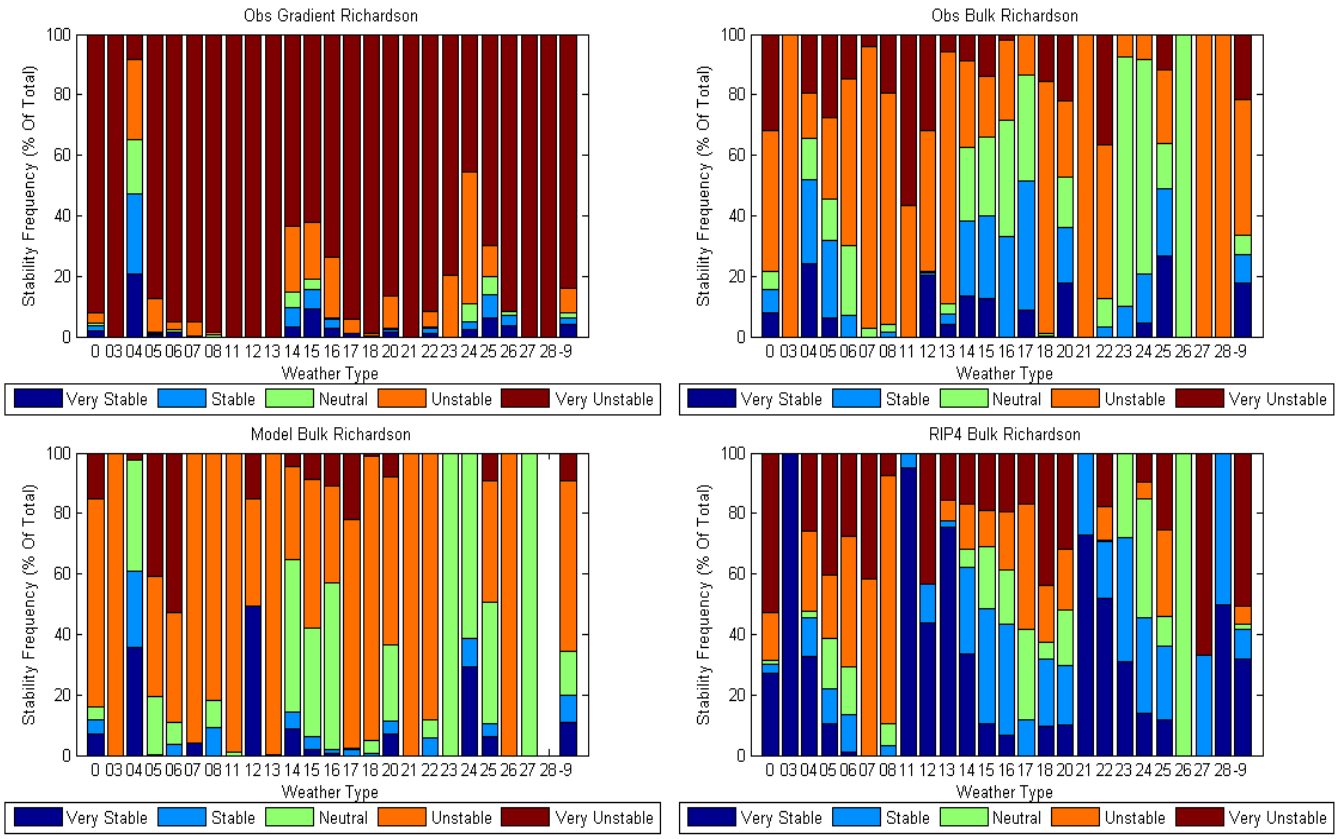

Figure 6.43 Observed and simulated stability at Shell Flats Mast 2 as a function of Lamb weather type.

6.4.3 Interaction between the different classifications of stability

Five variables were used to classify the occurrence of stability to see if and how the modelled values differed from those observed. While presented independently, it is important to remember these different classifications are entirely related. For example, considering the wind direction and time of year classifications, further investigation combining the two might confirm a number of related occurrences in particular stability classes. Take for example, the identification in the stability by wind direction analysis that Southerly flow tended to be less unstable than flow from the North. If this was then broken down further, by time of year, one might see a clearer distribution of stable and unstable conditions depending on time as a result of the thermal contrast through the seasons.

6.4.4 Assessment of the stability investigation at Shell Flats

6.4.4.1 Methods of approximating stability

Initially, there appeared little difference between the bulk and gradient Richardson number methods as approximations of stability when compared by

reference to observed wind shear. In the practical investigation where stability is calculated and classified by a number of variables for the Shell Flats resource assessment, there is stark contrast between the two Richardson measures in the proportion of stability classes observed. Not only is the proportion of stability classes different, but the variation in stability depending upon the variable by which stability is classified, can be different too. For example when classified by wind speed bin, the bulk Richardson number profiles appear similar to that seen in previous studies (e.g. Motta and Barthelmie, 2005), showing a rise in the proportion of neutral conditions with wind-speed, however the gradient Richardson number values maintain a strongly unstable dominance. Increased wind speeds tend to correspond to a more stratified flow which translates to a more stable or neutrally stratified atmosphere. As a result, based solely on these findings, the better approximation for stability in this work appears to be the bulk Richardson number method calculated using one measurement of wind speed at one height. What these results ultimately imply is that caution should be used when undertaking such investigations. It is not unlikely that differences between the two methods are artefacts arising from differences in the calculated layers and assumptions implicit in the Richardson number calculation and mapping to Obukhov length. It may be that the two measures are accurately reporting the atmospheric stability as intended and a small detail, perhaps a layer of air or a temperature inversion is translated into a big difference that separates the two measures. As a result one suggestion from this work is the standardisation of means of comparison. Approximations produced from different height levels are less valid than those made at the same levels because the factors influencing both may well be different and cannot be accounted for. In contrast, when using consistent height measurements, the influences should be the same. Furthermore, these measures of stability are only undertaken and representative for a particular location in the boundary layer, where local effects may be influencing approximations, which are not representative of the whole atmosphere either vertically or horizontally.

6.4.4.2 Model performance as a tool for simulating stability

Considering the performance of the model as a means to approximate stability, results here indicate definite potential. Comparing the bulk Richardson derived stability, from variables outputted by the model and observed at Shell Flats,

both series' showed a balance of stable and unstable conditions, though the modelled results favoured less neutral values than were observed. The OBR series displayed a stronger tendency towards unstable conditions while the MBR series showed a greater proportion of stable conditions. When OBR and MBR derived stability were compared using different variables to classify the incidence of stability, patterns which were observed were to a large extent replicated by the simulated stability, albeit with a slight tendency towards more stable conditions in the modelled data. In the practical context of wind farm operation, output projections based on the model simulation would likely be on the conservative side. Wake losses would probably not be as significant as originally thought because of the increased turbulent mixing arising from greater incidence of unstable conditions, which however, would also mean increased fatigue imparted to the turbines due to the higher level of turbulence. Ultimately the model simulates variation in stability to a an appreciable degree by reference to observations. A tendency towards more stable conditions was identified and with further work to establish and quantify the magnitude, could be accounted for by a systematic correction. Given the accuracy with which modelled stability reflects that observed throughout the classifications, it could be a successful addition to a wind resource assessment campaign. Clearly these results are applicable to a long term resource assessment where aggregated statistics are used for planning. While the results show the model has skill, further work would need to be undertaken to investigate the performance of the model on short timescales for use in an operational capacity such as short term forecasting.

6.5 Resource assessment for the Supergen Wind exemplar farm

6.5.1 The wind resource

To provide an example of the potential of NWP as a resource assessment tool, a resource assessment was performed for the Supergen Wind exemplar site. Wind speed, wind direction and temperature were produced to quantify the wind field of the site as well as the stability conditions. The variables were produced from June 2003-June 2004. Wind speed was produced at five heights to provide a vertical profile, stretching from the surface layer at 10m to 160m, around the height at which one would expect the rotating blade tips of a modern turbine to reach in operation. A vertical wind speed profile is of great use to operators as it will give an indication of

the shear expected at the site and an impression of how it changes through the year under different conditions. Average wind speed from June 2003 to June 2004 at hub height (90m) for the Exemplar farm is found to be 9.04 ms^{-1} with a standard deviation of 4.48 ms^{-1}. The two-parameter Weibull distribution statistics for the series are a scale (C) value of 10.22 ms^{-1} and a shape (k) value of 2.13 ms^{-1}, providing a more comprehensive impression of the wind speed distribution at the site.

Wind direction distribution is shown in Figure 6.44 with the prevailing wind direction simulated to be south westerly, with a strong north-westerly component also present. Easterly flow comprises relatively little of the general wind direction observations for the exemplar site. The average vertical windspeed profile is shown in Figure 6.45 which could be compared against similar profiles under different conditions for analysis. For example, much like with stability, it might be of benefit to the operator to classify vertical wind speed profile by weather type or wind direction to help inform a farm optimisation strategy for given synoptic conditions which relates to array performance.

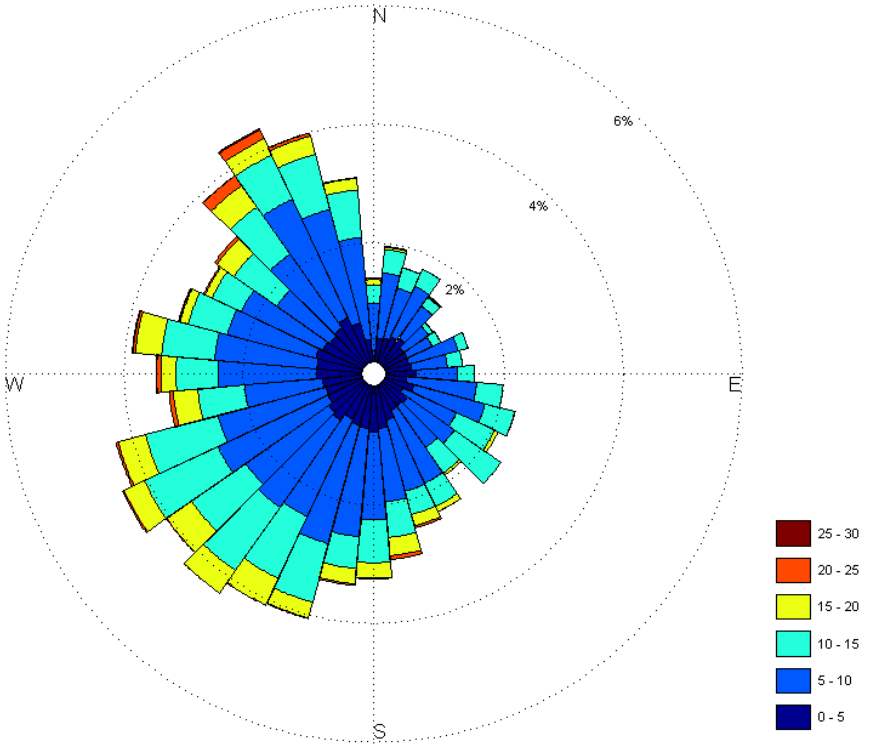

Figure 6.44 Wind rose at 40m for the Supergen Wind Exemplar site.

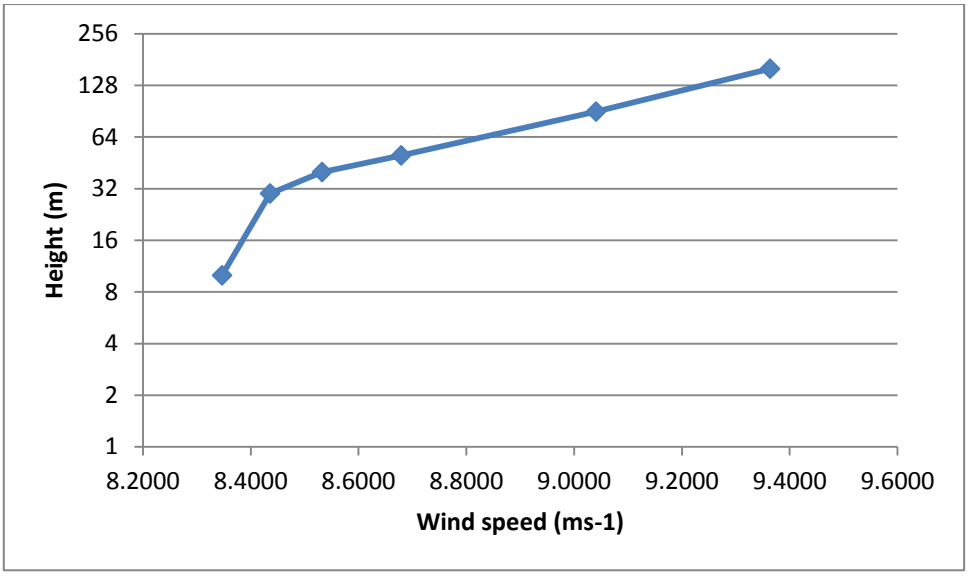

Figure 6.45 Average vertical wind speed profile at the Supergen Exemplar site from June 2003 to June 2004.

6.5.2 Stability at the Supergen Exemplar site

Stability as simulated at the Exemplar site is predominantly neutral (Figure 6.46) in contrast to the Shell Flats site, the difference could be related to the contrast in fetch between the two sites as the Shell Flats fetch includes a land-sea interface. With such a neutral atmosphere, wakes would not dissipate as quickly as if they conditions were more unstable, however turbulence levels would be lower and there would potentially be less fatiguing present. When considered in the context of the results from the Shell Flats resource assessment, model tendency was towards a more stable atmosphere than was observed, so if the same bias is present in this model run, actual conditions at the site may well be unstable. Figure 6.47 provides an insight into the variability of stability at the Exemplar site on diurnal and seasonal cycles as well as for different wind speed and direction values. Overwhelmingly the stability is neutral, as Figure 6.46 would suggest, but the variation of stability by reference to the other variables seems to follow a similar pattern to that observed at Shell Flats. For example more unstable conditions are observed at lower wind speeds as well as during the summer months.

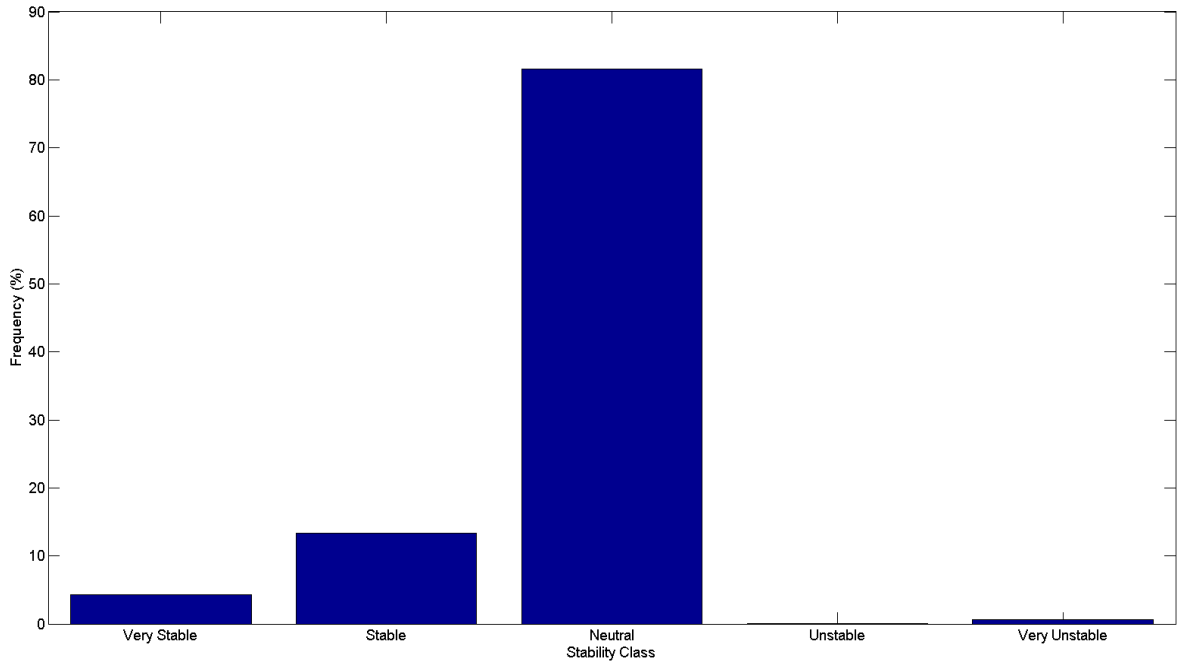

Figure 6.46 Simulated stability at the Supergen exemplar wind farm site for the duration of the resource assessment.

6.5.3 Variation across the farm site

Model output for the wind resource assessment of the Supergen exemplar site was produced for the centre point of the farm to be as representative as possible for the whole farm. Three months of simulations were performed to gain an impression of the deviation in conditions seen across the farm. Due to the size of the Exemplar farm, designed to be representative of a round three site, it is entirely possible that turbines at opposite extremities of the farm might be subject to different weather systems at the same time. A resource assessment for the farms centre point could thus be inapplicable for other parts of the wind farm. Such a scenario highlights the weakness of having one observational series representing a whole wind farm and supports the case for application of NWP models which, through observational nudging and data assimilation, can dynamically expand the scope of a single point observational series. Figure 6.48 is an example of one occasion in January 2004 where wind direction was variable over the extent of the wind farm area. What the schematic diagram shows is instantaneously sampled wind direction across the farm, which in this case could identify the presence of a high pressure system moving in.

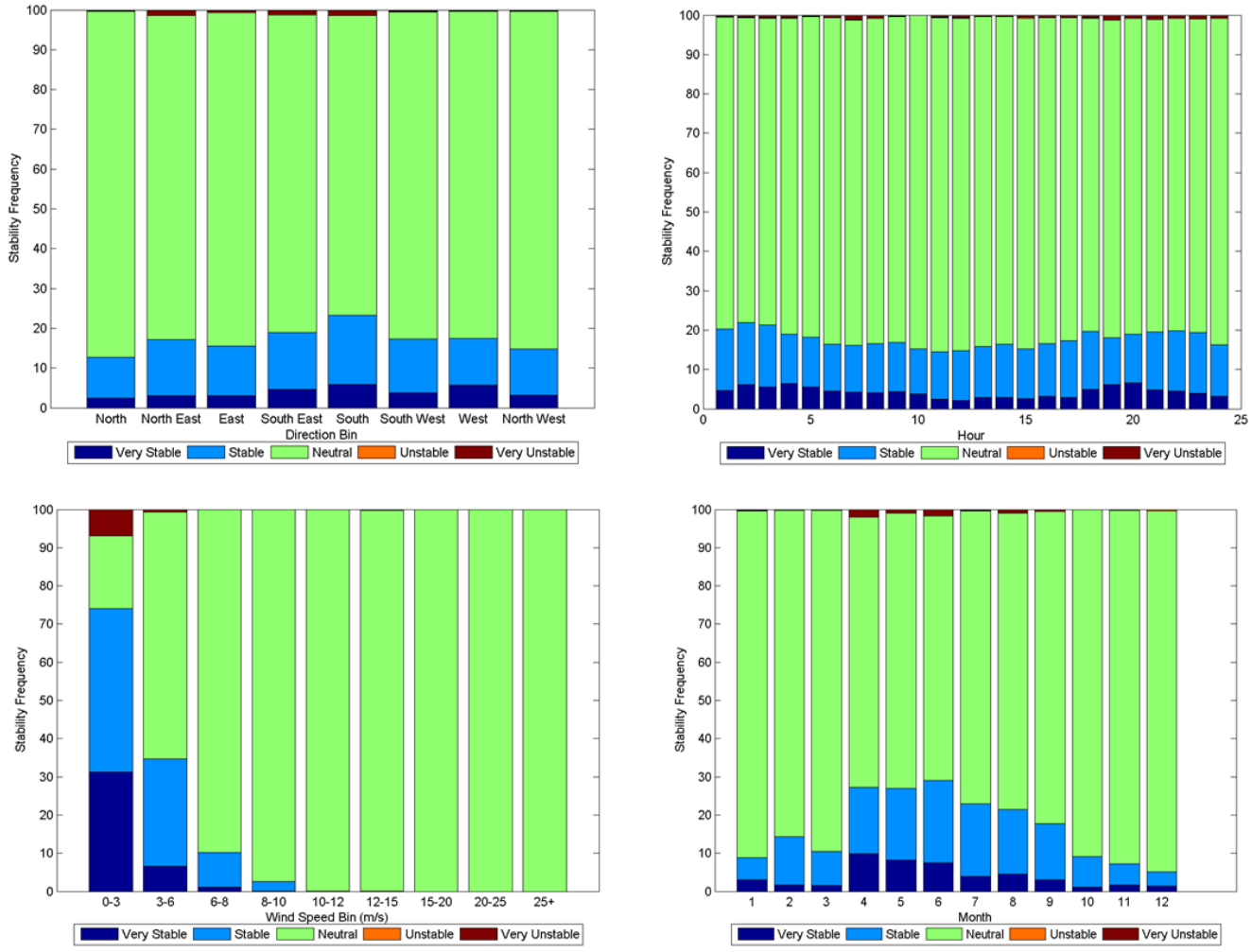

Figure 6.47 Simulated stability at the Supergen Exemplar site by reference to (clockwise from the bottom left) wind speed, wind direction, diurnal and seasonal timescales.

Table 6.22 provides an insight into the variation in the simulated variables across the exemplar site, something which could not be achieved using one observational series. Wind direction is 9 degrees different at the centre of the farm compared to the extremities, the reason for which is unknown. The wind has a slightly more Westerly component in the North and West stations compared to the South and East stations. Average wind speed is higher at the centre of the farm also, compared with the extremities, while the North and West stations see slightly higher speeds than the South and East stations which could be related to the slight difference in direction. The centre point of the farm also appears to be experience temperatures slightly low the rest of the farm. Stability, inferred by the bulk Richardson number appears

slightly nearer to neutral for the Centre, North and West points, while the Southern point appears to experience slightly more unstable conditions.

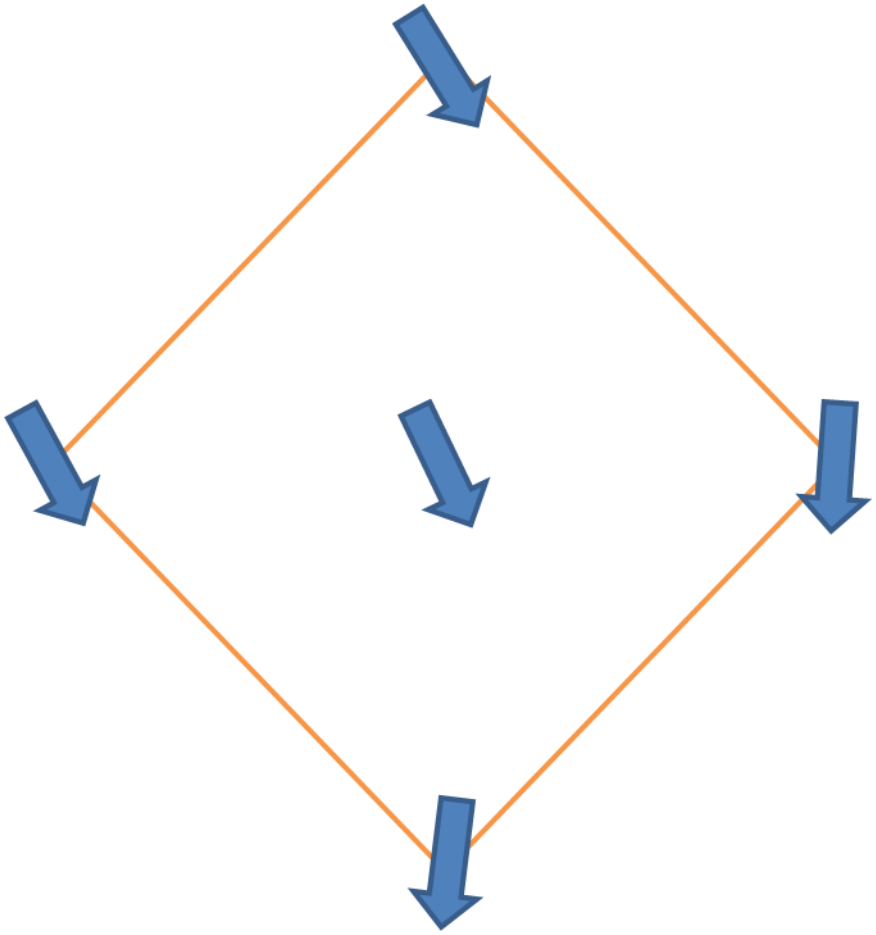

Figure 6.48 Schematic representation of wind direction variation across the Supergen exemplar farm on the 13th January 2004

Table 6.21 Average values of variables across the Supergen exemplar farm from the 3 months simulated.

		Centre	North	South	West	East
Bulk Richardson number	Average	0.0852	0.0857	0.5053	0.0846	0.1264
	Standard deviation	1.2199	1.1644	17.4306	0.9312	2.9106
10m Temperature (°K)	Average	281.0589	281.1292	281.1324	281.1526	281.1074
	Standard deviation	1.4943	1.4880	1.4900	1.4862	1.4905
50m temperature (°K)	Average	280.7523	280.8192	280.8364	280.8504	280.8031
	Standard deviation	1.5715	1.5649	1.5548	1.5656	1.5555
Wind Speed (m/s)	Average	8.6843	8.6233	8.6036	8.6099	8.6121
	Standard deviation	3.5772	3.6365	3.6605	3.6364	3.6547
Wind Direction (°)	Average	229.2715	221.1449	220.8757	220.7979	221.3610
	Standard deviation	89.0979	90.5928	91.0276	91.6048	93.3602

6.6 Summary of long term resource assessment analysis

The aim of this investigation was to provide a practical demonstration of the capability of WRF as a long term resource assessment tool. Initial comparison of model and observations showed excellent potential, particularly after the filtering process to focus on features corresponding to the resolved scale of the model. Not only was wind speed variability well accounted for, but wind speed distribution between the model output and observations was very similar which is of great importance to potential end users. The average correlation coefficient for wind direction was reasonably good, but showed a large RMSE which combined with the good accuracy of the wind speed results implies that the weather systems controlling the wind field are being accurately simulated in general apart from perhaps positioning of pressure systems might be the reason for the wind direction results. When model performance is considered relative to nearby observational series the results are, in general, encouraging. While the best series at representing observations at Shell Flats Mast 2 is observational data from Shell Flats Mast 1, the model performs to a high level within a reasonable margin of that achieved by observations from Mast 1, particularly when filtered to 6-hourly resolution, which given the constraints it operates within (6 hourly input and 2km spatial resolution), signifies great potential. Even with a short distance over water the RMSE of Mast 1 as a predictor of Mast 2 is 1.4, which is not much smaller than the model value. Model output comprehensively outperformed the nearest onshore met station, which historically might have been used for an MCP study during the planning stage, further justifying the application of an NWP model to providing a resource assessment for Shell Flats.

7 Optimising model performance

Information from the modelled runs undertaken previously was considered, alongside extensive reviewing of the literature, to develop an investigation which would aim to optimise model setup for the application to wind resource assessment. Ideally model performance should improve quantifiably by the same measures already used in the benchmarking exercise. In addition, the aim was to provide more information about the model performance, to be used in strengthening assertions made from analysis of the model output. For example if model performance can be shown to be particularly strong in one area/ scenario/ set of conditions, more confidence can be assigned to the output when those conditions recur. Conversely if model performance is found to be lacking, more uncertainty can be conveyed alongside the output to give the end user as much information as possible about the strength of the data on which they are basing key decisions. SST input was included and observational nudging of wind speed was employed. Two ensembles were created, one by offsetting the initialisation time of a run and combining the members for the overlapping period and the other by using different physical setups for the PBL. Twenty individual cases were chosen based on the prevailing weather type over the course of the run, for which five different boundary layer schemes were used and from three initialisation times, corresponding to a total of 300 runs.

7.1 Method

Results from the previous investigations had identified areas for improvement in model performance. The model optimisation investigation is intended to focus on those areas of uncertainty and try to improve model performance. As the most important variable to a wind resource assessment, wind speed is the variable model performance will be optimised for. Atmospheric features which cause changes in the wind field at low and medium frequencies exist at the medium to large scale which the model is able to directly resolve. Smaller sub-grid scale features are approximated by parameterisation schemes, which is one of the areas identified for improvement. Different PBL parameterisation schemes are available for WRF and a range were tested to see which performed best in the offshore environment. An ensemble of the different PBL schemes was generated to provide an insight into the

uncertainty associated with the PBL and see if an ensemble was a preferable option to an individual scheme. Another area of uncertainty related to the initial conditions provided to the model. While the CFSR reanalysis product is useful resource, a variety of factors (e.g. temporal and spatial resolution, interpolation method) mean that precisely representative values are unlikely to be provided. A time offset ensemble was created comprising members initialised at staggered intervals and combined for the period of overlap. This effectively provided three sets of initial conditions for each run which were updated throughout the run, which was intended to reduce divergence between model and observations. The investigation was undertaken for the Scroby Sands site, which provided a means of comparison by which to judge any improvement.

7.1.1 Computing setup

Model optimisation runs were undertaken on the HECToR facility using the second high performance computing account awarded to this research in the November 2012 resource allocation panel which required a peer reviewed application. Pre-processing of the input data and nudging steps were undertaken on CREST03 before the input files were compressed and sent to HECToR where the model solver was run for each case. Each case was run on 288 cores of HECToR which in combination with the resource allocation allowed around six runs to be undertaken simultaneously with another 6 in preparation or postprocessing depending upon the stage of the run. Post processing was also undertaken on HECToR after which the output files were transferred back to the working desktop for analysis in Matlab©.

7.1.2 Selection of run periods

Run periods were selected based upon the prevailing Lamb weather type as classified by Jones et al (2013) from the NCEP reanalysis product (Kalnay et al, 1996). Weather typing is a useful concept in synoptic meteorology whereby a classification of the atmosphere is performed by describing the type and location of the dominant pressure system affecting the UK. From this knowledge of the airmass can be inferred and assumptions made of the likely conditions. Choosing simulation periods dominated by consistent weather types tests if model performance is related to particular synoptic conditions, but also allows the classification of the wind observed at the site for given weather types. The benefit of relating wind conditions

to synoptic states is that models are better at simulating large scale circulation features. Therefore while longer term simulations will degrade in accuracy with look ahead time, if the correct synoptic features can be simulated then some properties of the wind might be inferred from large scale features simulated by the model. The investigation was undertaken for the year of 1996 to be able to compare results against those obtained in the benchmarking investigation. Daily weather types for the whole year were reviewed. Periods of consistent weather type were selected but it was important to get a balance of different weather types. Table 7.22 shows the cases eventually selected comprising cases dominated by both single and mixed weather types. The selection of cases dominated by a single weather type were made intentionally to identify pure weather type cases to allow the best chance of identifying related behaviours in stability. A number of different weather types which comprised mixed runs were undertaken for comparison, with the next step of research suggested to consider the sequence of weather types upon variations in stability. The number of cases selected was limited because of the number of ensemble member runs which needed to be undertaken to fulfil the aims. Five boundary layer options and three initialisations for 20 cases required 300 model runs. As identified in the early part of this research, optimal model run length is around 3-4 days. Model runs for this investigation were three days and 18 hours long with the first six hours discarded as spin-up. For the time offset ensemble runs one set of PBL members was initialised at the start of the run assigned the tag T00, one set of members was initialised 24 hours into the run assigned T24 and the final set of members were initialised 48 hours after the start of the run and were assigned T48.

Table 7.22 Twenty simulation periods selected for the optimisation runs with corresponding weather type.

Run dates		
From	**To**	**Weather type**
31/12/1995 00:00	03/01/1996 18:00	SE, SE, A, S
07/01/1996 00:00	10/01/1996 18:00	S
20/01/1996 00:00	23/01/1996 18:00	E
27/01/1996 00:00	30/01/1996 18:00	E
06/02/1996 00:00	09/02/1996 18:00	C, C, C, S
01/03/1996 00:00	04/03/1996 18:00	AN, AN, N, N
13/03/1996 00:00	16/03/1996 18:00	SE ,SE, SE, C
02/04/1996 00:00	05/04/1996 18:00	A
01/05/1996 00:00	04/05/1996 18:00	NE
22/05/1996 00:00	25/05/1996 18:00	CS, C, CW, CW
15/06/1996 00:00	18/06/1996 18:00	A
08/07/1996 00:00	11/07/1996 18:00	W
12/07/1996 00:00	15/07/1996 18:00	W, W, A, A
31/07/1996 00:00	03/08/1996 18:00	CW, CW, AW, A
23/08/1996 00:00	26/08/1996 18:00	C
04/09/1996 00:00	07/09/1996 18:00	AE
09/09/1996 00:00	12/09/1996 18:00	N, N, N, NW
17/10/1996 00:00	20/10/1996 18:00	SW
22/10/1996 00:00	25/10/1996 18:00	S, S, AS, CS
06/11/1996 00:00	09/11/1996 18:00	CW, CNW, W, CW

7.1.3 Model setup

7.1.3.1 Physical setup

The same domain setup was used for the optimisation runs as was used in the benchmarking runs which employed three domains at 18, 6 and 2 km resolution shown in Figure 5.17 and described in Table 5.6. Input data were sourced again from the 0.5° 6-hourly CFSR product. SST data was obtained from the CFSR archive to augment the standard skin temperature (TSK) field which is provided in the WRF-specific dataset. Updating the SST field was found to improve the performance of WRF and reduce bias in a wind resource assessment investigation by Shimada and Ohsawa (2011).

7.1.3.2 Dynamical setup

To preserve consistency between the runs, dynamical setup was the same as used in the benchmarking runs with the exception of some variations to the selection of PBL scheme used for the ensemble member runs. The MYJ scheme was used throughout the runs again for the purposes of consistency between the investigations, but also because it is a widely used and validated boundary layer scheme. The PBL schemes used for the PBL ensemble research have been described in the literature review and theory chapters. It was important to use a range of PBL schemes with different approaches to modelling the boundary layer to see which performed best but also utilise the skill present from each method in the ensemble. Local schemes tend to accompany higher turbulence closure models which provide a more complete simulation which is of benefit to this research. Non-local schemes however provide a more complete representation of fluxes through the depth of the boundary layer which is of most importance under unstable conditions. The MYJ scheme is a local 1.5 order closure scheme with a prognostic term for calculating TKE. MYJ was chosen because it is a widely used scheme and has been shown to perform well from stable to slightly unstable conditions. The first order nonlocal ACM2 scheme was used because of its novel treatment of fluxes through the boundary layer, which should offer good performance under unstable conditions. The MYNN 2.5 is a local 1.5 order closure scheme which simulates diffusion through the boundary layer in a slightly different manner to the MYJ scheme, but shares many other commonalities. The QNSE scheme operates locally and employs a 1.5 order spectral closure model, developed for stable conditions. The four schemes provide a diversity of approaches by which to approximate turbulent fluxes in the boundary layer under a range of stability conditions. Each PBL scheme is provided with input from a surface layer parameterisation scheme within WRF. There are a range of surface layer schemes which are generally developed to complement a particular PBL scheme. For this research, the surface layer scheme recommended in the WRF user's manual for the corresponding PBL scheme was used. The fifth and final ensemble member uses the MYJ PBL scheme but is not nudged. For the first two test cases (beginning 31/12/19950 and 07/01/1996), the YSU PBL scheme was tested while the QNSE scheme was not used. The investigation was undertaken with the QNSE scheme because it had not been

investigated in this work while the YSU scheme was exclusively used in the Shell Flats runs.

7.1.4 Model output

This investigation focussed solely on wind speed which was produced for the site of the Scroby Sands mast at 10 minute temporal resolution and 50m height. Each ensemble member is an individual model run with a different setup configuration or initialisation time. The process by which the members combine to become an ensemble is described in the next section.

7.1.5 Nudging

Nudging was employed to assimilate hourly 10m wind speed from Hemsby into the model input files for the cases comprising the optimisation runs. Nudging offered another method by which to account for some uncertainty associated with the initial conditions by providing information from a nearby site at a higher temporal resolution than the input data. Observations were, as with the Shell Flats resource assessment runs, integrated using the Obsgrid program once the data had been prepared into little-R format. All of the different setups were run with nudging and to test the benefit of the technique an extra MYJ PBL setup was run without observational nudging to test its performance, which, as a result provided another ensemble member.

7.1.6 Ensembles

Conceptually, the purpose of an ensemble is to evaluate the prediction of uncertainty. Model performance in the PBL is one of the areas, identified in this work, as requiring improvement, where sub-grid scale processes contribute to changes in wind speed which the model is unable to replicate. The other main source of uncertainty in NWP modelling is the accuracy of initial conditions, from which the model solves equations to simulate atmospheric evolution. The chaotic nature of the atmosphere makes accurate initial conditions very important so as to minimise divergence between the model solution and observations. The ensembles in this investigation are presented in the upcoming sections. The method by which they are generated and applied is discussed firstly for the PBL ensemble, secondly for the time offset ensemble and finally for the unified time offset ensemble system (TOES) which consists of members from both ensembles. Similar work has been published

by Deppe et al (2013), whereby an ensemble consisting of different PBL schemes is developed, as is a lagged initialisation ensemble.

7.1.6.1 PBL ensemble

A PBL ensemble addresses the uncertainty surrounding the representation of boundary layer processes by the model. PBL schemes have been reviewed and were shown to be variable in performance, depending upon the prevailing conditions (for example Deppe et al, 2013; Nolan et al, 2009). By producing an ensemble, multiple treatments of boundary layer processes are adopted. Either one PBL scheme will be identified as the best performer, or an ensemble mean with a diverse skill range will be produced from the combined skill of the individual members. The ensemble mean in this work is unweighted. As a pioneering study for the sites used, there are no other results upon which to base a weighting scheme, though results from the work will help inform future considerations for weighting the schemes accordingly. The unweighted ensemble mean will be the product of an average of each wind speed value from the five PBL options for each time step.

7.1.6.2 Time offset ensemble

The uncertainty associated with initial conditions is addressed by this work through the creation of the time offset ensemble. Rather than perturbing initial conditions from the start of the run, successively offset members are integrated into the ensemble as they are initialised later on through the run, which also effectively updates the earlier initialised run. The time offsets were at T+00, T+24 and T+48 hours for each case and each PBL option was run for each initialisation time. Where the time offset ensemble differs from the PBL ensemble is in the weighting of the members. Intuitively more weight should be afforded to the most recently initialised members because they have the latest information and have had the least amount of time to diverge from observations. This study investigates the different weighting strategies available to the user of a time offset ensemble by creating an unweighted scheme as well as two weighted schemes affording preference to the more recently initialised member(s), a technique applied by Lu et al (2007). The weighted schemes were generated by averaging the members of the previous lag to be equal to one member of the most recent time offset series. For the T48 ensemble this was achievable in two ways, firstly by providing equal weight to T24 and T48 members but averaging all the T00 members to account for the weight of one T24 and T48

member. Then, secondly, by affording more weight to T48 by averaging all the T00 and T24 members to be equal to one T48 ensemble member. Staggering the initialisation time of the ensemble members is a variant of a reinitialisation run, whereby a model run is comprised of a series of shorter runs, rather than undertaking one long model run for the duration. Lo et al (2008) found reinitialisation to provide better results than a traditional full length run, however the extra computing cost is a considerable addition.

7.1.6.3 Time offset ensemble system (TOES)

The time offset ensemble system (TOES) is a collection of all the ensemble members from both PBL and time offset ensembles. In essence the TOES is very similar to the time offset ensemble but considers the contribution of the PBL members more explicitly than simply averaging them for the purpose of creating a mean value for a given initialisation time. In addition the three weighting techniques detailed in the previous section are available with or without the inclusion of the nudged MYJ run to add another source of uncertainty into the ensemble system which in total provides eight variants of the TOES, though not all for the same time interval. Combining all the members from both ensembles provided a great range of skill throughout the run, but also a good opportunity to investigate the use of the spread error relationship used to identify model uncertainty during a run. While the ensemble spread-error relationship has been shown to offer value to NWP output, it is highly sensitive to the conditions in which it is used. Mentioned earlier in the literature review was the assertion that linear spread-error relationships are only of interest when spread is extreme and when compared to the climatological mean (Whitaker and Loughe 1998). This work will calculate the linear spread-error relationship for all the cases using every available ensemble member to maximise the potential for spread. The spread error relationship is defined by the correlation which exists between model mean absolute error and the ensemble spread. Ensemble spread is represented by the standard deviation of the ensemble members for a given time step, however the mean value used can be changed. This work will present results from the instantaneous mean value, which is calculated for every time step, as well as the climatological mean value, which is calculated from all available members for the duration of the run. To help identify when ensemble spread is anomalously high or low, plots for each run are produced which display an

indicator variable which show a nonzero value if the ensemble spread is greater than two standard deviations of the mean. Two standard deviations of the mean were selected to indicate anomalous values simply as a rough guide. In a Gaussian distribution 95% of data points are found within two standard deviations of the mean. While the wind speed distribution is not Gaussian, the indicator as a rough guide works well.

7.2 Model performance

7.2.1 General comments

To begin with, a general impression of the ensemble model performance is described, against which results from the optimisation strategies will have a frame of reference to which they can be compared. Average statistics for the nudged MYJ PBL scheme runs at TOES t+0 are presented as a rough indicator of baseline performance for this set of runs and to provide some initial comparisons against other model runs. As the MYJ scheme was used in the benchmarking investigation, it is logical to use the same PBL scheme for comparison. Average correlation coefficient across the 20 cases is 0.6, which is lower than the results from the benchmarking study (0.64). While a RMSE of 2.57 ms^{-1} is higher than the average result from the Scroby Sands benchmark runs (2.19 ms^{-1}). Initial performance for the optimised setup, including SST update and observational nudging of wind speed, is thus worse than results from the benchmarking performance study discussed in Chapter 5. A median correlation of 0.69 suggests it is likely the average performance of the optimised runs was affected by a few anomalously poor runs, such as the case of July the 31st where correlation was 0.08. It is vital to the successful understanding and development of the model, as a wind resource assessment tool, that such cases are identified and reviewed.

7.2.2 Wind speed variability

Results from the benchmarking and Shell Flats investigations imply that the degree of wind speed variability present in a run is related to the scale of the dominant atmospheric processes at the time. For example, small scale atmospheric processes such as convective cells are more likely to relate to large amounts of high frequency variation but lower overall variation through the run. In contrast a high

pressure system is likely to see suppressed high frequency variability but perhaps more pronounced medium or low frequency change which translates to larger variation over the course of the run. Standard deviation is used as a measure of variability because, as Figure 7.49 shows, runs with a higher standard deviation show a greater degree of change over the course of the run. However what standard deviation cannot represent is the type of variation seen, which relates to the frequency at which the change occurs. Synoptic weather typing allows an observer to infer characteristics of an airmass based on knowledge of its origin and path of travel. With information regarding the pressure tendency, assertions can be made about some likely properties of the dominant weather, such as wind speed variability. It is important to reiterate from the outset that any inferences made based on weather type are relative to one another, much like discussing pressure systems. For example a northerly flow is likely to bring a cooler, drier airmass than a south-westerly flow would. Due to the large number of ensemble runs needed to complete the investigation, the number of overall cases had to be limited. While efforts were made to provide a balance of diversity and consistency in weather types, there is a restriction on the assertions which can be made based on this limited sample. Analysis of the individual runs provides insight into the variability of windspeed resulting from different synoptic conditions and the ability of the model to recreate such variability. Both anticyclonic and Easterly weather types correspond to reduced variability while Northerly and cyclonic weather types tend to coincide with increased variability as represented by standard deviation. The runs which comprise Figure 49 were selected to illustrate the points made about variability relative to weather type and also show the degree of variation seen across the cases relative to standard deviation. Both of the simulations undertaken in May are examples of runs with larger variation, May the 1st is dominated by North-Easterly flow while May the 22nd is dominated by cyclonic conditions with varying directional components. The remaining two runs are examples of runs with a relatively low degree of variability, Jan the 20th is an example of an easterly dominated case while April the 2nd consistently experiences anticyclonic conditions.

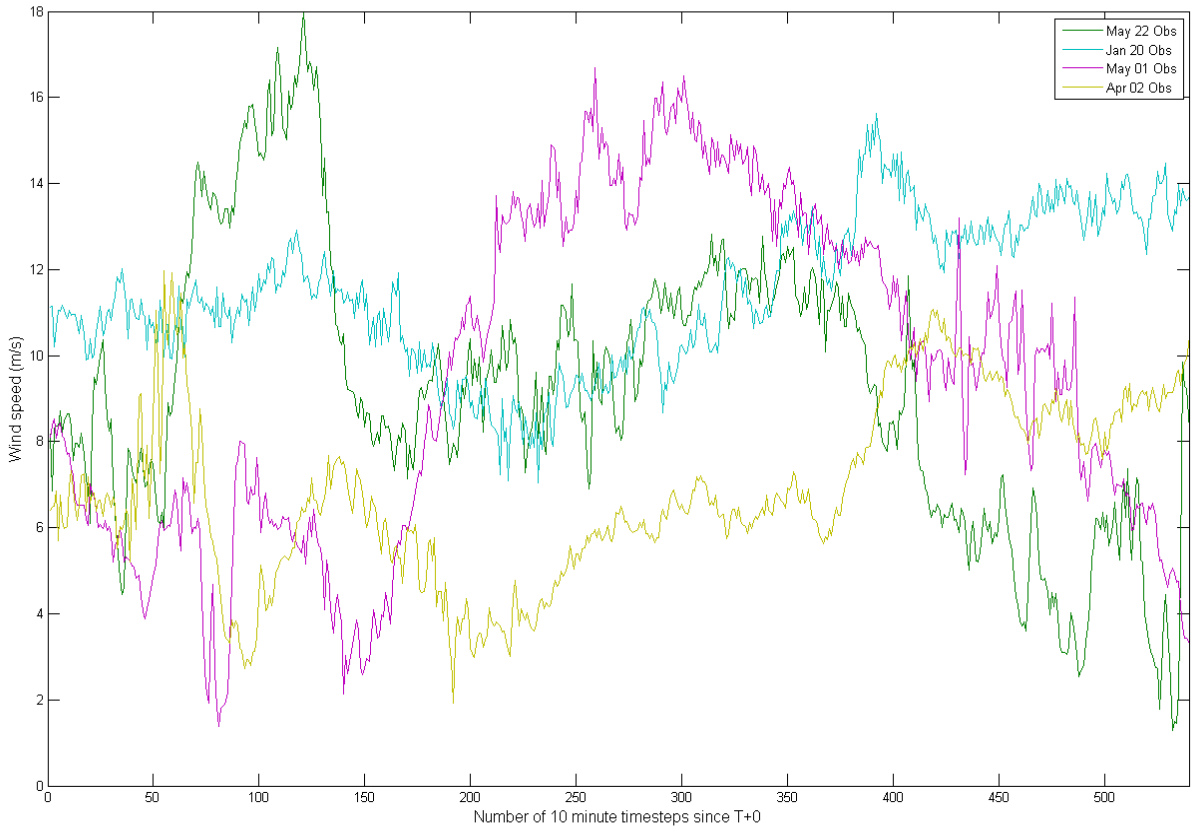

Figure 7.49 Observed wind speed from four cases illustrating the difference in variability through the run related to weather type. Standard Deviations for May 01 & 22, Jan 20 and Apr 02 are 3.9, 3.3, 1.7 and 2.0 ms^{-1} respectively.

7.2.3 Model performance by reference to weather type

The range of runs described in the methods section are undertaken for Scroby Sands, using a range of initialisation times and PBL schemes including a non-nudged run to simulate wind speed at Scroby Sands. The cases in Figure 7.49 were selected to illustrate the difference in observed variability through the runs with respect to weather type. For this part of the analysis, average statistics are comprised of all the available T+0 PBL schemes, including the non-nudged run, for the case in question. Despite the marked difference in variability through the runs and the contrast in dominant synoptic conditions, on the basis of these four runs there is little indication of state dependence in model performance. While the January the 20th run shows relatively little variation and is consistently under easterly flow conditions, model performance shows a moderate correlation of 0.52 and a reasonably high RMSE of 3.2 ms^{-1}. For the other case with low variability, April the 2nd, the model performs well showing a correlation of 0.77 and the lowest average

model RMSE of 1.5 ms^{-1}. A similar contrast in performance is evident in the runs with more variability. Model performance is poor for the May the 1st case showing a correlation with observations of 0.38 and a significant RMSE of 3.7 ms^{-1}. However the model performs very well in the May 22nd case, achieving a correlation of 0.8 and a RMSE of 2.09 ms^{-1}. Mentioned earlier in the chapter was that the poorest run in terms of model performance was the case of July the 31st. Figure 7.50 shows three TOES members which are the PBL ensemble mean runs. This is to show the best effort the model was able to make at simulating wind speed for the July 31st case, using all the PBL information and from the three different initialisation times. Statistics for the T+00 PBL ensemble mean exhibited a correlation of 0.01 and an RMSE of 2.89 ms^{-1}. The case is characterised by a change in dominant pressure system after 2 days with a transition from cyclonic to anticyclonic. The first two days show high frequency variation of significant magnitude dominating the mode of variation which the model struggles to simulate. In the latter half of the run, wind speed variability visibly smooth out as anticyclonic conditions dominate, but a couple of ramp events are observed which are not captured by the model. The TOES runs struggle to capture the observed change in the run, despite the T+48 run coinciding with the change to anticyclonic conditions. Model performance is variable across all the runs undertaken, while it appears to have greater ski under more calm stable conditions, there is little consistency. For example, model performance may be good under a few anticyclonic cases but then poor in another, which means the factors that influence model performance are not exclusively related to the conditions being simulated. This initial set of comparisons indicates that while model performance is variable across different weather types, it has skill when simulating wind speed throughout the range of synoptic conditions. Furthermore, inadequacies in model performance appear to be more subtle than a simple case of state dependence (a discernible level of performance related to particular conditions) because the model does not consistently perform at a specific level for a specific synoptic setting.

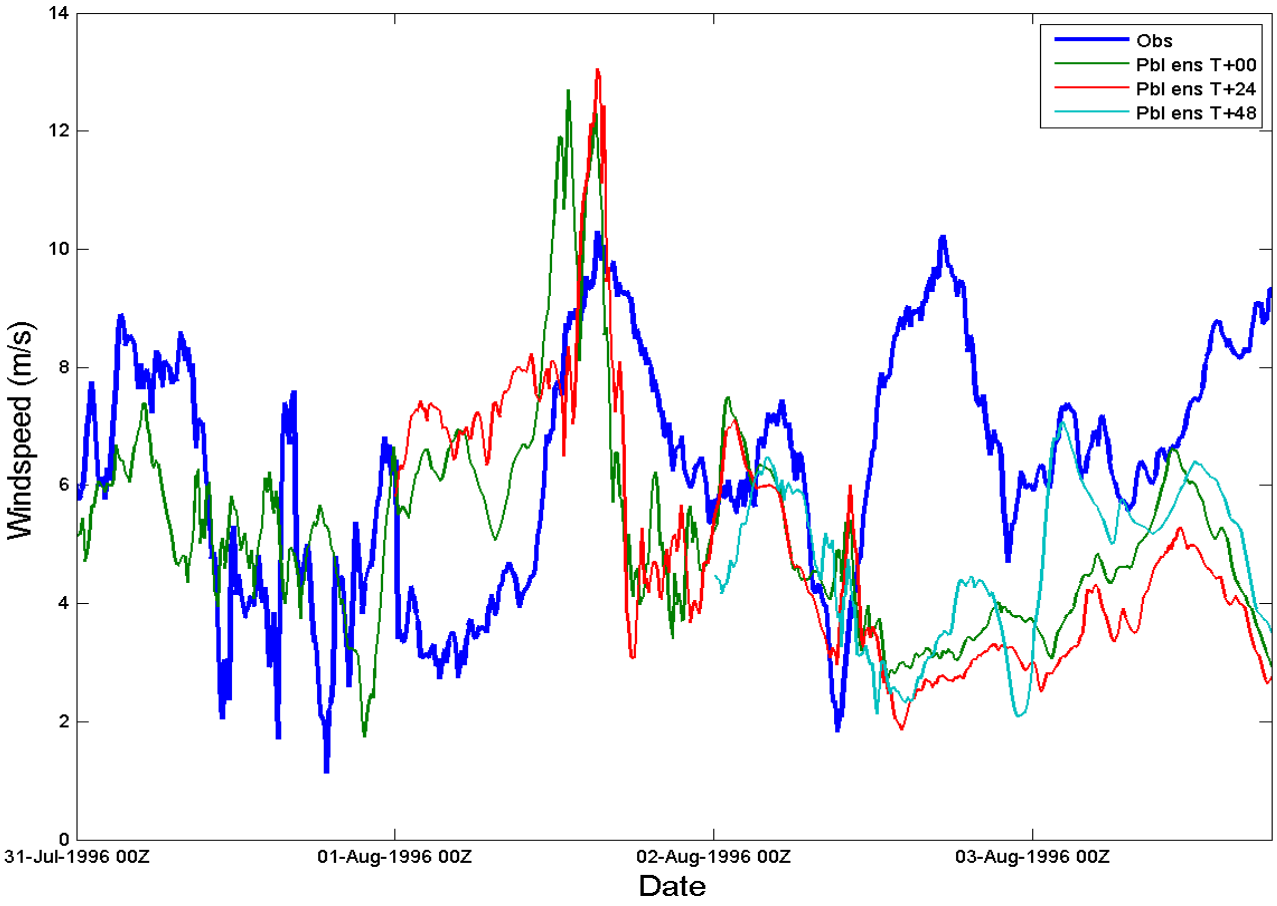

Figure 7.50 Observed and simulated 50m wind speed at Scroby Sands for the 31st of July case. Simulated wind speed is represented by the three time offset PBL ensemble means for the run.

7.2.4 Comprehensive analysis of model performance

When the full suite of runs is considered, more information regarding model performance becomes apparent. Table 7.23 shows the average statistics for the PBL averaged T+0 runs. The different statistical methods used to quantify model performance also act as a sorting method by which to conduct a detailed comparison between the model and observations.

7.2.4.1 Performance classified by correlation

Ordering the results by correlation from lowest to highest does not show any particular relationship to average wind speed, suggesting the model has skill throughout the wind speed range and no dependence on a particular level of wind speed. When standard deviation is classified by correlation, a slight inverse

relationship is identifiable, suggesting the model performs better when wind speed shows a large departure from the mean over the course of the run. An inverse relationship between correlation and standard deviation could be linked to the resolved scale of the model whereby larger scale features are more accurately simulated and likely to be responsible for more significant changes in wind speed, which is represented in these statistics by a larger standard deviation.

Table 7.23 Average statistics for the T+0 average PBL runs

Case Name	RMSE (ms-1)	Weather type	Average wind speed (observed ms^{-1})	Observed standard deviation (ms^{-1})	Correlation
Dec-31	2.7244	A,A,A,S	5.7175	2.9808	0.8082
Jan-07	2.1273	S	10.5320	3.1802	0.8006
Jan-20	3.2441	E	11.4647	1.7222	0.5237
Jan-27	2.6986	E	11.4263	2.7196	0.7038
Feb-06	3.5159	C	8.1918	4.3978	0.8164
Mar-01	3.6464	AN,AN,N,N	7.4081	3.4870	0.5423
Mar-13	2.5000	SE,SE,SE,C	10.4754	1.9929	0.3068
Apr-02	1.4666	A	6.8805	2.0370	0.7703
May-01	3.6572	NE	9.4972	3.8527	0.3818
May-22	2.0980	CS,C,CW,CW	9.2398	3.2580	0.7903
Jun-15	2.2220	A	4.2919	2.3819	0.7062
Jul-08	2.2289	W	5.8254	2.1820	0.4967
Jul-12	2.7865	W,W,A,A	4.7124	2.3041	0.2269
Jul-31	3.0614	CW,CW,AW,A	6.2967	2.0057	-0.0019
Aug-23	3.0575	C	8.5632	2.5156	0.4767
Sep-04	1.5974	AE	6.1865	2.0967	0.6879
Sep-09	2.2859	N,N,N,NW	10.3121	3.0418	0.7953
Oct-17	2.2627	SW	7.4809	3.4998	0.8086
Oct-22	1.9010	SS,AS,CS	8.4232	2.1194	0.5897
Nov-06	2.5765	CW,CNW,W,CW	10.1638	4.2148	0.8377

Correlation coefficients show some degree of dependence on weather type. In cases with a dominant anticyclonic tendency, strong correlations are often present which also coincides with low RMSE. When the weather type has a strong westerly disposition, correlation also appears high though with an RMSE closer to average ($2.57ms^{-1}$), while runs with a dominant easterly weather type tend to display a low

correlation. Model performance is more variable when considering runs with a cyclonic component. While cyclonic runs tend to correspond to more unstable conditions with high frequency variability, the top two runs in terms of correlation are cyclonically influenced. Assertions made thus far are by reference to dominant weather types persisting throughout a run. Analysis of cases which are dominated by mixed weather types, reveals that model performance is indifferent to changing weather type with mixed cases existing across the performance spectrum. When the runs are classified by correlation some assertions can be made, such as the likely low magnitude variation coinciding with a good correlation to model output under anticyclonic conditions. However what the results ultimately show is a fairly even distribution of performance across the range of weather types.

7.2.4.2 Performance classified by RMSE

Touched upon in the correlation classification was the tendency of model performance to exhibit a low RMSE under anticyclonic dominated conditions. Similarly, low RMSE values are observed under Southerly flow. Pure cyclonic runs tend to have large RMSE's, as do runs with a Northerly, Easterly or Westerly component. There is not a discernible relationship between RMSE and average windspeed or standard deviation, again implying model performance is not dependent upon a particular level of windspeed. RMSE is the first indicator of model performance which shows a possible element of state dependence, where model performance seems to be particularly related to certain weather types.

7.2.4.3 Performance classified by wind speed

Lowest average wind speeds tend to be seen under anticyclonic conditions, an observation which concurs with general weather conditions seen under the influence of a high pressure circulation. The highest wind speeds tend to occur under easterly conditions, with cyclonic tendency also figuring in many of the above average wind speed cases. Average wind speed does not appear to be strongly related to standard deviation, with a possible connection whereby cases with the highest average speeds possess lower than average standard deviation values. Model performance is unrelated to wind speed showing skill throughout the whole range. Some weather types tend to correspond to particular levels of wind speed but model performance does not seem affected.

7.3 Analysis of observational nudging

Section 7.2 looked at the general performance of the model using the nudged MYJ PBL setup and showed that performance was slightly worse than the benchmark established in Chapter 5. Observational nudging is employed as a model optimisation technique, with the intention of improving model performance by 'steering' the model towards an observational series near the site of interest. The major assumption in such work is that conditions at the two sites are uniform, where the wind observed at one is reflective of that observed at the other. Investigating the benefit of observational nudging is an important study in itself but also tests the extent of the assumption of uniformity. For the full length (t+0) of the individual case runs, the overall impression is that use of observational nudging is a beneficial endeavour. However there were a few cases (March the 1st, May the 1st and October the 17th) where nudging negatively affects the model run. Figure 7.51 shows observed and simulated wind speed beginning on October the 17th. Statistics for the run back up the visual impression that the non-nudged run performs best with a correlation and RMSE of 0.86 and 1.88 ms^{-1} versus 0.79 and 2.31 ms^{-1} for the nudged run. Nudging does not comprehensively influence the state of the run, but clear differences are visible in Figure 7.51. For example, the downward ramp event at around time step 220 is very well captured by the non-nudged model run, but by integrating the Hemsby data the ramp down is delayed and not as pronounced as observed or originally simulated. When the cases in which nudging negatively affects model performance are compared, the commonality is that they are dominated by consistent, directional weather types but different weather types for each of the cases mentioned. Considering that there must be a difference in conditions between Hemsby and Scroby Sands for the nudging process to be a negative influence, the presence of a consistent directional weather type has to mean the difference arises from local modification of the incoming air mass. For example, a situation may exist where stability conditions contrast between land and sea. Suppose the May 1st case is a warm, clear day, the land may heat up quickly and become warmer than the overlying air, causing an unstable atmosphere. The North Sea meanwhile has a greater heat capacity and sees little change in SST over the same time period, maintaining stable conditions as it cools the overlying air. Such a scenario is simply conjecture, but in order for a difference to occur over such a short distance with a

consistent air mass must require local modification, in which stability could be a key factor. The influence of nudging as a factor in model performance was also considered by reference to the simulation length. Analysis of nudging was extended by comparing the different TOES members comprising the same case. As simulation length decreases, it was found that the number of cases in which not nudging provided an advantage in terms of correlation increases, though only marginally. It would seem that the longer the run, the greater the benefit which might be gained from nudging. In shorter runs, however, the model has had less time to diverge from the initial conditions provided by the model and thus did not require extra 'steering'.

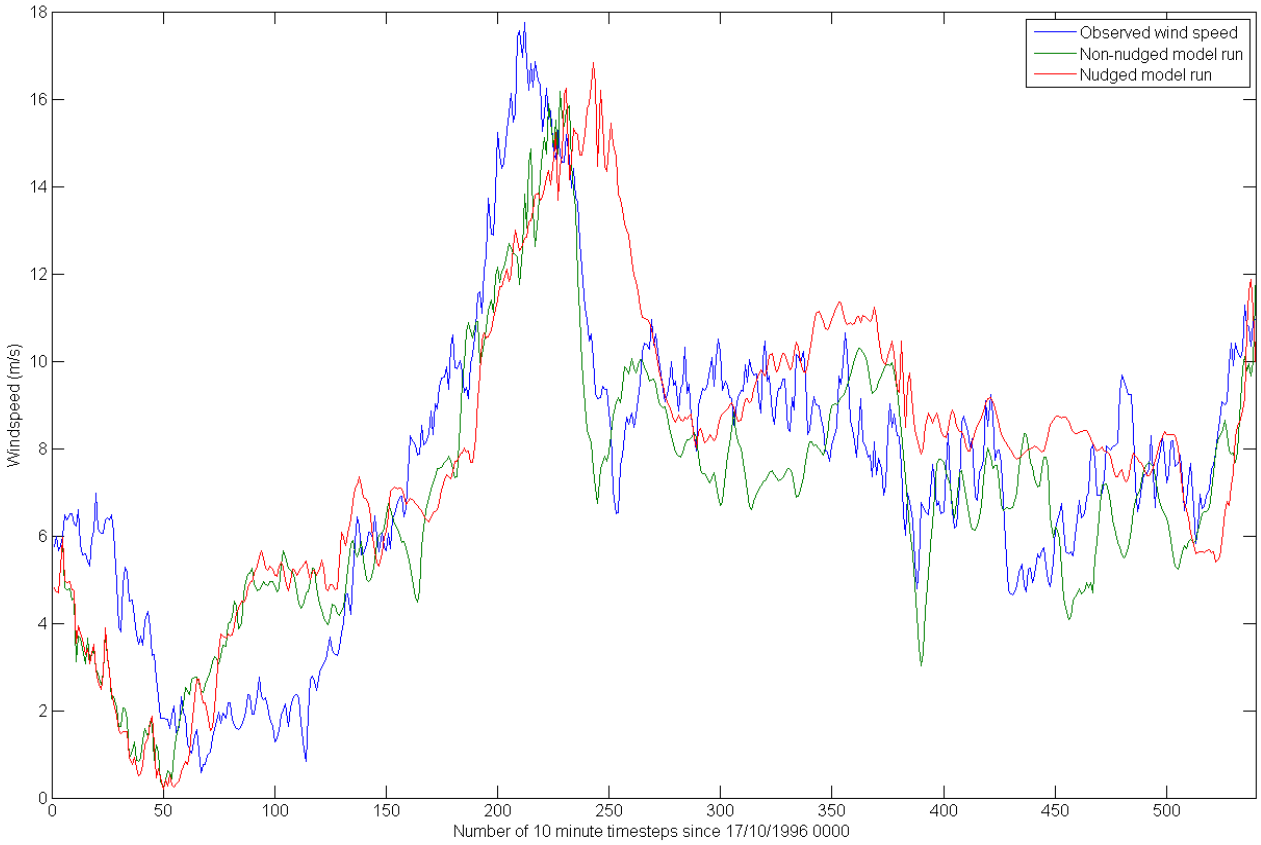

Figure 7.51 Observed and simulated (Nudged and non-nudged MYJ PBL) 10 minute wind speed at 50m for the 90 hour period beginning 17th October 1996.

7.4 Performance of the ensemble members

Before either of the two ensembles is considered as a whole, or combined to form the full PBL/TOES ensemble, the individual members are compared and contrasted. Firstly, investigation of performance in the PBL is addressed through

comparison of different PBL parameterisation setups, before the TOES members are considered as a means of accounting for uncertainty in initial conditions. It is important to review the performance of individual ensemble members. Firstly, a benchmark is established for the ensemble to be compared against, secondly to see how particular schemes perform in comparison with each other and finally to inform of future ensemble construction in terms of potential member weighting.

7.4.1 Individual PBL schemes

A number of PBL schemes exist for the WRF model because the PBL is such a complex and important part of the atmosphere, dominated by small scale processes which have to be approximated rather than resolved. Different schemes exist because of the complexity and philosophy by which they account for boundary layer processes. Accurate representation of the boundary layer is of importance to this research for two reasons. Firstly it has been identified that small scale features which give rise to short term, high frequency fluctuations in wind speed, are responsible for the greatest mode of inaccuracy in the model output. Secondly, with the focus of the research being wind resource assessment, the boundary layer is the region in which turbines mostly operate thus accurate representation of the processes are of the utmost importance. By utilising a range of PBL schemes which employ different methods to different levels of complexity, it is hoped firstly that identifying those which perform best might inform the priorities for future success in resolving the PBL and secondly that the strengths of each scheme will combine and contribute to the successful performance of the ensemble as a whole.

In general across the runs undertaken, statistical performance of the schemes is very similar. Performance of the individual schemes is summarised in Table 7.24 by average statistics and a count of the number of cases in which each scheme is the top performer. While the PBL ensemble performance will be discussed in an upcoming section, it is provided here as a means of comparison by which to judge the performance of individual schemes. The best performer, on average, is the PBL only ensemble showing the highest correlation and lowest RMSE. Individually, the PBL schemes show a good level of performance similar to the ensemble mean, however the MYNN and ACM2 schemes perform to the highest level compared to the remaining schemes.

Table 7.24 Average performance statistics over all 20 cases and for the three initialisation times for the different boundary layer setup options run. No_obs is a non-nudged MYJ run and PBL_only_ens is an unweighted ensemble mean of just the nudged PBL schemes.

Boundary layer setup	Number of cases as top performer		Average	
	Correlation	RMSE (ms^{-1})	Correlation	RMSE (ms^{-1})
MYJ	8	8	0.5767	2.4312
MYNN	12	8	0.6015	2.4128
ACM2	11	12	0.5993	2.4287
QNSE	3	5	0.5508	2.5068
No_obs	16	12	0.5577	2.5400
PBL_only_ens	10	15	0.6074	2.3803

The MYNN and ACM2 schemes display the best average statistics, very close to those of the ensemble mean, and perform the best in the highest number of cases for the nudged PBL schemes. Both actually perform best, in terms of correlation, in a higher number of cases than the ensemble mean. However because the MYNN and ACM2 members do not outperform the mean comprehensively, the ensemble mean represents the best option because it still includes their individual input, as well as the other PBL ensemble members when they represent the best individual option. Looking more closely at the high performing members, the ACM2 scheme is first order and non-local which approximates turbulence as a bidirectional cascade throughout the boundary layer upon numerous defined layers. Results from the Shell Flats resource assessment suggest a relatively balanced distribution of stability conditions offshore, which if applicable to Scroby Sands, implies the ACM2 scheme performs well in a variety of stability conditions. Formulation of the ACM2 PBL scheme suggests it should be a capable performer under unstable conditions, which might account for its level of relatively high performance compared to the other schemes. No dependence upon prevailing weather type is discernible from the results, confirming the value of the ACM2 scheme in the context of this research. The MYNN scheme is a local, 1.5 order closure scheme which relies on more complex equations than first order schemes, to simulate turbulent fluxes through the boundary layer. While local schemes utilise less information points through the boundary layer, performance of the MYNN scheme is shown to be skilful, suggesting accurate flux levels are generated through a range of conditions. While there did not

appear to be a state dependence in the performance of the ACM2 scheme, the MYNN scheme performs well in easterly and southerly conditions, which as previously mentioned, tends to promote increased variability in wind speed. The remaining schemes, MYJ and QNSE, are not anomalously poor performers, rather the MYNN and ACM schemes are able to operate more skilfully, with more consistency. The technical difference between the MYJ and MYNN schemes is in the formulation of the master mixing length scale, which might be the reason for the observed difference in performance in this study. In the MYJ scheme, the mixing length is a function of height, where in the MYNN scheme, turbulence, buoyancy and surface length scales are all used to form the mixing length scale, which all provide more detailed information regarding the turbulence present contributing to fluxes through the boundary layer. The QNSE scheme displaying the lowest performance statistics is not too surprising, because it is specifically tuned for stable conditions which are unlikely to continuously prevail offshore. The fact that it is not the best performer suggests that stability conditions offshore at Scroby Sands are mixed and not predominantly stable. Inclusion of the QNSE scheme was a positive undertaking because it did offer the highest performance in some instances, which justifies its inclusion in the ensemble. Further work is required to identify the specific nature of the test cases, for example identifying if they were stably stratified, which would feed into the development of the ensemble mean and potential weighting techniques. The results obtained here are reflective of those obtained by other researchers, in that there is no conclusive ‘best option’. All of the schemes perform well at times, some more consistently than others, but perform poorly in some cases too. Certain conditions are favourable for particular schemes where investigated at Scroby Sands, but the setting might well favour one scheme over another. For example, the ACM2 scheme has been shown to perform reasonably well in other studies, but it is the joint top performer here. Atmospheric circulation at Scroby Sands is subject to influence by the nearby coastal interface. Floors et al, (2013) found that depending upon wind direction, the atmospheric modification resulting from the coastal roughness change can affect the model simulation of wind speed as well as stability. While they found little difference in performance between the non-local YSU and local MYNN PBL schemes, it may well transpire that at Scroby Sands the non-local scheme ACM2 is able to perform to a higher level for such topography because of the transport mechanism employed through the PBL depth.

7.4.2 Nudging

Nudging has been discussed earlier but it is interesting to consider the performance of the non-nudged run in the context of the other schemes, which appear to be fairly 'hit and miss' given the statistics from Table 7.24. While the non-nudged setup shows the best correlation to observations in the largest number of cases, it has the lowest average correlation, with a similar story occurring by reference to the RMSE, which is above average. The results imply that on occasion, nudging inhibits the model run to the significant detriment of performance. However, results indicate the opposite is also true, where nudging can provide a clear performance advantage. Judging by the average values it appears a better choice to employ nudging for a higher average than not. Ultimately, results from analysing the individual ensemble members in Table 7.24 imply that it is beneficial to generate an ensemble over any individual option, however, inclusion of the non-nudged setup as one member is discussed later. Gryning et al, (2013) found the use of analysis nudging to be a beneficial process, reducing RMSE in wind speed simulations by $0.6ms^{-1}$.

7.4.3 Analysis of individual TOES member runs

Combining overlapping model runs with offset initialisation times allows the potential to address uncertainty in initial conditions provided to the model. Model output, after the point where the next time offset member is introduced, effectively has more recent information about the state of the atmosphere which should help keep it on track with observations. The process is a measure intended to account, to some extent, for divergence between model and observations due to the chaotic nature of the atmosphere. Table 7.25 shows that, generally, the T+48 members marginally provide the best level of performance relative to those initialised at different times because, while the correlations are very close, the RMSE is slightly better than the T+00 run. Performance of the T+48 runs is most likely aided by having the most recent information available and simulating the shortest run period. The number of cases in which the T+48 members perform best is the same as the T+00 members, with the T+24 a bit behind. Standard deviation is largest for the T+24 runs, and similar on average for the T+00 and T+48 runs. Average correlation

is better for the T+00 runs than the T+24 runs but standard deviation is higher, similar to RMSE, indicating the T+24 runs to be more variable over the duration.

Table 7.25 Average statistics for the members of the time offset ensemble system (TOES) by intialisation time.

	Correlation	RMSE (ms^{-1})
T+00	0.5981	2.6057
T+24	0.5591	2.6114
T+48	0.5862	2.3528

Figure 7.52 shows the case of February the 6th which is an ideal example of the practical application of the TOES concept. It is clear to see on the 7th of February that wind speeds simulated in the T+24 set of runs are considerably closer to the observations than is simulated by the members from the T+00 run. If the two series were combined, the output would be closer to observations than the T+00 mean would be, reducing the divergence of the original T+00 series. Correlations for the T+00 runs are just over 0.8 on average and RMSE is quite high at around 3.5 ms^{-1}, where performance of the T+24 members show correlations around 0.9 with RMSE around 2 ms^{-1}. Time offset ensemble members, like the full model runs, rely on the accuracy of the input data used to initialise the model. Input data have been of high enough quality to enable the model to perform to a high standard over the majority of runs undertaken in this research, but on occasion input data have been found to be contrasting to observations at Scroby Sands. Furthermore, different initial conditions can change the context of a model run, to the extent that the same period simulated by a model initialised from alternative initial conditions may lead to a very different outcome. While different initial conditions may contribute to alternative predictions from the TOES members, that is exactly the reason for undertaking them, to gain knowledge of potential outcomes which will aid the use of the model output. Either the different members will agree, in which case a degree of confidence can be assigned to the model output. Or the members will disagree, at which point more uncertainty can be assigned to the output and knowledge obtained regarding characteristics of model performance.

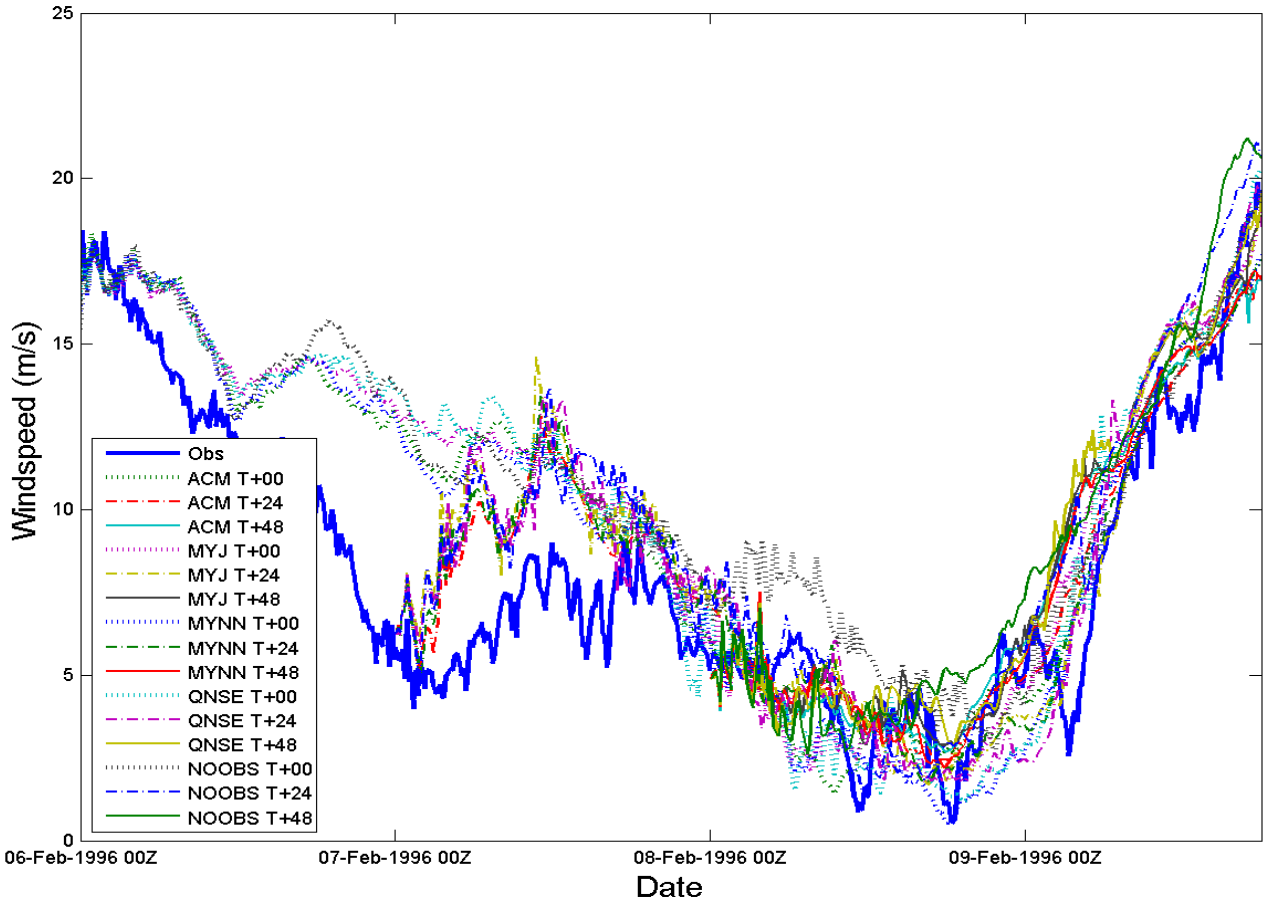

Figure 7.52 50m 10 minute wind speed as observed and simulated buy every TOES and PBL ensemble member for the February the 6th case.

Figure 7.53 shows the 7th of January case. Initially the T+00 members perform well with a correlation around 0.8 and an RMSE just over 2 ms^{-1}. Addition of the T+24 members augments performance for the duration of the T+24 run with statistics similar to the T+00 run. Addition of the T+48 members would be including members performing some way below the level of those already available for the TOES mean showing an average correlation just below 0.7 and an RMSE around 2.4ms^{-1}. Inspection of the final day of the 7th of January case reveals a conflict between ensemble members relating to wind speed variability, which at some points are completely out of phase. Such contrast between ensemble members shows uncertainty in the model output and would ultimately correspond to poor performance of the ensemble mean as variation from conflicting members effectively cancels out. In some cases, the application of time offset initialisation is a negative process in terms of model performance. However, it does provide more information about

model representation of the atmosphere under given conditions and model uncertainty given a particular set of starting conditions, which is all useful information that can be used to learn about model performance.

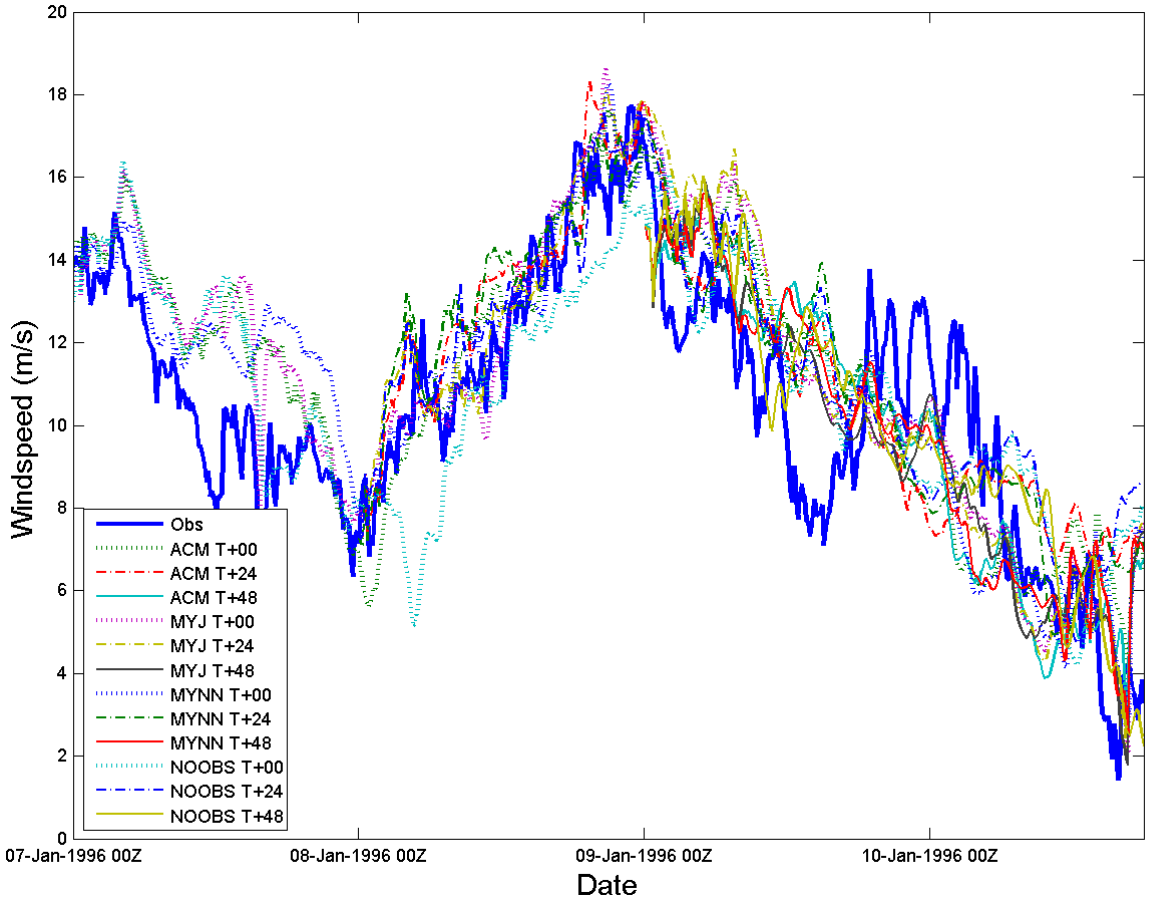

Figure 7.53 50m 10 minute Wind speed as observed and simulated buy every TOES and PBL ensemble member for the January 7th case.

Skill is present throughout the time offset members, apparently regardless of initialisation time, which is why it is beneficial to undertake such a run scheme because skill across the runs comes from varying members. The reason for the variability in performance may well be a result of coincidental setup optimisation for particular circumstances. Essentially, by running so many variants of the same run, some setups will naturally tend to be more appropriate. For example, meteorological features such as weather type or wind speed variability, which have been shown to affect model performance, may manifest themselves in a slightly different way over the course of the run across the individual members because of the contrast in initial conditions and model setup. Ultimately each member exists to provide individual input towards the ensemble as a whole.

7.5 Performance of the PBL ensemble and the TOES

7.5.1 Performance of the PBL ensemble

Mentioned in section 7.4.1 was the fact that, statistically, the best performing boundary layer simulation option was the PBL only ensemble. By combining the different schemes equally, the best performing option is always represented and augmented by the skill of the other schemes. It is interesting that despite having the highest average values, the PBL ensemble is not the leading performer in the highest number of cases. An ensemble mean can only perform within certain limits of its members by definition. While each scheme is different and generally produces a different solution, overall divergence between the schemes does not tend to be significant. As a result, performance of the ensemble mean will inevitably be of a similar level to its members. The two main reasons for producing an ensemble are, to account for uncertainty and to attain the level of skill of the individual members. In some instances, the ensemble mean outperforms the best individual scheme, clearly improved by the addition of the other schemes. Conversely, there are also instances where some of the schemes perform poorly compared to the best scheme holding back the performance of the ensemble. In the case of May the 22nd, shown in Figure 7.54, the PBL ensemble mean is the best performer with respect to correlation (0.85) and RMSE (1.79 ms^{-1}) while the ACM2 is the best performing individual scheme with respect to correlation (0.82) and RMSE (1.91 ms^{-1}). Between time steps 50 and 150 is a good example of where the ensemble mean outperforms the ACM2 scheme thanks to the input from the other members, despite the fact that over the course of the run the other members offer a worse prediction of observations than the ACM2 scheme.

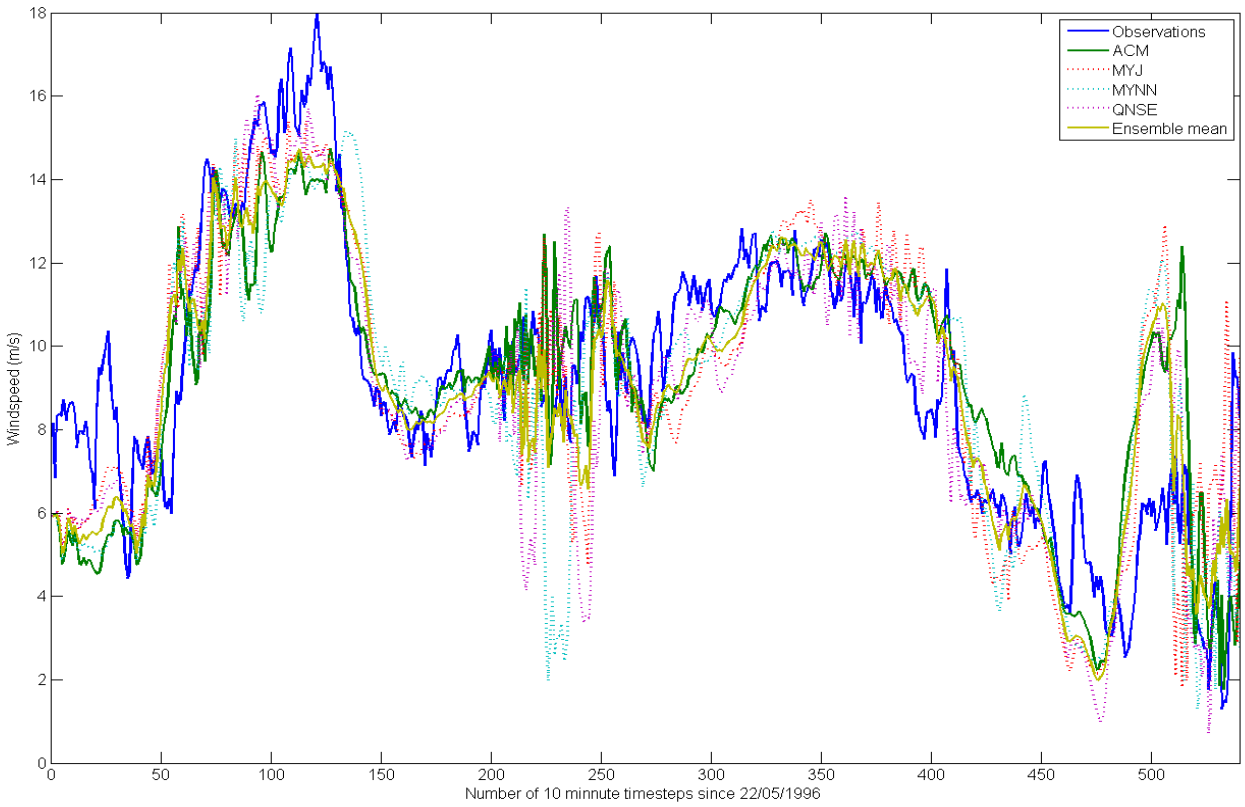

Figure 7.54 Wind speed at 50m observed and simulated by the different PBL members and ensemble mean. Observations, ACM2 and ensemble mean are solid lines to aid comparison between the series.

While the ensemble mean appears to be the best option when producing a model estimate of wind speed, the downside is that variability in the individual schemes is damped by the averaging effect. In one way this is beneficial because the high frequency range is where the model struggles, so damping may contribute to an improved performance by removing erroneous variation, but ultimately it is an artificial effect of combining the different members. Furthermore, the members are included because of their specific skills under different conditions and variability is a key parameter which would ideally be retained. Ideally, an ensemble mean would preferentially weight the most accurate member for a given time step to achieve the best result. Such a scheme is unlikely to be developed because of the difficulty involved, but the concept is not totally out of the question. Weighting an ensemble is one way of retaining more information from a particular source/selection of sources. For example, by attributing more weight to a member of choice, more variability from that member will be present in the ensemble mean. Results from the analysis of the individual members shows the best schemes were the MYNN and ACM2, with the

MYJ not far behind. For future work it would be of interest to investigate the weighting strategy whether it be a full analysis of runs and then a set weighting is assigned to each member reflecting the level of performance. Or potentially a dynamic ensemble where weighting is changed based on values of particular variables, such as weather type. The downsides of the ensemble mean presented here are the increased computing resource required to generate the ensemble members and the effect of the averaging used to produce the ensemble mean. Ultimately however, the ensemble mean is the best performing PBL option. By containing information from all the members it exhibits their accuracy and at times mediation against erroneous values and as a result displays the most consistent skill.

7.5.2 Performance of the time offset ensemble

Much of the information which pertains to the performance of the time offset ensemble mean is present in the analysis of the performance of the members. In general, the highest performing option is the latest initialised (T+48) run, which is likely the result of the run length. However, when the frequency of cases is reviewed, the T+00 runs perform best in the same number of cases as the T+48 runs. Much like the PBL ensemble, the critical issue is consistency, because no run stands significantly above the others in terms of performance. It is usually of benefit to combine the members where possible to utilise the inherent skill from the available sources where possible. Because of the way the runs were designed, performance of the time offset ensemble mean can be reviewed at two points. Firstly after the T+00 and T+24 runs were combined and secondly after the combination of all three runs again over the overlapping period beginning at T+48. Performance of the ensemble is compared against an average of the PBL options for the corresponding run initialised at the same time. For example, an ensemble of the T+00 and T+24 runs - are compared against the performance of the T+24 run. Comparison of the correlation and RMSE stats in Table 7.26 shows that the ensemble mean is the best performer.

Table 7.26 Raw versus ensemble average performance for the TOES ensemble.

		Correlation	RMSE
T+24	Raw	0.5591	2.6114
	Ensemble	0.6003	2.4282
T+48	Raw	0.5862	2.3528
	Ensemble	0.6374	2.2127

Given that analysis of the individual members implies performance is fairly evenly distributed across the different initialisation times, no one scheme is a clearly preferable option. Rather, the ensemble benefits from the periods of high performance from each member alongside the other members which provide mediation to the run. Equally when one member performs poorly, overall performance is not immediately sacrificed as the other members exist to provide an alternative solution. For example, Figure 7.55 shows the case of September the 4th where the three time offset PBL ensemble means are presented. Mentioned earlier was the high performance of the T+00 run, which is good in the early stage s of this run, but diverges from observations around September the 5th. Introduction of the T+24 series gives a better account of observations than the T+00 run in this case which helps to keep the ensemble mean on track. As with the PBL ensemble, the downside is the damping effect of averaging but these are preliminary results which can be built upon. Ultimately, the addition of extra information which has skill in its own right proves to be a valid addition to the modelling process as a tangible improvement in performance is evident. The next section talks about different approaches to weighting and the unified ensemble consisting of both PBL and time offset members.

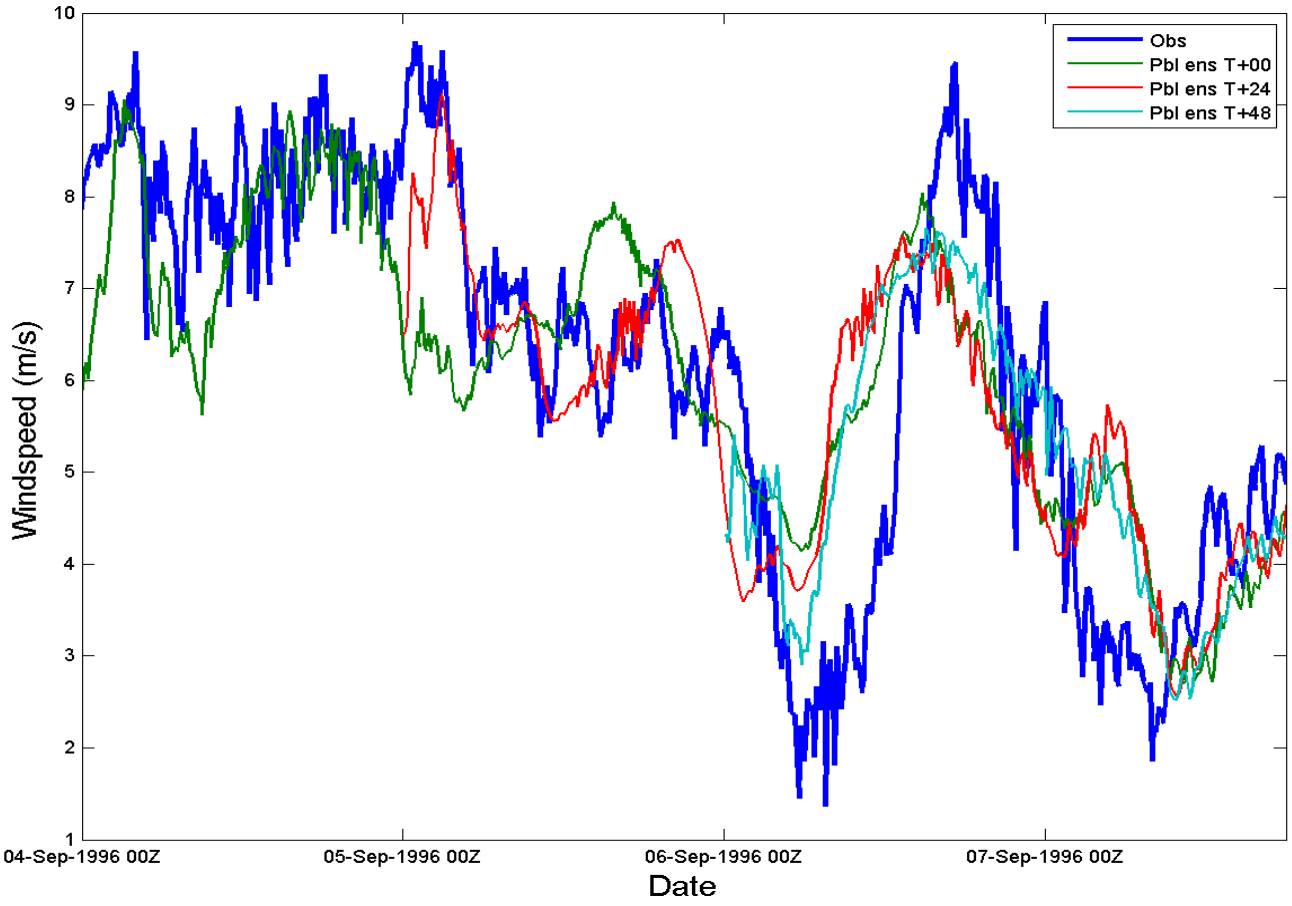

Figure 7.55 Wind speed at Scroby Sands for the September the 4th case simulated by the three time offset pbl ensembles

7.6 Performance of the TOES

7.6.1 Assessment of the ensemble mean

Multiple versions of the unified ensemble were produced. The first option was inclusion of the non-nudged model runs and the second was concerned with the weighting of the TOES members. Three weighting methods for generating the ensemble mean were employed and each were available with and without the non-nudged MYJ runs. Firstly an equal weighting scheme, which was created to provide equal importance to all members regardless of initialisation time, was applied to the overlapping periods from T+24 and T+48 shown in Equation 16. Then to provide more influence to the most recent members they were weighted more heavily by averaging the members of the previous lag to be equal to one member of the most recent time offset series. For the T+48 ensemble this was achievable in two ways,

firstly by providing equal weight to T+24 and T+48 members but averaging t0 to account for one member (Equation 7.17), then secondly by affording more weight to the T+48 members by averaging the T+00 and T+24 members to equate to one ensemble member each (Equation 7.18). The subscript n represents the number of ensemble members present for each initialisation time, for example $[T+00]_n$ represents the 4 ensembles (MYJ, MYNN, ACM, QNSE) thus n=4. A summary of the ensemble generation methods is provided in Table 7.27, which shows that the two ensemble methods in which ever member was equally weighted were ensemble 1 & 2. For ensemble methods 5a & 6a T+00 was equalled to one member while T+24 members were equally weighted (eq.7.17). Then in ensemble 5b and 6b equation 7.18 was used.

$$Mean = \frac{[T+00]_n + [T+12]_n + [T+48]_n}{3_n} \quad \text{Equation 7.16}$$

$$Mean = \frac{\frac{[T+00]_n}{n} + [T+12]_n + [T+48]_n}{2n+1} \quad \text{Equation 7.17}$$

$$Mean = \frac{\frac{[T+00]_n}{n} + \frac{[T+12]_n}{n} + [T+48]_n}{n+2} \quad \text{Equation 7.18}$$

Table 7.27 Description of ensemble method and relevant weightings

	Nudged	Non-nudged
Equally weighted	2	1
T+00 members combined to equal one member	6	5
T+00 and T+24 members combined to equal one member each	6a 6b	5a 5b

Results show that it is favourable to include the non-nudged run as part of the ensemble because the best performing ensembles were those which included the non-nudged runs. When analysed individually in section 7.3 at times the non-nudged runs were shown to be the best performing members, so it is not surprising that their inclusion improves ensemble performance. By including the non-nudged series in the ensemble uncertainty in the nudging process is accounted for to a small extent. Analysis of the different methods of ensemble generation is undertaken by reference

to the average statistics for each ensemble, presented in Table 7.28. The immediate observation is that very little difference in performance exists between the ensembles despite the alternative weighting methods. Considering the T+24 runs, ensemble method 2 provides the best average statistics and performs best in the highest number of cases when considering RMSE, but ensemble 6 performs best in the highest number of cases regarding correlation. For the T+48 runs, the method which performed highest, for both correlation and RMSE, in the most number of cases was shown to be ensemble 6b, the ensemble in which T+00 and T+24 members were averaged and given the same weight as each T+48 member. Ensemble 6b also provide the lowest RMSE value of the methods but was outperformed in terms of correlation by ensemble 2 which is the equally weighted, nudged ensemble. Essentially, the results imply the strongest performing option prioritises the most recent mode runs, but, performance of the members offset at different times is shown to be very close which is translated into the narrow difference between the ensembles' performance.

The most significant improvement to performance comes from creating the two ensembles: the time offset ensemble and PBL ensemble. Observational nudging does offer an improvement to model performance as well as another metric by which to address model uncertainty, but the biggest performance benefit of the optimisation work comes from combining the different ensemble members to form an ensemble mean. By doing this, skill from every member is always present in the output and results unequivocally prove that the ensemble as a whole has the potential to outperform any of the individual parts. No individual member is able to offer consistent performance close to the ensemble mean because of the variability in performance for given conditions. However, by combining all the members together, skill is always present. Different methods of generating the ensemble mean have been tested but are shown to provide minimal impact upon performance, with the main focus of performance coming from the skill of the individual members. Thus suggestions for future work are to optimise the boundary layer schemes and understand the levels of performance available more completely, which will allow for a careful selection of ensemble members to more fully address areas of model uncertainty. One issue which will require future work is the concern about variability damping as a result of averaging multiple ensemble members. Whilst it inadvertently

serves to eliminate much of the noisy error present in the model and focus on the lower frequency variation features at which the model has more skill, ultimately in the future, it should be able to fully resolve short term variation which would include high frequency variability.

Table 28 Performance of different ensemble generation methods

Comparison period beginning	Ensemble method	Correlation Coefficient	RMSE (ms^{-1})
T+24	Ensemble 1	0.6023	2.4256
	Ensemble 2	0.6067	2.3877
	Ensemble 5	0.5932	2.4705
	Ensemble 6	0.5989	2.4290
T+48	Ensemble 1	0.6373	2.2245
	Ensemble 2	0.6425	2.2067
	Ensemble 5a	0.6353	2.2235
	Ensemble 5b	0.6333	2.2151
	Ensemble 6a	0.6395	2.2062
	Ensemble 6b	0.6367	2.2004

7.6.2 Assessment of the ensemble spread

Part of the reason for producing an ensemble was to investigate the relationship between ensemble spread and model error to see if ensemble spread was able to act as a potential indicator of uncertainty. As suggested in the literature review, a link between ensemble spread and model error is conceivable, with instances of extreme ensemble spread more likely to correspond to a readily identifiable spread-error relationship. Ensemble spread is represented by the standard deviation of the ensemble measures for a given time step. Two methods of calculating ensemble spread were employed based on the review of literature which related to the mean value used to calculate the standard deviation. The first method calculated an instantaneous mean at each time step, whereas the second method calculated the climatological mean (in this case for each individual run). Correlation between both calculations of ensemble spread and absolute model error was calculated for each run and a plot of both ensemble spreads was produced

alongside model error to provide a visual component to the analysis. Indicators of extreme values were also integrated in to the plots to identify periods when a visible spread error relationship might be evident. In the context of this research extreme values were defined as being greater than two standard deviations from the mean, which in a Gaussian distribution would account for around 5% of data. Results from the correlation analysis indicate there is no discernible linear error spread relationship. On average the instantaneous spread mean achieves a correlation coefficient of 0.08 which is strongest in 12 of the 20 cases while the climatological spread mean achieves a correlation of 0.04 outperforming its counterpart in the remaining eight cases, which indicates the complete lack of a relationship between spread and error. The best individual correlation achieved is 0.5 which is for the instantaneous method, while the climatological method achieves a value of 0.4. The average correlation values are particularly low because for both measures of spread there are a number of cases where the correlation is negative. Negative correlations, however, only serve to support the argument that there is little to no relationship between ensemble spread and model error from the results in this study. Visual analysis of the model runs does, on occasion, identify some periods of runs where a spread-error relationship seems apparent. For example, Figure 7.56 shows the case of March the 1st in which the instantaneous ensemble spread achieves its highest correlation of 0.5 while the climatological spread shows a correlation of 0.01. There are definite periods over the course of the run where the instantaneous spread does reflect the behaviour of the error. However, even over the course of this run, which is the best performing instance, a relationship is difficult to identify. Despite the correlation and that some features are represented in both series, there is little consistency in the magnitude of change between spread and error and what little directional similarity is present is not consistent throughout the run. Instances of a spread-error relationship are present in most of the runs, but for very limited periods. There is usually little consistent timing change and the magnitude of change is hardly ever captured. When identified, extreme ensemble spread was not an indicator of periods when the spread-error relationship was identifiable. Ultimately in this work the ensemble spread as an indication of error was not of use, minimal spread of members did not correspond to a low model error and likewise large ensemble spread did not translate to a large error. Perhaps because many of the members were initialised from the same data, not enough uncertainty sources were introduced

to generate sufficiently large spread to make use of instances of extreme spread. Further work might be done into looking at nonlinear correlations, calibrating the output and perturbing initial conditions to generate more ensemble members and increase the potential for sources of error and thus spread.

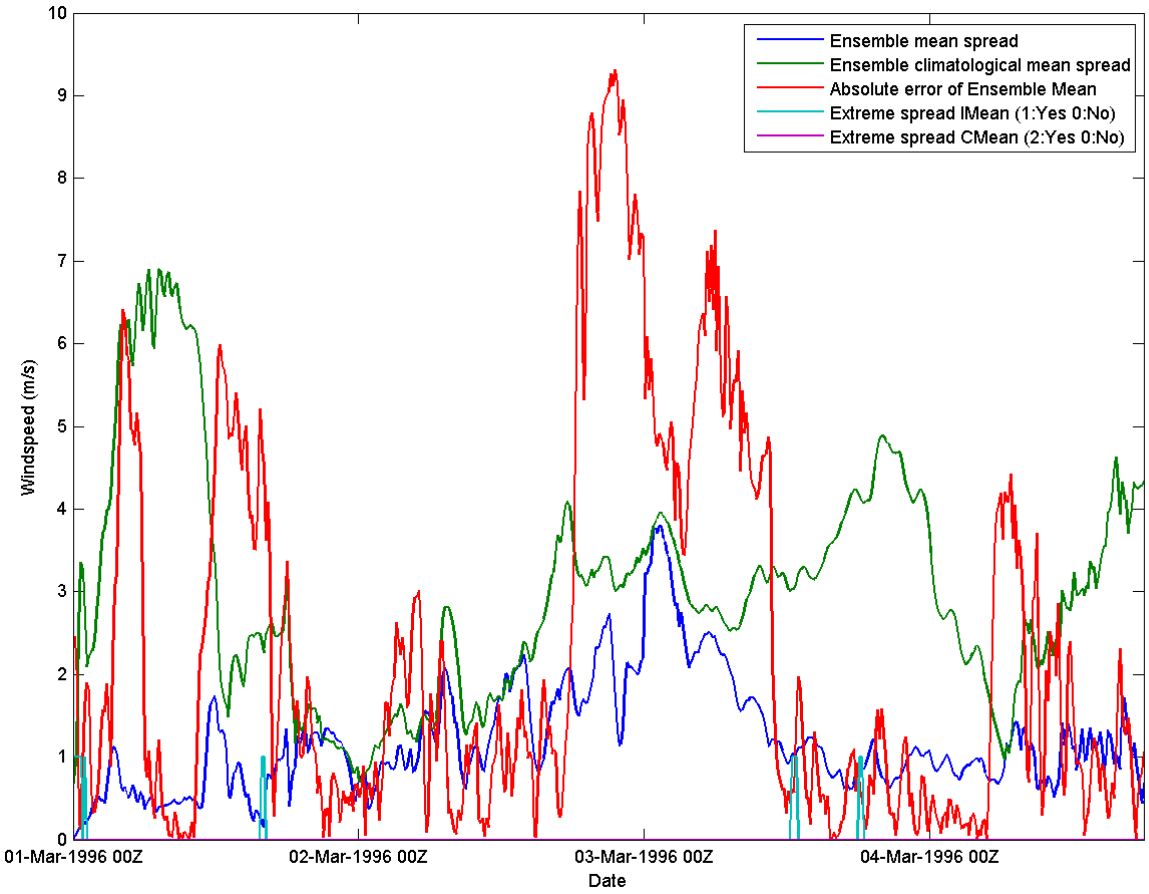

Figure 7.56 Ensemble spread and model error relating to wind speed calculated using the instantaneous and climatoilogical meanvalues for the case beginning 1st March 1996.

8 Conclusions

8.1 Introduction

Conclusions from the results are drawn in the following chapter. A consideration of the methodology is presented first, before a summary of each of the investigations. How the results addressed the research questions/objectives stated in the introduction chapter is then discussed before a few thoughts are presented on the overall application of mesoscale NWP to the field of offshore wind resource assessment. Finally suggestions for directions of future work are mooted.

8.2 Methodology development

As a relatively inductive investigation, one of the significant achievements of this research was developing the methodology by which the research aim was addressed. Flexibility, in terms of portability and setup, alongside a proven level of performance were the main reasons for selecting WRF, which offered a wide scope to many aspects of the investigation. Once the model was selected, three separate investigations were designed to explore the potential of WRF in a variety of applications relevant to the wind energy industry. Model performance in different locations was considered, as was the performance at different temporal resolutions over different timescales. Computing resource as a factor influencing performance was investigated and different variables such as stability were produced for investigation. Efforts were made to address the major sources of uncertainty in the modelling process used and throughout the investigations variables were characterised by a wealth of metrics, for example weather type. The focus of the research was to validate WRF as an offshore wind resource assessment tool, but the methodology also provided an investigation into the variability of the parameters which were simulated. Unique and novel techniques, such as ensemble generation and simulation of atmospheric stability, were applied to the investigations and provided a set of results from which performance could be analysed and conclusions drawn. Investigating so many facets of the modelling process was an ambitious aim, made possible through the careful and unique methodology developed.

8.3 Benchmarking model performance

8.3.1 Model performance

A level of performance was defined for two setups of the WRF mesoscale model as a predictor of 50m 10 minute wind speed. Average and standard deviation statistics provided a basic comparison between the predictors and observations, while the correlation coefficient and RMSE were calculated to quantify the relationship and absolute error of the predictors. For the more computationally restricted model setup, performance was relatively poor showing a correlation of 0.35 and an RMSE of 3.5 ms^{-1}. Elements of observed low frequency, long term, wind speed change were present in the model runs but no high frequency change was produced. By contrast, the model setup which adopted an unrestricted computing resource was able to produce levels of high frequency variation similar to those observed. Low and medium frequency change was generally well captured, however variability of high frequency change was less well represented. Access to a larger computing resource led to setup changes which resulted in improved model performance, the correlation coefficient rose to 0.65 and RMSE dropped to 2.2ms^{-1}. By expanding the computing resource available to the model, a more comprehensive setup could be used which not only provided more information to the model as input, but also allowed a larger area over which to simulate the controlling atmospheric features. The inner resolution of the unrestricted setup was 2km which according to the principle of effective grid resolution meant, in that domain, the smallest fully resolved features would be on the order of 10-15km. Features smaller than 10km correspond to changes in wind speed in the high frequency range where accuracy reduces. While they are not explicitly resolved, WRF does account for small scale atmospheric features. Such features are approximated by parameterisation schemes, themselves functions of resolved variables of a larger scale. The benchmarking exercise had initially provided results as required from which an initial indicator of model performance from two different setups was obtained. Analysis of the individual runs helped identify that high frequency changes in windspeed were the features which the model struggled to simulate.

8.3.2 Filtering

Model output and observations were temporally filtered to investigate the strength of the relationship at different timescales, where atmospheric features are

fully resolved by the model rather than approximated by the parameterisation schemes. Initially an unweighted moving average filter was applied before a low-pass Butterworth filter was developed. The application of both filters saw an improvement in model performance, with correlation coefficient improving to 0.73 for the six hour Butterworth filtered resolution with RMSE dropping to 1.8ms^{-1}. Comparison of the filters showed the unweighted moving average filter offered a marginally better level of performance but at the expense of sensitivity and a number of observations used to calculate the moving average. The Butterworth filter provided a more sensitive, flexible method by which to filter the series and was able to retain some of the key features in the wind speed profile to a greater extent than the moving average filter. The improvement of performance achieved through filtering the time series is evidence that the model has genuine skill as a predictor of single point wind speed when applied at resolved scales. Low and medium frequency features are well captured while high frequency features are not particularly well represented because they are approximated as functions of resolved variables by the parameterisation schemes rather than directly resolved. 'Out of the box' model performance was not quite able to match the accuracy of the local observational data from Hemsby as a predictor of wind speed, but performs to a similar level when filtered to a temporal resolution of three hours. When model RMSE is compared against that of a persistence forecast, the model becomes the favourable option after a three hour lead time, as RMSE for persistence exceeds 2ms^{-1}. The main outcome of the benchmarking exercise is the recommendation to optimise model setup as best possible. Resolution is shown to be the limiting factor of the runs undertaken here, with performance shown to drop when the model is applied to simulate sub grid scale features.

8.4 The Shell Flats resource assessment

8.4.1 General performance

The Shell Flats resource assessment was an investigation designed to test the suitability of WRF as a long term offshore resource assessment tool. Multiple variables were simulated to provide a comprehensive atmospheric analysis upon which to calculate wind farm yield predictions. Simulations covered 489 days at Shell Flats from June 2002 to December 2003 and were compared against corresponding observations to validate the model performance. WRF performed to a very high

standard when simulating fifty metre, ten minute wind speed at Shell Flats. Descriptive statistics were very similar between model and observations, with the 2 parameter Weibull distributions closely reflecting one another. Absolute error as quantified by RMSE was 2.1ms^{-1} while a strong relationship between model output and observations was signified by a correlation coefficient of 0.86. The model comprehensively outperformed 10m hourly observational data from the onshore station at Squires Gate (~14km away), but fell short of the performance achieved by data from Mast 1 as a predictor of wind speed at Shell Flats Mast 2. Wind direction was not simulated to the same high level of accuracy as wind speed. Descriptive statistics however did show agreement between the two directional series, with the modelled wind rose showing a considerable likeness to the observed wind rose.

8.4.2 Stability

Atmospheric stability at Shell Flats was investigated by calculating variants of the Richardson number from observed and simulated variables. The bulk Richardson number was found to produce a reasonably good impression of observed stability by comparison to the calculated gradient Richardson number. The bulk Richardson number was also calculated from model outputted variables and then compared to the bulk Richardson derived stability calculated from the observations. The absolute balance of stability, in terms of whether the atmosphere was either stable, neutral or unstable, was fairly similar between observed and simulated variables, however the model tended towards more stable conditions while, in reality, more neutral conditions were observed. When classified by other variables, observed variations in stability were broadly reflected in the model output, in some cases with bias present and thus modification to tuning clearly required.

8.4.3 Performance classification

Atmospheric classification schemes offer an extra dimension of information when analysing performance. Model performance is shown to be better when changes in wind speed are associated with large scale atmospheric features. Given that some variables show dependence upon the prevailing weather type, a weather type analysis of model output would serve to add value to the model output, for example as historic distributions of the variable under that weather type could be queried to provide a probabilistic output. Results from the descriptive statistics and the time series analysis imply that the model is able to simulate the dominant modes

of atmospheric variability in the long term for Shell Flats. Large scale atmospheric features dominate variability in the long-term, which exist within the resolved spatial domain of the model. Large scale features contribute to low and medium frequency change in the modelled variables which the model is able to reproduce to a high degree of accuracy, corroborating the findings from the Scroby Sands benchmarking exercise.

8.4.4 Temporal filtering

To isolate change in the low and medium frequency range, the modelled and observed wind speed series were temporally filtered using a first order low-pass Butterworth filter. Temporally filtering the model output and observations to a six-hourly temporal resolution saw an improvement in performance to a correlation coefficient of 0.92 and an RMSE of 1.7ms^{-1}. Such performance figures bring the model much closer to the level achieved by the observations from Mast 1 as a predictor of Mast 2, albeit at a lower temporal resolution. Results of the temporal filtering process show that the model is unable to simulate variability in the high frequency domain as well as in the low and medium frequency domain. Variability on such timescales is reliant upon information from the model's parameterisation schemes because the controlling processes exist at sub-grid scales and cannot be directly resolved by the model.

8.4.5 Nudging

Observational nudging by data from Mast 1 was employed for the Shell Flats runs. On occasion the model output was detrimentally affected by nudging but on balance it was found to be a positive influence, improving model performance more than it inhibited it. WRF has shown itself to be a viable wind resource assessment tool for Shell Flats. Wind speed, the most important variable in a wind resource assessment, is simulated to a very high level, particularly when considered at the resolved scale of the model. Additional variables, such as wind direction, are simulated to a good level providing more information for a potential end user by which to predict a potential wind farm output. The resource assessment produced for the Supergen exemplar farm shows the capacity of WRF to be able to produce a full range of outputs over a wide spatial area both horizontally and vertically, displaying a great degree of flexibility, particularly in comparison with established techniques.

8.5 Optimising model performance

A new set of runs at Scroby Sands was undertaken to test optimisation techniques. Average model performance of the runs comprising the optimisation investigation was below the level achieved in the benchmarking runs prior to the application of optimisation techniques. Such an occurrence identifies the variance in model performance across the runs undertaken at Scroby Sands. The cases selected for the optimisation runs were chosen based on prevailing weather type over the duration of the run. Optimisation techniques employed included; observational nudging, SST update, analysis by reference to weather type and the creation of PBL and time offset initialisation ensembles to address physical and dynamical uncertainty in the modelling process. Optimisation techniques were shown to improve performance and offer insight into dependencies of the model performance. Weather typing was used to classify model performance providing an extra dimension of information to augment NWP forecasts, for example, by providing probabilities of tendency or likely change in a variable under a particular weather type. Nudging was shown to be a positive process to incorporate in to the model runs. In the majority of instances a nudged run outperformed its non-nudged equal, however it proved beneficial to include both as members in an ensemble to account for the runs in which the nudged series underperformed and inhibited model performance.

8.5.1 Ensemble runs

Two different ensembles were created to address uncertainty in the accuracy of initial conditions provided to the model and uncertainty regarding model performance in the boundary layer. Creation of the PBL ensemble afforded the opportunity to directly compare the performance of individual schemes. The findings reflected very much those of the general literature which, on balance, was to identify no single scheme as the best performer, rather, that different individual schemes performed best at different times. Higher levels of performance at Scroby Sands were seen for by the ACM2 and MYNN schemes, however these findings may not be applicable in another environment. Because the PBL ensemble is comprised of members with different skill levels, it excels in many conditions rather than being restricted as a single scheme would be. Even in the worst cases, the performance of the ensemble mean was not far below the best individual scheme because it possessed the same

information, but, was misguided by other schemes poor performance. Further research will allow the identification of appropriate weighting strategies for the ensemble which, ideally, will optimise performance where the best schemes are selected and weighted with a higher importance. The time offset ensemble also provided an array of benefits on top of the ensemble mean. Staggering the initialisation time identified a dependence upon initial conditions, the accuracy of which was shown to vary as in a number of runs the very first point showed a discrepancy between the model and observations. Given that the runs initialised at different times performed, on average, to a similar level, in some individual cases performance between the staggered members often differed to a notable extent. Thus, the undertaking of staggered initialisation proved beneficial as more successful inputs were combined to improve the performance of less accurately initialised runs. Staggered initialisation improved performance, not only by providing different initial conditions, but also by effectively reinitialising the process. Of course, retrospectively it can be said that combining two members of varying performance is to reduce the performance of one, but when the solution is as yet unknown, more confidence can be applied to an ensemble approach than selection of an individual member *a priori*. Ensemble spread was investigated as a potential indicator of model error, however no discernible relationship between ensemble spread and model error was found for any of the runs. It may be an avenue worth investigating in the future if ensembles can be designed which produce a greater degree of spread, but served little purpose in this research.

8.6 Ease of model use and application

To answer the question “How accessible is this technology?” the whole modelling process must be considered. This comprises obtaining the source code then compiling the model and its ancillaries, developing the methodology relating to setup, then running the model and finally post processing the output. It took around a year and a half before running the model was a trivial process by which results for analysis were being generated routinely. A big consideration is familiarisation with the Linux computing systems on which the model is to be run, once this is achieved the priority becomes devising a run strategy. For example addressing questions such as; “where will each stage of the model run be processed?” and “at what point will data be transferred?” etc. Support for WRF is superb and once some computing

skills are learned, acquisition and compilation of the model is a relatively simple process. Developing model setups for operational use by which to generate results requires a period of trial and error whereby domain setups are devised and tested to optimise the balance between the computing resource used and the model runtime. Once the run procedure on all three computing facilities was adopted the model runs themselves were relatively simple to undertake and the process was simply about repetition to generate the results required for the investigations. It was found to be of benefit to post process the model output in the same location as the model run is undertaken simply because of the size of the model output files, which if transferring across multiple computers would be a considerable undertaking. The requirement for a high performance computing resource is discussed shortly, but ultimately relates to the accessibility of this mesoscale NWP technology. While a modest desktop PC is capable of running WRF, access to the model's full potential will only be available with a significantly more powerful computing facility which must be a consideration to potential end users.

8.7 Implications of computing resource

One outcome of the benchmarking performance study at Scroby Sands was the identification that model performance is dependent upon the available computing resource. In the benchmarking exercise at Scroby Sands, simulations were undertaken for the same periods using model configurations optimised for two different computing systems. Results implied a considerable difference in performance was present due to the available computing resource. The need to use the maximum available computing resource for the remaining investigations was overtly apparent. From a practical perspective it meant running the model on multiple computing facilities, which despite a few teething problems with compilation on both HPC facilities used, was not a significant problem. Because WRF is well-supported and can be readily compiled on facilities with a diversity of compilation options, the technology is highly accessible. While a restricted computing resource has been shown to perform to an inferior level, it still offers some potential regarding longer term lower frequency features to a potential end user. With a large computing resource available for the Shell Flats investigation, a high level of performance was observed. A large domain was practical to use and afforded the model sufficient capacity to perform well. The simulations could be run simultaneously (assuming

availability on the computing facility) with approximately five undertaken at a time, which from start to finish took around three days. These results were achieved using the HPC facility at Loughborough University to give some impression of the operators of such a computing facility. Similarly, with the optimisation runs comprising the third investigation, a large computing resource was used, namely the UK's national HPC facility HECToR. Like the long term resource assessment investigation, the awarded computing resource was ample for the requirements of the study, with absolute performance compromised for the benefit of runtime. Multiple runs were undertaken simultaneously, which was vital to achieving the aims of the research within the allotted time. Ultimately, while the available computing resource is shown to dictate the level to which an NWP model can perform, it is also related to the duration of a study. Efficient use of the available computing resource is related to the number and duration of runs which can be undertaken simultaneously, not exclusively the outright computing capacity the model can utilise. A number of recommendations can be made with these considerations in mind for potential end users applying NWP to the field of offshore wind resource assessment. Where available, it is recommended that setup of the model domain should aim to provide an optimal compromise of spatial coverage and inner resolution. All the optimisation techniques used in this research are also recommended to not only improve performance, but also increase understanding about model performance over the run. When computing resource is restricted, results obtained in this research show that the biggest gain in model performance arises from affording the model as much resource as possible through an efficient setup compared to the relatively small improvements available from the optimisation techniques. Thus it is recommended that the resolution of the inner domain be around 4-10 km with the priority of the domain setup being spatial coverage of the outermost domain

8.8 Optimal grid resolution

Analysis of the results obtained from the three investigations enables some recommendations to be made pertaining to optimal grid resolution given a large computing resource. It is first important to establish the definition of optimal in this context and the considerations which inform that definition. In this research, an optimal setup will give the highest grid resolution whilst minimising computing time. In the literature review a study by Gibbs et al (2011) suggested mesoscale model

resolutions higher than ~2 - 4km were of limited benefit as the increase in computing resource outweighed the observed improvement in performance which became increasingly small. Results from this study cannot confirm or refute that assertion, but they can provide additional information. The comparison of two model setups in the benchmarking exercise showed that despite the higher inner resolution of the NMM-setup, the ARW-setup was the better performer. The major physical differences between the two model setups were the resolution of the input data and the spatial coverage of the domains. By providing the ARW-setup with more information, the model was able to perform to a higher standard, again despite the higher resolution of the inner domain used in the NMM-setup. Effectively, these results agree with one assertion from Gibbs et al (2011), that when using mesoscale models at high resolution (~1-4km), inner grid resolution should be prioritised below computing resource, which should be allocated to a larger spatial coverage with higher resolution input data.

Temporal filtering of the benchmarking and long-term resource assessment investigations allowed an analysis of the practical implications of effective grid resolution. Filtering increased the temporal period of the comparison, which because the size of an atmospheric feature is related to time period over which it exists. The resultant effect was to shift the focus to larger atmospheric features responsible for lower frequency changes in wind speed. With an inner grid resolution of 2km (standard for the ARW runs) the effective grid resolution was around 14km, meaning the model is expected to fully resolve features of that size, which typically occur on the order of an hour or so. By reference to the Van der Hoven (1957) spectrum (Figure 3.11), comparison at ten minute resolution includes changes in wind speed caused by turbulent structures far below the effective resolution of the model. Temporally filtering the simulated and observed wind speed to one, three and six hours shifted the focus of the runs to the left of the Van der Hoven spectrum where low frequency features dominate wind speed variability. In both the benchmarking and long-term resource assessment investigations, filtering the modelled and observed series resulted in an improved level of performance achieved by the model. These results confirm the importance of effective resolution when designing an NWP investigation. Furthermore they are of particular relevance when justifying the application of mesoscale NWP models to long term wind resource assessments,

where wind speed variability is dominated by large scale features which are more successfully resolved by the model. Temporal analysis of model performance in this research identified high frequency variability as being the area corresponding to most model uncertainty, which relates to the approximation of the causal small scale features by parameterisation schemes. Until representative grid resolutions can be achieved where turbulent structures are resolved, mesoscale NWP models are unlikely to be able to perform to a high enough standard in short term situations where high frequency change dominates. It has been shown, in both the benchmarking exercise and the long term resource assessment exercise, that WRF is capable of high levels of accuracy regarding lower frequency wind speed change. At longer timescales, lower frequency features are the dominant mode of change in wind speed, so the application of a mesoscale model to long term resource assessments is appropriate. Therefore for future work regarding mesoscale NWP in wind resource assessment, it is suggested the comparison between model and observations be at a lower temporal resolution than 10 minutes for example around 1-3 hours. Clearly, developers and operators want to know about wind speed change at shorter timescales but since the model parameterisation schemes are unable to account for turbulent features to a satisfactory degree, model performance should be evaluated at timescales at which it is designed to perform. These findings suggest that increasing resolution might improve performance in the high frequency temporal domain, but as Gibbs et al (2011) suggest, such an undertaking will likely not have the desired 'silver bullet' effect and alternative solutions must also be investigated. With a significantly greater computing resource, increasing model resolution and spatial domains in tandem may provide the ideal conditions to address performance in the high frequency domain, but requires further investigation.

8.9 Temporal filtering

As an addendum to the previous discussion, which was enabled due to the application of temporal filtering, it is argued that filtering a high resolution series provides more information of model performance than simply simulating and comparing at a temporal resolution of interest. Extra information, pertaining to tendency in the series between the compared points, is provided by filtering a series at higher temporal resolution. For example, at an hourly resolution a straight line would join two data points an hour apart, where filtering a ten minute series to hourly

resolution will give a shape between the intervening time steps to indicate any tendency in the time series. Observations used in this research were ten minute averaged values while the model produced an instantaneous value for the corresponding ten minute interval. Thus, comparing an average value with an instantaneous value does not represent a like with like comparison. There was no other option for the comparison at ten minute intervals because that was the format of the available data. However, filtering offered an option to by which to make the comparison between model output and observations more appropriate, by filtering the data to longer periods the model output was effectively averaged for the given time step.

8.10 Variability in model performance with location

A considerable difference in model performance is evident with location, the simulation of the ten minute wind speed is much more accurate at Shell Flats than both investigations at Scroby Sands. Application of the Butterworth temporal filter to both Scroby Sands and Shell Flats yielded improvements in both locations but to a greater extent at Scroby Sands compared to Shell Flats. The fact that the improvement was greater at Scroby Sands is interesting but does not provide an explanation as to why. The simple fact that performance was worse meant that there was greater potential for improvement at Scroby Sands, however that by no means translates to a greater improvement by applying the filter. What the application of the filter to the Scroby Sands data did, was identify that the filtered series were far more similar than the unfiltered series, inferring that the model struggled with high frequency change at Scroby Sands to a greater extent than at Shell Flats. No comparison was made between the sites to offer a reason as to why this might be the case, however, a discussion comprising a number of suggestions will follow.

Before addressing potentially viable sources for the performance discrepancy, one option can be ruled out. Computing resource is unlikely to be the source of the performance difference because the Shell Flats runs had a slightly lower allocation of resources compared to the Scroby Sands runs. An element of the discrepancy in performance might arise from procedural differences between the two investigations. There is a greater amount of data comprising the Shell Flats run than the Scroby Sands runs which might have a slight bearing on performance, but the magnitude of the difference suggests there is a more fundamental underlying reason for the

performance gap between the two sites. Alternatively the input data provided to the model might differ in quality for the two sites which would have a significant bearing on the success of the model. For example, more observations may be available for use in the CFSR product to make the accuracy over the Irish Sea more accurate than the North Sea.

After examining the method by which the simulations were undertaken, the fundamental differences between the two sites must be considered. In terms of differences between the sites which might cause rise to a performance discrepancy, the potential candidates can be grouped into physical differences and climatic differences. Physical differences refer to the physical domain of the site, while climatological differences relate to the prevailing atmospheric conditions seen at the site. Beginning with the physical properties, Shell Flats is farther offshore than Scroby Sands, so while a coastal interface is present in the inner domain it is farther away from the point of interest. Scroby Sands however is located close to the shore which means the model output at the point of interest is heavily influenced by model performance in a coastal zone. Mentioned in the literature review was that WRF exhibited a positive wind speed bias over land, which could well affect the model solution at a coastal interface, particularly given small scale perturbations such as turbulence giving rise to short term fluctuations in wind speed. In contrast, the extra distance to the coastal interface in the Shell Flats domain provides something of a relaxation zone where the effect of the coastal interface has more time to be damped in the model solution so as not to be too influential at the point of interest. A coastal interface presents a significant challenge to a numerical model, representing changing values in roughness, heat capacity and height which all have a bearing on the incident wind flow. Climatic differences between the sites relate to the type of weather seen at the sites, specifically the degree of variability and the prevailing conditions. The model may physically simulate both sites to the same degree but if one site experiences particular synoptic or driving conditions more often which the model struggles with then performance may suffer. For example there may simply be a lesser degree of high frequency wind speed variability observed at the Shell Flats site than Scroby Sands, so the model is able to perform to a higher standard. Equally there may be a set of atmospheric features that affect one site but not the other for example a sea breeze circulation affecting the Scroby Sands site or the presence of

a low level jet. With the prevailing south westerly wind the British Isles experiences, the fetch (physical landscape over which the incident wind flows) also impacts the physical differences between the sites despite being a climatological parameter. At Scroby Sands, a South-Westerly flow would involve a land to sea wind flowing over the coastal interface, while the Shell Flats site has a much longer ocean fetch with minimal roughness. Ultimately the variations between the sites, both physically and climatologically could translate to differences in model performance simply because one site is more complex than the other or because of the way the sites are represented by the model. Further work is required to elucidate these differences more comprehensively from which a more complete understanding of the models performance can be obtained.

8.11 Model performance as a wind resource assessment tool

Table 2, provided in the literature review, summarised the level of performance achieved by WRF when simulating wind speed in a number of other studies. It is presented below (Table 8.29), with the addition of results obtained in the three investigations comprising this research. Direct comparison between the studies is not applicable because results from this study show how variable one model setup can be in the same location, let alone in different configurations for different locations. As a result, the different studies are presented as a reference point by which to consider the results obtained in this research and provided with some information pertaining to key differences between the studies. The results obtained in this work are broadly comparable to the results obtained by others shown in Table 8.29. The NMM-setup performs to a lower standard than the other studies presented, but was conducted on a more computationally restricted setup than all of them. The ARW-setup varies in performance with location but is well within the range provided by the other studies. The temporal resolution of the other studies is also important because most studies tend to examine wind speed at lower temporal resolution which, according to the results of the filtering process undertaken in this research, would improve performance. Variability in wind speed, as represented by correlation coefficient, is captured to varying degrees of success across the different studies ranging from around 0.6 to 0.9. Absolute error seems to be consistent with studies finding an RMSE of around 2 ms^{-1}. Optimisation techniques applied in the third investigation of this research were not used in any of the other studies implying an

extra level of performance is achievable using such techniques. Furthermore, the process of temporally filtering some of the higher resolution runs would likely improve the performance of some of the runs, in accordance with the results from the benchmarking and long term resource assessment investigations. Ultimately, these results show that WRF can capture variability in offshore wind for a range of locations over a range of timescales and using a diverse range of model setup strategies. RMSE statistics imply a consistent absolute error which is comparable to the error associated with MCP studies. Optimisation strategies and temporal filtering offer means by which to improve upon the results presented which make the operational application of the technique viable.

Table 8.29 Collection of statistics describing accuracy of WRF as a predictor of wind speed including the results achieved in this research (Hughes, 2013*).

Study	Notable setup options	Resolution	Correlation coefficient	RMSE
Shimada and Ohsawa	ARW, FDDA, MYJ, SST	10 minute	0.8	46% mean ~2.8ms^{-1}
Kwun et al 2009	ARW, MYJ	Correlation – hourly RMSE – daily	0.64	1.1 ms^{-1}
Pena et al, 2011	ARW	Hourly	-	2 ms^{-1}
Raubenheimer et al, 2012	ARW	Diurnal	0.94	1.8-2.1 ms^{-1}
Nawri et al, 2012	ARW	Monthly	0.57	-
Liu et al, 2012	ARW	Hourly	0.48	2.8 ms^{-1}
Hughes, 2013*	NMM, MYJ	10-minute	0.35	3.5 ms^{-1}
Hughes, 2013*	ARW (Shell Flats)	10-minute	0.86	2.1 ms^{-1}
Hughes, 2013*	ARW (Shell Flats)	6-hourly	0.9	1.7 ms^{-1}
Hughes, 2013*	ARW (Scroby)	10-minute	0.64	2.2 ms^{-1}
Hughes, 2013*	ARW (Scroby Optimised)	10-minute	0.64	2.2 ms^{-1}

Hughes, 2013*	ARW (Scroby)	3-hourly	0.72	1.9 ms^{-1}

What the investigations have achieved is a definition of performance for two locations with different priorities, with short individual runs comprising the benchmark exercise and short runs concatenated to form a continuous run comprising the long term resource assessment. The optimisation investigation then required another set of short runs for Scroby Sands by which to test the optimisation techniques. Performance improved, seeing an increase in correlation coefficient of 0.05 and a reduction on RMSE of 0.2 ms^{-1} or roughly 10% in each case. To understand how applicable it would be to assume the same level of improvement for different sites, the impact of temporal filtering performed upon the shell flats and Scroby Sands benchmarking studies is compared. At Shell Flats, the correlation coefficient between the model and observations was reasonably high at 0.856, when filtered to three hourly resolution (three hourly values are used to compare against a likewise resolution at Scroby Sands) it improved to 0.883, a margin of 0.027 or by around 3% of the original value. For RMSE at Shell Flats, the raw ten minute value was 2.12 ms^{-1} while the three hour filtered value was 1.88 ms^{-1}, a difference of 0.24 ms^{-1} or around 11%. By comparison, the Scroby Sands benchmarking results showed an initial correlation coefficient at ten minute resolution of 0.64, which when filtered to a three hourly resolution, improved to 0.72 a difference of 0.08 or 11% of the original value. RMSE in the benchmarking runs at Scroby Sands improved from 2.2 to 1.9 ms^{-1} a change of 0.3 ms^{-1} or 13.6%. The improvements were of a greater magnitude at Scroby Sands than Shell Flats, the reasons for this are unknown and could simply relate to the fact that there was more room for improvement at Scroby Sands.

At this point no factor can be applied to infer the likely benefit of the optimisation techniques for different locations. It could be asserted with some confidence, that the application of the optimisation techniques to the benchmarking runs at Scroby Sands may well yield a 10% improvement. However at Shell Flats, because of the difference in performance seen, resulting from the temporal filtering process, no quantification regarding improvement can be made. What can be said is that because temporal filtering improved performance improved at Scroby Sands as well as Shell Flats, the optimisation techniques are likely to improve performance at Shell Flats and thus other locations, however the degree to which is unknown. Thus

far, wind speed has been the focus of this section, however WRF is shown to simulate a wide range of variables and has displayed its potential by producing a number of those variables critical to offshore wind resource assessments. Wind direction has been simulated and while time series analysis suggests direct variability is not well captured, aggregated statistics show a discernible level of skill in the model output. Stability is a variable of growing importance to the wind industry as farms increase in size and parameters which influence wake propagation play a big part in farm production. As with wind direction, the instantaneous representation of stability was found to be lacking but the general distribution was found to represent that observed. Stability was classified by outright proportion but also by wind speed bin, wind direction, weather type and time (hour and month) in which distinct likenesses between the modelled and observed distributions were evident. All of these factors combined with the potential of the model to simulate for any location globally make it an extremely capable option by which to produce a wind resource assessment. One example of the flexibility of NWP as a resource assessment tool was provided by the Supergen exemplar farm assessment. Where a met mast can only represent one location, the model output was used to provide a spatial field to identify change in the wind field through the farm. While wind direction results from the Shell Flats resource assessment may not invoke confidence, the model could be used to provide a more simple output relating to tendency rather than trying to account for precise changes. NWP provides a readily accessible source of such information which considering the size of the round 3 wind farms would be of huge use to the operators. It is anticipated that with research and development in the application of NWP to wind resource assessment, its use will be commonplace in the future. Indications are that absolute error will be difficult to reduce to the level achieved by in situ observations, but it is entirely feasible that with development and the use of a single mast, the addition of an NWP campaign will extend the assessment to provide what is required by the developers. Results from Shell Flats show that WRF is not far off the accuracy of an inter-mast interpolation procedure, which with development is an accuracy which could very well be achieved by the model negating the need for multiple masts at a site of interest.

8.12 Application of WRF to the field of offshore wind resource assessment

The benchmarking performance runs showed that WRF has a reasonable level of skill as an offshore wind resource assessment tool when used 'out of the box', provided a comprehensive computing resource is available. Low frequency wind speed change is generally captured by the computationally restricted NMM-setup runs, suggesting that large scale features can be simulated to an appreciable degree of accuracy. Beyond that however, with the NMM-setup, model performance is limited. Production of wind speed change in the medium frequency range is minimal and no high frequency variability is present in the runs. In terms of practical application, the restricted computing setup might be of use in a preliminary site assessment, undertaken over a very long period to review the long-term trend at a site. The computationally 'unrestricted' ARW-setup runs showed a much higher level of skill 'out of the box' compared to the restricted NMM setup runs. Wind speed change in the low and medium frequencies was well captured, however high frequency change proved harder to simulate for the model. Levels of high frequency wind speed change simulated by the model reflected those observed, but the timing and direction of change was less accurately simulated. 'Out of the box' skill is implies that the model in both configurations would be suitable for use in a preliminary site assessment and with a larger computing resource a long-term resource assessment, due to their ability to simulate wind speed well in the low and medium frequency range. As an operational resource assessment tool, where forecast horizons are short and simulation of high frequency features is critical, the model offers some potential, but to a lesser extent than for longer term simulations due to uncertainty in production of short term changes in wind speed. High frequency change dominates short term forecasting, which has been shown to be a weakness throughout these investigations.

The Shell Flats long term resource assessment enabled a review of the models performance with a large computing resource, to simulate for a continuous period as a direct example of what would be required by the industry. Performance regarding the simulation of wind speed was much improved over that seen at Scroby Sands. Given the consistency of the model setup between Shell Flats and Scroby Sands, the difference in model performance at the two sites was attributed to physical contrasts between the sites which, with further research, should be accounted for to

some extent through model setup. The level of performance seen in the Shell Flats investigation confirms the potential of WRF as an offshore wind resource assessment tool for both long and short term studies. In both the Scroby Sands and Shell Flats studies, temporal filtering was applied to the observed and predicted series to shift the focus of the simulations to larger scale synoptic features at the effective resolution of the model grid. Performance improved by a significant margin, which served to confirm the performance of the model for longer term studies and its uncertainty regarding short term wind speed variation. Optimisation techniques were developed and applied to modelling runs throughout the investigation with a view to improving accuracy and understanding of model performance.

Observational nudging was employed for the Shell Flats resource assessment and in the optimisation runs at Scroby Sands. On balance, nudging proved to be a beneficial technique which helped improve model performance at the site of interest. Interestingly, inclusion of a non-nudged series in the PBL ensemble also proved a beneficial undertaking, to account for occasions when nudging the model run inhibited performance.

When examining the effect of different PBL parameterisation schemes, model performance was found to vary depending upon the PBL scheme used. No individual scheme was found to be consistently preferable confirming the findings of other studies which imply performance to be dependent upon the atmospheric conditions. An ensemble of model solutions, perturbed by virtue of using different PBL schemes, was created to mitigate such an effect and was found, on average, to perform to a higher standard than any individual scheme. The main benefits arising from applying the PBL ensemble resulted in; increased accuracy of the mean compared to any individual member, greater understanding of model performance based on ensemble member distribution and a reduced level of uncertainty regarding the model output. Generation of the time offset ensemble not only provided multiple sets of initial conditions for a model run but did so at different times to effectively reinitialise the runs, to an extent. Like the PBL ensemble, one of the main benefits of this technique is a reduction in the uncertainty of the model output in line with that associated with the initial conditions. Specifically, this technique offered potential to model performance in short term applications such as the forecasting resource assessment field. The reinitialisation process inherent in a time offset ensemble, updated the

initial conditions by incorporating new members into the run at later intervals in the simulation, which has the effect of reducing the inevitable divergence between the modelled and observed series. WRF has been shown to perform to a high standard when simulating wind speed, but not to the level of accuracy achieved by in situ observations.

The flexibility of an NWP platform was demonstrated in the Shell Flats investigation where a range of variables critical to the wind resource assessment process were produced. Wind direction and stability were simulated and aggregated statistics comparing the simulated values with those observed for the same time period, showed the skill present in the model. The flexibility of WRF was extended further in the Supergen Exemplar site where a demonstration of the spatial coverage of the model domain showed wind direction variation across the farm. Such information could not be obtained from a single mast and adds great value to the case for using NWP in some form during a resource assessment. A number of considerable handicaps are imparted onto the numerical simulation process, such as the fact that input conditions were provided at 50km resolution and boundary conditions were updated at 6 hourly intervals. Despite these limitations, WRF does provide a viable option by which to generate a wind resource assessment. Performance is not at a level to consider suggesting NWP as a replacement for in situ observational campaigns, but at this stage certainly consideration should be given to using NWP as an augmentation to them. Use of NWP model output alongside in situ data might aid the improvement of the model and setup techniques to develop NWP into a genuine standalone resource assessment tool, but as yet performance is not to a high enough standard.

8.13 Closing remarks

Practicality was a key consideration of this research which strived to assess the potential of NWP to offshore wind resource assessments for a range of potential end users. Undertaking the ensemble runs required a considerable investment in time and computing resource, reducing the practicality of the approach, but the benefits are evident. The number of runs required to complete the ensembles was high and constituted a considerable undertaking in terms of time as well as computing resource. For end users with a well-staffed team and a high end computing resource, such an undertaking would be feasible for most applications, such as forecasting and

historic site assessments. However, for an individual researcher, such a technique is unlikely to be able to produce forecasts at the required rate given the number of ensemble runs required. For a long term assessment, the time available to undertake the runs is greater than for a forecasting application which makes the ensemble technique more appropriate, again depending on the availability of a large computing resource and well-structured run procedure. The ensemble technique offers a lot of benefits to a forecasting application and is recommended where possible. In this work the process could have been streamlined by selecting fewer members, for example only using the ACM and MYNN PBL schemes, but it is suggested that the TOES technique be employed as extensively as possible to account for initialisation errors and afford the reinitialisation process. For users with a limited resource it is suggested that computing resource be allocated to maximising the model run for one output, rather than employing the supplementary techniques such as ensembles which would requires a vast addition of computing time and restrict the base model setup in the first place. Instead it is recommended that the NMM core be used with an inner resolution of around 4-10 km with the priority being spatial coverage of the outermost domain.

When compared to alternative resource assessment methods, NWP was able to match and outperform land based data used in MCP studies and come close to the level of performance achieved by one offshore mast as a predictor of another at Shell Flats. A lack of data for validation has hindered the development of this technology in this field, but results presented in this study underline the potential of NWP in the field of wind resource assessment. Without question, NWP has a lot to offer the field of wind resource assessment. With appropriate progress in developing the technology and specifically the process by which NWP is applied to the field, strides will be taken in improving performance to a level which makes it acceptable for operational use. The legacy of this work is twofold, firstly the results have provided a level of performance for a range of scenarios by which other studies can be compared. It is hoped the second legacy of the work is the stimulation of future research. Many questions arose over the course of the three investigations and are posed to be addressed by future research, suggestions for which are summarised in the following section. With the application of research in the relevant areas the potential of mesoscale NWP modelling in the field of offshore wind resource

assessment can be realised. The planning phase of an offshore wind farm will reduce in cost, achieving the aim of Supergen Wind and increasing the penetration of offshore wind in the U.K.'s energy future to achieve renewable energy and carbon emissions targets.

8.14 Future work

8.14.1 Areas for improvement

8.14.1.1 Location dependence

Ultimately WRF is capable of performing to a very high standard, shown by results for the long term resource assessment work at Shell Flats. However for some as yet unknown reasons, the model was not able to perform to the same level at Scroby Sands. Given that dynamically, model setup was almost identical for the two sites, it is logical to suggest the gap in performance is due to a fundamental difference between how the model physically treats the two sites. Either Scroby Sands isn't as well represented by input data as Shell Flats, which would set the model run off with inaccurate initial conditions and tendencies and certainly affect performance. Or, the model doesn't represent the physical domain well, which given that Scroby Sands is very close to a coastal interface, is a legitimate theory. It is suggested a comparative study of the Shell Flats and Scroby Sands sites be undertaken to elucidate the differences between the sites and try to understand why model performance was so varied. The study needs to be extensive in order to identify differences between the sites themselves and how they might be treated differently by WRF. Analysis of how both sites are physically represented by WRF is an important place to start. Observational data from both sites should be compared, as should data from the CFSR product used to initialise WRF. CFSR data should also be compared against observations at both sites to identify any discrepancies translating to inaccurate initial and boundary conditions being provided to the model. Once the reasons for model performance are known, steps can be taken to address the performance gap and either improve model performance at Scroby Sands to the level of Shell Flats or fundamentally improve model performance in general, seen at both locations.

8.14.1.2 The PBL

A review of literature presented in chapter 2 identified the PBL as a source of uncertainty in the process of wind resource assessment. Results from this research agreed and showed that while it's possible to improve performance in the boundary layer by combining the schemes outputs in an ensemble, no individual scheme is able to comprehensively offer a preferable option. It is strongly suggested that research into performance in the PBL be pursued, as extra information from different investigations will only help develop understanding. One option is the application of more complex schemes such as the MYNN 3.0, which wasn't used in this research because it didn't run with the setup used. Alternatively, further development of an ensemble combining the skill of different schemes, perhaps more carefully weighted given particular conditions might prove beneficial and are discussed shortly. Time restrictions meant stability was not investigated in the optimisation runs at Scroby Sands, but it would be of great interest to see how the PBL schemes vary in performance by stability class. The results of which could help in selecting a dynamic weighting scheme for generating an ensemble mean based on a weather type analysis, perhaps of an aggregate number of previous time steps for a long term resource assessment and an initial low resolution pilot run in a short term forecasting assessment again to establish the weather type.

8.14.1.3 PBL scheme modification

A number of studies have been presented which highlight the inherent variability in performance not only between different schemes, but for the same scheme in different conditions/ locations. Some research has been undertaken to more directly address the issue of inconsistent performance offshore, by modifying the existing scheme. The MYJ scheme was found to underperform when representing the vertical diffusion of turbulence (Cheng et al 2002; Trini Castelli et al, 2006), particularly under stable conditions (Hanna et al, 2010), where under unstable and near-neutral conditions, performance improved. Two schools of thought exist as to the potential source of error, one attributes uncertainty to the model closure constants (Foreman and Emeis, 2010), the other to the master length scale (Suselj and Sood, 2010) which controls the properties of the vertical diffusivity constant. It is thought (Foreman and Emeis, 2010) that one of the processes contributing to turbulent kinetic energy (TKE) in the surface layer had been overlooked. The MYJ scheme was developed for horizontally homogeneous terrain (Pahlow et al, 2001)

yet the ocean surface is dynamic and wavy which contributes to the forces imparted upon the air, the added contribution of stress enhances TKE in the surface layer (Shaikh and Siddiqui, 2010). Two solutions have been suggested which involve modifications to either the closure constants (Foreman and Emeis 2010) or the master length scale (Tambke et al, 2005; Suselj and Sood, 2010) of the parameterisation scheme. Both methods showed improvements in the accuracy of the schemes, Foreman and Emeis (2010) improved the accuracy of the MYJ scheme by altering the model closure constants (Figure 8.57). Suselj and Sood (2010) found that modifications to the master length scale produce similarly accurate results in unstable and near-neutral conditions but also significantly improved performance under stable conditions. Nolan et al (2009) found the impact if the surface layer scheme to be of great importance regarding model performance in the PBL, suggesting a more comprehensive review of performance through the model treatment of the surface rather than exclusively focussing on the PBL scheme.

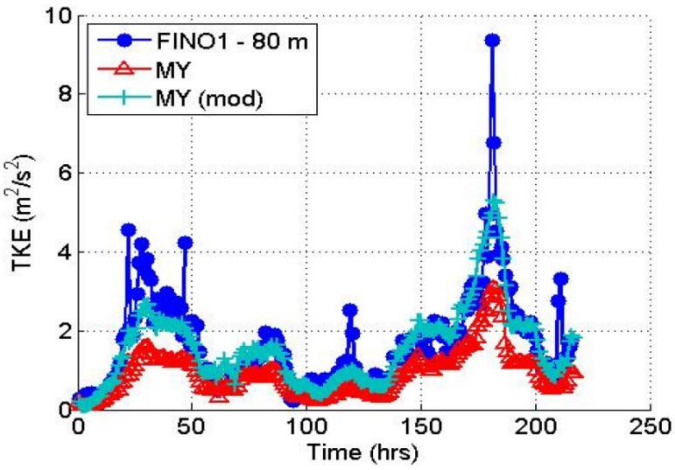

Figure 8.57 Turbulent kinetic energy at 80 m above sea level during a storm in Jan. 1- 10, 2005. Dots: FINO1 observations, triangles: simulation with onshore MYJ scheme, bars: WRF simulation with modified offshore MYJ scheme (Foreman and Emeis, 2010).

8.14.2 Techniques

A range of techniques are presented which might aid the future investigations to be undertaken using NWP to improve performance as an offshore wind resource assessment tool. The suggestions are simply that, by no means are they intended to instruct future research and be taken verbatim, merely as a guide.

8.14.2.1 Nudging

Overall, nudging was shown to be a positive process in enhancing the performance of WRF, however not exclusively. This study only nudged wind speed from local observations in the outer domain. It would be of great interest to expand the investigation into nudging which could have a significant effect on model performance if optimised correctly. Nudging could be performed for multiple locations, at multiple vertical levels. The radius of influence could be tuned for particular investigations, for example changing with different applications of the same simulation. Furthermore, only wind speed was ingested in this research for the sake of simplicity, however WRF is able to integrate multiple variables which may help the model more comprehensively simulate the atmospheric state and improve performance more completely. For example nudging temperature might provide more accurate information about local energy distribution improving the resolution of local gradients which have an impact upon the local circulation. Results from this research showed the positive effect nudging wind speed had regarding the accuracy of simulating of wind direction which gives reason to undertake such an investigation.

8.14.2.2 Weather typing

Weather typing is a powerful technique which could provide an extra level of information for any wind resource assessment. Weather type analysis was introduced and used in this research as a means of quantifying the atmospheric setting to infer likely properties. The depth of a weather typing analysis could be more detailed however by undertaking a more comprehensive analysis of each case. Careful consideration of the implications associated with a prevailing weather type, compared to the atmospheric properties as they are observed might allow a deeper understanding of how weather type affects model performance and also what conditions can be expected from particular weather types when they are simulated by the model. For example, it has been asserted in this research that under anticyclonic conditions the atmosphere is more stable, less turbulent and wind speeds are lower. However, there is more information that could be inferred from an anticyclonic weather type such as humidity, temperature profile and vorticity which all affect the wind field. The importance of using weather typing alongside NWP relates to the scale dependent performance of WRF observed in this study. Given that WRF was found to simulate large scale features well, one might afford more confidence to

their simulation into the future. Consultation of a weather type analysis for the future simulation might add an extra level of information to the analysis, for example tendencies of variables such as pressure or temperature and likely stability conditions.

8.14.2.3 Ensemble analysis

An ensemble can provide a wealth of information for an end user. Given that end users will invariably use the data differently from one another, there are some features some users will utilise which other will not. One example is the ensemble spread, which in this research was found to have no relationship to model error, but remains a technique employed in other studies. Comprehensive analysis of the ensemble system will provide a wealth of information that users may have not considered previously. It is suggested that an exhaustive investigation into the information which can be obtained from an ensemble is performed. For example features such as member clustering, where a group of members tends towards similar values either at particular times through the run or over the course of the run might help identify periods of increased model confidence. Such identification might help the end user for example associate less risk with that given value and it might help the model user identify particular periods of strength in the model performance. Another area of potential regarding the output of an ensemble system is the production of a probabilistic output, where a time series is provided with a distribution of values for a given time step, perhaps shaded to give the likelihood, according to the ensemble member distribution, of the actual value at any time.

8.14.2.4 Ensemble weighting

Detailed analysis of ensemble members, for example by employing a classification method, could lead to the development of a tool which apportions weight to each member preferentially under particular conditions. This research has presented a simple method by which to deliver an ensemble output which was via a mean value, however in the optimisation runs weighting towards the more recently initialised run was investigated. The purpose of such an undertaking is to account for the variability in model performance seen throughout the model runs undertaken in this research. There is huge potential for investigating the performance of each member and having a more customised ensembling process, classified for example by; location, time of day, time of year, wind speed bin, wind direction bin or weather

type. To take the concept one step further a dynamic ensemble might be developed which would analysis on an ad-hoc basis to generate the most appropriate member weighting scheme.

8.14.2.5 Ensemble spread

No spread error correlation was found in the model optimisation investigation, such that small member spread did not necessarily relate to low error and large spread to high error. This could be for a number of reasons, firstly this work was uncalibrated, which according to the literature wouldn't make much of a difference but might have some effect. Secondly, the cases for which the model was run were selected based upon periods of consistent weather type, more research would have to be undertaken but it's possible the synoptic consistency was a factor in producing a minimal level of member spread. Finally, there were not particularly many incidents of extreme ensemble spread to relate to model error, therefore it might be of interest to produce a wider range of ensemble members for a wider array or uncertainties to try and maximise spread for the benefit of identifying periods of uncertainty.

8.14.3 Short term forecasting

Performance at small scales which contribute to short term, high frequency change in wind speed will only truly be solved dynamically by running the model at the correct effective resolution. That is to say until a model is able to be run where desired scales are directly simulated for rather than approximated. Some options exist, but are very computationally heavy, and would require input from larger scale models as initialisation data. The larger scale models would also need running to provide input to the smaller high resolution domains, again increasing compute time. Given results of the persistence forecasting, a practical solution might consist of a statistical approach, perhaps using an ARIMA model. A stage further might make use of an artificial neural network which could be fed with some key larger scale indicators from a dynamical model. Such undertakings would require significant preparation times to learn prior occurrences but might offer a performance improvement once operational to augment model output.

8.14.4 Spatial coverage

One of the great strengths of NWP is its flexibility, it can be applied to any global location for any size domain, which in a practical context simulating for a large wind farm may require multiple met masts to satisfy a developers requirements. With

the size of offshore installations continuing to increase, such flexibility could save developers millions in the planning phase as NWP is used to provide an insight into conditions across the farm working alongside output from a reduced number of met masts. It would be of interest to conduct a study whereby a model run is undertaken for a site which contains multiple masts, then the output of the model could be assessed as a predictor for masts throughout the domain and compared against data from the other masts. It would seem from the Shell Flats investigation that 6km is a short enough distance to allow a reasonable replication from one mast to another so it would be interesting to test the limits of such extrapolations.

8.14.5 Model resolution

The main area for improvement in model performance has been identified as small scale short term features. Many alternatives and mitigations have been presented, employed and discussed apart from a frank consideration of simply increasing model resolution. It is a lot to ask that a PBL scheme accounts for turbulent structures giving rise to changes in wind speed, based solely upon values of larger resolved variables, but at the moment that is how the PBL is treated in WRF. Improvements will continue to be made regarding the PBL schemes but ultimately confidence will come when the boundary layer is actually resolved, at least to some extent. The literature review mentioned how small improvements seen by increasing resolution were compared to the increase in computing resource, but another factor to consider is the validity of mesoscale model equations at small scales. WRF is capable of running in LES (Large eddy simulation) mode which provides a more appropriate representation of smaller scale atmospheric features. Such a domain could be used to simulate at high resolutions on the order of metres, though are very computationally expensive and difficult to implement. Alternatively combining WRF output with a CFD (computational fluid dynamics) code might yield interesting results but again is likely to be computationally expensive and require a great investment setting up.

8.14.6 Stability

Originally intended as an additional variable by which to assess model performance, stability proved to be an interesting subject of investigation which stimulated many questions requiring future work. What the results from this research did was establish a set of scenarios, for example stability variation as classified by

weather type, and compared the performance of the model to observation under those classifications. However it would be of great use to know the reasons for the variation in stability as a function of those other variables as observed and to then qualify that by reference to the model results to see if the reasons for variations in stability are consistent. Using the example of weather type, a number of inferences can be made regarding the atmospheric conditions which might contribute to a certain stability class, for example, the thermodynamic characteristics of an airmass. But, without further investigation of those properties, by reference to the model and observations, identification of the mechanism causing the relationship between weather type and stability cannot be confirmed. Such an investigation requires a detailed knowledge of stability to be able to carefully plan an appropriate methodology, stability is a complex parameter which could stimulate multiple tangential investigations away from the original aim. The benefit of such a study would help qualify the skill present in the mesoscale model because if it were found that the reasons the model output followed that observed were though correct appreciation of the controlling mechanisms, more confidence could be afforded to the model output.

8.14.7 Model bias

WRF has shown a capacity to simulate observed wind speed, correlation statistics imply the model has great skill but is dependent upon location. Once model performance is improved to a level where correlation is consistently high, it will be worth investigating the presence of bias in model output. While RMSE quantifies the absolute error in a series, it is also important to know the degree of bias associated with a predictor. Bias is a measure of systematic error in a model, for example variability may be well resolved by a model but with a consistent offset in magnitude whereby the model under- or over-predicts reality. Bias is represented by averaging the residuals, produced by subtracting the concurrent modelled value from that observed. A positive value indicates an under prediction by the model and a negative value signifies an over prediction. The magnitude of the bias relative to the absolute error, in this case as represented by RMSE, gives an indication of the systematic error present in the model. A bias similar to RMSE implies that the systematic error can be accounted for by applying a correction. Bias is an important factor to account for in model performance, but will be more evident if and when the correlation

coefficient between model and observations is at a consistently high level. A good place to start such an investigation might be on the Shell Flats resource assessment work. With a reasonably high correlation between the model and observations, it should be possible to undertake a reliable trend analysis which might identify any model bias which could then be corrected.

References

Anderson, J.L. 1996. A method for producing and evaluating probabilistic forecasts from ensemble model integrations. *J. Climate*, **9**, 1518–1530.

Arribas, A., Robertson, K.B. and Mylne, K.R. 2005. Test of a poor man's ensemble prediction system for short-range probability forecasting. *Mon. Wea. Rev*., **133**, 1825–1839.

Badger, M., Badger, J., Nielsen, M., Hasager, C.B. and Peña, A. 2010 Wind class sampling of satellite SAR imagery for offshore wind resource mapping. *J. Appl. Meteorol. Climatol.*

Bailey, B.H., McDonald, S.L., Bernadett, D.W., Markus, M.J. and Elsholz, K.V. 1997. Wind Resource Assessment Handbook" (PDF). *Subcontract No. TAT-5-15283-01*. National Renewable Energy Laboratory.

Ballantyne, A.P., Alden, C.B., Miller, J.B., Tans, P.P. and White, J.W.C. 2012. Increase in observed net carbon dioxide uptake by land and oceans during the past 50 years. *Nature*, **488**, 70–72, doi:10.1038/nature11299.

Barry, R.G. ad Chorley, R.J. 2003. *Atmosphere, Weather and Climate (8th ed)*. Routledge, London.

Barthelmie, R.J. and Jensen, L.E. 2010. Evaluation of power losses due to wind turbine wakes at the Nysted offshore wind farm. *Wind Energy*; **13**: 573–586.

Bengtsson, L., Kanamitsu, M., Kallberg, P. and Uppala, S. 1982 FGGE 4-dimensional data assimilation at ECMWF. *Bull. Am. Meteorol. Soc.*, **63,** 29–43.

Bengtsson, L. and Shukla, J. 1988. Integration of space and in situ observations to study global climate change. *Bull. Amer. Meteorol. Soc.,* **69**,1130-143.

Betz, A. 1966. Introduction to the Theory of Flow Machines. *Pergamon,* Oxford, UK.

Borge, R., Alexandrov, V., del Vas, J.J., Lumbreras, J., Rodrıguez, E., 2008. A comprehensive sensitivity analysis of the WRF model for air quality applications over the Iberian Peninsula. *Atmos. Environ.* **42**, 8560–8574

Brodeau, L., Barnier, B., Penduff, T., Treguier, A.-M., and Gulev, S. 2010. An ERA40-based atmospheric forcing for global ocean circulation models. *Ocean Model*., **31(3-4)**, 88–104.

Bright, D.R., Mullen, S.L., 2002. The sensitivity of the numerical simulation of the Southwest monsoon boundary layer to the choice of PBL turbulence parameterization in MM5. *Wea. and Fore.* **17**, 99–114.

Bryan, G.H., Wyngaard, J.C. and Fritsch, J.M. 2003. Resolution requirements for the simulation of deep moist convection.*Mon Weather Rev,* **131**, 2394–2416.

Buizza, R., 1997: Potential forecast skill of ensemble prediction and spread and skill distributions of the ECMWF ensemble prediction system. *Mon. Wea. Rev*., **125**, 99–119.

Buizza, R., Houtekamer, P.L., Toth, Z., Pellerin, G., Wei, M. and Zhu, Y. 2005. A comparison of the ECMWF, MSC, and NCEP global ensemble prediction systems. *Mon. Wea. Rev*., **133**, 1076–1097.

Burton, T., Sharpe, D., Jenkins, N. and Bossanyi, E. 2001. Wind energy handbook. Chichester, UK: J. Wiley & Sons.

Carvalho, D., Rocha, A., and Gómez-Gesteira, M. 2012. Ocean surface wind simulation forced by different reanalyses: Comparison with observed data along the Iberian Peninsula coast. *Ocean Modelling*, **56**, 31-42.

Challa, V.S., Indracanti, J., Rabarison, M.K., Patrick, C., Baham, J.M., Young, J., Hughes, R., Hardy, M.G., Swanier, S.J. and Yerramilli, A. 2009. A simulation study of mesoscale coastal circulations in Mississippi Gulf coast. *Atmospheric Research* **91**, 9– 25.

Chin, H.N.S., Glascoe, L., Lundquist, J. and Wharton, S. 2010. Impact of WRF Physics and Grid Resolution on Low-level Wind Prediction: Towards the Assessment

of Climate Change Impact on Future Wind Power.*Lawrence Livermore National Laboratory* (LLNL), LLNL-PROC-425038.

Crooks, S.A. and L.J. Gray. 2005. Characterization of the 11-year solar signal using a multiple regression analysis of the ERA-40 dataset, *J. Clim*., **18**, 996– 1015

Dalcher, A., Kalnay, E. and Hoffman, R.N. 1988. Medium range lagged forecasts. *Mon. Wea. Rev.*, **116**, 402–416.

DECC, 2013. 2012 UK GREENHOUSE GAS EMISSIONS, PROVISIONAL FIGURES AND 2011 UK GREENHOUSE GAS EMISSIONS, FINAL FIGURES BY FUEL TYPE AND END-USER. Available from https://www.gov.uk/government/uploads/system/uploads/attachment_data/file/193414/280313_ghg_national_statistics_release_2012_provisional.pdf [Accessed 23/09/2013].

Deng, A., and Stauffer, D. R. 2005. On improving 4-km mesoscale model simulations. *J. Appl. Meteor*., **45**, 361–381.

Deppe, A. J., Gallus, W. A. and Takle, E.S. 2013. A WRF Ensemble for Improved Wind Speed Forecasts at Turbine Height. *Wea. Forecasting*, **28**, 212–228.

Draxl, C., Hahmann, A. N. Peña, A. and Giebel. G. 2012. Evaluating winds and vertical wind shear from Weather Research and Forecasting model forecasts using seven planetary boundary layer schemes, *Wind Energy*

Dumais,R. E., Passner, J. E., Flanigan, R., Sauter, B. and Kirby, S. 2009. High Resolution WRF-ARW Studies at the U.S. Army Research Laboratory for use in Short-Range Forecast Applications. *P2.4. 23rd Conference on Weather Analysis and Forecasting/19th Conference on numerical Weather Prediction*. Omaha, NE,June 1–5, 2009.

ECMWF, 2012. *ECMWF 2012 Annual report*. Available from: http://www.ecmwf.int/publications/annual_report/2012/pdf/Annual-report-2012.pdf. [Accessed 05/09/2013]

Floors, R., Vincent, C.L., Gryning, S-E., Pena, A. and Batchvarova, E. 2013. The Wind Profile in the Coastal Boundary Layer: Wind Lidar Measurements and Numerical Modelling. *Boundary-Layer Meteorol,* **147,** 469–491

García-Díez, M., Fernández, J., Fita, L., Menéndez, M., Méndez, F. J., Gutiérrez, J.M., 2012. Using WRF to generate high resolution offshore wind climatologies, *Poster, 8 Congreso Internacional AEC, Salamanca*, (Spain).

Gibbs, Jeremy A., Fedorovich, E. and van Eijk, A.M.J. 2011. Evaluating Weather Research and Forecasting (WRF) Model Predictions of Turbulent Flow Parameters in a Dry Convective Boundary Layer. *J. Appl. Meteor. Climatol.*, **50**, 2429–2444.

Grachev, A.A. and Fairall, C.W. 1997. Dependence of the Monin–Obukhov stability parameter on the bulk Richardson number over the ocean. *Journal of Applied Meteorology.* **36**, 406–414.

Great Britain, 2008. *Climate Change Act 2008: Elizabeth II. Chapter 27.* London, The Stationery Office.

Grimit, E.P. and Mass, C. F. 2002. Initial results of a mesoscale shortrange ensemble forecasting system over the Pacific Northwest. *Wea. Forecasting*, **17**, 192–205.

Grimit, E.P. and Mass, C.F. 2007. Measuring the Ensemble Spread–Error Relationship with a Probabilistic Approach: Stochastic Ensemble Results. *Mon. Wea. Rev.*, **135**, 203–221.

Gryning, S.-E., Batchvarova, E. and Floors, R. 2013. A Study on the Effect of Nudging on Long-Term Boundary Layer Profiles of Wind and Weibull Distribution Parameters in a Rural Coastal Area. *J. Appl. Meteor. Climatol.*, **52**, 1201–1207.

Hamill, T.M. and Colucci, S.J. 1998. Evaluation of Eta-RSM ensemble probabilistic precipitation forecasts. *Mon. Wea. Rev*., **126**, 711–724.

Hamill, T. M. 2001. Interpretation of rank histograms for verifying ensemble forecasts. *Mon. Wea. Rev*., **129**, 550–560

Hanna, S.R., Reen, B., Hendrick E., et al., 2010. Comparison of observed, MM5 and WRF-NMM model-simulated, and HPAC-assumed boundary-layer meteorological

variables for 3 days during the IHOP field experiment," *Boundary-Layer Meteorology*, **134(2),** 285–306.

Hansen, K.S., Barthelmie, R.J., Jensen, L. and Sommer, A. 2012. The impact of turbulence intensity and atmospheric stability on power deficits due to wind turbine wakes at Horns Rev wind farm. *Wind Energy*. **15**(1), 183–196.

Harrison, M. S. J., Palmer, T. N., Richardson, D. S. and Buizza, R. 1999. Analysis and model dependencies in medium-range ensembles: Two transplant case studies. *Quart. J. Roy. Meteor. Soc*., **125**, 2487–2516.

Hasager, C., Badger, J., Bingol. F., Clausen, N-E., Hahmann, A., Karagali, I., Badger, M and Pena, A. 2011. Wind energy resources of the South Baltic Sea. *World renewable energy congress 2011.* Sweden.

Hasager, C.B., Peña, A.; Christiansen, M.B., Astrup, P.; Nielsen, M.; Monaldo, F.M., Thompson, D.R. and Nielsen, P. 2008**.** Remote sensing observation used in offshore wind energy. *IEEE J. Sel. Topics Appl. Earth Obs. Remote Sens.*, **1**, 67-79.

Hays, J.D., Imbrie, J. and Shackleton, N.J. 1976. Variations in the Earth's Orbit: Pacemaker of the Ice Ages. *Science* **194** (4270): 1121–1132.

Heikkila, U., Sandvik, A. and Sorteberg, A. 2010. Dynamical downscaling of ERA-40 in complex terrain using the WRF regional climate model. *Climate Dyn*., **37**, 1551–1564,

Hoffman, R.N. and Kalnay, E. 1983. Lagged average forecasting, an alternative to Monte Carlo forecasting. *Tellus*, **35A**, 100-118.

Holtslag, A.A.M. and Boville, B.A. 1993. Local versus nonlocal boundary layer diffusion in a global climate model*. J. Climate*, **6**, 1825.

Hong, S.Y., Noh, Y. and Dudhia, J. 2006 A new vertical diffusion package with explicit treatment of entrainment processes, *Mon. Weather Rev.* **134** pp. 2318–2341.

Honirubia, A., et al. 2011. Comparison of wind speed measurements over complex terrain using a LIDAR system. EWEA 2011 Proceedings. Available from http://proceedings.ewea.org/annual2011/allfiles2/1114_EWEA2011presentation.pdf. [Accessed 13/05/2013].

Horseman, A. 2013. Lamb weather type data website. Available from: http://www.weathertypes.info/ [Accessed 20/09/2013].

Horstmann, J., Koch, W. and Lehner, S. 2004. Ocean wind fields retrieved from the advanced synthetic aperture radar aboard ENVISAT. *Ocean Dyn.* **54**, 570-576.

Hou, D., Kalnay, E. and Droegemeier, K.K. 2001. Objective verification of the SAMEX' 98 ensemble forecasts. *Mon. Wea. Rev.*, **129**, 73–91

Hughes, J.G. and Watson S.J. 2012. Correlation v RMSE: The difference in priorities when meteorological research is applied to industry. *Poster: RMetS, Renewable Energy and future of energy meteorology.* London.

Hu, X.-M., Nielson-Gammon, J. W. and Zhang, F. 2010. Evaluation of three planetary boundary layer schemes in the WRF model. *J. Appl. Meteor. Climatol*., **49**, 1831–1844.

IEC, 2005. IEC 61400-12-1 "Wind turbines – Part 12-1: Power Performance Measurement of Electricity Producing Wind Turbines", Geneva, Switzerland..

Janjic, Z. I. 2001. Nonsingular Implementation of the Mellor–Yamada Level 2.5 Scheme in the NCEP Meso model. NCEP Office Note No. 437, p. 61.

Janjic, Z. I., 2003: A Nonhydrostatic Model Based on a New Approach. *Met. Atmos. Phy*., **82**, 271-285.

Janjic, Z et al. Date unknown. User's Guide for the NMM Core of the Weather Research and Forecast (WRF) Modeling System Version 3. Available online at: http://www.dtcenter.org/wrf-nmm/users/docs/user_guide/V3/users_guide_nmm_chap1-7.pdf [Accessed 16/09/2013]

Jenkinson, A.F. and Collison, F.P., 1977. An initial climatology of gales over the North Sea. *Synoptic Climatology Branch Memorandum No. 62*, Meteorological Office, Bracknell.

Jiminez, P.A. et al. 2010. Surface Wind Regionalization over Complex Terrain: Evaluation and Analysis of a High-Resolution WRF Simulation. *J. Appl. Meteor. Climatol.*, **49**, 268–287.

Jiménez, P. A. and Dudhia, J. 2012. Improving the Representation of Resolved and Unresolved Topographic Effects on Surface Wind in the WRF Model. *J. Appl. Meteor. Climatol.*, **51**, 300–316

Joffre, S.M. 1984. Power laws and the empirical representation of velocity and directional shear. *Journal of Climate and Applied Meteorology*, **12,** 1196–1203.

Jones, P.D., Harpham, C. and Briffa, K.R. 2012. Lamb weather types derived from reanalysis products. *International Journal of Climatology*, **33** (5), 1129-1139.

Jorba, O. Jiminez-Guerrero, P. and Baldasano J.M. 2008. Annual evaluation of WRF-ARW and WRF-NMM meteorological simulations over Europe. *9th annual WRF users worksho*. Available from: http://www.mmm.ucar.edu/wrf/users/workshops/WS2008/abstracts/P9-18.pdf. [Accessed 13/09/2013]

Kalnay, E., Kanamitsu, M., Kistler, R., Collins, W., Deaven, D., Gandin, L., Iredell, M., Saha, S., White, G., Wollen, J., Zhu, Y., Chelliah, M., Ebisuzaki, W., Higgins.,W., Janowiak, J., Mo, K.C., Ropelewski, C., Wang, J., Leetmaa, A., Reynolds, R., Jenne, R. and Joseph, D. 1996. The NCEP/NCAR 40-year reanalysis project. *Bulletin of the American Meteorological Society*, **77**, 437-471.

Kalnay, E. 2003. Atmospheric modelling, data assimilation and predictability*. Cambridge University Press*, Cambridge.

Kang, S-L. 2009. Temporal Oscillations in the Convective Boundary Layer Forced by Mesoscale Surface Heat-Flux Variations. *Boundary-Layer Meteorol,* **132**, 59–81.

Kellert, S.H. 1993 In the Wake of Chaos: Unpredictable Order in Dynamical Systems*. University of Chicago Press*, Chicago.

Kristensen, L. 1999. The Perennial Cup Anemometer. *Wind Energy*, **2**, 59-75.

Kwun, J.H., Kim, Y-K., Seo, J-W., Jeong, J.H. and You, S.H. 2009. Sensitivity of MM5 and WRF mesoscale model predictions of surface winds in a typhoon to planetary boundary layer parameterizations. *Nat Hazards* **51**, 63–77.

Lackner, M.A., Rogers, A.L. and Manwell, J.F. 2007. Uncertainty analysis in wind resource assessment and wind energy production estimation*. 45th AIAA Aerospace Sciences Meeting and Exhibit*, Reno, US.

Lamb, H.H. 1972. British Isles Weather types and a register of daily sequence of circulation patterns, 1861-1971. *Geophysical Memoir 116*, HMSO, London, 85pp.

Leith, C.E. 1974. Theoretical skill of Monte Carlo forecasts. *Mon. Wea. Rev*., **102**, 409–418.

Levin, I. 2012. Earth science: The balance of the carbon budget. *Nature*, **488,** 35–36, doi:10.1038/488035a.

Liléo, S. and Petrik, O. 2011. Investigation on the use of NCEP/NCAR, MERRA and NCEP/CFSR reanalysis data in wind resource analysis. *EWEA 2011 conference proceedings*.

Litta, A. J. and Mohanty, U. C. 2008. Simulation of a severe thunderstorm event during the field experiment of STORM programme 2006, using WRF-NMM model. *Current Sci*., **95**, 204–214.

Liu, Z., Liu, S., hu, F., Ma, Y. and Liu, H. 2012. A comparison study of the simulation accuracy between WRF and MM5 in simulating local atmospheric circulations over Greater Beijing. *Science China Earth Sciences,* **55(3),** 418-427.

Lo, J. C. F., Yang, Z. L. and Pielke Sr., R. A. 2008. Assessment of three dynamical climate downscaling methods using the Weather Research and Forecasting (WRF) model. *J. Geophys. Res.,* **113**, D09112.

Lorenz, E.N. 1989. Comptutaional Chaos – A prelude to computational instability. *Physica D* **35**, 299-317.

Lu, C., Yuan, H., Schwartz, B.E. and Benjamin, S.G. 2007. Short-Range Numerical Weather Prediction Using Time-Lagged Ensembles. *Wea. Forecasting*, **22**, 580–595.

Lukas, R. Date Unknown. *Turbulence Closure and Parameterisation*. Available from: ftp://mana.soest.hawaii.edu/pub/rlukas/OCN-MET665/turbulence/Turbulence%20parameterization.pdf. [Accessed 21/08/2013].

Mahrt, L., Sun, J., Blumen, W., Delany, T. and Oncley, S. 1998. Nocturnal boundary-layer regimes. *Boundary-Layer Meteorology*, **88,** 255–278

Manwell, McGowan, and Rogers, 2002. *Wind Energy Explained; Theory, Design and Application*. Wiley.

Mass, C. and Ovens D. 2011. Fixing WRF's high speed wind bias: A new subgrid scale drag parameterization and the role of detailed verification. *Preprints, 24th Conf. on Weather and Forecasting/20th Conf. on Numerical Weather Prediction, Seattle, WA, Amer. Meteor. Soc*., **9B.6**. Available online at http://ams.confex.com/ams/91Annual/webprogram/Paper180011.html [Accessed 13/09/2013]

Mckie, R. 2013. Droughts and floods 'will be common events in Britain', *The Guardian*. Available from http://www.guardian.co.uk/uk/2013/mar/02/britain-faces-more-floods-and-droughts. [Accessed 07/02/2013].

McQueen, D. and Watson, S. J. 2006. Validation of Wind Speed Prediction Methods at Offshore Sites. *Wind Energy,* **9,** 75–85.

Meehl, G.A., T.F. Stocker, W.D. Collins, P. Friedlingstein, A.T. Gaye, J.M. Gregory, A. Kitoh, R. Knutti, J.M. Murphy, A. Noda, S.C.B. Raper, I.G. Watterson, A.J. Weaver and Z.-C. Zhao, 2007: Global Climate Projections. In: Climate Change 2007: *The Physical Science Basis. Contribution of Working Group I to the Fourth Assessment Report of the Intergovernmental Panel on Climate Change* [Solomon, S., D. Qin, M. Manning, Z. Chen, M. Marquis, K.B. Averyt, M. Tignor and H.L. Miller (eds.)]. Cambridge University Press, Cambridge, United Kingdom and New York, NY, USA.

Mellor, G.L. and Yamada, T. 1982. Development of a turbulence closure model for geophysical fluid problems. *Reviews of Geophysics and Space Physics* **20** (4), 851–875.

Misenis, C., and Zhang, Y. 2010. An examination of sensitivity of WRF/Chem predictions to physical parameterizations, horizontal grid spacing, and nesting options. *Atmos. Res*., **97**, 315–334,

Motta, M. and Barthelmie, R.J. 2005. The influence of non-logarithmic wind speed profiles on potential power output at Danish offshore sites. *Wind Energy*, **8,** 219-236.

Munoz-Esparza, D., Canadillas, B., Neumann, T. and van Beeck, J. 2012. Turbulent fluxes, stability and shear in the offshore environment: Mesoscale modelling and field observations at FINO1 *J. Renewable Sustainable Energy* **4**, 063136.

Muñoz-Esparza, D., van Beeck, J. and Cañadillas, B. 2011. Impact of turbulence modelling on the performance of the WRF model for offshore short-term wind energy applications. *13th International Conference on Wind Engineering*, Amsterdam, The Netherlands.

Munteanu, I., Bratcu. A.I., Cutululis, N-A. and Ceanga, E. 2008. *Optimal Control of Wind Energy Systems*. Springer.

Murphy, J.M. 1988. The impact of ensemble forecasts on predictability. *Quart. J. Roy. Meteor. Soc.*, **114**, 463–493.

Nakanishi, M. and Niino, H. 2004. An improved Mellor-Yamada level-3 model with condensation physics: Its design and verification. *Bound.-Layer Meteor*., **112**, 1–31.

Nakanishi, M., and Niino, H. 2009. Development of an improved turbulence closure model for the atmospheric boundary layer. *J. Meteor. Soc. Japan*, **87**, 905–909.

Nawri, N., Petersen, G.N., Björnsson, H. and Jónasson, K. 2012. Evaluation of WRF mesoscale model simulations of surface wind over Iceland. Report VI2012–010. Icelandic Meteorological Office, ISSN 1670-8261. http://www.vedur.is/media/2012_010_web.pdf [Accessed 16/09/2013]

Nolan, D.S., Zhang, J.A. and Stern, D.P. 2009. Evaluation of planetary boundary layer parameterizations in tropical cyclones by comparison of in situ observations and high-resolution simulations of hurricane Isabel (2003). Part I: initialization, maximum winds, and the outer-core boundary layer. *Mon Weather Rev* **137,** 3651–3674.

Nunalee, C.G. and Basu, S. 2013. Mesoscale Modeling of Coastal Low-Level Jets: Implications for Offshore Wind Resource Estimation. *Wind Energy*, In review.

Olson, J.B. and Brown, J.M. 2009. A comparison of two mellor-yamada-based PBL schemes in simulating a hybrid barrier jet. The 23rd Conference on Weather

Analysis and Forecasting/19th Conference on Numerical Weather Prediction, *Omaha*, NE, June 1-5.

Otte, T. L., 2007. The impact of nudging in the meteorological model for retrospective air quality simulations. Part I: Evaluation against national observation networks. *J. Appl. Meteor. Climatol.,* **47**, 1853–1867.

Pedersen, T.F. 2003. Development of a Classification System for Cup Anemometers – CLASSCUP. *Risø National Laboratory*, Roskilde.

Rareshide, E., Tindal. A., Johnson. C., Graves, A. M., Simpson, E., Bleeg, J., Harris, T. and Schoborg, D. 2009. Effects of complex wind regimes on turbine performance *Proc. American Wind Energy Association,* WINDPOWER Conference (Chicago, IL)

Raubenheimer, B., Ralston, D.K., Elgar, S., Giffen, D., Signell, R.P. 2012. Observations and predictions of summertime winds on the Skagit tidal flats, Washington. *Continental Shelf Research,* **60**, s13-s21.

RenewableUK. 2013. Offshore wind. Available from: http://www.renewableuk.com/en/renewable-energy/wind-energy/offshore-wind/ [Accessed 23/09/2013].

Reiter, E.R. and Lester, P.F. 1968. Richardson's number in the free atmosphere. *Archiv für Meteorologie, Geophysik und Bioklimatologie*, Serie A, **17(1)**, 1-7.

Peña, A., Hahmann, A.N., Hasager, C.B., Bingöl, F., Karagali, I., Badger, J., Badger, M., and Clausen, N.E. 2011. South Baltic Wind Atlas. South Baltic Offshore Wind Energy Regions Project. *ISBN: 978-87-550-3899-8 Risø-R-1775(EN)*, Risø DTU.

Pleim, J. E., 2007. A combined local and nonlocal closure model for the atmospheric boundary layer. Part I: Model description and testing. *J. Appl. Meteor. Climatol*., **46**, 1383–1395.

Saha, S., and Coauthors, 2010: The NCEP Climate Forecast System Reanalysis. *Bull. Amer. Meteor. Soc*., **91**, 1015–1057.

Santos-Alamillos, F. J., Pozo-Vázquez, D., Ruiz-Arias, J. A., Lara-Fanego, V. and Tovar-Pescador, J. 2013. Analysis of WRF Model Wind Estimate Sensitivity to

Physics Parameterization Choice and Terrain Representation in Andalusia (Southern Spain). *J. Appl. Meteor. Climatol.*, **52**, 1592–1609

Shimada, S. and Ohsawa, T. 2011 Accuracy and characteristics of offshore wind speeds simulated by WRF. *SOLA*. **7**, 21-24.

Skamarock, W.C. 2004. Evaluating mesoscale NWP models using kinetic energy spectra. *Mon Weather Rev, **132***, 3019–3032.

Skamarock, W. C. 2005. Why is there more than one dynamical core in WRF? A technical perspective. Available from: http://www.mmm.ucar.edu/people/skamarock/one core 2005.pdf. [Accessed 13/09/2013].

Skamarock, W.C., Klemp, J.B., Dudhia, J., Gill, D.O., Barker, D.M., Duda, M.G., Huang, X-Y., Wang, W. and Powers, J.G. 2008. A description of the Advanced Research WRF Version 3. NCAR/TN-475=STR, *NCAR Technical Note, Mesoscale and Microscale Meteorology Division, National Center of Atmospheric Research, June 2008*, 113 pp.

Stensrud, D.J., Brooks, H.E., Tracton, M.S. and Rogers, E. 1999. Using ensembles for short-range forecasting. *Mon. Wea. Rev*., **127**, 433–446.

Stensrud, D.J., Bao, J.-W. and Warner, T. T. 2000. Using initial condition and model physics perturbations in short-range ensemble simulations of mesoscale convective systems. *Mon. Wea. Rev*., **128**, 2077–2107.

Stensrud, D.J., and Yussouf, N. 2003. Short-range ensemble predictions of 2-m temperature and dewpoint temperature over New England. *Mon. Wea. Rev*., **131**, 2510–2524.

Stensrud, D.J. 2007. Parameterization schemes: keys to understanding numerical weather prediction models. Cambridge University Press, Cambridge.

Storm B, Dudhia J, Basu S, Swift A, Giammanco I. 2009. Evaluation of the Weather Research and Forecasting Model onForecasting Low-level Jets: Implications for Wind Energy. *Wind Energy*, **12**, 81–90

Stull, R.B. 1988. An introduction to boundary layer meteorology. *Kluwer Acad. Press*, Dordrecht, The Netherlands.

Sukoriansky, S., Galperin, B. and Perov, V. 2005. Application of a new spectral theory of stable stratified turbulence to the atmospheric boundary layer over sea ice. *Boundary-Layer Meteorol*, **117**, 231–257.

Supergen Wind, 2012. Homepage, Supergen Wind website. Available from http://www.supergen-wind.org.uk/. [Accessed 16/11/2012].

Suselj, K. And Sood, A. 2010. Improving the Mellor–Yamada–Janjic parameterization for wind conditions in the marine planetary boundary layer. *Boundary-Layer Meteorol,* **136**, 301–324.

Tastula, E.-M., Vihma, T. and Andreas, E. L. 2012. Evaluation of Polar WRF from modeling of the atmospheric boundary layer over Antarctic sea ice in autumn and winter. *Mon. Wea. Rev*., **140**, 3919–3935.

Teixeira, J., Stevens, B., Bretherton, C.S., Cederwall, R., Doyle, J.D., Golaz, J.C., Holtslag, A.M.M., Klein, S.A., Lundquist, J.K., Randall, D.A., Siebesma, A.P. and Soares, P.M.M. 2008. Parameterization of the atmospheric boundary layer: a view from just above the inversion. *Bull Am Meteorol Soc* **89,** 453–458.

Tindal, A., Johnson, C., LeBlanc, M., Harman, K., Rareshide, E. and Graves, A.-M. 2008. Site-specific adjustments to wind turbine power curves *Proc. American Wind Energy Association WINDPOWER Conference* (Houston, TX).

Toth, Z., 1992. Quasi-stationary and transient periods in the Northern Hemisphere circulation series. *J. Climate*, **5**, 1235–1247.

Trenberth, K. E., and Olson, J. G. 1988. An evaluation and intercomparison of global analyses from NMC and ECMWF. *Bull. Amer. Meteor. Soc.,* **69**, 1047–1057.

Türk, M. and Emeis, S. 2010. The dependence of offshore turbulence intensity on wind speed. *Journal of Wind Engineering and Industrial Aerodynamics*; **98**(8–9), 466–471.

UCAR, Date Unknown. *The Greenhouse effect*. Available from http://www.ucar.edu/learn/1_3_1.htm. [Accessed 02/07/2013].

Uppala, S. M., et al. 2005. The ERA-40 re-analysis, *Q. J. R. Meteorol. Soc*., **131**, 2961–3012.

van den Dool, H.M., and Rukhovets, L. 1994. On the weights for an ensemble-averaged 6–10-day forecast. *Wea. Forecasting,* **9**, 457–465.

Van der Hoven, I. 1957. Power spectrum of horizontal wind speed in the frequency range from 0.0007 to 900 cycles per hour. *J Meteorol,* **14,** 160-164.

van Wijk, A. J.M., Beljaars, A.C.M., Holtslag, A.A.M. and Turkenburg, W.C. 1990 "Evaluation of stability corrections in wind speed profiles over the North Sea," *J. Wind Eng. Ind. Aerodyn*. **33**, 551.

von Storch H. 2001. Models. In: von Storch H, Floser G, eds. *Models in Environmental Research*. Springer Verlag; 17–33.

Wagner, R., Antoniou, I., Pedersen, S.M., Courtney, M.S. and Jørgensen, H.E. 2009. The influence of the wind speed profile on wind turbine performance measurements. *Wind Energy*, **12,** 348–62.

Walser, A., Luthi, D. and Schar, C. 2004. Predictability of precipitation in a cloud-resolving model. *Mon. Wea. Rev*., **132**, 560–577.

Watson, S.J. 2012. Wind Farm Spacing. Personal communication via email. 13/09/2012.

WMO 2012. WMO GREENHOUSE GAS BULLETIN, No. 8. Available online from http://www.wmo.int/pages/mediacentre/press_releases/documents/GHG_Bulletin_No.8_en.pdf. [Accessed 23/11/2012].

Wharton, S. and Lundquist, J.K. 2012a. Atmospheric stability affects wind turbine power collection. *Environ. Res. Lett.* **7.**

Wharton, S. and Lundquist, J.K. 2012b. Assessing atmospheric stability and its impacts on rotor-disk wind characteristics at an onshore wind farm. *Wind Energ.* **15**, 525–546.

Whitaker, J.S. and Loughe, A.F. 1998. The Relationship between Ensemble Spread and Ensemble Mean Skill. *Monthly Weather Review*, **126**, 3292-3302.

Xie, B., Fung, J. C.-H., Chan, A. and Lau, A. K.-H. 2012. Evaluation of nonlocal and local planetary boundary layer schemes in the WRF model. *J. Geophys. Res*., **117**.

Zhao, P., Wang, J., Xia, J., Dai, Y., Sheng, Y. and Yue, J. 2012. Performance evaluation and accuracy enhancement of a day-ahead wind power forecasting system in China. *Renewable Energy,* **43**, 234-241.

Zhao, T. B., and C. B. Fu, 2009: Intercomparison of the summertime subtropical high from the ERA-40 and NCEP/NCAR reanalysis over East Eurasia and the western North Pacific. *Adv. Atmos. Sci.*, **26**, 119-131

Ziehmann, C. 2001. Skill prediction of local weather forecasts based on the ECMWF ensemble. *Nonlinear Processes Geophys*., **8**, 419–428.

Zoumakis, N.M. and Kelessis, A.G. 1991. The dependence of the bulk Richardson number on stability in the surface layer. *Boundary-Layer Meteorology*. **57(4),** 407.

9 Appendix I

Example Namelists for the pre-processing (namelist.wps) and Model run (namelist.input) stages for the Scroby Sands simulations using WRF-NMM.

Namelist.wps

```
&share
 wrf_core = 'NMM',
 max_dom = 5,
 start_date = '1996-05-10_00:00:00', '1996-05-10_00:00:00',
'1996-05-10_00:00:00', '1996-05-10_00:00:00', '1996-05-
10_00:00:00',
 end_date   = '1996-05-14_18:00:00','1996-05-
14_18:00:00','1996-05-14_18:00:00','1996-05-
14_18:00:00','1996-05-14_18:00:00',
 interval_seconds = 21600
 io_form_geogrid = 2,
/

&geogrid
 parent_id         =   1,   1,     2,   3,   4,
 parent_grid_ratio =   1,   3,     3,   3,   3,
 i_parent_start    =   1,   6,     7,   11,  8,
 j_parent_start    =   1,   6,     7,   10,  8,
 e_we              =  18,   22,    28,  22,  19,
 e_sn              =  18,   22,    28,  22,  22,
 geog_data_res     = '10m',  '5m', '2m',     '30s', '30s',
 dx = 0.842,
 dy = 0.837,
 map_proj = 'rotated_ll',
 ref_lat   = 53.032,
 ref_lon   = 1.112,
 geog_data_path = '/usr/local/WRF-NMM/geog'
 opt_geogrid_tbl_path = '/usr/local/WRF-NMM/WRF/WPS/geogrid'
/

&ungrib
 out_format = 'WPS',
 prefix = 'FILE',
/

&metgrid

 fg_name = 'FILE'
 io_form_metgrid = 2,
 opt_metgrid_tbl_path = '/usr/local/WRF-NMM/WRF/WPS/metgrid'
/
```

Namelist.input

```
&time_control
 run_days                            = 3,
 run_hours                           = 18,
 run_minutes                         = 0,
 run_seconds                         = 0,
 start_year                          = 1996,     1996, 1996,
1996,     1996,
 start_month                         = 07,       07,       07,
07,       07,
 start_day                           = 10,       10,       10,
10,       10,
 start_hour                          = 00,       00,   00,
    00,  00,
 start_minute                        = 00,       00,   00,
    00,  00,
 start_second                        = 00,       00,   00,
    00,  00,
 tstart                              = 00,
 end_year                            = 1996,     1996, 1996,
    1996,     1996,
 end_month                           = 07,       07,       07,
07,       07,
 end_day                             = 13,       13,       13,
13,       13,
 end_hour                            = 18,       18,       18,
18,       18,
 end_minute                          = 00,       00,   00,
    00,  00,
 end_second                          = 00,       00,   00,
    00,  00,
 interval_seconds                    = 21600,
 input_from_file = T,F,F,F,F,
 history_interval                    = 360,       360, 60,
    10,  10
 auxinput1_inname = "met_nmm.d<domain>.<date>",
 frames_per_outfile                  = 1,        1,    1,   1,
    1,
 restart                             = .false.,
 restart_interval                    = 5760,
 reset_simulation_start              = F,
 io_form_input                       = 2
 io_form_history                     = 2
 io_form_restart                     = 2
```

```
 io_form_boundary                    = 2
 io_form_auxinput1                   = 2
 debug_level                         = 0
 /

 &domains
 time_step                           = 150,
 time_step_fract_num                 = 0,
 time_step_fract_den                 = 10,
 max_dom                             = 5,
 e_we                                = 18,      22,    28,
     22,  19,
 e_sn                                = 18,      22,    28,
     22,  22,
 e_vert                              = 65,      65,    65,
     65,  65,
 num_metgrid_levels                  = 24,
 dx                                  = .8420,  .2810,  0.0940,
0.0310,  0.0100
 dy                                  = .8370,  .2790,  0.0930,
0.0310,  0.0100
 p_top_requested                     = 5000.
 ptsgm                               = 42000.,
 grid_id                             = 1,       2,     3,   4,
     5,
 parent_id                           = 0,       1,     2,   3,
     4,
 i_parent_start                      = 1,       6,     6,   6,
     6,
 j_parent_start                      = 1,       6,     6,   6,
     6,
 parent_grid_ratio                   = 1,       3,     3,   3,
     3,
 parent_time_step_ratio              = 1,       3,     3,   3,
     3,
 eta_levels                     = 1.000, 0.997, 0.995, 0.993,
0.991,
                0.988, 0.9851, 0.9802, 0.9753, 0.9703,
                0.965, 0.9595, 0.9537, 0.9476, 0.9412,
                0.9344, 0.9272, 0.9195, 0.9113, 0.9024,
                0.8826, 0.8716, 0.8596, 0.8467, 0.8327,
                0.8014, 0.7839, 0.7652, 0.7451, 0.7238,
                0.6772, 0.6521, 0.6259, 0.5988, 0.5708,
                0.5421, 0.5129, 0.4835, 0.4539, 0.4244,
                0.3953, 0.3665, 0.3384, 0.3111, 0.2847,
                0.2594, 0.2351, 0.212, 0.19, 0.167,
                0.1478, 0.1301, 0.1138, 0.0988, 0.0851,
                0.0726, 0.0611, 0.0507, 0.0412, 0.0326,
                0.0247, 0.0176, 0.0112, 0.0053, 0.000,
 feedback = 1,
 /
```

```
 &physics
 mp_physics                          = 5,        5,    5,   5,
     5,
 ra_lw_physics                       = 99,       99,   99,
     99,  99,
 ra_sw_physics                       = 99,       99,   99,
     99,  99,
 nrads                               = 12,      36,    108,
     324, 972,
 nradl                               = 12,      36,    108,
     324, 972,
 co2tf                               = 1,
 sf_sfclay_physics                   = 2,        2,    2,   2,
     2,
 sf_surface_physics                  = 2,        2,    2,   2,
     2,
 bl_pbl_physics                      = 2,        2,    2,   2,
     2,
 nphs                                = 2,         6,   18,
     54,  162,
 cu_physics                          = 2,         2,   2,   0,
     0,
 ncnvc                               = 2,         6,   18,
     54,  162,
 tprec                               = 3,         3,   3,   3,
     3,
 theat                               = 6,         6,   6,   6,
     6,
 tclod                               = 6,         6,   6,   6,
     6,
 trdsw                               = 6,         6,   6,   6,
     6,
 trdlw                               = 6,         6,   6,   6,
     6,
 tsrfc                               = 6,         6,   6,   6,
     6,
 pcpflg                              = .false., .false.,
.false., .false., .false.,
 isfflx                              = 0,
 ifsnow                              = 0,
 icloud                              = 0,
 num_soil_layers                     = 4,
 mp_zero_out                         = 0
 gwd_opt                             = 0
 /

 &dynamics
 /

 &bdy_control
```

```
 spec_bdy_width                      = 1,
 specified                           = .true., .false.,
.false., .false., .false.,
 nested                              = .false., .true.,
.true., .true., .true.,
 /

 &fdda
 /

 &grib2
 /

 &namelist_quilt
 nio_tasks_per_group = 0,
 nio_groups = 1
 /
```

Example Namelists for the pre-processing (namelist.wps) and Model run (namelist.input) stages for the Scroby Sands simulations using WRF-ARW.

Namelist.wps

```
&share
 wrf_core = 'ARW',
 max_dom = 3,
 start_date = '1996-04-02_00:00:00','1996-04-02_00:00:00',
'1996-04-02_00:00:00','1996-03-13_00:00:00',
 end_date   = '1996-04-05_18:00:00','1996-04-05_18:00:00',
'1996-04-05_18:00:00','1996-03-15_00:00:00',
 interval_seconds = 21600
 io_form_geogrid = 2,
/

&geogrid
 parent_id         = 1,1,2,
 parent_grid_ratio = 1,3,3,
 i_parent_start    = 1,81,97,
 j_parent_start    = 1,34,57,
 e_we          = 178,208,241,
 e_sn          = 130,169,169,
 geog_data_res = '10m','5m','30s',
 dx = 18000,
 dy = 18000,
 map_proj =  'lambert',
 ref_lat   = 53.559,
 ref_lon   = -7.395,
 truelat1  = 53.559,
 truelat2  = 53.559,
 stand_lon = -7.395,
 geog_data_path = '/usr/local/WRF-NMM/geog',
 opt_geogrid_tbl_path = '/home/eljh3/runs/WPS/geogrid'
 ref_x = 89.0,
 ref_y = 65.0,
/

&ungrib
 out_format = 'WPS',
 prefix = 'FILE',
/

&metgrid
 fg_name = 'FILE', 'SST'
 io_form_metgrid = 2,
 opt_metgrid_tbl_path = '/home/eljh3/runs/WPS/metgrid'
/
```

Namelist.input

```
&time_control
 run_days                            = 1,
 run_hours                           = 18,
 run_minutes                         = 0,
 run_seconds                         = 0,
 start_year                          = 1996, 1996, 1996, 1996,
 start_month                         = 04,   04,   04,    11,
 start_day                           = 04,   04,   04,   00,
 start_hour                          = 00,   00,   00,   00,
 start_minute                        = 00,   00,   00,   00,
 start_second                        = 00,   00,   00,   00,
 end_year                            = 1996, 1996, 1996, 1996
 end_month                           = 04,   04,   04,  11,
 end_day                             = 05,   05, 05,   13,
 end_hour                            = 18,   18,   18,   18,
 end_minute                          = 00,   00,   00,  00,
 end_second                          = 00,   00,   00,  00,
 interval_seconds                    = 21600
 input_from_file                     = .true., .true., .true.,
.true.,
 history_interval                    = 180,  60,   10, 10,
 frames_per_outfile                  = 1, 1, 1, 1,
 restart                             = .false.,
 restart_interval                    = 50000,
 io_form_history          = 2,
 io_form_restart          = 2,
 io_form_input            = 2,
 io_form_boundary         = 2,
 debug_level              = 0,
 io_form_auxinput4 = 2,
 auxinput4_inname = "wrflowinp_d01",
 auxinput4_interval = 360,


/

 &domains
 eta_levels               = 1.000, 0.9974, 0.9947, 0.9921,
0.9895,
                0.9869, 0.9843, 0.9817, 0.9791, 0.9765,
                0.9725, 0.9671, 0.9602, 0.9516, 0.9412,
                0.9291, 0.9151, 0.8992, 0.8814, 0.8616,
                0.8398, 0.816, 0.7904, 0.7629, 0.7338,
                0.703, 0.6709, 0.6375, 0.603, 0.5677,
                0.5318, 0.4955, 0.4592, 0.4229, 0.387,
                0.3517, 0.3172, 0.2837, 0.2513, 0.2203,
                0.1906, 0.1625, 0.1335, 0.1087, 0.086,
                0.0652, 0.0463, 0.0292, 0.0138, 0.000,
 time_step                = 90,
```

```
 time_step_fract_num      = 0,
 time_step_fract_den      = 1,
 max_dom                  = 3,
 e_we                     = 168,      208,      241,
 e_sn                     = 120,      169,      169,
 e_vert                   = 50,       50,       50,
 p_top_requested          = 5000,
 num_metgrid_levels       = 38,
 num_metgrid_soil_levels  = 4,
 dx                       = 18000,     6000,     2000,
 dy                       = 18000,     6000,     2000,
 grid_id                  = 1,        2,        3,
 parent_id                = 1,        1,        2,
 i_parent_start           = 1,       81,       97,
 j_parent_start           = 1,       34,       57,
 parent_grid_ratio        = 1,        3,        3,
 parent_time_step_ratio   = 1,        3,        3,
 feedback                 = 1,
 smooth_option            = 0,
 /

 &physics
 mp_physics                          = 2,     2, 2,     2,
 ra_lw_physics                       = 99,     99, 99,     99,
 ra_sw_physics                       = 99,     99,     99,
99,
 radt                                = 30,    30,    30, 30,
 sf_sfclay_physics                   = 2,     2,     2, 2,
 sf_surface_physics                  = 2,     2,     2, 2,
 bl_pbl_physics                      = 2,     2,     2, 2,
 bldt                                = 0,     0,     0, 0,
 cu_physics                          = 2,     2,     0, 0,
 cudt                                = 5,     5,     5, 5,
 isfflx                              = 1,
 ifsnow                              = 0,
 icloud                              = 1,
 surface_input_source                = 1,
 num_soil_layers                     = 4,
 sf_urban_physics                    = 0,     0,     0, 0,
 sst_update = 1
 /

 &fdda
   grid_fdda = 1, 0,
   gfdda_inname = "wrffdda_d<domain>",
   gfdda_end_h = 90, 24,
   gfdda_interval_m = 360, 360,
   fgdt = 0, 0,
   if_no_pbl_nudging_uv = 0, 0,
   if_no_pbl_nudging_t = 1, 1,
   if_no_pbl_nudging_q = 1, 1,
```

```
   if_zfac_uv = 0, 0,
   k_zfac_uv = 10, 10,
   if_zfac_t = 0, 0,
   k_zfac_t = 10, 10,
   if_zfac_q = 0, 0,
   k_zfac_q = 10, 10,
   guv = 0.0003, 0.0003,
   gt = 0.0003, 0.0003,
   gq = 0.0003, 0.0003,
   if_ramping = 1,
   dtramp_min = 60.0,
   io_form_gfdda = 2,

  grid_sfdda = 1, 0, 0,
  sgfdda_inname = "wrfsfdda_d<domain>",
  sgfdda_end_h = 90, 24,
  sgfdda_interval_m = 60, 360,
  io_form_sgfdda = 2,
  guv_sfc = 0.0003, 0.0003,
  gt_sfc = 0.0003, 0.0003,
  gq_sfc = 0.0003, 0.0003,
  rinblw = 250.,
 /

 &dynamics
 w_damping                           = 0,
 diff_opt                            = 1,
 km_opt                              = 4,
 diff_6th_opt                        = 0,      0,      0, 0,
 diff_6th_factor                     = 0.12,   0.12,   0.12,
0.12,
 base_temp                           = 290.
 damp_opt                            = 0,
 zdamp                               = 5000.,  5000.,  5000.,
5000.,
 dampcoef                            = 0.2,    0.2,    0.2,
0.2,
 khdif                               = 0,      0,      0, 0,
 kvdif                               = 0,      0,      0, 0,
 non_hydrostatic                     = .true., .true., .true.,
.true.,
 moist_adv_opt                       = 1,      1,      1, 1,
 scalar_adv_opt                      = 1,      1,      1, 1,
  /
 &bdy_control
 spec_bdy_width                      = 5,
 spec_zone                           = 1,
 relax_zone                          = 4,
 specified                           = .true.,
.false.,.false., .false.,
```

```
 nested                              = .false., .true.,
.true., .true.,
  /

 &grib2
 /

 &namelist_quilt
 nio_tasks_per_group = 0,
 nio_groups = 1,
 /
```

Example Namelists for the pre-processing (namelist.wps) and Model run (namelist.input) stages for the Shell Flats simulations.

Namelist.wps

```
&share
 wrf_core = 'ARW',
 max_dom = 3,
 start_date = '2003-06-10_00:00:00','2003-06-
10_00:00:00','2003-06-10_00:00:00',
 end_date   = '2003-12-06_00:00:00','2003-12-
06_00:00:00','2003-12-06_00:00:00',
 interval_seconds = 21600
 io_form_geogrid = 2,
/

&geogrid
 parent_id         = 1,1,2,
 parent_grid_ratio = 1,3,3,
 i_parent_start    = 1,48,47,
 j_parent_start    = 1,36,36,
 e_we          = 107,112,97,
 e_sn          = 90,94,82,
 geog_data_res = '10m','2m','30s',
 dx = 27000,
 dy = 27000,
 map_proj =  'lambert',
 ref_lat   = 52.048,
 ref_lon   = -9.439,
 truelat1  = 52.048,
 truelat2  = 52.048,
 stand_lon = -9.439,
 geog_data_path = '/usr/local/WRF-NMM/geog',
 opt_geogrid_tbl_path = '/home/eljh3/runs/WPS/geogrid'
 ref_x = 53.5,
 ref_y = 45.0,
/
&ungrib
 out_format = 'WPS',
 prefix = 'FILE',
/

&metgrid
 fg_name = 'FILE',
 io_form_metgrid = 2,
 opt_metgrid_tbl_path = '/home/eljh3/runs/WPS/metgrid'
/
```

Namelist.input

```
&time_control
run_days                  = 4,
run_hours                 = 0,
run_minutes               = 0,
run_seconds               = 0,
start_year                = 2003,     2003,     2003,
start_month               = 10,       10,       10,
start_day                 = 20,       20,       20,
start_hour                = 00,       00,       00,
start_minute              = 00,       00,       00,
start_second              = 00,       00,       00,
end_year                  = 2003,     2003,     2003,
end_month                 = 10,       10,       10,
end_day                   = 24,       24,       24,
end_hour                  = 00,       00,       00,
end_minute                = 00,       00,       00,
end_second                = 00,       00,       00,
interval_seconds          = 21600,
input_from_file           = .true.,   .true.,   .true.,
history_interval          = 180,       60,       10,
frames_per_outfile        = 1000,     1000,     1000,
restart                   = .false.,
restart_interval          = 5000,
io_form_history           = 2,
io_form_restart           = 2,
io_form_input             = 2,
io_form_boundary          = 2,
debug_level               = 0,
/

&domains
eta_levels                = 1.000, 0.9943, 0.9886, 0.983,
0.9774,
                0.9718, 0.9658, 0.9592, 0.952, 0.944,
                0.935, 0.9248, 0.913, 0.8995, 0.8838,
                0.8656, 0.8446, 0.8205, 0.7929, 0.7619,
                0.7273, 0.6895, 0.6487, 0.6054, 0.5603,
                0.514, 0.4673, 0.4208, 0.3751, 0.3307,
                0.288, 0.2472, 0.2085, 0.1722, 0.1381,
                0.1064, 0.077, 0.0471, 0.0223, 0.000,
time_step                 = 90,
time_step_fract_num       = 0,
time_step_fract_den       = 1,
max_dom                   = 3,
e_we                      = 107,      112,       97,
e_sn                      = 90,       94,       82,
e_vert                    = 40,       40,       40,
p_top_requested           = 16992.0,
num_metgrid_levels        = 38,
```

```
num_metgrid_soil_levels  = 4,
dx                       = 27000,     9000,     3000,
dy                       = 27000,     9000,     3000,
grid_id                  = 1,         2,        3,
parent_id                = 1,         1,        2,
i_parent_start           = 1,        48,       47,
j_parent_start           = 1,        36,       36,
parent_grid_ratio        = 1,         3,        3,
parent_time_step_ratio   = 1,         3,        3,
feedback                 = 1,
smooth_option            = 0,
/

&physics
mp_physics               = 3,         3,        3,
ra_lw_physics            = 1,         1,        1,
ra_sw_physics            = 1,         1,        1,
radt                     = 30,        30,       30,
sf_sfclay_physics        = 1,         1,        1,
sf_surface_physics       = 2,         2,        2,
bl_pbl_physics           = 1,         1,        1,
bldt                     = 0,         0,        0,
cu_physics               = 1,         1,        0,
cudt                     = 5,         5,        5,
isfflx                   = 1,
ifsnow                   = 0,
icloud                   = 1,
surface_input_source     = 1,
num_soil_layers          = 4,
sf_urban_physics         = 0,         0,        0,
maxiens                  = 1,
maxens                   = 3,
maxens2                  = 3,
maxens3                  = 16,
ensdim                   = 144,
/

&fdda
   grid_fdda = 1, 0, 0,
   gfdda_inname = "wrffdda_d<domain>",
   gfdda_end_h = 96, 24,
   gfdda_interval_m = 360, 360,
   fgdt = 0, 0,
   if_no_pbl_nudging_uv = 0, 0,
   if_no_pbl_nudging_t = 1, 1,
   if_no_pbl_nudging_q = 1, 1,
   if_zfac_uv = 0, 0,
   k_zfac_uv = 10, 10,
   if_zfac_t = 0, 0,
   k_zfac_t = 10, 10,
   if_zfac_q = 0, 0,
```

```
   k_zfac_q = 10, 10,
   guv = 0.0003, 0.0003,
   gt = 0.0003, 0.0003,
   gq = 0.0003, 0.0003,
   if_ramping = 1,
   dtramp_min = 60.0,
   io_form_gfdda = 2,

  grid_sfdda = 1, 0, 0,
  sgfdda_inname = "wrfsfdda_d<domain>",
  sgfdda_end_h = 96, 24,
  sgfdda_interval_m = 60, 360,
  io_form_sgfdda = 2,
  guv_sfc = 0.0003, 0.0003,
  gt_sfc = 0.0003, 0.0003,
  gq_sfc = 0.0003, 0.0003,
  rinblw = 250.,
/

&dynamics
w_damping                = 0,
diff_opt                 = 1,
km_opt                   = 4,
diff_6th_opt             = 0,        0,        0,
diff_6th_factor          = 0.12,     0.12,     0.12,
base_temp                = 290.,
damp_opt                 = 0,
zdamp                    = 5000.,    5000.,    5000.,
dampcoef                 = 0.2,      0.2,      0.2,
khdif                    = 0,        0,        0,
kvdif                    = 0,        0,        0,
non_hydrostatic          = .true.,   .true.,   .true.,
moist_adv_opt            = 1,        1,        1,
scalar_adv_opt           = 1,        1,        1,
/

&bdy_control
spec_bdy_width           = 5,
spec_zone                = 1,
relax_zone               = 4,
specified                = .true.,  .false.,  .false.,
nested                   = .false.,   .true.,   .true.,
/

&grib2
/

&namelist_quilt
nio_tasks_per_group      = 0,
nio_groups               = 1,
/
```

Example Namelists for the pre-processing (namelist.wps) and Model run (namelist.input) stages for the Supergen exemplar simulations.

Namelist.wps

```
&share
 wrf_core = 'ARW',
 max_dom = 3,
 start_date = '2003-12-01_00:00:00','2003-12-
01_00:00:00','2003-12-01_00:00:00',
 end_date   = '2004-06-10_00:00:00','2004-06-
10_00:00:00','2004-06-10_00:00:00',
 interval_seconds = 21600
 io_form_geogrid = 2,
/

&geogrid
 parent_id         = 1,1,2,
 parent_grid_ratio = 1,3,3,
 i_parent_start    = 1,42,38,
 j_parent_start    = 1,32,40,
 e_we          = 107,112,121,
 e_sn          = 90,94,103,
 geog_data_res = '10m','2m','30s',
 dx = 27000,
 dy = 27000,
 map_proj =  'lambert',
 ref_lat   = 53.637,
 ref_lon   = -1.038,
 truelat1  = 52.048,
 truelat2  = 52.048,
 stand_lon = -9.439,
 geog_data_path = '/usr/local/WRF-NMM/geog',
 opt_geogrid_tbl_path = '/home/eljh3/runs/WPS/geogrid'
 ref_x = 53.5,
 ref_y = 45.0,
/
&ungrib
 out_format = 'WPS',
 prefix = 'FILE',
/

&metgrid
 fg_name = 'FILE',
 io_form_metgrid = 2,
 opt_metgrid_tbl_path = '/home/eljh3/runs/WPS/metgrid'
/
```

Namelist.input

```
&time_control
run_days                  = 4,
run_hours                 = 0,
run_minutes               = 0,
run_seconds               = 0,
start_year                = 2004,     2004,     2004,
start_month               = 04,       04,       04,
start_day                 = 25,       25,       25,
start_hour                = 00,       00,       00,
start_minute              = 00,       00,       00,
start_second              = 00,       00,       00,
end_year                  = 2004,     2004,     2004,
end_month                 = 04,       04,       04,
end_day                   = 29,       29,       29,
end_hour                  = 00,       00,       00,
end_minute                = 00,       00,       00,
end_second                = 00,       00,       00,
interval_seconds          = 21600,
input_from_file           = .true.,   .true.,   .true.,
history_interval          = 180,       60,       10,
frames_per_outfile        = 1000,     1000,     1000,
restart                   = .false.,
restart_interval          = 4000,
io_form_history           = 2,
io_form_restart           = 2,
io_form_input             = 2,
io_form_boundary          = 2,
debug_level               = 0,
/

&domains
eta_levels                = 1.000, 0.9943, 0.9886, 0.983,
0.9774,
                 0.9718, 0.9658, 0.9592, 0.952, 0.944,
                 0.935, 0.9248, 0.913, 0.8995, 0.8838,
                 0.8656, 0.8446, 0.8205, 0.7929, 0.7619,
                 0.7273, 0.6895, 0.6487, 0.6054, 0.5603,
                 0.514, 0.4673, 0.4208, 0.3751, 0.3307,
                 0.288, 0.2472, 0.2085, 0.1722, 0.1381,
                 0.1064, 0.077, 0.0471, 0.0223, 0.000,
time_step                 = 90,
time_step_fract_num       = 0,
time_step_fract_den       = 1,
max_dom                   = 3,
e_we                      = 107,      112,      121,
e_sn                      = 90,       94,      103,
e_vert                    = 40,       40,       40,
```

```
p_top_requested          = 5000,
num_metgrid_levels       = 38,
num_metgrid_soil_levels  = 4,
dx                       = 27000,     9000,     3000,
dy                       = 27000,     9000,     3000,
grid_id                  = 1,         2,        3,
parent_id                = 1,         1,        2,
i_parent_start           = 1,        42,       38,
j_parent_start           = 1,        32,       40,
parent_grid_ratio        = 1,         3,        3,
parent_time_step_ratio   = 1,         3,        3,
feedback                 = 1,
smooth_option            = 0,
/

&physics
mp_physics               = 3,         3,        3,
ra_lw_physics            = 1,         1,        1,
ra_sw_physics            = 1,         1,        1,
radt                     = 30,        30,       30,
sf_sfclay_physics        = 1,         1,        1,
sf_surface_physics       = 2,         2,        2,
bl_pbl_physics           = 1,         1,        1,
bldt                     = 0,         0,        0,
cu_physics               = 1,         1,        0,
cudt                     = 5,         5,        5,
isfflx                   = 1,
ifsnow                   = 0,
icloud                   = 1,
surface_input_source     = 1,
num_soil_layers          = 4,
sf_urban_physics         = 0,         0,        0,
maxiens                  = 1,
maxens                   = 3,
maxens2                  = 3,
maxens3                  = 16,
ensdim                   = 144,
/

&dynamics
w_damping                = 0,
diff_opt                 = 1,
km_opt                   = 4,
diff_6th_opt             = 0,         0,        0,
diff_6th_factor          = 0.12,      0.12,     0.12,
base_temp                = 290.,
damp_opt                 = 0,
zdamp                    = 5000.,     5000.,    5000.,
dampcoef                 = 0.2,       0.2,      0.2,
khdif                    = 0,         0,        0,
kvdif                    = 0,         0,        0,
```

```
non_hydrostatic          = .true.,   .true.,   .true.,
moist_adv_opt            = 1,        1,        1,
scalar_adv_opt           = 1,        1,        1,
/

&bdy_control
spec_bdy_width           = 5,
spec_zone                = 1,
relax_zone               = 4,
specified                = .true.,  .false.,  .false.,
nested                   = .false.,   .true.,   .true.,
/

&grib2
/

&namelist_quilt
nio_tasks_per_group      = 0,
nio_groups               = 1,
/
```